

**INVESTIGATION INTO THE HEPATOTOXICITY OF THE NOVEL
ANTI-CANCER DRUG ECTEINASCIDIN –743 (ET-743)**

Thesis submitted for the degree of Doctor of Philosophy
at the University of Leicester

Sarah Donald BSc. (Hons)
Department of Oncology
University of Leicester

May 2003

UMI Number: U495640

All rights reserved

INFORMATION TO ALL USERS

The quality of this reproduction is dependent upon the quality of the copy submitted.

In the unlikely event that the author did not send a complete manuscript and there are missing pages, these will be noted. Also, if material had to be removed, a note will indicate the deletion.



UMI U495640

Published by ProQuest LLC 2015. Copyright in the Dissertation held by the Author.
Microform Edition © ProQuest LLC.

All rights reserved. This work is protected against
unauthorized copying under Title 17, United States Code.



ProQuest LLC
789 East Eisenhower Parkway
P.O. Box 1346
Ann Arbor, MI 48106-1346



Investigation into the hepatotoxicity of the novel anti-cancer drug ecteinascidin-743 (ET-743)

Sarah Donald

Ecteinascidin-743 (ET-743) is a novel marine-derived anti-cancer drug with demonstrated anti-tumour activity in clinical trials against sarcoma, breast and ovarian carcinoma. Reversible transaminitis and subclinical cholangitis have frequently been described in patients who receive ET-743. To facilitate understanding of this adverse effect and help design suitable therapeutic rescue strategies, the hepatic effects of ET-743, administered as a single i.v. dose of 40 µg/kg, were characterised in female Wistar rats by histopathology, electron microscopy, hepatic and plasma biochemistry and DNA microarray analysis. Plasma levels of bilirubin were elevated up to 7-fold over those in untreated rats and activities of alkaline phosphatase and aspartate aminotransferase in plasma were slightly elevated. Livers displayed degeneration and necrosis of bile duct epithelia associated with mild inflammation followed by fibrosis. DNA microarray analysis of livers from ET-743-treated rats showed a significant increase in the expression of ATP binding cassette transport genes *abcb1a* and *abcb1b* and cell cycle genes *cdc2a* and *ccnd1*. The cell cycle gene expression changes mirrored ET-743-induced increases in liver weight and Ki-67 labelling of liver nuclei. The results suggest that the toxicity exerted by ET-743 in the rat liver is a consequence of biliary damage and is accompanied by a wave of mitogenic activity.

Pre-treatment with dexamethasone (10 mg/kg p.o.) 24 hours prior to ET-743 abrogated the biochemical and histopathological manifestations of ET-743-induced liver changes without interfering with the anti-tumour activity. Dexamethasone pre-treatment decreased hepatic levels of ET-743 dramatically compared to those obtained after administration of ET-743 alone. Pre-treatment with dexamethasone effectively protected against ET-743-mediated hepatic damage by decreasing hepatic exposure to ET-743, probably linked to induction of certain cytochrome P450 enzymes. Pre-treatment with cytochrome P450 inducers β-naphthoflavone, phenobarbitone or indole-3-carbinol also reduced ET-743-mediated hepatotoxicity. In conclusion, the results strongly advocate the clinical evaluation of pre-treatment with dexamethasone in patients who receive ET-743 to ameliorate its unwanted effects in the liver.

This thesis is dedicated to my dad

Acknowledgements

Firstly, I would like to thank PharmaMar for giving me the opportunity to carry out the work for this thesis and for financial support.

My supervisor, Professor Andy Gescher deserves special thanks for his advice, support and enthusiasm throughout this project. I would also like to thank Dr Verschoyle for much advice and assistance with animal experiments and expertise in cytochrome P450-enzymes.

I am indebted to Dr Peter Greaves for his expert advice and his time spent examining the pathology. I would also like to thank David Dinsdale for carrying out electron microscopy. In addition, I would like to acknowledge Richards Edwards, for immunohistochemistry, Jenny Edwards and Lynda Wilkinson, for the histological preparation, and Judy McWilliams, for electron microscopy.

I would like to thank the MRC microarray group: Dr Reg Davies, Joan Riley and David Judah, for assistance with the microarray technology, but especially Dr Tim Gant, for his advice and help with the data analysis and statistics.

Also I would like to thank Maurizio D'Incalci, Massimo Zuchetti and other collaborators at the Mario Negri Institute who worked on the anti-tumour activity and analytical chemistry experiments.

The TACD/oncology group, past and present, require special thanks, for all the tea breaks and fun nights out, which made my time in the departments very enjoyable.

Finally, I need to thank my family and friends, for their support, especially my Mum and Bill for putting up with me, and a special thank you to Paul.

Contents	Page
Abstract	i
Dedication	ii
Acknowledgements	iii
Contents	iv
Figures	xi
Tables	xvii
Abbreviations	xix

Chapter 1: Introduction

1.1 Scope of introduction	1
1.2 Cancer and chemotherapy	1
1.3 Drug induced liver disease	5
1.4 Bile flow	7
1.5 Phase I and II drug metabolism	10
1.5.1 Mechanisms of induction and inhibition of cytochrome P450	14
1.5.2 Species differences in metabolism	18
1.6 Mechanisms of hepatotoxicity	21
1.7 Mechanism of α -naphthylisothiocyanate (ANIT) hepatotoxicity	24
1.8 Liver disease induced by chemotherapy	27
1.9 Evaluation of hepatotoxicity <i>in vitro</i>	33

1.10 ET-743	35
1.10.1 Mechanism of action of ET-743	37
1.10.2 <i>In vivo</i> antitumour activity of ET-743	40
1.10.3 Clinical investigations	41
1.10.4 Preclinical toxicity	43
1.10.5 Metabolism of ET-743	46
1.11 Aims	49

Chapter 2: Materials and methods

2.1 Materials

2.1.1 Materials	52
2.1.2 Animals	52
2.1.3 Histopathology and immunocytochemistry	52
2.1.4 Electron microscopy	53
2.1.5 CYP assays	53
2.1.6 Microarray	53
2.1.7 Bradford protein assay	53
2.1.8 Polyacrylamide gel electrophoresis	54
2.1.9 Isolation of hepatocytes	54

2.2 Methods

2.2.1 Study of the hepatotoxicity of ET-743 <i>in vivo</i> .	55
2.2.2 Effect of ET-743 on hepatic gene expression	55

2.2.3 Study of the hepatotoxicity of ANIT	56
2.2.4 Study of the effect of dexamethasone on ET-743 hepatotoxicity	56
2.2.5 Study of the effect of dexamethasone and ET-743 on hepatic gene expression changes	56
2.2.6 Study of the modulation of the hepatotoxicity <i>in vivo</i>	57
2.2.7 Study of the modulation of the hepatotoxicity <i>in vitro</i>	58
2.2.8 Study of the effect of I3C on ET-743 hepatotoxicity	58
2.2.9 Study of anti-tumour activity	58
2.2.10 Histopathology and immunocytochemistry	60
2.2.11 Electron microscopy	61
2.2.12 Measurement of liver enzymes	62
2.2.12.1 ALP	62
2.2.12.2 AST	62
2.2.12.3 Bilirubin	63
2.2.13 Preparation of microsomes	63
2.2.14 CYP2E1 assay	63
2.2.15 CYP1A1/2 assay	64
2.2.16 CYP3A2 assay	64
2.2.17 Total cytochrome P450 assay	65
2.2.18 Measurement of glutathione levels in liver	65
2.2.19 Bradford protein assay	66
2.2.20 Microarray analysis, an overview	66

2.2.20.1 Preparation of mRNA	67
2.2.20.2 Printing the arrays	67
2.2.20.3 Labelling and hybridisation	68
2.2.20.4 Purification of RNA	69
2.2.20.5 Preparation of hybridisation to microarray slides	69
2.2.20.6 Washing of array coverslips	69
2.2.20.7 Microarray slide blocking, prescan and prehybridisation	70
2.2.20.8 Hybridisation	70
2.2.20.9 Analysis of fluorescence and data processing	70
2.2.21 Preparation of membrane liver fractions for Western blotting	71
2.2.22 Polyacrylamide gel electrophoresis and Western blotting analysis, an overview	71
2.2.22.1 Preparation of the gel	72
2.2.22.2 Loading and running the gels	73
2.2.22.3 Detection of P-glycoprotein expression	74
2.2.23 Cell cycle analysis	74
2.2.24 Isolation of primary rat hepatocytes	75
2.2.25 Incubations with hepatocytes	76
2.2.26 Study of ET-743 levels in liver and plasma	77
2.2.27 MCF-7 cells	77
2.2.28 Effect of ET-743 on MCF-7 cell growth	78
2.2.29 <i>In vitro</i> bioassay to assess the cytotoxicity of ET-743 after incubation with rat liver microsomes	78
2.2.30 Statistical analysis	79

Chapter 3: ET-743 hepatotoxicity

3.1 Introduction	80
3.2 Effects of ET-743 on liver biochemistry	82
3.3 Effect of ET-743 on liver cell pathology	85
3.4 Effects of ET-743 on hepatic gene expression	89
3.5 Effects of ET-743 on indices of hepatic cell proliferation	98
3.6 Effects of ET-743 on liver biochemistry and pathology in male rats	102
3.7 The effect of ANIT on liver pathology, biochemistry and gene expression changes	104
3.8 Discussion	108

Chapter 4: Evaluation of the protective efficacy of dexamethasone against ET-743 induced hepatotoxicity *in vivo*

4.1 Introduction	112
4.2 Effect of dexamethasone pre-treatment on ET-743-induced liver damage	114
4.3 The effect of dexamethasone on ET-743 hepatotoxicity when both are administered concurrently	118
4.4 Effect of pre-treatment with dexamethasone on changes in hepatic gene expression caused by ET-743	120
4.5 Effect of dexamethasone on hepatic CYP3A	123
4.6 Effect of pre-treatment with dexamethasone on levels of ET-743 in liver and	

blood	127
4.7 Effect of pre-treatment with dexamethasone on anti-tumour activity of ET-743	129
4.8 <i>In vitro</i> bioassay to predict toxicity of ET-743 metabolites.	132
4.9 Discussion	134

Chapter 5: Evaluation of the protective efficacy of β -naphthoflavone, phenobarbitone and N-acetylcysteine against ET-743 –induced toxicity *in vivo*

5.1 Introduction	139
5.2 Effect of β -naphthoflavone, phenobarbitone and N-acetylcysteine on ET-743-induced elevations of plasma indicators of hepatotoxicity	141
5.3 Effects of β -naphthoflavone, phenobarbitone and N-acetylcysteine on ET-743 induced histopathological changes in liver	143
5.4 Effects of ET-743 on hepatic glutathione levels	145
5.5 Discussion	146

Chapter 6: Toxicity of ET-743 in hepatocytes in culture and evaluation of protection by modulators of metabolism

6.1 Introduction	149
6.2 Effect of ET-743 on hepatocytes isolated from female rats	150
6.3 Effects of dexamethasone, β -naphthoflavone, phenobarbitone and N-acetylcysteine on ET-743 induced toxicity in hepatocytes	154

6.4 Discussion	156
----------------	-----

Chapter 7: Evaluation of the protective efficacy of indole-3-carbinol against ET-743 induced hepatotoxicity

7.1. Introduction	158
7.2 The effect of I3C pre-treatment on ET-743-induced liver changes	161
7.3 The effect of DIM pre-treatment on ET-743-induced liver changes	166
7.4 The effect of I3C on hepatic cytochrome P450 enzymes	168
7.5 Discussion	171

Chapter 8: Final discussion

8.1 Final discussion	173
----------------------	-----

Bibliography	180
---------------------	-----

Appendix	201
-----------------	-----

Figures

Chapter 1

Figure 1.1 Major transport systems in bile formation.	9
Figure 1.2 Metabolism of paracetamol.	23
Figure 1.3 Mechanisms of ANIT hepatotoxicity.	26
Figure 1.4 Photograph of <i>Ecteinascidia turbinata</i>	36
Figure 1.5 Structure of ET-743	36
Figure 1.6 Structures of potential metabolites of ET-743	48

Chapter 3

Figure 3.1 Time course of changes in concentration of total bilirubin and activities of liver enzymes alkaline phosphatase and aspartate aminotransferase in plasma from female rats that received ET-743 (40 µg/kg, i.v.).	83
Figure 3.2 Time course of changes of cytochrome P450 protein levels and activities of CYP1A1/2, CYP2E and CYP3A2 in liver microsomes obtained from female rats that received ET-743 (40 µg/kg, i.v.).	84
Figure 3.3 Photomicrographs of liver sections from female rats that received ET-743 (40 µg/kg, i.v.).	86/87
Figure 3.4 Electron micrographs of a bile duct and a typical hepatocyte observed in female rats 2 days after treatment with ET-743 (40 µg/kg, i.v.).	88

Figure 3.5 A cluster of genes up-regulated after ET-743 (40 µg/kg, i.v.) administration.	94
Figure 3.6 Time course of changes in hepatic expression of ABC genes <i>abcb4</i> , <i>abcb1a</i> and <i>abcb1b</i> in livers of female rats that received ET-743 (40 µg/kg, i.v.).	95
Figure 3.7 Western blot showing the expression of P-glycoprotein in the liver after ET-743 treatment (40 µg/kg, i.v.), compared to control.	95
Figure 3.8 A cluster of genes down-regulated after ET-743 (40 µg/kg, i.v.) administration	96
Figure 3.9 Time course of changes in expression in <i>hba-x</i> , <i>hba-a1</i> , <i>hbb-b1</i> , <i>hbb-bh1</i> and <i>hbb-y</i> genes in livers of female rats that received ET-743 (40 µg/kg, i.v.).	97
Figure 3.10 Time course of changes in expression of <i>cdc2a</i> and <i>ccnd1</i> genes in livers of female rats that received ET-743 (40 µg/kg, i.v.).	99
Figure 3.11 Time course of changes in liver weight and Ki-67 labelling nuclei in female rats that received ET-743 (40 µg/kg, i.v.).	100
Figure 3.12 Change in liver cell cycle distribution in rats given ET-743 (40 µg/kg, i.v.), compared to untreated rats.	101
Figure 3.13 Plasma aspartate aminotransferase, alkaline phosphatase and bilirubin levels in male Wistar rats after ET-743 at two dose levels.	103
Figure 3.14 Plasma aspartate aminotransferase, alkaline phosphatase and bilirubin levels measured in female Wistar rats after ANIT treatment (100 mg/kg, p.o.) or vehicle only.	105

Figure 3.15 Gene changes after ANIT (100 mg/kg, p.o.) and ET-743 (40 µg/kg, i.v.) administration. 106

Figure 3.16 Gene expression changes 2 days post ANIT (100 mg/kg, p.o.) and 3 days post ET-743 (40 µg/kg, i.v.) and 6 days post ANIT and 12 days post ET-743 treatment. 107

Chapter 4

Figure 4.1 Dose dependency of the effect of dexamethasone administered p.o. 24 hours prior to ET-743 (40 µg/kg, i.v.) on ET-743 induced elevations of plasma activity of alkaline phosphatase, aspartate aminotransferase and of plasma bilirubin levels in female rats measured 3 days after ET-743. 115

Figure 4.2 Liver section from female Wistar rats at 3 days after ET-743 treatment (40 µg/kg, i.v.) alone or 24 hours after dexamethasone (10 mg/kg, p.o.). 117

Figure 4.3 The effect of dexamethasone (10 mg/kg, p.o.) administered immediately prior to ET-743 (40 µg/kg) on ET-743-induced elevation of plasma activity of alkaline phosphatase, aspartate aminotransferase and of plasma bilirubin levels in female rats measured 3 days after ET-743. 119

Figure 4.4 Gene expression changes elicited by ET-743 (40 µg/kg, i.v.) without pre-treatment and after pre-treatment with dexamethasone (10 mg/kg, p.o.) in livers of female rats. 121

Figure 4.5 Gene expression changes in livers of female rats elicited by ET-743 (40 µg/kg, i.v.), dexamethasone (10 mg/kg, p.o.) and the combination. 122

Figure 4.6 Gene expression changes in livers of female rats 24 h after oral administration of dexamethasone (10 mg/kg, p.o.). 124

Figure 4.7 CYP3A activity in female rats treated with dexamethasone (1-20 mg/kg, p.o.) compared to untreated female rats and untreated male rats.	126
Figure 4.8 Effect of pre-treatment with dexamethasone on the disposition of ET-743 in liver tissue of female rats.	128
Figure 4.9 Anti-tumour activity of dexamethasone, ET-743 or ET-743 in combination with dexamethasone, the latter given 24 hours prior to ET-743, in female Fischer rats bearing the 13762 mammary carcinoma.	130
Figure 4.10 The effect of ET-743, and ET-743 after microsomal metabolism, on cytotoxicity towards MCF-7 cells.	133

Chapter 5

Figure 5.1 The effect of dexamethasone, β -naphthoflavone, phenobarbitone and N-acetylcysteine when administration prior to ET-743 (40 μ g/kg, i.v.) on ET-743 induced increases in the plasma activities of ALP, AST and of plasma levels of bilirubin in female Wistar rats.	142
Figure 5.2 The effect of N-acetylcysteine and β -naphthoflavone on ET-743-induced changes in liver pathology.	144
Figure 5.3 The effect of ET-743 on hepatic glutathione levels.	145

Chapter 6

Figure 6.1 Effect of ET-743 on viability of hepatocytes isolated from female Wistar rats.	151
---	-----

Figure 6.2 Effect of ET-743 on MCF-7 cell proliferation	152
Figure 6.3 Effect of ET-743 on viability of hepatocytes from rats and humans after 48, 72 and 96 hours exposure to the drug.	153
Figure 6.4 Effect of ET-743 on viability of hepatocytes isolated from rats which have been pre-treated with dexamethasone, β -naphthoflavone, or phenobarbitone or of cells which have been incubated with N-acetylcysteine.	155

Chapter 7

Figure 7.1 Structure of I3C and one of its condensation products, DIM.	159
Figure 7.2 Effect of 0.5 % I3C in the diet on ET-743-induced elevations of plasma activity of aspartate aminotransferase, alkaline phosphatase and of plasma bilirubin levels in female rats.	163
Figure 7.3. Photomicrographs of liver sections from female Wistar rats which received ET-743 (40 μ g/kg, i.v.) alone or after 0.5 % I3C in the diet for one week prior to ET-743 and throughout the study period.	164
Figure 7.4 Effect of 0.1 % I3C in the diet on ET-743-induced elevations of plasma activity of aspartate aminotransferase, alkaline phosphatase and of plasma bilirubin levels in female rats.	165
Figure 7.5 Effect of 0.2 % DIM in the diet on ET-743-induced elevations of plasma activity of aspartate aminotransferase, alkaline phosphatase and of plasma bilirubin levels in female rats.	167
Figure 7.6 CYP3A activity in female rats after 0.5 % I3C or 0.2 % DIM feeding for one week compared to untreated female rats.	169

Figure 7.7 CYP1A1/2 activity in female rats after 0.5 % I3C or 0.2 % DIM feeding for one week compared to untreated female rats.

170

Tables

Chapter 1

Table 1.1 Glutathione S-Transferases	13
Table 1.2 Inducers of CYP enzymes.	17
Table 1.3 Antiproliferative effect of ET-743 in vitro using NCI cell line screen.	37
Table 1.4 Table showing the maximum tolerated doses for ET-743 from animal toxicity studies.	44

Chapter 2

Table 2.1 The dosing schedule used in the five tumour models to investigate the antitumour properties of the combination of ET-743 and dexamethasone.	60
---	----

Chapter 3

Table 3.1 Genes up-regulated at one or more time points after ET-743 (40 µg/kg, i.v.) administration in female rats.	90/91
Table 3.2 Genes down-regulated at one or more time points after ET-743 (40 µg/kg, i.v.) administration in female rats.	92/93

Chapter 4

Table 4.1. Gene expression changes in female rat liver elicited by dexamethasone (10 mg/kg, p.o.) in livers of female rats 24 hours after dosing.	125
Table 4.2 The AUC values for plasma between 0 and 6 hours obtained from rats which received ET-743 alone or after dexamethasone pre-treatment.	127

Table 4.3 Activity of dexamethasone, ET-743 and the combination against mouse
B-16 melanoma, M5076 reticulum sarcoma, IGROV-1 ovarian carcinoma
and TE-671 rhabdomyosarcoma 131

Abbreviations

Ah	aryl hydrocarbon
ALP	alkaline phosphatase
ALT	alanine aminotransferase
ANIT	α -naphthylisothiocyanate
ANOVA	analysis of variance
Ara-C	cytosine arabinoside
AST	aspartate aminotransferase
AUC	areas under the plasma concentration time curve
BIBRA	British Industrial Biological Research Association
7-BQ	7-benzyloxyquinoline
CAR	constitutive androstane receptor
CYP	cytochrome P450 enzyme
DEPC	diethyl pyrocarbonate
DIM	3,3-diindolylmethane
dNTP	2'-deoxyribonucleoside-5'-triphosphate
DTNB	5,5-dithio <i>bis</i> 2-nitrobenzoic acid
DTT	dithiothreitol
dTTP	2'-deoxythymidine 5'-triphosphate
dUTP	2'-deoxyuridine 5'-triphosphate
DMSO	dimethyl sulphoxide
DNA	deoxynucleic acid
EDTA	ethylenediaminetetraacetic acid
EGTA	ethylene glycol-bis (2-aminoethylether)-N, N, N', N'-tetraacetic acid
FACS	fluorescence-assisted cell-sorting scan
FCS	fetal calf serum
5-FU	5-fluorouracil
GGT	γ -glutamyltranspeptidase

GR	glucocorticoid receptor
H&E	haematoxylin and eosin
HPLC	high performance liquid chromatography
7-HQ	7-hydroxyquinoline
I3C	indole-3-carbinol
ICZ	indolyl-carbazole
i.m.	intra muscular
i.p.	intra peritoneal
i.v.	intra venous
LC-MS	liquid chromatography/mass spectrometry
LDH	lactate dehydrogenase
LTr-1	2-(indol-3-ylmethyl)-3,3'-diindolylmethane
6-MP	6-Mercaptopurine
MTD	maximum tolerated dose
NADP	nicotinamide adenine dinucleotide phosphate
NADPH	nicotinamide adenine dinucleotide phosphate reduced form
NAPQI	N-acetyl- <i>p</i> -benzoquinone imine
NER	nucleotide excision repair
NSCLC	non-small cell lung cancer
PBRU	phenobarbital-responsive enhancer unit
PBS	phosphate buffered saline
P-gp	P-glycoprotein
PMA	phorbol myristate acetate
PMSF	phenylmethylsulphonylfluoride
p.o.	per os
PXR	pregnane X receptor
RNA	ribonucleic acid
Rnase	ribonuclease
RXR	retinoid X receptor
s.c.	subcutaneous

SD	standard deviation
SDS	sodium dodecyl sulphate
SSC	saline sodium citrate
SSPE	saline sodium phosphate EDTA
TBS	tris buffered saline
TBS-T	tris buffered saline tween
T/E	trypsin/EDTA
TEMED	N,N,N',N',-tetramethylethylenediamine
Tris	2-amino-2-hydroxymethyl-1,3-propanediol
TWI	Tumour weight inhibition
UGT	UDP-glucuronyl transferases

CHAPTER 1

Introduction

1.1 Scope of introduction

The work described in this thesis concerns the elucidation and manipulation in rats of the hepatotoxicity of ET-743, a novel, experimental anti-cancer drug. In order to place the experiments described into an appropriate context this introduction reminds the reader of general features of cancer chemotherapy with cytotoxicants, it introduces factors which determine the organism's susceptibility towards hepatotoxic chemicals, it introduces biochemical and physiological factors which can be targets of hepatotoxicants, and it describes the mechanisms by which known hepatotoxicants exert their effects. As experiments were performed in which the hypothesis of the involvement of cytochrome P450 enzymes in the toxicity of ET-743 was tested, an introductory section is devoted to the physiological and pharmacological regulation of such enzymes. Special emphasis is placed in the introduction on examples of anti-cancer drugs which are known to damage the liver. Finally, the mechanism by which ET-743 is thought to exert its anti-cancer activity is summarised and the literature on its efficacy and unwanted effects in animals and humans is reviewed.

1.2 Cancer and chemotherapy

Cancer is a leading cause of death in the Western world. Around a quarter of a million cases of cancer are diagnosed in the UK each year, with around 156,000 deaths. At current rates, about one in three of the population will develop cancer and one in four of the population will die from the disease (Cancer Research UK). In 1930, the medical cure rate for those afflicted with cancer was about one in five. Today, approximately two in five are cured (Pitot and Loeb, 2002). This decline in cancer mortality is due to the effect of cancer prevention and improved cancer treatment through radiation, surgery and chemotherapy. Significant advances have been made during the past three decades in the successful treatment of neoplasms that were not curable by surgery or radiation alone. Chemotherapy, by use of an increased spectrum of drugs, hormones and other natural products is the principle regime that has resulted in significant improvement in the treatment of a number of cancers.

Chemotherapy as well as a significant number of its basic scientific concepts originated in the work of Paul Ehrlich in the early 1900s. He developed a system that allowed the transplantation of neoplasms in rodents, on which he could test the effectiveness of drugs in slowing or eliminating neoplastic development. Although the concept of treating cancers with drugs may be traced back several centuries, there is no example of successful cancer chemotherapy before the 1940s (Donehower et al., 1995). In World War II an explosion on a ship containing mustard gas resulted in the exposure of a number of individuals to this agent. It was noted at that time that exposed individuals exhibited a significant degree of bone marrow and lymphoid hypoplasia (Infield, 1971). As a result of this finding, Gilman and Philips studied and reported the first clinical trials of nitrogen mustard in patients with malignant lymphomas (Gilman and Philips, 1946). Their results demonstrated dramatic, although somewhat transient, regression of lymphomas. In the 1960s, the potential of the nitrosoureas first came to light from an early screening programme searching for chemicals cytotoxic towards malignant cells (Priestman, 1989). It resulted in a large chemical synthesis programme intended to improve the effectiveness of such compounds by reducing the unwanted toxicity. The anthracyclines were also discovered in the 1960s during a search for natural products with anti-cancer activity. Since that time, there has been not only an increasing number of drugs used for chemotherapy but also increased understanding of their mechanism of action. New chemicals with stronger cytotoxic actions are constantly being developed.

Clinically, cancer is a large group of diseases that vary in age of onset, rate of growth, state of cell differentiation, invasiveness, metastatic potential, response to treatment and prognosis. However, in terms of molecular biology, cancer may represent diseases caused by a similar molecular defect in cell function and similar alterations in the cell's genes. Carcinogenesis is a multistep process which leads ultimately to a disease of abnormal gene expression. Cancer cells have the following general properties: They proliferate in a deregulated manner and have limitless replicative potential. Cancer cells are insensitive to anti-growth signals and evade apoptosis. They invade surrounding tissues, probably through secretion of certain proteolytic enzymes. They metastasise to secondary sites throughout the body. Cancer cells also show

alterations of cell surface components such as antigens and enzymes. Cancers growing in the body occupy space and crowd out normal cells, sustaining themselves by angiogenesis. They can invade through tissues and cause haemorrhage and infection. Cancer cells also decrease host defence mechanisms against infection. In general, there are few unique or specific biochemical and biological differences between normal and cancer cells (Ruddon 1995).

Cancer chemotherapy is the use of anti-cancer drugs to eliminate cancer cells or alter their neoplastic phenotype. The challenge of cytotoxic chemotherapy is to maximize the killing of neoplastic cells while minimizing the damage to most or all other host cells. Most cytotoxic anti-cancer drugs interfere with the ability of cells to divide and reproduce. In general such drugs cannot distinguish between normal and malignant cells. Therefore cytotoxic anti-cancer drugs attack not only dividing cancer cells but also normal cells, which are actively dividing, such as the bone marrow, the hair follicles, and the digestive system. In addition to their shared activity against replicating tissues, individual cytotoxic agents have their own specific toxicity profile which can be severe or potentially lethal. In addition, anti-cancer drugs are often used clinically at or near the maximum tolerated dose and frequently cause unwanted side effects.

Many anti-cancer drugs exert their cytotoxic effect by inhibiting cell replication in a variety of ways. Alkylating agents such as cisplatin and cyclophosphamide alkylate nucleotide residues of DNA and cause cross-linking of DNA that interferes with its replication. Alkylating agents can also form covalent links with RNA and protein. Antimetabolites such as methotrexate and fluorouracil inhibit enzymes such as dihydrofolate reductase and thymidylate synthase which are essential for purine and pyrimidine synthesis and therefore RNA and DNA synthesis. Agents such as vincristine and taxanes interfere with polymerisation or depolymerisation of cell microtubules. Actinomycin D is an example of drug which acts via intercalation of DNA which inhibits RNA and DNA synthesis. Other mechanism of action include induction of apoptosis and disruption of a variety of signal transduction pathways (King, 2000; Priestman, 1989).

The history of the development of novel anti-cancer drugs is crowded with molecules which, in spite of impressive antineoplastic activity in preclinical models, struggled or failed to reach the stage of routine clinical application because of severe host toxicity. Paclitaxel provides an instructive example. Whilst the structural elucidation of the cytotoxic molecule in extracts of the bark of the pacific yew tree goes back to 1971(Wani et al., 1971), the commencement of its clinical development was delayed until the mid-1980s due mainly to toxicity problems. Toxicities included hypersensitivity which proved fatal in at least one case. Despite such detrimental side effects, research and development of this compound was pursued and investigators found that the toxicity could be minimised by pre-treatment with glucocorticoids and antihistamines. Currently there are over 500 molecules in clinical development by 43 pharmaceutical companies (Pitot and Loeb, 2002). The National Cancer Institute estimates that fewer than 1 in 15, 000 drugs reach the final stage of development.

1.3 Drug induced liver disease

Drug induced liver disease is a multifaceted phenomenon. It may occur in response to a toxic metabolite, unique to the injured individual after a therapeutic dose of a drug (idiosyncratic reaction) or as a consequence of the intrinsic toxicity of an agent taken in a sufficiently large dose to cause liver damage (Zimmerman, 1993). Drug induced liver damage includes all known hepatic lesions, both chronic and acute. Acute liver injury can be cytotoxic, characterised by overt damage to hepatocytes, or cholestatic, manifested by damage to the biliary system with decreased bile flow and jaundice. Some agents lead to a mixed type, with simultaneous features of cytotoxic and cholestatic injury. Cytotoxic injury includes necrosis, steatosis, both, or only degeneration.

Novel pharmaceutical agents which are found to cause hepatic necrosis at a modest dose level by a direct mechanism in preclinical toxicity studies are not usually developed in man. Hepatic necrosis can occur following treatment with a high doses of therapeutic agents as a result of an indirect mechanism. Necrosis may be zonal (centrilobular, mid-zonal or periportal), or focal or affect individual hepatocytes (Zimmerman and Ishak, 1995). Centrilobular necrosis is particularly liable to occur following administration of drugs or chemicals. As centrilobular hepatocytes are well endowed with drug metabolising enzymes, reactive metabolites are liable to be formed in the centrilobular zones and damage tissue by covalent binding directly with vital organelles. The centrilobular zones are also vulnerable to ischaemic damage by virtue of the vascular supply within the liver and the oxygen gradient (Greaves, 2000). Periportal necrosis is seen in periportal zones following treatment with agents such as α -naphthylisothiocyanate and allyl alcohol, which damage the bile ducts or periportal hepatocytes, or following bile duct ligation which increases intrahepatic bile levels (Greaves, 2000; Kountouras et al., 1984). Hepatic necrosis leads to hepatocellular jaundice. The syndrome and biochemical values resemble those of viral hepatitis. Aminotransferase levels are elevated 8- to 500- fold and alkaline phosphatase (ALP) levels usually less than three-fold (Zimmerman and Ishak, 1995). The most important aspect of drug induced cytotoxic injury is its tendency to progress to liver failure.

A large number of agents can produce fatty acid change. The microscopic appearance of fatty change is broadly of two main types. Macrovascular, characterised by large single vacuoles within each cell, which displaces the nucleus to the periphery, is the most common form. It is a relatively benign change associated with a variety of nutritional or metabolic alterations. It has been suggested that most agents that lead to the development of steatosis do so by interfering with the process of removal of lipid from the cell rather than increased entry of lipid into the cell (Zimmerman, 1978). Microvesicular steatosis comprises fine, lipid containing vacuoles, often giving a foamy appearance. This type of steatosis is associated with fatty liver in pregnancy and Reye's syndrome (Belay et al., 1999; Bernuau et al., 1986). Microvesicular steatitis has been reported after administration of tetracycline and valproic acid (Fromenty and Pessayre, 1997). Jaundice is usually relatively slight, and aminotransferase levels are usually not as high as those in hepatic necrosis. Although the precise mechanisms that cause these conditions are not fully understood, it appears that the mitochondrion is a likely target, through inhibition of β -oxidation or impairment of mitochondrial function.

Cholestasis is defined as the decreased flow of bile resulting from suppressed secretion or anatomical blockade of the biliary tree. Inflammation or blockage of the bile duct results in retention of bile salts as well as bilirubin accumulation, an event which leads to jaundice. Cholestasis is accompanied by little or no overt injury to the hepatic parenchyma. Zimmerman and Lewis reported six types of drug induced cholestasis (Zimmerman and Lewis, 1987). Three types of cholestasis may be attributed to injury to the hepatocytes: hepatocanalicular cholestasis, canalicular cholestasis and hepatocellular cholestasis and three types due to lesions of the biliary tree: ductal cholestasis, ductular cholestasis and dissociated cholestasis. All have elevated levels of conjugated bilirubin. The degree of elevated bilirubin, alkaline phosphatase, cholesterol and aminotransferase and the prominence of histological markers of parenchymal hepatic injury provide some distinction between the disease types.

1.4 Bile flow

Bile is formed by several energy-dependent transport processes. Bile consists of two components: canalicular and ductular. The passage of bile acids into the biliary canaliculus is the most important factor promoting bile formation (Boyer, 1980). This is known as bile acid-dependent bile flow. A fraction of bile flow is independent of bile acid secretion which is called bile acid-independent bile flow (Erlinger, 1981).

The hepatocyte is a polarised secretory epithelial cell. Most endogenous and exogenous substances secreted in the bile are taken up by the hepatocytes through the sinusoidal (basolateral) membrane, transported through the hepatocyte and excreted across the canalicular membrane. Tight junctions between hepatocytes seal the biliary space from the blood and delimit the canaliculus. The actin containing microfilaments of the cytoskeleton are important in the maintenance of the integrity and orientation of the surface membranes and junctional complexes of the canaliculus.

The secretory process depends on a coordinated action of a number of transporter proteins in the sinusoidal and canalicular domains of the hepatocyte (see figure 1.1). During recent years, many of these proteins have been identified and cloned, and their function has been characterised (Erlinger, 1996; Muller and Jansen, 1997). The sinusoidal membrane contains a $\text{Na}^+\text{-K}^+$ ATPase which maintains a chemical gradient and potential difference between the hepatocyte and its surroundings. The multispecific 'organic anion transporting polypeptide' (OATP) transports organic anions and amphiphilic compounds including organic cations. The 'Na⁺-bile acid co-transporting protein' (NTCP) mediates the uptake of bile acids, probably accounting for the major part of conjugated bile acid uptake.

Transport of bile across the cell involves cytosolic proteins. The major protein is 3- α -hydroxysteroid dehydrogenase, while glutathione-S-transferase and fatty acid binding proteins are less important. The endoplasmic reticulum and Golgi apparatus are implicated in the transfer of bile acid.

The canalicular membrane contains transporters responsible for transporting substances into the bile against steep concentration gradients. Several ATP-dependent transport processes have been identified which are mediated by an ATP-binding cassette (ABC) superfamily of proteins (see figure 1.1). Two members of the ABC family are important for canalicular transport. ABCB1 is a transporter of organic cations, and is also responsible for multidrug resistance, hence its name, MDR1 (Arias, 1990). ABCB4 is a phospholipid translocator that acts as a flippase for phosphatidylcholine, and is important in the secretion of phospholipid into bile. The canalicular membrane also contains a 'canalicular multispecific organic transporter' (cMOAT) which carries glucuronide and glutathione-S-conjugates and a 'canalicular bile acid transporter' (cBAT), which carries bile acids. It also contains enzymes such as alkaline phosphatase and gamma glutamyl transpeptidase. Water and inorganic ions enter canalicular bile by diffusion across tight junctions, via an osmotic gradient.

Bile acid independent bile flow results from the secretion of non bile acid organic ions and glutathione into bile. It is dependent on bicarbonate uptake, which in turn is dependent on active proton transport, or facilitated by a bicarbonate chloride exchanger. The ductular components of bile consist of the fluid and electrolytes which are added during the passage of bile along the bile ductules and duct (Reichen and Simon, 1984). Ductular cells secrete bicarbonate rich fluid. This secretion is under hormonal control. Secretin stimulates the 'cystic fibrosis transmembrane conductance regulator' (CFTR)-associated chloride channel and a chloride-bicarbonate exchanger by a cAMP-dependent mechanism.

Disruption of the well-coordinated transport process can lead to the retention of substrates with resulting cholestasis. Cholestasis represents impairment in the excretion of bile that results in the retention of biliary constituents both in the liver and the blood. Drug induced cholestatic injury can be produced by the compound itself, by a drug metabolite, by a metabolic idiosyncrasy or by an immunological idiosyncrasy. Cholestasis may follow disturbance of the anatomical structures involved in bile duct formation and flow as a result of damage to the canalicular membrane itself, the microfibrillar network, microtubules and microvesicles, tight junctions around canaliculi, bile ducts or bile ductules (Erlinger, 1985;

Reichen and Simon, 1984; Tuchweber et al., 1986). Functional alterations may also be important; impaired formation of canalicular bile can result from decreased uptake of bile acids and other key constituents from sinusoidal blood, deficient transport into the canaliculus and impaired propulsive action of the canalicular network. Other factors such as electrolyte balance and bile viscosity also influence bile flow independently of bile acids.

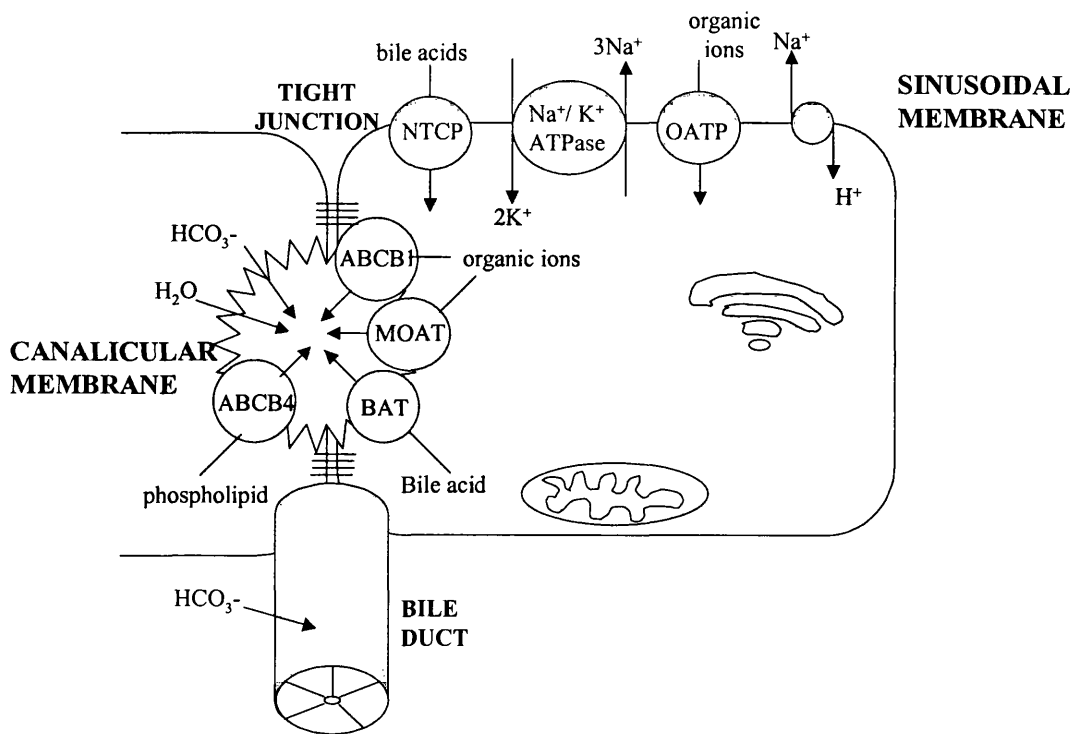


Figure 1.1 Major transport systems in bile formation. The sinusoidal transporters are the Na⁺-K⁺ATPase, the Na⁺ taurocholate co-transporting protein (NCTP), the multispecific organic anion transporter (OATP) and the Na⁺-H⁺ exchanger. The canalicular membrane transporters are the ATP dependent bile acid transporter (BAT), the multispecific organic anion transporter (MOAT), the ATP-dependent transporter of organic cations (ABCB1) and the ATP-dependent phospholipid (ABCB4). Adapted from Zimmerman and Lewis, 1987.

1.5 Phase I and II drug metabolism

Most drugs and toxins absorbed by the gastrointestinal tract are lipophilic, which facilitates their uptake into cellular membranes of the enterocytes. Conversely, to prevent uptake into other cells and to promote elimination from the body requires chemical modification to increase the water solubility of foreign compounds. These biotransformation reactions are of two types, phase I and phase II. In phase I reactions, polar groups are introduced into the molecule by oxidation, reduction or hydrolysis (Watkins, 1990). This type of reaction is most commonly mediated by cytochrome-P450 enzymes (CYP). In phase II reactions, the molecule is conjugated to a water soluble ligand, such as glucuronic acid, sulfate, glycine or glutathione.

The majority of CYP is located in the endoplasmic reticulum and is anchored on the cytoplasmic side of the membrane. There is a haem binding sequence that contains a conserved cysteine moiety, a substrate binding site in close proximity to the heme group, and a poorly characterised site that interacts with NADPH: cytochrome P-450 reductase. Electrons are taken from NADPH to reduce oxygen and oxidize or hydroxylate nitrogen and carbon. CYP selectivity for substrates is determined by both the chemical reactivity of the substrate and the three dimensional structure of the substrate binding site. CYPs have overlapping substrate specificity that catalyse a variety of oxidation and reduction reactions including carbon hydroxylation and the dealkylation of substituted heteroatoms such as N, O, and S (Black and Coon, 1987).

Over the last 20 years a variety of different names have been used for the hundreds of different forms of CYP that have been isolated in different laboratories. Based on sequence similarity CYPs are now grouped into families termed CYP1, CYP2, CYP3 etc and subfamilies designated by a capital letter CYP1A, CYP1B etc. Arabic numbers are used to identify the individual letters with subfamilies. CYPs within the same family share a primary sequence homology of at least 59 % whereas CYPs within the same subfamily should be at least 70 % similar (Gonzalez, 1988).

CYPs can be placed in two categories. CYP4 and higher members are generally involved in the metabolism of endogenous compounds. These CYP families are often highly specific for their substrate, non-inducible by exogenous compounds and are well conserved through evolution. These enzymes play a role in steroidogenesis, synthesis of cholesterol and bile acids, and hydroxylation of fatty acids and prostaglandins. The second category consists of CYPs 1-3, which metabolise exogenous compounds and show overlapping substrate specificity. They are often inducible by exogenous compounds and have been poorly conserved through evolution.

Phase II reactions involve the conjugation of chemicals with hydrophilic moieties such as glutathione, glucuronic acid, sulfate or amino acids. These reactions are usually considered detoxification pathways because they result in the formation of a more water soluble and easily excreted species. Glucuronidation can occur directly with the parent compound or with a metabolite formed by a phase I reaction. Glucuronic acid can be conjugated with alcohols, carboxylic acids, thiols and acids to form an ether, ester, thiol or amide glucuronide. UDP-glucuronyl transferases (UGT) are a family of enzymes which catalyse the conjugation of glucuronic acid with both endogenous and exogenous substrates. Over 35 different UGT gene products have been described from several different species. UGTs have been divided into two distinct subfamilies based on sequence identities, UGT1 and UGT2. Substrates for the UGT1 subfamily include bilirubin, amines, and phenols. The UGT2 subfamily consists of numerous enzymes which catalyze the glucuronidation of a diverse chemical base including steroids, bile acids, and opioids (King et al., 2000).

Sulfation has evolved as a key step in xenobiotic metabolism, and it also plays a critical role in steroid biosynthesis and in modulating the biological activity and facilitating the inactivation and elimination of potent endogenous chemicals including hormones and steroids. These reactions involve the transfer of a sulfate group from 3'-phosphoadenosine 5'-phosphosulfate (PAPS) to the hydroxyl/amino groups of acceptor molecules. Sulfation is catalysed by a category of enzymes known as sulfotransferases. In mammals, two classes of sulfotransferase have been distinguished. One class metabolises macromolecular endogenous structures and

comprises mainly membrane-bound forms localized in the Golgi apparatus. The other class of enzymes is cytosolic and metabolises xenobiotics and small endogenous compounds (Glatt, 2000).

Glutathione (GSH) detoxifies electrophiles and oxidants and is therefore extremely important in the prevention of hepatotoxicity. The reactions catalysed by glutathione S-transferases (GST) may be substitutions, additions or reductions. In substitution and addition reactions, GSH is conjugated with an electrophilic substrate either by displacing a leaving group or by binding to the electrophilic site. For reduction reactions, the enzyme can function as a peroxidase with reduction of organic hydroperoxides and oxidation of GSH to GSSG. Another role for GSH is reduction of oxidants catalysed by GSH peroxidase. In these reactions, the oxidant is reduced and GSH is oxidised to GSSG. The GSSG can be reduced back to GSH at the expense of one molecule of NADPH (Kretzschmar, 1996).

GSH is a tripeptide consisting of glutamine, cysteine and glycine. GSH is synthesised in cytoplasm from the three constitutive amino acids in two enzymatic steps involving ATP. The first enzymatic step, catalysed by γ -glutamylcysteine synthetase, is rate limiting and controlled by negative feedback. The other rate limiting factor is the availability of cysteine. Circulating cysteine in the plasma is low because it auto-oxidizes to cystine. In a process unique to the hepatocytes and the ocular lens, cells use methionine and serine to synthesis cysteine. Cells which can transport cystine may reduce it intracellularly and release cysteine into plasma. Other cells use cysteine broken down from GSH (DeLeve and Kaplowitz, 1991). The most widely used cysteine prodrug is N-acetylcysteine, which is used to treat paracetamol overdosing (Lyons et al., 1977).

The liver has the highest concentration of GSH, approximately 5-10 mM, and supplies nearly all the GSH in the plasma. There are two GSH transporters, one located on the canalicular membrane and the other on the sinusoidal pole of the hepatocyte. The latter is responsible for the efflux of GSH from the liver into the blood (Yi et al., 1995). On a subcellular level, 90 % of GSH is in the cytosol and the remainder in the mitochondria. Mitochondrial GSH is a

particularly important pool of GSH. About 2-5 % of oxygen that passes through the respiratory chain escapes as oxygen radicals which are converted to hydrogen peroxide. Mitochondrial GSH is the main antioxidant that reduces hydrogen peroxide, preventing lipid peroxidation. Therefore, under physiological conditions mitochondrial GSH protects cells against endogenous oxidative stress. Pathological conditions that reduce mitochondrial GSH can be lethal to the cell. It has been shown that in paracetamol poisoning, depletion of mitochondrial GSH, rather than cytosolic GSH is the key event is rendering the mitochondria susceptible to toxic alkylation by N-acetyl-*p*-benzoquinone imine (NAPQI) or oxidant stress from hydrogen peroxide (DeLeve and Kaplowitz, 1995).

GST consists of a family of enzymes with broad, overlapping substrate specificities. There are four human cytoplasmic GST forms: alpha, mu, pi and theta and two microsomal forms: mGST and LTC₄ synthase (Armstrong, 1994; Awasthi et al., 1994). Table 1.1 provides information about the different classes of GST. GSTs are usually composed of 2 subunits, with an active site on each subunit (Danielson and Mannervik, 1985). The active site has a highly specific binding site for GSH adjacent to a partly hydrophobic binding site for the electrophilic substrate. The major functions of the GSTs are catalysis of GSH conjugation of electrophiles, peroxidation of lipid hydroperoxides and intracellular transport.

Class	Tissue expression	Substrates
Alpha	Liver , skin	Organic hydroperoxides
Mu	Liver, muscle, brain	Epoxides
Pi	Placanta, intestine, bile duct, tumours	
Theta	Liver, erythrocyte	Dichloromethane
mGST	Liver, small intestine, adrenal, testes	Polyhalogenated hydrocarbons, lipid hydroperoxides

Table 1.1 Glutathione S-Transferases (from DeLeve and Kaplowitz, 1991)

The process of biotransformation is intimately involved in chemically induced hepatotoxicity. Metabolism can modulate the properties of hepatotoxic agents in two general ways depending on whether the parent compound or its metabolite are the ultimate hepatotoxicant. Metabolism can either increase toxicity or decrease toxicity. The toxic potential of a hepatotoxic compound depends on the relative rates of toxification and detoxification. Enzyme induction can lead to metabolic activation or detoxification of toxic agents. A CYP inducer may increase the amount of toxic metabolite formed, for example alcohol induction of CYP2E1 may increase formation of the toxic product, NAPQI, from paracetamol. Conversely, inhibition of CYP, responsible for the inactivation of a parent compound, can lead to the toxic accumulation of the compound.

1.5.1 Mechanisms of induction and inhibition of cytochrome P450

The mechanisms of induction differ for the different CYPs. Induction can result either from increased production of enzymes, through increased transcription or translation, or a reduction in rate of enzyme breakdown. Well characterised is the induction of CYP1A1 and 1A2 by polycyclic aromatic hydrocarbons. The inducer interacts with a cytosolic protein, the aryl hydrocarbon (Ah) receptor, which then undergoes translocation to the nucleus. In the nucleus, the complex binds to a DNA regulatory sequence termed the xenobiotic responsive element (XRE), leading to transcriptional activation of the CYP1A gene. The regulation of expression of the gene is complex, involving multiple negative and positive control sequences with which the inducer can interact (Nebert and Jones, 1989). There is evidence that the mechanism involved are very similar between species, such as the rat, mouse, rabbit and human.

Another CYP inducer which should be mentioned as it is investigated in this project is indole-3-carbinol (I3C). I3C has been shown to inhibit chemically induced tumourigenesis in a number of models and is being investigated by the NCI as a potential chemopreventive against breast cancer (Stoner et al., 2002; Wong et al., 1997). The postulated mechanism for the blocking effects of I3C administered before a carcinogen is through the ability of I3C to

induce phase I and II metabolism resulting in increased capacity for detoxification of carcinogens (Manson et al., 2000). I3C is unstable in acidic conditions and is converted into several condensation products. I3C induce phase I and II enzymes but it is not clear which of the condensation products are acting as a ligand for the Ah receptor (Bjeldanes et al., 1991; Vang et al., 1999).

The influence of I3C on the metabolism of the carcinogen aflatoxin B₁ was examined. I3C was found to preferentially induce CYP1A, 1A2, 3A and 2B1/2 (Stresser et al., 1994). This resulted in a significant increase in the formation of aflatoxin B₁-epoxide, aflatoxin Q₁ and aflatoxin M₁ (Manson et al., 1997). I3C also induced a number of phase II enzymes, in particular GST A5, which is very effective at conjugating the AFB₁-epoxide to glutathione (Hayes et al., 1991). In addition, I3C has been shown to suppress spontaneous carcinogenesis at estrogen-susceptible sites such as mammary gland and endometrium. Estradiol is normally metabolised to 16 α -hydroxyestrone, 2-hydroxyestrone and to a lesser extent 4-hydroxyestrone. 16 α -hydroxyestrone is thought to be tumorigenic and is elevated in breast cancer whilst 2-hydroxyestrone is reported to have anti-estrogenic effects (Schneider et al., 1982). It has been shown that I3C induces CYP activity, increasing 2-hydroxylation of oestrogens, leading to increased 2-hydroxyestrone and decreasing 16 α -hydroxylation leading to 16 α -hydroxyestrone.

Phenobarbitone induces expression of CYP2B1 and CYP2B2 and, to a lesser extent CYP2A1, CYP2C6, CYP3A1 and CYP3A2. It also increases the quantity of endoplasmic reticulum in hepatocytes, increases total microsomal protein, and increases NADPH: cytochrome P450 reductase as well as phase II metabolising enzymes. Its induction of the CYPs occurs at the transcriptional level, but the molecular mechanism by which phenobarbitone induces gene expression remains unknown; no receptors for phenobarbitone have been found. However, in the last five years, PB-responsive sequences have been identified in the 5' flanking regions of several CYP genes (Kemper, 1998). The phenobarbital-responsive enhancer unit (PBRU) of CYP2B gene family members contain two potential nuclear receptor binding sites (NR1 and NR2) and a nuclear factor 1 (NF-1) binding motif (Honkakoski and Negishi, 1998; Honkakoski et al., 1998; Sueyoshi et al., 1999). The nuclear factors that regulate PBRU

activity have not yet been identified. Responding to phenobarbitone, the constitutive androstane receptor (CAR), translocates to the nucleus, forms a heterodimer with the retinoid receptor (RXR) and activates the PBRU via binding to NR1 and NR2. It is possible that the pleiotropic effects of phenobarbitone can be explained by the ability of the CAR-RXR heterodimer to bind to a variety of nuclear receptor binding motifs.

Expression of CYP3A is markedly induced *in vivo* in the liver and *in vitro* in cultured hepatocytes in response to a variety of xenobiotics and drugs, including glucocorticoids such as dexamethasone and antibiotics such as rifampicin. Two nuclear receptors, pregnane X receptor (PXR) and CAR have been proposed to mediate CYP3A4 gene induction, as these receptors bind to, and transactivate, DNA nuclear response elements located in the promoter of the gene *in vitro*. Both CAR and PXR form heterodimers with RXR which bind to, and transactivate, DNA response elements located in the proximal and distal CYP3A4 regulatory region. The mechanism by which dexamethasone and glucocorticoids induce CYP3A4 is still unclear. Dexamethasone is an efficacious inducer in rodents and humans, but seems to be a relatively weak activator of mouse PXR (Pascussi et al., 2001). Several observations suggest that the glucocorticoid receptor plays an important part in the expression and xenobiotic-mediated inducibility of CYP3A4. There is a functional glucocorticoid response element (GRE) in the rat CYP3A23 (Pereira et al., 1998), while the human CYP3A5 promoter gene contains two GRE sites (Schuetz et al., 1996). Transcriptional activation of CYP3A4 by dexamethasone is partially inhibited by the anti-glucocorticoid, mifepristone (RU486) (Quattrochi et al., 1998). Conversely, studies in glucocorticoid receptor (GR)-null mouse model suggest that GR has no effect on CYP3A induction by PXR activators (Schuetz et al., 2000). Recent studies by Pascussi et al suggest that dexamethasone induces CYP3A4 via a two step mechanism (Pascussi et al., 2001). At low (submicromolar) concentrations activation of the glucocorticoid receptor positively controls the expression of PXR and CAR which in turn activates CYP3A4 transcription in a ligand-dependent manner. At high (supramicromolar) concentration dexamethasone binds to and activates PXR which induces CYP3A4 transcription.

Class of Inducer	Examples	Induced P450
Polycyclic hydrocarbon type	3-methylcholanthrene TCDD β -naphthoflavone Chlorpromazine Benzo(a)pyrene	CYP1A1, CYP1A2
Phenobarbital type	Phenobarbitone Phenytoin Griseofulvin	CYP2A1, CYP2B1, CYP2B2 CYP2C6, CYP3A2
Ethanol	Ethanol Acetone, Heptane	CYP2E1
Glucocorticoid	Dexamethasone, pregnenolone-16 α -carbonitrile Prednisolone Rifampicin	CYP3A1, CYP3A2, CYP3A4
Clofibrate	Clofibrate	CYP4A1

Table 1.2 Inducers of CYP enzymes.

Various drugs inhibit the activities of CYPs. Inhibition can occur as a result of different mechanisms, reversible, irreversible or by alteration of the synthesis or degradation of CYP. Reversible or competitive inhibition occurs due to simple interaction with the substrate binding site of the CYP. Reversible inhibitors can act directly such as carbon monoxide, alcohols and imidazole derivatives, or act indirectly such as aromatic amines and hydrazines. Indirect inhibitors act through metabolic intermediates forming complexes with CYP. Irreversible or non-competitive inhibitors bind covalently at an allosteric site, not the substrate binding site, and include compounds that act directly with CYP and those that undergo metabolic activation to form reactive intermediates. Irreversible inhibitors generate stable complexes with the enzyme so that the cytochrome is sequestered in a functionally inactive state, or the metabolite may inactivate the enzyme via haem or apoprotein modifications.

Metals ions such as cobalt, cadmium, nickel and copper inhibit CYP by inhibition of its biosynthesis. Haem oxygenase, an enzymes which oxidises CYP to biliverdin, and may increase the conversion of cytochrome P450 to cytochrome P420, is an example of inhibition by degradation of CYP (Testa and Jenner, 1981).

1.5.2 Species differences in metabolism

Significant differences exist between humans and rodents with respect to the metabolism of xenobiotics. The difference can be divided broadly into three categories, occurrence of the isoenzyme, substrate specificity and rate of metabolism.

The CYP superfamily can display very significant species, strain and gender differences in expression and catalytic activity. The classic example of this difference is the sexual dimorphism observed for the metabolism of compounds by rats that is not observed in any other species. In addition species specific CYPs have evolved through the process of gene duplication and the fixation of duplicated genes through natural selection. An example of this is the species variation in the CYP2E subfamily. Rabbits, rats and humans diverged about 75 million years ago. The CYP2E subfamily in rats and humans contains a single gene, however, two highly similar 2E genes are present in rabbits. Another example is the species difference in the CYP2D family. In the rat there are four CYP2D genes with 73 to 95 % amino acid similarity, whereas in the human there are three genes with 89 to 95 % amino acid similarity. Based on the speciation period of rodent and human lines, about 75 million years ago, and the amino acid similarities of the rat and human CYP, it appears that four CYP2D genes existed in the ancestor to humans and rats. Subsequent to the formation of these 2 species, 3 genes were lost in humans and an additional two genes formed more recently by gene duplication. In rats, four genes were maintained and one newer gene formed (Gonzalez and Nebert, 1990).

The substrate specificity of many enzymes is similar in different species, however a few exceptions have been reported. Different CYPs in the various species may perform, with high specificity, the same metabolic function. For example, S-mephenytoin is metabolised in the rat

by a 3A subfamily, whereas in man it is metabolised by a member of the 2C family. In addition, highly structurally related CYPs in different species may have different substrate specificities. For example, 4-hydroxylation of debrisoquine is catalysed largely by CYP2D both in rat and human, however the competitive inhibitor, quinidine is a much more potent inhibitor of this activity in humans than in rats. Quinine, the stereoisomer of quinidine, is a much less potent inhibitor of debrisoquine 4-hydroxylase activity in humans, however, in the rat, the potency of the two inhibitors is reversed with quinine being more potent than quinidine. The reason for the species difference in the specificity of these inhibitors may be due to differences in the geometry of the active site of the enzyme (Boobis et al., 1990).

Species differences exist for the rate of metabolism. The rat clears drugs which are substrates for CYP2D at higher rates than humans and dogs. Another example is the faster clearance rate of S-mephenytoin in humans compared to rats. In humans, R-mephenytoin is metabolised by CYP3A4 whilst the S-enantiomer is metabolised by CYP2C, whereas in rats both the R and S form are metabolised by CYP3A4 (Yasumori et al., 1993). Therefore the interspecies differences in the rate of metabolism are a consequence of different substrate specificities.

Species differences in biotransformation are responsible for most of the known species differences in chemical hepatotoxicity. For example, hamsters and mice are sensitive to the hepatotoxic effects of paracetamol whereas rats and human require high doses to produce similar toxicities. These species differences are due to differences in the rate of production of the toxic metabolite NABQI. Another example is the sex difference in the hepatotoxicity of the pyrrolizidine alkaloid senecionine observed in rats with the male being much more sensitive than the females. Senecionine requires CYP mediated biotransformation to form the toxic metabolite that reacts with critical cellular macromolecules to produce hepatic cytotoxicity. Female rats lack the CYP3A isoform involved in the metabolism of senecionine. However, when female rats are treated with dexamethasone to induce enzymes of the CYP3A family, they become as sensitive to senecionine hepatotoxicity as male rats (Williams et al., 1989).

There are also species variations in the response of CYP to different inducers and inhibitors which lead to species differences in the metabolism of xenobiotics. One reason for species differences in the effects of inhibitors includes different active sites of the enzyme amongst species (Boobis et al., 1990). Substrates for the same enzyme will compete for the active site and inhibit each others metabolism, whereas substrates metabolised at different enzyme sites will not compete. Another reason is due to different inhibitory binding sites between species. The inhibitor interacts with an allosteric site on the protein which results in an alteration in catalytic activity of the enzyme causing a conformational change. In addition, species differences exist in the pharmacokinetics of the inhibitor. The potency of the inhibitor *in vivo* will depend not only upon the nature of the interaction with enzyme but also on the rate of elimination of the inhibitor. Species differences in the metabolism of the inhibitor will explain discrepancies in inhibitor potential.

In many cases the human CYP analogue is similarly inducible to the isoenzyme in rodents. Examples are the CYP1A subfamily, CYP2E and CYP3A. Species differences in induction can be due to differences in the mechanism of induction. The mechanism of CYP1A induction is very similar amongst species such as rat, rabbit, mouse and human. Nevertheless there are important differences in effectiveness of inducer-receptor coupling. Some strains of mouse are resistant to the inducing effects of polycyclic aromatic hydrocarbons. Species differences may also be due to alterations in competing pathways and differences in the pharmacokinetics of the inducer. As for inhibitors, the extent of induction will depend on the concentration of the inducing agent at the site of action (Boobis et al., 1990).

1.6 Mechanisms of hepatotoxicity

Hepatotoxicity is often the result of inadequate detoxification, or of an imbalance between phase I reactions that produce reactive molecules and phase II reactions which detoxify them. This is not always the case as both phase I and II reactions can function as activating or detoxification reactions. Some compounds are toxic without any metabolism. Toxicants such as chlorpromazine and other phenothiazines can have direct surfactant effects on the hepatocyte membrane (Seeman, 1972). These effects ultimately disrupt cellular volume homeostasis and lead to cell death. The mushroom poison phalloidin binds to actin and disrupts the cell cytoskeleton, resulting in increased plasma membrane permeability (Govindan et al., 1972). Various chemicals and metal ions bind to mitochondrial membranes and enzymes, disrupting energy metabolism and cellular respiration. The majority of compounds with hepatotoxic properties require metabolic activation to exert toxicity, and CYP mediated activation is a common pathway. This pathway forms electrophiles or free radicals by oxidative metabolism (Kedderis, 1996). The unstable intermediates react with crucial cellular macromolecules that can donate electrons. Free radicals can lead to peroxidative injury of membrane lipids and subsequent membrane perturbation, leading to necrosis. An example is carbon tetrachloride. Electrophiles bind covalently to nucleic acids, proteins, or other nucleophilic species, disturbing critical cellular function and eliciting cell death.

Glutathione is quantitatively the major soluble cellular nucleophile, and it provides an efficient detoxification pathway for electrophilic reactive metabolites. Thus, glutathione depletion renders cells more susceptible to the toxic effects of chemicals. Paracetamol is an example of a drug metabolised to a toxic free radical, NAPQI that reacts with protein thiols when GSH is depleted (figure 1.2).

In addition to covalent binding and depletion of glutathione, reactive intermediates can initiate redox cycling and lipid peroxidation. Compounds such as quinone, may undergo reversible one electron transfer catalysed by a reducing enzyme such as NADPH: cytochrome P450-reductase. In the presence of molecular oxygen, such chemicals can donate a single electron to

oxygen and the chemical itself ultimately reverts to the original form. The oxygen free radical formed, superoxide, is converted to hydrogen peroxide (H_2O_2) by superoxide dismutase. In the presence of iron, H_2O_2 is converted by the Fenton reaction to a highly reactive hydroxyl radical which is presumed to be the ultimate toxic metabolite generated from this pathway. The hydroxyl radical may oxidize protein thiols or membrane lipids to cause peroxidation (Kedderis, 1996). Lipid peroxidation is thought to be an important mechanism for the cytotoxicity of some agents (Tribble et al., 1987).

Disruption of calcium homeostasis is a common feature of chemical hepatotoxicity. Calcium is kept within a narrow range in the cytosol by calcium pumps (Ca^{2+} -ATPase) that store calcium in the endoplasmic reticulum and that maintain the 1000-fold gradient between the intracellular and extracellular compartment. Reactive metabolites may damage these pumps by covalent binding or protein thiol oxidation. Alternatively, lipid peroxidation may disrupt normal membrane function and disturb calcium homeostasis. Elevated intracellular calcium levels disrupt the cytoskeleton, leading to blebbing, and activates degradative enzymes in the cytosol (Nicotera et al., 1986). Activated Ca^{2+} -dependent proteases can degrade enzymes and structural proteins, Ca^{2+} -dependent phospholipases can digest membranes and release arachidonate, and Ca^{2+} -dependent endonuclease can fragment DNA (Nicotera et al., 1990; Nicotera et al., 1986). Furthermore, elevated intracellular calcium levels may impair mitochondrial function, which may lead to cell death (Meyers et al., 1988). Elevation of cytosolic calcium has been implicated in the course of events leading to cell death for compounds, such as paracetamol, diquat and carbon tetrachloride.

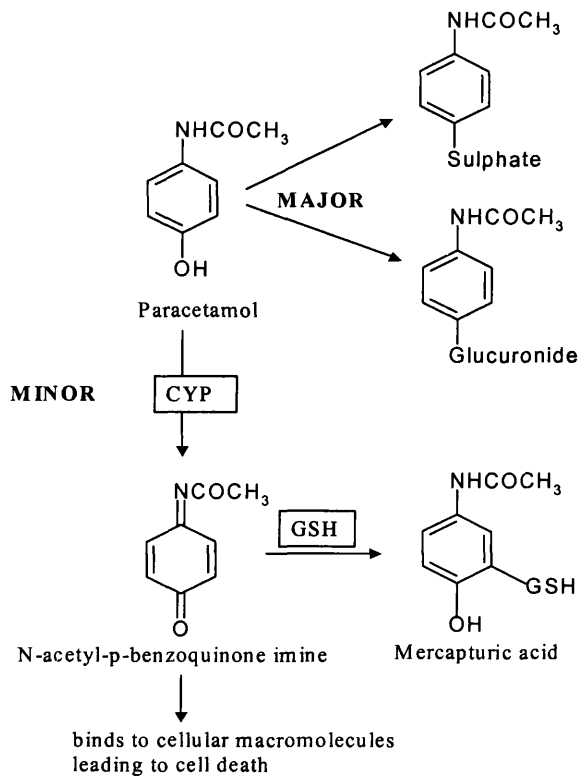


Figure 1.2 Metabolism of paracetamol. Paracetamol is extensively metabolised by sulphation and glucuronidation. A small amount is metabolised by CYPs to form a toxic metabolite, N-acetyl-p-benzoquinone imine. With normal therapeutic doses of paracetamol, this metabolite is quickly metabolised to a non-toxic derivative by glutathione and is excreted in the urine. With high doses of paracetamol glutathione becomes depleted and the toxic metabolite interacts with proteins leading to cell damage. Adapted from Zimmerman, 1993.

1.7 Mechanism of α -naphthylisothiocyanate (ANIT) hepatotoxicity

ANIT has attracted attention because it produces cholestasis and hepatic lesions in rats which mimic biliary cirrhosis in humans (Plaa and Priestly, 1976). Animal models of ANIT hepatotoxicity may be useful for studying the mechanism of drug-induced cholestasis. Within 24 hours of administration, ANIT causes cholestasis with marked injury to bile duct epithelial cells accompanied by a mild injury to periportal hepatic parenchymal cells (Desmet et al., 1968; Goldfarb et al., 1962). An inflammatory response in the periportal region of the liver encompasses oedema and infiltration of inflammatory cells, especially neutrophils. Injury to the parenchymal cells is reflected by elevations in AST and alanine aminotransferase (ALT) activities. Injury to bile duct epithelial cells is reflected by an increase in plasma γ -glutamyltranspeptidase (GGT) activity, bile acids and bilirubin and decreased bile flow (Krell et al., 1982; Leonard et al., 1984).

The pronounced neutrophilic infiltration after ANIT administration led to the hypothesis that neutrophils participate in its hepatotoxicity. The neutrophil not only protects mammals from certain invading pathogens by phagocytosis and killing, but can participate in tissue injury in the host through the extracellular release of toxic oxygen metabolites, lysosomal enzymes, and metabolites of arachidonic acid. To determine whether a reduction in the numbers of blood neutrophils would alter ANIT hepatotoxicity, an antiserum to rat neutrophil was injected before administration of ANIT (Dahm and Roth, 1991). The reduction in blood neutrophil numbers was associated with protection against ANIT hepatotoxicity, as reflected in less pronounced changes in several plasma markers as well as a reduction in histopathologic change. Accompanying studies *in vitro* revealed that ANIT was capable of stimulating neutrophils to release reactive oxygen species and lysosomal enzymes (Roth and Hewett, 1990). When hepatocytes were co-cultured with neutrophils activated by phorbol myristate acetate (PMA), hepatocytes developed blebs and released ALT into the medium indicating hepatic parenchymal cell damage (Ganey et al., 1994).

Other studies have suggested that glutathione plays a role in ANIT hepatotoxicity (figure 1.3). Unlike many other hepatotoxicants, ANIT hepatotoxicity is not associated with a decrease in liver glutathione and hepatic glutathione increases as cholestasis develops (Dahm et al., 1991). Interestingly when animals were pretreated with an inhibitor of glutathione biosynthesis, buthionine sulfoximine, the resultant decrease in hepatic glutathione concentration was associated with protection from hepatotoxicity (Dahm and Roth, 1991). Pre-treatment of animals with other agents that deplete liver glutathione by different mechanisms also afforded protection. These studies indicate that glutathione participates in ANIT-induced liver damage.

Evidence has accumulated during the last several years to suggest that glutathione's critical role involves formation of an S-conjugate with ANIT. Initial evidence came from studies in isolated hepatocytes in which incubation with ANIT resulted in an enhanced rate of efflux of glutathione from these cells. Carpenter-Deyo et al discovered the formation of an unstable glutathionyl conjugate formed in hepatocytes which dissociates to release the original reactants (Carpenter-Deyo et al., 1991). This led to the hypothesis that a glutathione conjugate formed in hepatocytes is exported into bile, where it dissociates to free ANIT and GSH, thereby exposing bile duct epithelial cells to high concentrations of ANIT, resulting in further injury to these cells (Dahm and Roth, 1991). Support for this includes the finding that ANIT administration in rats leads to increased concentration of both reduced GSH and ANIT in bile (Jean et al., 1995). Moreover, depletion of hepatic glutathione with buthionine sulfoximine prevented both the hepatotoxicity and the accumulation of ANIT in bile (Jean and Roth, 1995).

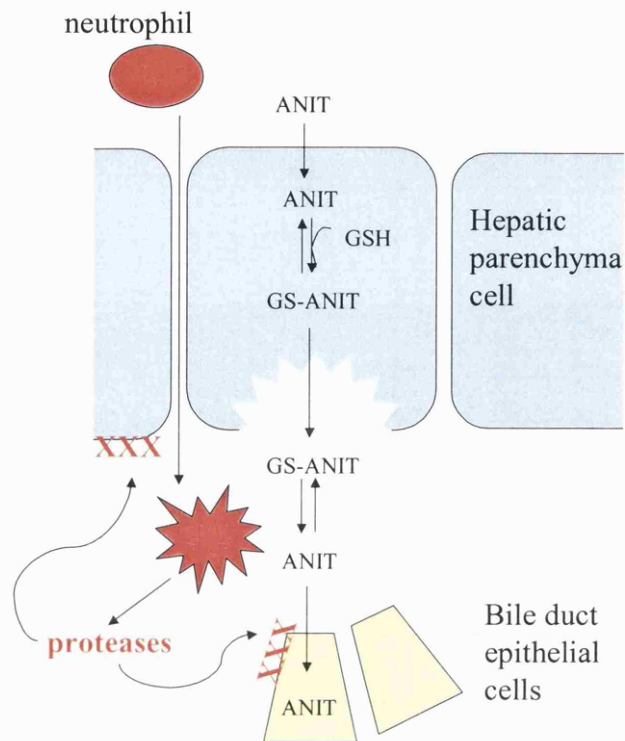


Figure 1.3 Mechanisms of ANIT hepatotoxicity. ANIT is lipid soluble and enters by passive diffusion into hepatic parenchymal cells where it forms a reversible conjugate with GSH. This conjugate is actively transported into bile, where it dissociates, exposing bile duct epithelial cells to large and possibly toxic concentrations of ANIT. Factors produced because of the resultant cellular homeostatic changes or the large concentration gradient of ANIT itself, between bile and plasma, recruits neutrophils to periportal regions of the liver. When activated these neutrophils release lysosomal proteases, which cause cell damage (indicated by **XXX**). Adapted from Roth and Dahm, 1997.

1.8 Liver disease induced by chemotherapy

The liver is a frequent target for drug toxicity because it is exposed to high concentrations of drugs. It is particularly efficient in removing xenobiotics from the blood and promoting their excretion from the body. Thus the liver is exposed to high concentrations of compounds that may be toxic either in their native form or after metabolism by the liver. Orally administered drugs usually enter the portal circulation, exposing the liver to high concentrations of the ingested drug. The liver is also exposed to high concentrations of intravenously administered drugs because it receives 25 % of the cardiac output. Therefore the concentrations seen by the liver may greatly exceed those seen by other organs, especially if first pass metabolism occurs.

The spectrum of hepatic toxicities ranges from transient elevations of transaminases to life threatening hepatic necrosis. In chemotherapy patients, there are multiple other potential causes of abnormal liver function tests that must be considered. Patients with metastatic disease may have hepatic metastases. All patients may have been exposed to hepatotoxins, including medication, alcohol and other chemicals. Patients may have other co-existing medical conditions that affect the liver, or because of their immunocompromised state, be prone to complications such as infection.

In general, alkylating agents are rarely associated with hepatic toxicity, however there are several reports linking individual alkylating agents to liver toxicities (Perry, 1992). Cyclophosphamide undergoes metabolism in the liver to produce 4-hydroxycyclophosphamide, which is in equilibrium with its acyclic tautomeric form, aldophosphamide. Non-enzymatic cleavage of aldophosphamide yields phosphoramidate mustard and acrolein which are highly cytotoxic and may represent the active form of the drug (King and Perry, 1995). Despite its requirement for hepatic metabolism for activity, there are only a few reports of elevated hepatic enzymes attributed to the drug, and this effect is likely to be due to idiosyncratic reactions rather than direct toxicity (Aubrey, 1970; Bacon and Rosenberg, 1982; Goldberg and Lidsky, 1985; Walters et al., 1972). Chlorambucil was linked to the development of liver damage in six patients from an autopsy series of 181 patients with

leukaemia or lymphoma (Amromin et al., 1962). Two patients had post necrotic cirrhosis, and a third had areas of fibrosis. All six patients had jaundice, and variable degrees of centrilobular or periportal liver degeneration and necrosis were seen. All patients in the series had abnormal liver enzyme levels. Busulfan, at standard doses, rarely causes hepatic damage, but it has been linked to at least one case of cholestatic hepatitis (Morris and Guthrie, 1988) and another of cholestatic jaundice (Underwood et al., 1971).

The nitrosoureas are commonly the cause of hepatotoxicity, perhaps because of their dual mechanism of action, acting as alkylating and carbamoylating agents (Pratt et al., 1994). Carmustine (BCNU) induces liver function abnormalities in 26 % of patients from 6 to 127 days after treatment (DeVita et al., 1965). Serum transaminases, ALP and bilirubin increases are usually mild and revert to normal within a short period, although fatalities have occurred. Lomustine (CCNU) produces similar effects (Hoogstraten et al., 1973).

The antimetabolites currently in clinical use include cytosine arabinoside (ara-C), 5-fluorouracil (5-FU), 6-mercaptopurine, azathioprine, 6-thioguanine and methotrexate. Although their mechanisms differ, individual antimetabolites are common causes of hepatotoxicity. Ara-C is currently the main treatment for acute myelogenous leukaemia and its variants. It is metabolised in three successive phosphorylation reactions to the triphosphate derivative araCTP, which inhibits DNA synthesis by inhibiting DNA polymerase and by misincorporation into the DNA molecule. In one of the first series using ara-C, abnormal liver function tests were noted in 37 of 85 patients, but many had abnormal liver function tests before treatment (Ellison et al., 1968). Because these patients are particularly prone to infections, have received many medications, and are not often candidates for liver biopsy because of thrombocytopenia, establishing ara-C as a hepatotoxicant has been difficult. In those patients in whom biopsies have been possible, drug-induced intrahepatic cholestasis has been reported (George et al., 1984; Pizzuto et al., 1983). Although 24 of 27 leukaemia patients given high-dose ara-C by continuous infusion over 72 hours developed abnormal liver tests, the effects were reversible and not dose limiting (Donehower et al., 1986). Although ara-C may be hepatotoxic, this toxicity does not appear to limit its use.

5-FU is used in the treatment of breast, head and neck cancer, and gastrointestinal cancers. When given intravenously, 5-FU is largely catabolised in the liver with 15 % of the drug excreted unchanged in the urine. Although the liver plays a key role in the metabolism of 5-FU, hepatotoxicity has only rarely been reported. Fluorodeoxyuridine, a derivative of 5-FU is given intra-arterially by an implantable pump to treat hepatic metastases from colorectal carcinoma. Two types of hepatotoxicity occur: chemical hepatitis with increases in transaminases, ALP and serum bilirubin, or stricture of the intrahepatic or extrahepatic bile ducts accompanied by increased alkaline phosphatase and bilirubin levels (Chang et al., 1987; Doria et al., 1986; Kemeny et al., 1987). Toxicity appears to be both time- and dose-dependent. With rare exceptions patients with hepatitis usually experience normalisation of liver function tests with temporary cessation of therapy, whereas the development of secondary sclerosing cholangitis is irreversible (Pettavel et al., 1986; Shepard et al., 1987). When compared to 5-FU treatment, fluorodeoxyuridine treatment offers a better anti-cancer response but at the cost of increased toxicity.

6-Mercaptopurine (6MP), a drug used for the treatment of leukaemia and to a lesser extent, immunosuppression, has been reported to produce liver toxicity. In animal experiments with rats and mice, it was noted that 6MP caused hepatic necrosis (Phillips et al., 1957). Subsequent studies in dogs and humans showed engorged bile canaliculi, suggestive of cholestasis, with minimal hepatic necrosis (Clark et al., 1960; McIlvanie and MacCarthy, 1959). Shortly after its introduction 6MP was reported to result in jaundice. 6MP induces hepatocellular damage and cholestasis, especially when the daily dose exceeds the usual 2 mg/kg (Einhorn and Davidson, 1964). The histological pattern includes features of both intrahepatic cholestasis and parenchymal cell necrosis, with either predominating (Shorey et al., 1968). Serum bilirubin levels are usually between 3 to 7 mg/dL (compared to the normal range of 0.2-1 mg/dL), with moderate increases in transaminase and alkaline phosphatase. Most episodes of jaundice occur more than 30 days after the start of therapy and are usually cleared when treatment is stopped.

Azathioprine, a derivative of 6MP used mainly as an immunosuppressant, has been reported to cause cholestatic injury. It has also been incriminated in a number of instances of hepatocellular injury (King and Perry, 1995). Hepatotoxicity was reflected by increased serum bilirubin and ALP levels with moderate increases in transaminases. The mechanism of azathiopurine-related hepatic injury is unknown. It has been speculated that patients who develop hepatotoxicity are those who convert azathiopurine to 6MP at an unusually fast rate.

The folic acid analogue methotrexate is often a component of combination chemotherapy programs for breast cancer, head and neck cancer, gestational trophoblastic disease, acute lymphoblastic leukaemia, osteosarcoma and non-Hodgkins lymphoma. It is also used to treat a variety of non-malignant diseases such as psoriasis, psoriatic arthritis and rheumatoid arthritis. Methotrexate was the first chemotherapeutic agent to be implicated in causing hepatic toxicity. Treatment of children with acute leukaemia led to the development of hepatic cirrhosis and fibrosis (Hutter et al., 1960; McIntosh et al., 1977). Fatty change, focal hepatitis or portal fibrosis in previously untreated patients made the evaluation of the role of methotrexate in hepatotoxicity difficult. Increases in transaminases and serum lactate dehydrogenase are quite common after methotrexate therapy. The enzymes may increase with each course of therapy and are higher in patients treated on a daily schedule than those treated on an intermittent schedule. In one report of treatment of gestational trophoblastic disease 14 % of patients had elevated transaminases (Berkowitz et al., 1986). High dose methotrexate therapy results in acute hypertransaminasemia, which is transient, reversible, and at least in children does not result in chronic liver disease (Weber et al., 1987).

The role of methotrexate therapy, used in the treatment of psoriasis and rheumatoid arthritis, in the production of hepatotoxicity is much less clear. Patients who take daily, oral methotrexate are reported to develop fibrosis or cirrhosis more than twice as frequently as those who take the drug intermittently parenterally (Weinstein, 1977). When administered continuously by mouth, methotrexate hepatotoxicity increases with the length of therapy or cumulative dose. One study showed that patients administered cumulative doses of less than 2 g had a low incidence of hepatotoxicity, even though the therapy lasted between 24 and 48 months (Mackenzie, 1985;

Tolman et al., 1985). This evidence suggests that cumulative dose is more important than duration of therapy for the development of toxicity. Cirrhosis affected 24 % of patients treated with daily oral methotrexate (Podurgiel et al., 1973). Hepatic fibrosis tends to remain stable or regress when therapy is stopped. The possibility that low- dose weekly methotrexate can cause hepatotoxicity has been debated. Age, obesity, decreased renal function and diabetes mellitus have also been associated with an increased risk of toxicity (Sznol et al., 1987). Alcohol was the most important determinant of significant hepatic fibrosis in patients treated with methotrexate. The risk of progressive hepatic fibrosis was 73 % in those who drank more than 15 g of alcohol daily compared to 26 % in those who did not.

The class of anti-tumour antibiotics include doxorubicin, daunorubicin, mitoxantrone, bleomycin, mitomycin, plicamycin (formerly mithramycin) and dactinomycin. Bleomycin causes hepatotoxicity in a very low number of patients and the toxicity could not be attributed to the drug itself (Blum et al., 1973). Doxorubicin has been reported to cause hepatotoxicity when combined with vincristine and prednisone (Aviles et al., 1984). Shortly after administration, increases in AST, ALP and bilirubin were associated with focal inflammation and steatosis. However the toxicity was considered to be due to an idiosyncratic reaction. Mitoxantrone has produced transient elevations in AST and ALT levels in leukaemia patients (Crooke and Bradner, 1976; Paciucci and Sklarin, 1986). Dactinomycin has been reported to cause liver toxicity in children who have previously received radiotherapy. Hepatotoxicity manifested itself as transient increases in AST levels. It is possible that dactinomycin treatment may reactivate prior radiation damage in the liver. In addition severe hepatotoxicity, in the form of veno-occlusive disease, has been reported in Wilm's tumour patients treated with dactinomycin and vincristine (Bjork et al., 1985; Green et al., 1988; Pritchard et al., 1989).

Plicamycin is one of the most hepatotoxic chemotherapeutic agents available (Kennedy et al., 1965) (Kennedy, 1970). With the discovery of less toxic and more effective drugs it is rarely used except for the treatment of refractory tumour hypercalcemia (Green and Donehower, 1984). The drug binds to DNA and is a potent inhibitor of RNA synthesis which leads to

inhibition of protein translation. Plicamycin could therefore block the production of many intracellular enzyme systems necessary for normal hepatic function. Elevations of aminotransferases and LDH occur in 100 % of patients treated with plicamycin. Milder elevations of ALP occur, but serum bilirubin is usually normal. These changes occur on the day of drug administration, peak on the second day and return to normal levels by day 4-21 after treatment. In addition, coagulation factors II, V, VII and X, which are synthesised by the liver, are depressed. The toxicity can be lessened by a reduction in drug dose. A review of patients treated with low dose plicamycin revealed a 16 % incidence of mild reversible hepatic dysfunction (Green and Donehower, 1984). Also, changing the schedule to an alternate-day schedule can decrease the toxicity (Yarbro and Kennedy, 1967).

Etoposide is a topoisomerase 2 inhibitor, excreted primarily via the bile. One report identified three patients who experienced severe hepatocellular injury at standard doses (Tran et al., 1991). At high doses, etoposide produces hyperbilirubinemia with elevated aminotransferases and ALP levels 3 weeks after administration (Johnson et al., 1983).

Cisplatin is a rare cause of steatosis and cholestasis at standard doses. At high doses, it has been reported to produce hepatocellular injury with elevations in AST and ALT (Pollera et al., 1987).

1.9 Evaluation of hepatotoxicity *in vitro*

In vitro systems offer the possibility of assessing liver toxicity in the absence of extrahepatic factors such as the absorption, distribution, extrahepatic metabolism and humoral factors. In the light of the current trend to reduce animal experimentation, *in vitro* models are often used to screen drugs for hepatotoxic potential and to reveal insights into mechanisms by which they may exert such toxicity. *In vitro* models include isolated perfused organs, tissue slices, isolated hepatocytes, primary hepatocyte cultures, cell lines and subcellular fractions. All of them have advantages and limitations, but isolated hepatocytes appear to be the most widely used model.

The technique of isolation of hepatocytes was derived from the pioneering work of Berry and Friend (Berry and Friend, 1969). It was modified and simplified by Seglen, who developed the two-step collagenase perfusion method (Seglen, 1976). The first step involves perfusion of a calcium free buffer. The second step is circulation of a calcium supplemented buffer containing collagenase. The initial perfusion facilitates desmosomal cleavage and further dispersion of liver cells. The addition of calcium to the enzyme solution ensures adequate collagenase activity. The method yields large numbers of parenchymal cells. About 40 to 60 x 10⁶ hepatocytes/g tissue are obtained from a young rat liver; cell viability ranges between 85 and 95 % as determined by the trypan blue exclusion assay; the preparation contains less than 5 % non parenchymal cells. The cells remain viable for about 4 hours. The cells retain the characteristics and functions present *in vivo* such as intact subcellular organelles, enzymes co-factors and interacting enzymes. The activity of phase I and II metabolising enzymes is maintained for a few hours. However, isolated hepatocytes lack the anatomical architecture, heterogeneity and plasma membrane polarity of hepatocytes *in vivo*.

To increase the survival of hepatocytes, the cells can be maintained in culture. Cultured hepatocytes can survive for several days. The mRNA levels and activities of various CYP isoforms are differentially expressed over time in culture. In general, there is a time-dependent decrease in the expression of mRNA for all major CYP genes over the first 1-2 days.

However, CYP3A4 and CYP2D6 return to nearly equal or greater levels than those expressed at the time of isolation over the subsequent 24-48 hours in the presence of low levels of glucocorticoids (0.1 μM) (Skett, 1994). In contrast, mRNA levels for other CYP450 enzymes including CYP1A2 and CYP2E do not return to the levels at the time of isolation during the ensuing 2-3 days in culture. These temporal changes in CYP expression should be taken into account when interpreting results obtained in cultured hepatocytes for long term studies of toxicants metabolism and enzyme induction. Nevertheless, many researchers utilise cultured hepatocytes for drug metabolism and toxicity studies. A major advantage of using isolated hepatocytes is that human cells can be used, thereby helping in the extrapolation of observations from laboratory animals to humans.

1.10 ET-743

A large proportion of the anti-cancer drugs currently used today are derived from natural sources. They include the vinca alkaloids, camptothecins, anthracyclines and taxanes. Cytarabine was the first marine-derived anti-cancer drug marketed and is now an essential component in the treatment of acute myeloid leukaemia. Several marine-derived compounds e.g., bryostatin, dolestatin, didemnim and aplidin are under clinical development (da Rocha et al., 2001). Ecteinascidins are a class of novel chemicals that belong to the tetrahydroisoquinoline alkaloids, extracted from the Caribbean tunicate, *Ecteinascidia turbinata*. The potent cytotoxicity of extracts from the tunicate was first discovered in the late 1960s, although attempts to isolate the active compounds were not successful for more than 15 years (Rinehart, 2000). More than 10 different ecteinascidins have been isolated; ET-743 was selected for further development as an anti-cancer agent because of its high cytotoxic potency and its relative abundance in the tunicate compared to the other ecteinascidins. Cytotoxicity was observed *in vitro* at very low doses in various tumour cell lines including melanoma and non-small cell lung (NSCL), ovarian, renal, prostate and breast cancer (Jimeno et al., 1996). This cytotoxicity data is shown in table 1.3.



Figure 1.4 Photograph of *Ecteinascidia turbinata*

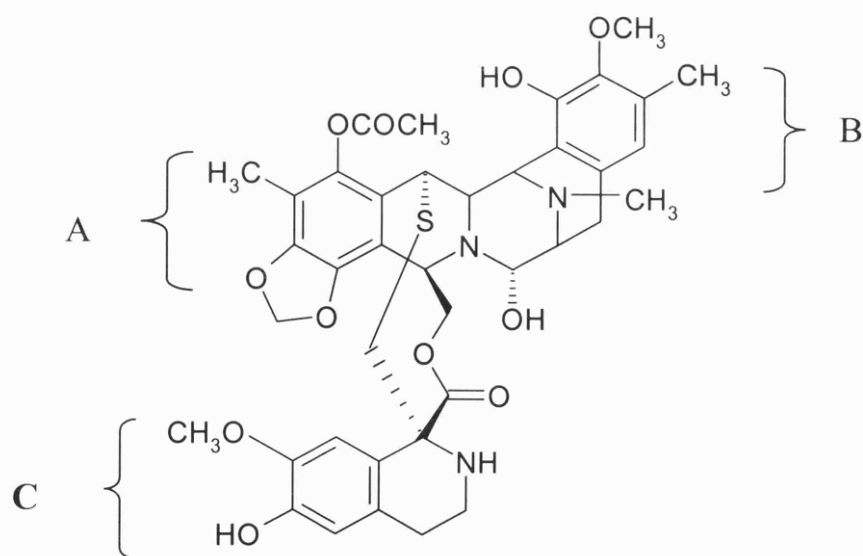


Figure 1.5 Structure of ET-743.

Molecular formula: $C_{39}H_{43}N_3O_{11}S$

Relative molecular mass: 762

Physical form and solubility: White to pale yellow amorphous powder. It is hydrophobic and very soluble in methanol, ethanol, chloroform, ethyl acetate and acetone.

Cell type	LC ₅₀	Number of cell lines
Colon	<1 pM	6
CNS	<1 pM	5
Melanoma	<1 pM	8
Renal	<1 pM	8
NSCL	4 pM	9
Breast	<100 pM	6
Ovarian	2.02 nM	6
Prostate	3.43 nM	2
Leukaemia	>10 nM	5

Table 1.3 Antiproliferative effect of ET-743 in vitro using NCI cell line screen (from Jimeno, 1996). LD₅₀ is the amount of ET-743 which causes the death of 50 % of the cells

1.10.1 Mechanism of action of ET-743

ET-743 consists of three fused tetrahydroisoquinoline rings (Figure 1.5). The A and B subunits of the drug are responsible for DNA recognition and covalent interaction with DNA, while ring C protrudes from the DNA duplex. Early *in vitro* studies indicated that ET-743 forms DNA adducts mediated through an intramolecular acid-catalysed dehydration of the carbinolamine moiety, resulting in an iminium intermediate that is the DNA-reactive species (Moore et al., 1997; Pommier et al., 1996). By gel mobility shift assays and nuclear magnetic resonance studies, it has been demonstrated that the alkylation of DNA by ET-743 occurs at guanines located either in the sequence 5'-PuGC or 5'-PyGG (Moore et al., 1997). One unique feature of ET-743 is that it is the first example of a minor groove alkylator that bends DNA towards the major groove (Zewail-Foote and Hurley, 1999). It has been suggested that the protrusion of the C subunit may be responsible for the biological activity of ET-743, since Saframycin, a structurally related compound which lacks the C subunit, does not possess anti-tumour properties (Pommier et al., 1996). Despite the large number of studies investigating the

mode of action of ET-743 the precise mechanism of action has not yet been fully elucidated. Many cellular systems and transcription factors have been identified as possible targets for ET-743 *in vitro*. However, the high concentration of ET-743 required in such studies, much greater than the concentrations which cause cytotoxicity *in vivo*, has led to contradictory reports concerning the mechanism of action.

Topoisomerase I was identified as a cellular target as it forms protein-linked DNA breaks in the presence of ET-743 (Takebayashi et al., 1999). However, the high concentrations of ET-743 required to produce DNA breaks suggest that topoisomerase binding is only an auxiliary effect and not the primary effect of ET-743. In addition, ET-743 is equally cytotoxic in wild-type yeast and in yeast with a deletion in the DNA topoisomerase gene suggesting that topoisomerase 1 is not the primary target of ET-743 (Damia et al., 2001). Studies have shown that ET-743 affects the regulation of transcription by inhibiting the complex between the transcription factor, NF-Y and the CCAAT box (Jin et al., 2000; Minuzzo et al., 2000). The CCAAT box is a conserved sequence of nucleotides in promoter regions upstream of the transcription start site of the gene. Bonfanti et al investigated the ability of ET-743 to inhibit the binding of different transcription factors. Many of the transcription factors tested required very high concentrations of ET-743 (300 μ M) while for NF-Y, the ET-743 concentration required to interfere with DNA-protein interactions were lower, but still higher than those showing significant cytotoxic activity *in vitro*. The authors propose that ET-743 might target histones and interfere with the process of nucleosome assembly (Bonfanti et al., 1999). In addition, ET-743 can inhibit activation of the multidrug resistance 1 (MDR1) gene by interfering with NF-Y (Jin et al., 2000). This inhibition was selective for activated transcription, as constitutive MDR1 promoter activity was not repressed at pharmacological concentrations of ET-743. Induction of MDR1 gene expression in tumour cells leads to drug resistance which represents a major obstacle to successful chemotherapy. ET-743 is the only cytotoxic drug found thus far to selectively inhibit activation of MDR1 gene transcription in tumour cells.

In vitro exposure to clinically relevant concentrations of ET-743 induces strong perturbations of the cell cycle with slowed cell cycle progression in S phase and cell cycle arrest in G₂. Cell cycle response of human colon carcinoma HCT116 cells was examined by Takebayashi (Takebayashi et al., 2001). ET-743 at 10 nM induced a marked accumulation of cells in the S and G₂M phases at 14 hours and in the G₂M phase at 24 hours after drug removal. At 0.1 μM, ET-743 induced a G₁ arrest at 6 hours after drug removal and an increase of cells in S phase at later time points. In addition, pulse labelling studies with methyl-³[H]-thymidine showed that DNA synthesis was inhibited by ET-743 at 1 or 10 μM. ET-743 at 2 nM disrupted S phase progression after a 12 hour treatment resulting in a late S phase and G₂M accumulation after 24 hours in the same cell line (Martinez et al., 2001). Erba et al examined the effects of ET-743 on LoVo and SW640 human intestinal carcinoma cell lines (Erba et al., 2001). At 14 hours after ET-743 treatment at 80 nM for 1 hour, there was an increase in percentage of cells in S phase. At 24 hours after drug removal, the majority of the cells were blocked in the G₂M phase.

The sensitivity of SW620 cells in different phases of the cell cycle was compared. The results showed that SW620 cells in G₁ were most sensitive to ET-743, and G₂M phase cells had the lowest sensitivity (Erba et al., 2001). This phase specificity is unusual for DNA-interacting agents as most anti-cancer drugs that interact with DNA are effective in S-phase cells. ET-743 induces a significant increase in p53 levels, which promotes apoptosis in cell lines expressing wild-type p53. However, cell cycle blockade does not appear to be p53-dependent, as no significant differences in ET-743 cytotoxicity were found when the treatment was carried out in cells with different p53 status.

Recently it has been observed that DNA repair capability appears to be a pre-requisite for ET-743-mediated toxicity. Damia and colleagues observed that nucleotide excision repair (NER)-deficient hamster cell lines were 2-8 fold less sensitive to ET-743 than NER-proficient cell lines and this decrease in sensitivity was also observed in fibroblasts from patients suffering from XPA (Damia et al., 2001). Takebayashi show that xeroderma pigmentosum cells deficient in the NER genes XPG, XPA, XPD or XPF, were resistant to ET-743, and sensitivity

was restored by complementation with wild type genes. In addition, ET-743 interacted with transcription-coupled NER machinery to induce lethal DNA strand breaks (Takahashi et al., 2001). Zewail-Foote et al used the bacterial Uvr ABC endonuclease to characterise how the NER pathway recognises and repairs ET-743 DNA adducts that differ in their hydrogen-bonding induced stability in the DNA helix (Zewail-Foote et al., 2001). The ET-743 adducts at the non-preferred and less stable sequences (5'AGT) were incised with the highest efficiency, whereas adducts at the preferred, more stable sequences (5'AGC) were incised to a lesser extent. Generally, DNA-interacting drugs are more effective in cell lines with specific mutants in NER mechanisms than in cells with proficient NER mechanisms. These findings that ET-743 is less cytotoxic in NER deficient cell lines further highlight the unique mechanism of action of ET-743. The anti-tumour activity of ET-743 may also be the result of interaction with the microtubule network of the cell. ET-743, at high concentrations, has been shown to disorganise microtubule bundles, but does not appear to interact directly with tubulin (Garcia-Rocha et al., 1996).

1.10.2 *In vivo* anti-tumour activity of ET-743

The anti-tumour activity of ET-743 was investigated in human tumour xenografts from melanoma, NSCL and ovarian cancer grown subcutaneously in nude mice (Hendriks et al., 1999). ET-743 was given at the maximum tolerated dose (MTD) of 0.2 mg/kg intermittently on days 0, 4, 8 and at the MTD of 0.1 mg/kg given i.v. on days 0-2 and 13-15. ET-743 caused complete regression in the chemo-sensitive human tumour xenografts MEXF 989, LXFL529, HOC22. In addition, strong tumour inhibition was observed at half of the MTD. The drug was inactive in two chemo-resistant tumour xenografts, MEXF 514 and LXFA 629. The results indicated that ET-743 has a broad therapeutic index and is a candidate for clinical development.

The anti-tumour activity of ET-743 was evaluated against a panel of human ovarian carcinomas transplanted into nude mice (Valoti et al., 1998). The tumour models included three xenografts transplanted s.c., HOC18, HOC22-S and MNB-PTX-1 which are

characterised by different levels of sensitivity to cisplatin. In addition, the anti-tumour activity was measured in two highly malignant xenografts HOC22 and HOC8, grown in the peritoneal cavity. At the maximum tolerated dose of 0.2 mg/kg using an intermittent schedule of one i.v. injection every 4 days, ET-743 was highly active against HOC22-S (sensitive to cisplatin) and HOC18 (marginally sensitive to cisplatin). In contrast, ET-743 was not active against MNB-PTX-1, a tumour that is highly resistant to chemotherapy. In the i.p. ovarian carcinoma xenograft model, ET-743 at the maximum tolerated dose induced complete tumour remissions in all mice bearing HOC22 tumour, but only marginal tumour delay against HOC8. These results indicate that ET-743 is a potent drug against ovarian carcinoma xenografts, being equally or more efficacious than cisplatin in the same tumour line (Valoti et al., 1998). Studies have indicated that ET-743 forms adducts in the minor groove of DNA whereas cisplatin and conventional alkylators form adducts mainly in the major groove (Broggini and D'Incalci, 1994). These mechanistic differences provide a rationale for exploring combinations of ET-743 and cisplatin in future preclinical and clinical studies.

A clonogenic assay system using fresh tumour specimens isolated directly from patients was used to determine the concentration of ET-743 to achieve anti-tumour activity and to determine the spectrum of activity of ET-743 (Izbicka et al., 1998). Continuous exposure to ET-743 at 100 nM, inhibited tumour cell growth by 79 % in breast, 69 % in NSCL, 58 % ovary and 88 % in melanoma specimens. At 1 μ M, ET-743 inhibited tumour growth by 100 % in breast, 85 % in NSCL, 67 % in ovary and 86 % in melanoma specimens. These results indicate that breast, NSCL, and ovarian cancers as well as melanoma may warrant clinical investigation.

1.10.3 Clinical investigations

The phase I programme in which ET-743 was tested included six trials investigating different schedules and doses. ET-743 was administered intravenously over 1, 3, 24 or 72 hours or administered over 1 hour on five consecutive days; all regimes were repeated at 3 weekly intervals at doses ranging from 6-1800 μ g/m². For 3- and 24- hour infusion schedules of ET-

743, peak plasma drug concentrations (C_{max}) and areas under the plasma concentration time curve (AUC) were proportional to the administered dose (Beijnen et al., 1999; van Kesteren et al., 2000). Non-linearity of pharmacokinetics was found when the drug was administered over 1- and 72- hours (Beijnen, 2001; Lopez Lazaro et al., 2001; Ryan et al., 2001). A study in 25 patients with solid tumours who received a single 24-hour intravenous infusion of ET-743 ($1500 \mu\text{g}/\text{m}^2$) reported mean (\pm SD) C_{max} and AUC values of $1.8 \pm 1.1 \mu\text{g}/\text{L}$ and $55 \pm 25 \mu\text{g}/\text{h}/\text{L}$, respectively (van Kesteren et al., 2000). ET-743 showed considerable interpatient variability of AUC and total body clearance at all dose levels. ET-743 is extensively bound to plasma proteins and shows a high degree of tissue binding. The pharmacokinetic profile of ET-743 after a 24 hour infusion is best described by a 2-compartment model with median distribution and elimination half lives of 0.5 and 45.6 hours, respectively (Lopez Lazaro et al., 2001). Dose-limiting toxicities were neutropaenia and thrombocytopenia. At the recommended dose, reversible and noncumulative transaminitis was noted in most of the patients. The dose, C_{max} and AUC of ET-743 were found to be significantly correlated with percentage reduction in white cell count and absolute neutrophil count, whereas elevation of transaminases and percentage decrease in platelet count showed a positive correlation only with AUC values. Evidence of objective activity, including long lasting responses, was noted in melanoma, breast cancer, ovarian cancer, mesothelioma and sarcoma. Among 20 patients with advanced pretreated sarcoma entered into phase 1 trials at the recommended dose or at the maximum tolerated dose, one had a complete response, three had partial responses, and two had minor responses.

ET-743 is currently under phase II/II investigation in different tumour types. The efficacy in patients with advanced soft tissue sarcoma has been investigated in three non-randomised multicentre phase II trials. ET-743 was administered by 24-hour infusion at $1500 \mu\text{g}/\text{m}^2$ every three weeks, as this was well tolerated in phase I trials. The majority of patients had received prior chemotherapy, but for some patients ET-743 was the first line treatment. The results of these phase II trial are only available as abstracts. In one clinical trial comprising of 36 patients with advanced soft tissue sarcoma receiving ET-743 as second or third line treatment, one patient had a complete tumour response, three patients had a partial tumour response and

two had a minor tumour responses (Demetri et al., 2001). In the other two studies, ET-743 treatment resulted in a partial tumour response in 9 of 99 patients (8 %) and 3 of 52 patients (6 %). Minor responses were observed in an additional 7 (8 %) and 4 (8 %) patients, respectively, while disease stabilisation occurred in 50 % and 42 % of patients, respectively (Le Cesne et al., 2001; Yovine et al., 2001). In patients receiving ET-743 as first line therapy the partial tumour response rate was 6 of 34 patients (18 %). Results from 127 patients in a pooled analysis of three multicentre phase II trials showed that the tumour response (partial or minor) or stable disease was reported in 57 % of patients.

In addition, there is preliminary evidence of ET-743 activity in heavily treated advanced, metastatic breast cancer (Zelev et al., 2000). Twenty-six women were enrolled in a phase II study with the following metastatic disease sites: liver 57 %, bone 46 %, cutaneous 42 %, lymph nodes 38 % and pleuropulmonary 38 %. All of the patients had been previously pre-treated with anthracyclines and 22 had also received taxanes. Of the 24 patients, 7 showed partial response, two of these responses were in taxane resistant patients, and 11 patients achieved disease stabilisation. This ongoing study suggests clinical activity for ET-743 in heavily pre-treated advanced, metastatic breast cancer. Furthermore, data available suggest a therapeutic benefit in patients with advanced ovarian cancer resistant to chemotherapy with 1 of 17 patients showing complete tumour response, 3 of 17 showing partial tumour response and 2 of 17 showing minor tumour response (Curigliano et al., 2001).

1.10.4 Preclinical toxicity

A preclinical toxicology program was carried out for ET-743 following the guidelines set out by the EORTC, the Cancer Research Campaign and the NCI. Further studies were performed in dogs for U.S. regulatory requirements. Despite full evaluation, very little information has been published. Toxicity studies have been performed in mice, rats, dogs and monkeys. Dose limiting haematological toxicities were observed in all species, but of at least equal concern was the hepatotoxicity observed in rats, dogs and monkeys (Mirsalis et al., 1996). Female rats were found to be the most sensitive towards the hepatotoxicity followed by male rats, dogs,

mice and monkeys (Jimeno et al., 1996). The maximum tolerated doses for the four species are displayed in table 1.4. Single and multiple-dose studies were performed with additional sequential studies carried out in mice and rats to assess cumulative and reversible toxicity.

Animal model	Schedule	MTD ($\mu\text{g}/\text{m}^2$)	MTD ($\mu\text{g}/\text{kg}$)
Mouse	Single i.v. dose	600	200
	Divided i.v. dose (dailyx5)	600	200
Rat (female)	Single i.v. dose	450	75
Rat (male)	Single i.v. dose	540	90
	Divided i.v.dose (dailyx5)	525	105
Dog	Single i.v. dose	700	35
	Divided i.v. dose (dailyx5)	1100	>60
Monkey	Single i.v. dose	1065	93

Table 1.4 Table showing the maximum tolerated doses for ET-743 from animal toxicity studies (adapted from Jimeno et al., 1996).

In mice, rats and dogs, the toxicity profiles were similar between single and multiple-dose schedules. However, the incidence and severity of pathological effects reduced with the multiple-dose schedule, suggesting that the incidence and severity of dose-limiting toxicities may be related to peak blood concentrations. Hepatic effects were observed as reflected by increases in bilirubin, ALP, AST and ALT, evidence of cholangitis in rats and dogs and coagulative focal necrosis in rats. At high doses, haematological side effects included leukopaenia, anaemia and thrombocytopenia. Haematological and pathological disorders were generally reversible but for some parameters complete pathological recovery was not seen. Monkeys experienced haematological toxicity and mild hepatotoxicity at the MTD level. A single dose toxicity study using ET-743 at 200 $\mu\text{g}/\text{kg}$ was performed in mice (British Industrial Biological Research Association (BIBRA) project no. 1589/6). The liver was the

most severely affected tissue, with the appearance of liver necrosis. This damage was accompanied by increases in serum levels of ALT and AST. The levels of these enzymes and histopathology returned to control levels by day 28 in most animals. Mice also showed decreased levels of red blood cells, haemoglobin, haematocrit and platelets and these changes were reversible. Multiple administration studies were performed to mimic the clinical situation (BIBRA project no 1589/2). Serum enzyme levels were substantially raised at 7 days after treatment but without adverse histopathological effects. The main effect of treatment was seen in the bone marrow, of which there was minimal to marked depletion. The effects were seen to be reversible and by day 32, both the number of bone marrow cells and the level of liver enzymes had returned to normal.

In male and female rats, multiple dose studies were performed at doses of 2 or 17.5 µg/kg ET-743 for 5 consecutive days (BIBRA Project no. 1589/3). Histopathological examination indicated toxicological damage in the liver, spleen, bone marrow and thymus of all male and female rats given 17.5 µg/kg ET-743. Liver toxicities were also seen in female rats given 2 µg/kg. The histopathological examination showed damage to the bile duct cells with increases in liver enzymes, especially aspartate aminotransferase. Many toxicity parameters were reversible, but at higher doses elevated levels of bilirubin and bile acids were irreversible.

ET-743 was administered to dogs for five consecutive days at dose levels of 5, 8 and 11 µg/kg. Toxic effects of ET-743 were seen in the bone marrow, liver, gallbladder, thymus and lymph nodes. Animals treated with 8 and 11 µg/kg ET-743 experienced haematological toxicities such as leukopaenia and thrombocytopaenia. At these dose levels, ET-743 induced hepatocellular and hepatobiliary damage. Liver damage was characterised by marked changes in ALT, AST, ALP and GGT. Histopathological changes included glycogen depletion, subacute periportal inflammation, bile duct hyperplasia and periportal oedema.

1.10.5 Metabolism of ET-743

Data about ET-743 metabolism is very limited. In early *in vitro* studies, rat CYP3A enzymes were the major CYPs that catalysed ET-743 metabolism as measured by the disappearance of the parent compound (Kuffel et al., 1997). Inhibition of metabolism was observed with inhibitors of CYP3A, CYP2C and CYP1A (Kuffel et al., 1997; Reid et al., 2002). Furthermore, metabolism in rats was induced by pre-treatment with dexamethasone and phenobarbitone, inducers of CYP3A and CYP2B respectively, but not by 3-methylcholanthrene, an inducer of CYP1A. In a study using incubations of ET-743 with lymphoblasts expressing specific CYP enzymes, it was demonstrated that human CYP3A4, CYP2D6, CYP2E1 and CYP2C9 had ET-743 metabolising activity as reflected by a decrease in parent compound (Rinehart et al., 1999). Human CYP1A2, CYP1B, CYP2B6, CYP2C8 and CYP2C19 did not metabolise ET-743. Three potential metabolites (figure 1.6) were discovered with incubations of lymphoblasts expressing a CYP3A4 isoform. Two metabolites were formed by oxidative degeneration (S1 and S2) and the third was a N-demethylated derivative of ET-743, ET-729 (Reid et al., 2002; Sparidans et al., 2001).

CYP3A is known to be expressed in much greater amounts in male than in female rats. A key observation in support of a major role of CYP3A in ET-743 metabolism is the observation that liver microsomes from male rat catalyse metabolism of ET-743 to a greater extent than did liver microsomes from female rats (Reid et al., 2002). The gender-dependent toxicity in rats is consistent with metabolism by CYP3A which shows gender specific expression. Metabolism of CYP3A enzyme in rats often predicts CYP3A catalysed metabolism in humans although CYP3A enzymes do not exhibit gender specific differences in expression in humans. In human liver microsomes ET-743 disappearance was highly correlated with CYP3A activity (Reid et al., 2002).

In a recent study, a four-step approach was used to discover potential metabolites in human samples (Sparidans et al., 2001). Potential metabolites were generated using several incubations with human microsomes, human plasma and uridine 5'-diphosphoglucuronyl

transferase. The compounds were identified using liquid chromatography (LC)-UV and LC-mass spectrometry (MS)(-MS). Samples of urine, plasma and bile from treated patients from phase I studies were screened for presence of potential metabolites. Eight compounds were discovered in the *in vitro* incubations which included non-enzymatic breakdown products (S1 and S2), deacetylated ET-743 and a glucuronidated ET-743. In the urine, bile and plasma samples the metabolites could not be detected. Concentrations of metabolites *in vivo* may be too low to detect. These low concentrations are the result from the low ET-743 dose (maximum concentration in plasma is 2 ng/ml), large volume of distribution and the slow rate of conversion.

Substantial amount of ET-729 are formed in some animal species, including mice, dog and rats. However, no ET-729 was formed in patients receiving the highest dose of ET-743 (1800 $\mu\text{g}/\text{m}^2$). It is reported that ET-729 has greater cytotoxicity than ET-743 (Reid et al., 1996; Wright et al., 1990). Biliary excretion of ET-729 was 5-fold greater in female rats compared with male rats. Because ET-729 has greater cytotoxicity than ET-743, the greater biliary excretion of this metabolite may contribute to the greater hepato- and biliary toxicity of ET-743 in female rats. ET-729 toxicity was evaluated in an *in vivo* model and it was found to be 2-4 times more toxic than ET-743 (Reid et al., 2002).

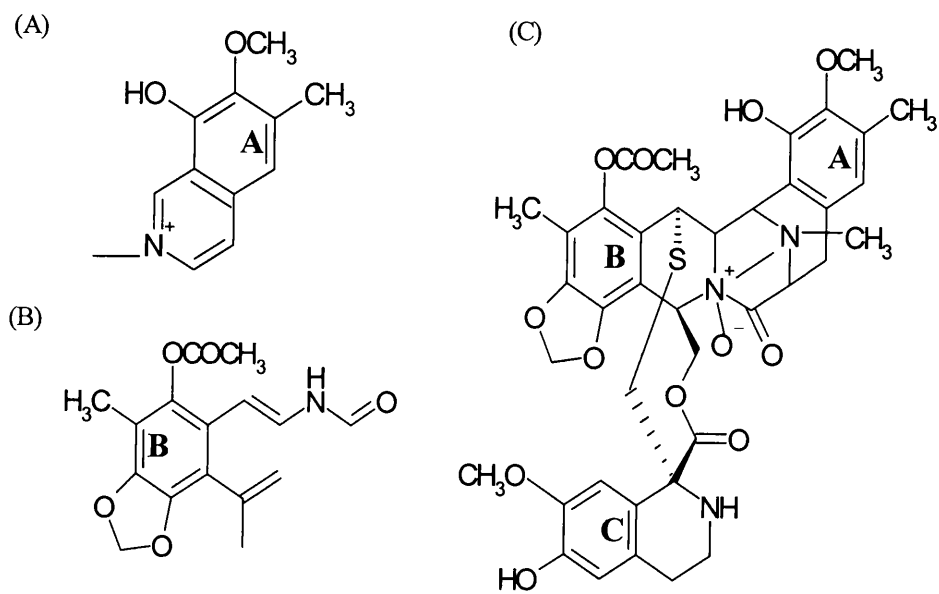


Figure 1.6 Structures of potential metabolites of ET-743 (A) S1, (B) S2 and (C) ETM-775.

1.11 Aims

ET-743 is a very promising anti-cancer drug currently in phase II clinical trial (section 1.10.3). Anti-tumour activity was observed in all Phase I studies, which were conducted on patients with advanced-stage breast, colon, ovarian and lung cancer, melanoma, mesothelioma and several types of sarcoma. ET-743 showed particularly high activity in cases of advanced sarcoma that had relapsed or were resistant to conventional therapy. Sarcoma is an example of a malignancy for which there is no effective treatment. In each study, hepatotoxicity was identified as a major adverse effect (section 1.10.3). Preclinical toxicity studies identified liver toxicity as a dose limiting toxicity in mice, rats, dogs and monkeys (section 1.10.4). The female rat was identified as the species with highest susceptibility to the hepatotoxicity of ET-743 and showed treatment related blood chemistry alterations, not dissimilar to those accompanying hepatotoxicity seen in clinical trials. Information on the detail and extent of the liver toxicity is extremely scarce as the initial toxicity study by the NCI and contract work commissioned by PharmaMar were never published.

The main overall aim of this project was to fully evaluate the liver toxicity of ET-743 in the most sensitive species, the female rat by *in vivo* and *in vitro* studies. The second overall aim was to investigate potential therapeutic strategies which may attenuate the hepatotoxicity of ET-743. These two main aims governed the design of experiments with the following specific objectives in mind:

i) To fully characterise the toxicity of ET-743 in the female rat. This was achieved by pathological examinations of ET-743 treated liver by electron and light microscopy. In addition, biochemical markers of liver toxicity were measured. In order to identify biological events underlying the observed hepatic alteration caused by ET-743, RNA from ET-743 treated liver and control liver were subjected to gene expression analysis by cDNA microarray.

ii) To compare the hepatotoxicity of ET-743 with that of ANIT. ANIT produces cholestasis in the rat that has been extensively characterised (chapter 1.7) and used for many years as a model for cholestatic liver damage. This comparison was used to clarify mechanisms by which ET-743 elicits hepatotoxicity in the rat.

iii) To investigate the toxicity of ET-743 in male rats and to compare the sensitivities of male and female rats towards ET-743 hepatotoxicity.

iv) To develop an *in vitro* model to study the hepatotoxicity of ET-743. The method of isolating and culturing hepatocytes from female rats was developed. The toxicity of ET-743 to hepatocytes in culture was evaluated and compared with the toxicity of ET-743 to the liver *in vivo*. In a preliminary experiment, isolated human hepatocytes were cultured and the toxicity of ET-743 towards rat and human hepatocytes was compared.

v) To investigate the effect of a CYP3A inducer, dexamethasone, on the hepatotoxicity of ET-743. There is evidence to suggest that CYP3A is involved in the metabolism of ET-743 (chapter 1.10.5). The choice of dexamethasone has more than one implication. Dexamethasone is given to ET-743 patients as an anti-emetic. In addition, there is evidence to suggest that dexamethasone pre-treatment enhances the efficacy of ET-743 (unpublished work by PharmaMar). Different doses and schedules of dexamethasone were investigated to find the optimum dose. The effect of dexamethasone on ET-743 toxicity was investigated by pathological and biochemical examination together with microarray analysis of gene expression changes. Dexamethasone has pleiotropic pharmacological effects. To investigate the mechanism of protection by dexamethasone, microarray analysis was performed with RNA from dexamethasone treated rats and control rats, to identify potential gene expression changes which may alter ET-743 mediated toxicity. CYP3A activity after dexamethasone treatment was measured to test the hypothesis that dexamethasone induces metabolism of ET-743 by CYP3A induction (chapter 1.10.5). In addition, in work carried out in parallel with the research submitted for PhD here, levels of ET-743 in the liver and plasma of rats pretreated

with dexamethasone were measured. Furthermore, collaborators in Italy studied the effect on anti-tumour activity of combining ET-743 with dexamethasone in different rodent models.

vi) To assess the effects of other modulators of drug metabolism on ET-743 metabolism. The potential hepatoprotective capacity of β -naphthoflavone, phenobarbitone and N-acetylcysteine were compared with that of dexamethasone. β -Naphthoflavone and phenobarbitone induce CYP 1A1/2 and 2B respectively (section 1.5.1) and can induce the oxidative metabolism of drugs. N-acetylcysteine replenishes intrahepatocellular stores of thiol moieties and increases levels of glutathione thus increasing the cell's capacity to detoxify potential harmful chemically reactive intermediates. In addition, the effects of these compounds on ET-743 hepatic changes displayed *in vivo* were investigated *in vitro* using cultured hepatocytes.

vii) Finally, to investigate of the effect the natural dietary constituent, indole-3-carbinol on the hepatotoxicity of ET-743. It has been shown that I3C pre-treatment (0.5 % in the diet) can prevent hepatic malignancies induced by aflatoxin B₁ (Manson et al., 1997). In addition, I3C pre-treatment inhibited the liver necrosis associated with carbon tetrachloride (Shertzer et al., 1987). On the basis of these findings it was hypothesised that I3C might protect against ET-743-induced liver damage in rats. I3C undergoes acid-induced polymerisation to diindolylmethane (DIM) in the stomach (Bjeldanes et al., 1991). Therefore, the effect of DIM on ET-743 hepatotoxicity was also tested. I3C is known to induce CYP enzymes (Manson et al., 1998), and in the light of the results with dexamethasone, that CYP3A induction may be involved in the metabolism of ET-743, the activity of CYP3A after I3C treatment was also measured.

CHAPTER 2

Materials and methods

2.1 Materials

2.1.1 General chemicals

All chemicals and reagents were purchased from Sigma-Aldrich Company Ltd. (Poole, UK) unless otherwise stated. ET-743 was obtained from PharmaMar SA (Colmenar Viejo, Madrid, Spain), the drug manufacturer. In *in vivo* experiments the ET-743 formulation for injection was used. ET-743 was supplied as a sterile lyophilised product freeze dried in a glass vial, which was reconstituted in sterile water prior to injection. Vials contained ET-743 (250 µg), mannitol (250 mg), potassium phosphate (34 mg) and phosphoric acid. In the hepatocyte cultures pure ET-743 was added after dissolution in DMSO.

2.1.2 Animals

Wistar rats aged 6 weeks old (200-250 g) were purchased from Charles River UK Ltd (Margate, Kent, UK). Rats were kept in a purpose built animal house in negative pressure isolators (19-23 °C) under a 12 hour light /dark cycle. The rats received RMI rodent maintenance diet supplied by Special Dietary Services, (Witham, UK) and water *ad libitum*. Experiments using animals were conducted as stipulated by Project license 80-1250 granted to the Medical Research Council Toxicology Unit by the UK Home Office. The experimental design was vetted and approved by the Leicester University Ethical Committee for Animal Experimentation.

2.1.3 Histopathology and immunocytochemistry.

Ki-67, primary polyclonal rabbit antibody and normal rabbit immunoglobulin were purchased from Novacastra (Peterborough, UK) and DAKO (Cambridge, UK), respectively and detected by the StreptABComplex/HRP Duet System obtained from DAKO. Smooth muscle actin,

mouse monoclonal antibody and negative control IgG2a antibodies were obtained from DAKO. VIP substrate kit was obtained from Vector Laboratories Ltd. (Peterborough, UK).

2.1.4 Electron microscopy

Epoxy resin was obtained from Taab Laboratories Equipment Ltd. (Berkshire, U.K.).

2.1.5 CYP assays

Ethoxy resorufin and resorufin were kindly donated from Dr A.G. Smith (MRC toxicology Unit, Leicester). 7-Benzyloxy-4-(trifluoromethyl)-coumarin (BFC) and 7-hydroxy-4-(trifluoromethyl)-coumarin were purchased from Cambridge Biosciences (Cambridge UK).

2.1.6 Microarray

Guanadinium thiocyanate and caesium chloride were purchased from ICN Pharmaceuticals (Basingstoke, UK). Cy3-dUTP and Cy5-dUTP and dNTP's were purchased from Amersham Pharmacia Biotech Ltd (Little Chalfont, UK). Superscript II reverse transcriptase, 5X superscript buffer, 0.1M DTT, tRNA and mouse Cot DNA were purchased from Gibco Life Technologies (Paisley, UK). RNAsin RNAase inhibitor was obtained from Promega (Southampton, UK), and micron columns were purchased from Milipore Corp (Bedford, MA, USA).

2.1.7 Bradford protein assay

Protein assay reagent was purchased from Bio-Rad Laboratories (Hemel Hempstead, UK).

2.1.8 Polyacrylamide gel electrophoresis

Acrylamide was purchased from Anachem Ltd. (Luton, UK). The ECL reagents, hyperfilm and hybond cellulose were supplied by Amersham Pharmacia Biotech Ltd. (Little Chalfont, UK). The wet blotting system and prestained broad range SDS-page standards were purchased from Bio-Rad Laboratories (Hemel Hempstead, UK). P-glycoprotein mouse monoclonal antibody was obtained from Signet laboratories (Dedham, MA, USA).

2.1.9 Isolation of hepatocytes

Cannulas were purchased from Southern Syringe Services. Hanks's buffered saline solution (HBSS) and sodium bicarbonate were purchased from Gibco Life technologies (Paisley, UK). Nylon gauze was obtained from Fischer Scientific (Leicester, U.K.).

2.2 Methods

2.2.1 Study of the hepatotoxicity of ET-743 *in vivo*.

Groups of 4 female Wistar rats (230 - 250 g) received either a single dose of ET-743 (40 µg/kg dissolved in water, 0.8 ml/kg body weight) i.v. under light halothane anaesthetic or the vehicle (water) *via* the lateral tail vein. In a preliminary dose-finding orientation experiment ET-743 administered at 75 µg/kg, the maximum tolerated dose in the female rat, elicited severe toxicity, resulting in mortality. Therefore the dose was reduced to 40 µg/kg, which caused toxicity but avoided mortality. This dose is close to 1500 µg/m² (approximately 38 µg/kg) recommended for infusion in phase II studies in patients (Taamma et al., 2001; van Kesteren et al., 2000). Animals were exsanguinated under halothane anaesthetic at 6, 12 and 24 hours, or 2, 3, 6, 12, 24 or 48 days or 3 months after administration. Blood was taken for measurements of liver enzymes and bilirubin. Blood was removed by cardiac puncture and collected in heparinised tubes, and blood cells were separated from plasma by centrifugation at 2 000 g for 25 min. Livers were removed and sections taken and stored in neutral buffered formalin for histologic examination or stored in ice cold buffer for microsomal preparation for CYP450 assays (chapter 2.2.13). Other tissues (including stomach, small intestine, thymus, spleen, heart, lungs, kidneys and bone marrow) from rats killed at periods of up to 14 days following treatment were taken for histologic examination and stored in buffered formalin..

2.2.2 Effect of ET-743 on hepatic gene expression

A separate study was performed to study the hepatic gene changes. Female Wistar rats were treated with ET-743 (40 µg/kg, i.v.) or the vehicle (water). The liver of each ET-743-treated rat was paired with a liver from an age-matched vehicle-treated control rat. Groups of three ET-743-treated rats paired with 3 untreated rats were killed 6 hours or 1, 2, 3, 6 and 24 days after dosing. Liver sections were removed and stored at -80 °C for up to 3 months for RNA isolation (chapter 2.2.20).

2.2.3 Study of the hepatotoxicity of ANIT

Groups of 6 female Wistar rats (230 - 250 g) received either a single dose of ANIT p.o. (100 mg/kg, dissolved in corn oil, 2 ml/kg body weight) or vehicle (corn oil). Animals were killed at 2 or 6 days after administration. Blood was taken for measurements of liver enzymes and bilirubin. Blood was removed by cardiac puncture and collected in heparinised tubes, and blood cells were separated from plasma by centrifugation at 2 000 g for 25 min. Livers were removed and sections taken and stored in neutral buffered formalin for histologic examination. To study hepatic gene expression, liver sections of each ANIT-treated rat was paired with liver sections from an age-matched vehicle-treated control rat. Liver sections were stored at -80°C for up to 3 months for RNA isolation (chapter 2.2.20).

2.2.4 Study of the effect of dexamethasone on ET-743 hepatotoxicity

Female Wistar rats (230 - 250 g) were pre-treated with a single dose of dexamethasone p.o. (1 to 20 mg/kg, dissolved in glycerol formal, 1 ml/kg body weight) 24 hours prior to, or concomitant with, a hepatotoxic dose of ET-743 (40 µg/kg, i.v. *via* the lateral tail vein). Control animals received the vehicles used, i.e. glycerol formal in the case of dexamethasone, and water as the vehicle for ET-743. Each treatment group comprised 5 animals. Animals were killed at 3, 6 or 12 days after administration. Blood was taken for measurements of liver enzymes and bilirubin. Blood was removed by cardiac puncture and collected in heparinised tubes, and blood cells were separated from plasma by centrifugation at 2 000 g for 25 min. Livers were removed and sections taken for histologic examination.

2.2.5 Study of the effect of dexamethasone and ET-743 on hepatic gene expression changes.

For the analysis of differential gene expression, three control rats were paired with three rats which had received either ET-743 (40 µg/kg, i.v.), dexamethasone (10 mg/kg, p.o.), or the

combination of dexamethasone and ET-743, the latter given 24 hours after dexamethasone. Animals were killed and livers sections were collected at 3 days *post* administration of ET-743. Liver sections were stored at -80°C for up to 3 months for RNA isolation (chapter 2.2.20). A separate study was performed to determine the gene expression changes 24 hours after dexamethasone administration. Control rats were paired with rats which had received dexamethasone or the combination, and animals were culled 24 hours later.

2.2.6 Study of the modulation of ET-743 hepatotoxicity *in vivo*.

Female Wistar rats (230 - 250 g) were pre-treated as follows, the choice of dose was based on relevant literature quoted below so as to produce optimal induction of the metabolising enzyme involved in the case of β -naphthoflavone or phenobarbitone or maximum electrophilic scavenging activity in the case of N-acetylcysteine: β -naphthoflavone (dissolved in glycerol formal, 3 ml/kg body weight), three consecutive daily doses of 80 mg/kg, p.o. finishing 24 hours prior to ET-743 injection; phenobarbitone, 500 mg/l of drinking water for 7 days finishing 24 hours prior to ET-743 (Fentem and Fry, 1991); N-acetylcysteine (dissolved in saline, 1 ml/kg body weight), given as a single i.p. dose of 200 mg/kg one hour prior to ET-743 (Gomez et al., 1994). Control animals received the vehicle only, *i.e.* glycerol formal in the case of β -naphthoflavone, saline for N-acetylcysteine and water for ET-743. Animals were killed 3 or 12 days after ET-743 administration. Blood was taken for measurements of liver enzymes and bilirubin. Blood was removed by cardiac puncture and collected in heparinised tubes, and blood cells were separated from plasma by centrifugation at 2 000 g for 25 min. Livers were removed and sections taken for histologic examination.

2.2.7 Study of the modulation of ET-743 hepatotoxicity *in vitro*.

Rats were treated with dexamethasone (three daily doses of 50 mg/kg /day), β -naphthoflavone (dose as above) or phenobarbitone (dose as above). Hepatocytes were isolated 24 hours after treatment as described in section 2.2.24.

2.2.8 Study of the effect of I3C on ET-743 hepatotoxicity.

Female Wistar rats (230 - 250 g) received indole-3-carbinol (0.1 % or 0.5 %) in the diet for one week prior to a hepatotoxic dose of ET-743 (40 μ g/kg, i.v. *via* the lateral tail vein). Control animals received the vehicles used, i.e. 2 % arachis oil in the case of indole-3-carbinol, and water as the vehicle for ET-743. Each treatment group comprised 4 animals. Animals were killed at 3 or 12 days after administration of ET-743. Blood was taken for measurements of liver enzymes and bilirubin. Blood was removed by cardiac puncture and collected in heparinised tubes, and blood cells were separated from plasma by centrifugation at 2 000 g for 25 min. Liver sections were fixed and stained with H & E for histopathological examination. To study the effect of DIM on ET-743-induced hepatotoxicity the same protocol was used replacing I3C with 0.2 % DIM.

2.2.9 Study of anti-tumour activity.

These experiments were performed by collaborators at Istituto di Ricerca Farmacologiche Mario Negri, Milan, Italy. The 13762 tumour was propagated in female Fischer rats. Tumour fragments (100-200 mg weight) were implanted (s.c.) into the flank of rats (100-120 g). Female C57Bl/6 mice (20 \pm 2 g body weight) received 10⁶ B16F1 melanoma cells s.c., or 10⁵ M5076 reticulum sarcoma cells i.m. Female MCr-nu/nu mice (22 \pm 2 g body weight) received 5x10⁶ Igrov/1 ovarian carcinoma cells s.c. Male CDI nu/nu mice (20 \pm 2 g body weight) received 1.5x10⁶ TE-671 rhabdomyosarcoma cells s.c. Properties of the tumour models have

been described in the following representative references: 13762 (Braunschweiger and Schiffer, 1980), B16F1 (Pendergrast et al., 1976), M5076 (Talmadge et al., 1981), Igrov/1 (Formelli and Cleris, 1993) and TE 671 (Chen et al., 1989). Rats (8 per group) received dexamethasone (10 mg/kg, in glycerol formal, i.p.) on day 9 *post* 13762 tumour implantation. ET-743 (40 µg/kg, i.v.) was administered 24 hours after dexamethasone. Thus the treatment protocol in the rat tumour model mimics faithfully the protocol used in the hepatoprotection studies. In the athymic murine models, mice (10 per group) received repeated doses of dexamethasone (20 or 40 mg/kg in glycerol formal, i.p.) daily between days 7 and 24 *post* tumour implantation. ET-743 (0.15 or 0.2 mg/kg, i.v.) was administered either once, twice or 3 times between days 10 and 25 after tumour implantation. The specific dosing schedules used in each model are listed in Table 2.1. Tumour weight (TW) was determined on days 14 and 17 *post* tumour implantation in rats, and between days 23 to 34 *post* tumour implantation in mice, as detailed for each model in Table 2.1. TW was calculated *via* tumour diameter, using a Vernier caliper and the formula $TW \text{ (in mg)} = \text{tumour volume (m}^3\text{)} = d^2 \times D/2$, in which *d* and *D* represent the shortest and longest diameter, respectively.

Procedures involving animal care and treatment were conducted as stipulated in Italian National Guidelines (D.L. No. 116 G.U., suppl. 40, 18.2.1992, circolare No. 8, G.U. luglio 1994) and appropriate European directives (EEC Council Directive 86/609, 1.12.1987) and adhered to the Guide for the Care and Use of Laboratory Animals (US National Research Council, 1996).

Tumour model	Dexamethasone dose schedule	ET-743 dose schedule
B-16	40 mg/kg on days 7, 8, 9, 14, 15, 16.	0.15 mg/kg on days 10, 17
M5076	40 mg/kg on days 11, 12, 13, 18, 19, 20.	0.15 mg/kg on days 14, 21
IGROV-1	40 mg/kg on days 8, 9, 10, 15, 16, 17, 22, 23, 24.	0.2 mg/kg on days 11, 18, 25
TE-671	20 mg/kg on days 12, 13, 14, 15.	0.2 mg/kg on day 15

Table 2.1 The dosing schedule used in the four tumour models to investigate the anti-tumour properties of the combination of ET-743 and dexamethasone.

2.2.10 Histopathology and immunocytochemistry.

Fixing and staining of sections were carried out by Jenny Edwards and Lynda Wilkinson and immunohistochemistry was performed by Richard Edwards. Histopathological analysis of the tissue sections was performed by Dr Peter Greaves.

Tissues were fixed in neutral buffered formalin and embedded in paraffin wax. Sternum samples were decalcified for examination of bone marrow cellularity. Sections (5 µm thick)

were cut and stained with haematoxylin and eosin. Selected hepatic sections were stained with van Gieson's stain for collagen.

Ki-67 was demonstrated in sections of formalin-fixed, paraffin wax-embedded liver tissue at all time points between 6 hours and 12 days *post* dosing. Sections were dewaxed in xylene, taken to water and microwaved in citrate buffer pH 6.0 for 30 min at 700 Watts. A primary polyclonal rabbit antibody to a 1086bp Ki-67 motif-containing cDNA fragment was applied at a dilution of 1/500 for 3 hours at room temperature. Normal rabbit immunoglobulin was used as a negative control. The primary antibody was detected with the DAKO StreptABCComplex/HRP Duet System. Positive nuclei were visualized using 3,3'-diaminobenzidine tetrahydrochloride, and sections were lightly counterstained with haematoxylin. The total number of nuclei per unit area was calculated by counting the number of nuclei in a rectangular frame (0.32 mm x 0.225 mm) using the x 40 Diaplan microscope objective on the haematoxylin and eosin-stained sections, counting was repeated in 10 randomly chosen frames. The proliferation index was calculated as the number of Ki-67-stained nuclei per 1000 hepatocyte nuclei.

Presence of α -smooth muscle actin was demonstrated using a mouse monoclonal antibody against the N-terminal decapeptide of human α -smooth muscle actin. Sections were pre-treated as above and the primary antibody was applied at a dilution of 1/100 for 3 hours at room temperature. Mouse IgG2a negative control antibody was used as control. The primary antibody was detected as above. The peroxidase label was visualized using the VIP substrate kit followed by a light haematoxylin counterstain.

2.2.11 Electron microscopy.

Tissues were processed by Judy McWilliams and analysed by electron microscopy by Dr David Dinsdale. Livers were fixed by vascular perfusion with 2 % glutaraldehyde in 0.1 M sodium cacodylate buffer (pH 7.4) and stored overnight (4 °C) in the fixative. Slices (<1mm

thick) were post-fixed with 1 % osmium tetroxide/1 % potassium ferrocyanide, stained *en bloc* with 5 % uranyl acetate and embedded in Taab epoxy resin. Ultra-thin sections were examined unstained or following staining with lead citrate and/or uranyl acetate.

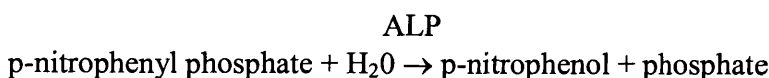
2.2.12 Measurement of Liver Enzymes.

Plasma levels of alkaline phosphatase (ALP), aspartate aminotransferase (AST) and total plasma bilirubin were measured using commercially available kits and established protocols (Sigma-Aldrich).

2.2.12.1 ALP

The method for ALP is a colourimetric, kinetic method.

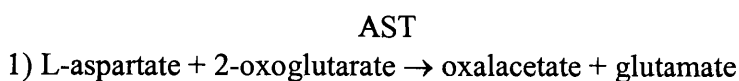
ALP catalyses the following reaction:



The hydrolysis occurs at alkaline pH and the p-nitrophenol formed shows an absorbance maximum at 405 nm. The rate of increase in absorbance at 405 nm is directly proportional to ALP activity in the sample.

2.2.12.2 AST

The method for AST is an ultraviolet, kinetic method.



The rate of decrease in absorbance at 340 nm due to the oxidation of NADH to NAD and hence AST activity.

2.2.12.3 Bilirubin

The method for bilirubin measurement is a colourimetric, endpoint method. Direct (conjugated) bilirubin couples with diazotised sulfanilic acid, forming a blue colour at alkaline pH. Indirect (unconjugated) bilirubin requires a caffeine-benzoate-acetate accelerating agent. The blue colour originates from both the direct and indirect bilirubin and is measured at 600 nm, giving total bilirubin.

2.2.13 Preparation of microsomes.

Three grams of liver was homogenised using a Potter-Elvehjem type teflon glass homogeniser (clearance 0.125 mm, 10 passes at 1100 rpm) in 15 ml ice cold Tris buffer (0.05 M Tris, 0.154 M KCl, 0.25 M sucrose, pH 7.6). Tissues were kept at 4 °C during the preparation of microsomes. The homogenate was centrifuged at 10 000 g for 20 min at 4 °C. The supernatant was decanted and centrifuged at 100 000 g for 60 min at 4 °C. The pellet was resuspended in Tris buffer and respun again at 100 000 g for 60 min. The final pellet was resuspended in 5 mls storage buffer (0.25 M potassium phosphate buffer containing 30 % glycerol), aliquoted and stored at -80 °C.

2.2.14 CYP2E1 assay.

This procedure was based on a method by Carlson, (Carlson, 1991). An incubation mixture containing 0.2 mM p-nitrophenol, 5 mM MgCl₂, 1 mM NADPH, 0.05 Tris buffer pH 7.4 and 3 mg microsomal protein was incubated at 37 °C for 30 min. The reaction was stopped by the addition of 0.5 ml 6 M perchloric acid. The samples were centrifuged at 2 000 g for 10 min. The supernatant was removed and 1 ml was added to 0.1 ml 10 M NaOH. This was centrifuged at 3 000 g for 5 min and the absorbance was determined at 546 nm. A standard curve was prepared using 4-nitrocatechol treated in the same manner.

2.2.15 CYP1A1/2 assay

Measurement of the 7-hydroxylation of ethoxyresorufin to resorufin was carried out by a method based on that of Burke and Mayer (Burke and Mayer, 1974). To a cuvette containing 2.35 ml Tris buffer (0.05 M Tris, 0.154 M KCl, pH 7.6) 12 μ l of ethoxyresorufin in DMSO (final concentration 2 μ M) and 50 μ l microsomes (0.6-0.8 mg protein), 12 μ l of NADPH (50 mM) was added to start the reaction. The rate of conversion to resorufin was measured by a decrease in fluorescence using a fluorimeter (Varian). Fluorescence was measured for 5 min at 37 °C at an excitation wavelength of 540 nm, slit width 2.5 nm and emission wavelength of 585 nm, slit width 10 nm. A standard curve was prepared using pure resorufin.

2.2.16 CYP3A2 assay

Measurement of the hydroxylation of benzyloxy-4-trifluoromethylcoumarin to hydroxy-4-trifluoromethylcoumarin was carried out by a method based on that of Stresser et al (Stresser et al., 2000). To a cuvette containing 2.35 ml 0.2 M phosphate buffer (pH 7.4), 12 μ l of benzyloxy-4-trifluoromethylcoumarin in DMSO (final concentration 50 μ M) and 50 μ l microsomes (0.6-0.8 mg protein), 12 μ l of NADPH (50 mM) was added to start the reaction. The rate of conversion to hydroxy-4-trifluoromethylcoumarin was measured by fluorescence using a fluorimeter (Varian). Fluorescence increase was measured for 3 min at 37°C at an excitation wavelength of 409 nm, slit width 10 nm and an emission wavelength of 530 nm, slit width 20 nm. A standard curve was prepared using hydroxy-4-trifluoromethylcoumarin.

It was reported that benzyloxy-4-trifluoromethylcoumarin was not a specific probe for CYP3A while 7-benzyloxyquinoline has greater specificity for the isozyme (Renwick et al., 2001). Therefore the above method was replaced with the following method which measures the oxidative de-benzoylation of 7-benzyloxyquinoline (7-BQ) to 7-hydroxyquinoline (7-HQ).

To a cuvette containing 2.35 ml 0.2 M phosphate buffer (pH 7.4), 25 μ l of 7-BQ (5 mM) and 50 μ l microsome (0.6-0.8 mg protein), 12 μ l of NADPH (50 mM) was added to start the reaction. The rate of conversion to 7-HQ was measured by fluorescence increase using a fluorimeter (Varian). The fluorescence was measured for 10 min at 37 °C at an excitation wavelength 410 nm, slit width 10 and an emission wavelength of 510 nm, slit width 10. A standard curve was prepared using 7-HQ.

2.2.17 Total cytochrome P450 assay

0.5 ml liver microsomes (2-10 mg protein) was added to 5 ml 0.1 M phosphate buffer pH 7.4. Carbon monoxide was vigorously bubbled through the microsomes for 30 sec and the tube stoppered. 2.5 ml was aliquoted into each of two cuvettes and a few crystals of sodium dithionite were added to the test sample. The cuvette was inverted to dissolve the crystals. The absorption spectrum between 400 and 550 nm was recorded. The 490 nm absorption reading was subtracted from the 450 nm absorption reading to obtain the cytochrome P450 peak. Using the extinction coefficient for cytochrome P450 of 91 cm^2/mmol , the cytochrome P450 concentration was obtained using the following formula:

$$\text{Cytochrome P450 (nmol/ml)} = \Delta A (450-490) \times 1000/91$$

2.2.18 Measurement of glutathione levels in liver

Measurement of glutathione in liver was carried out based on a method by White (White, 1976). Approximately 1 g of fresh liver was homogenised in 9 ml of homogenisation medium (100 ml of 24 mM potassium dihydrogen orthophosphate and 1 mM EDTA mixed with 300 ml ethanol) at 4 °C using a Teflon glass homogeniser. The homogenate was centrifuged at 10 000 g for 15 min at 4 °C. The supernatant was removed and 0.3 ml was added to 2.4 ml of phosphate buffer (0.3 M, pH 7.4). To this 1 ml DTNB (5,5-dithio *bis* 2-nitrobenzoic acid) (40

mg in 100 ml 0.03 M phosphate buffer, pH 7.4) was added and mixed. The absorbance was read at 412 nm. Glutathione concentration was calculated from a glutathione standard curve.

2.2.19 Bradford protein assay

This procedure was based on a method by Bradford (Bradford, 1976). Bovin serum albumin (BSA) standards were prepared in distilled water at a concentration range of 0-20 µg/ml protein. The protein samples were diluted 1:500 in distilled water in duplicate. The standards and samples (800 µl) were placed in a cuvette with 200 µl of protein reagent. The absorbance was read at 595 nm against a blank control sample and protein concentration was calculated from a standard curve.

2.2.20 Microarray analysis, an overview

The cDNA microarray technique is a recently developed tool that can be used to measure the expression patterns of genes in parallel, generating clues to gene expression changes in response to drug treatment. DNA microarray technology encompasses arraying of DNA onto a glass slide, hybridisation and detection methods, links to software and databases that facilitate data analysis. In a microarray experiment, single stranded DNA molecules are deposited onto a glass slide at fixed locations (chapter 2.2.20.2). RNA is prepared from the control and experimental tissue (chapter 2.2.20.1) and labelled using oligo dT-primed reverse transcription by utilising nucleotides tagged with fluorescent dyes, Cy3 and Cy5 (chapter 2.2.20.3). Both fluorescence-labelled cDNA samples are hybridised to the microarray, as gene sequences from the tissue hybridise to the complementary sequence on the array (chapter 2.2.20.3 to 2.2.20.8). To measure the relative abundance of the hybridized RNA the array is excited by a laser and the expression of each gene is detected and quantitated. From the fluorescence intensities and colour of each spot, the relative expression levels of the genes in the control and test tissue can be estimated.

2.2.20.1 Preparation of mRNA

This procedure was based on a method by Turton et al (Turton et al., 2001). Approximately 0.5 g of frozen liver was homogenised in 7 ml of 4 M guanidium thiocyanate and 525 µl β-mercaptoethanol and 200 µl of sarkosyl was then added to the homogenate. 4.5 ml cesium chloride solution was pipetted into a clean centrifuge tube and the homogenate was layered on top. The homogenate was then spun at 10 000 g for 18 hours at 20 °C. The supernatant was removed to leave a clear pellet at the bottom. The pellet was rinsed with 2 x 500 µl of 70 % ethanol. This was centrifuged at 10 000 g for 3 min to pellet the RNA, the excess ethanol was removed and the pellet left to dry before being resuspended in diethyl pyrocarbonate (DEPC) treated water. The RNA was extracted by adding an equal volume phenol/chloroform (1:1) followed by centrifugation at 10 000 g for 3 min. This step was repeated and then the RNA was extracted again using chloroform. The RNA was precipitated with sodium acetate: ethanol (0.1:3). The pellet was washed twice with 70 % ethanol. Finally the pellet was resuspended in 200 µl (DEPC) treated water. The concentration of RNA in aqueous solution was determined by measuring the absorbance of a dilution of the solution at 260 nm. The samples were diluted 1 in 500 with sterile water and the absorbance measured at 260 and 280 nm.

$$[\text{RNA } \mu\text{g/ml}] = \text{OD}_{260} \times \text{dilution factor} \times 40.$$

Comparison of absorbance at 260 and 280 nm of a nucleic acid solution provides an estimate of the purity of the preparation. A 260:280 ratio of approximately 1.6-1.9 indicates a protein free preparation, ratios lower than these indicate protein contamination

2.2.20.2 Printing the arrays

The arrays comprised 4,246 mouse sequence tag (EST) clones (2, 783 individual Genbank clusters). Two-thirds of the clones were obtained from the IMAGE collections held at the MRC Human Gene Mapping Project (<http://www.hgmp.mrc.ac.uk/>). The remaining one-third of the EST clones were obtained from Research Genetics (RG9 set, <http://www.resgen.com>). All clones described in this thesis were verified by sequence analysis. CDNA from the EST

was obtained via PCR amplification using plasmid-specific primers. The PCR products were all separated by electrophoresis on agarose gels to make sure that only single product was obtained for each clone. The reactions products were precipitated and prepared for array, using methods described (DeRisi et al., 1997; Eisen and Brown, 1999). Arrays were printed on poly-*L*-lysine-coated slides, UV-crosslinked and blocked prior to use (DeRisi et al., 1997; Eisen and Brown, 1999; Turton et al, 2001). The arrays were printed using an arrayer built essentially according to the Stanford designs (*cf.* http://www.le.ac.uk/cmht/microarray_lab/Home.htm). This was carried out by members of the Bioinformatics Group, MRC Toxicology Unit, University of Leicester, UK. The centre-to-centre distance of the features was 210 μm , and each feature was 90-100 μm in diameter.

2.2.20.3 Labelling and hybridisation

RNA samples (50 μg in 10 μl) were incubated with 4 μg oligo dT₍₂₅₎ (0.5 μl). After denaturation at 70 °C for 8 min annealing was allowed to occur as the temperature fell to 42 °C over 30 min. At this point dNTPs were added to a final concentration of 0.5 mM with the exception of dTTP which was added at 0.2 mM. The desired Cy labelled dUTP was added at a final concentration of 0.1 mM. Test RNA was incubated with Cy5 and control RNA was incubated with Cy3 for two pairs of samples and reversed for the third pair. The buffer used was 1X first strand buffer and 20U of RNAsin was added to the reaction. Transcription was initiated by the addition of superscript II 100 U and allowed to proceed for 1 hour at 42 °C before addition of a second 100U of superscript II and another 1 hour incubation at 42 °C. RNA was removed from the synthesised cDNA by addition of 1 μl EDTA (0.5 M) followed by 1 μl SDS (10 %) and 3 μl NaOH (3 M) and incubated at 70 °C for 10 min. Finally, 3 μl HCl (2 M) followed by 10 μl Tris/HCl (1 M) was added to neutralise the reaction mixture.

2.2.20.4 Purification of RNA.

The samples were purified using a microcon YM-30 micro-concentrator method. 140 µl Tris-EDTA buffer (1 M, pH 8) was added to each dye tube and then paired probes were combined into one centricon prior to microfugation (10 000 g, 7 min) and the flow through discarded. 450 µl Tris-EDTA buffer (1M, pH 8) was then added to each sample, microfuged (as previously) and the flow through discarded. The process was repeated with the addition of mouse Cot 1 DNA (10 µg), poly A (1 µg) and tRNA (4 µg) with the Tris-EDTA buffer. The samples were microfuged (10 000 g, 2 min) until the filter was dry in the middle and the probe formed a liquid ring. The flow through was discarded. The columns were then inverted in a fresh tube and microfuged (10 000 g, 2 min). Finally the samples were dried in a Speedvac.

2.2.20.5 Preparation of hybridisation to microarray slides

Probes were resuspended in 14 µl of hybridisation buffer (deionised formamide: 50X Denhardt's solution: water: 10% SDS; 10:1:2:1 filtered through a 0.45µ syringe filter) and added to 20X SSPE (6 µl; 3 M NaCl, 1 mM Na H₂PO₄ and 20 mM EDTA). Samples were denatured by heated at 100 °C at 2 min followed by incubation at 42 °C for 1 hour.

2.2.20.6 Washing of array coverslips

Coverslips were placed in racks and then washed in 1 % SDS for 30 min with occasional agitation followed by 5 rinses in fresh changes of pure water for 5 min per wash. The coverslips were then centrifuged (1000 g, 5 min) to remove residual water and stored in a dust free environment.

2.2.20.7 Microarray slide blocking, prescan and prehybridisation

Slides were heated at 100 °C for 2 min, washed in double distilled water to remove salts and centrifuged to dryness. Slides were pre-scanned to discard badly printed slides. To reduce non-specific binding of material to the array and the inherent green fluorescence, the slides were prehybridised under a coverslip at 40 °C, for 45 min using prehybridisation solution (55 % H₂O, 30 % 20X SSPE, 1 % Denhardtts, 0.5 % SDS and 1 % w/v BSA, filtered through a 0.45µ membrane). Slides were washed in 1 X SSC containing 0.03 % SDS for 10 min, allowing the coverslip to gently slide off, transferred to 0.2X SSC for 5 min and then 0.05X SSC for 5 min. The slides were dried by centrifugation.

2.2.20.8 Hybridisation

Using an array template as a guide, 20 µl of probe was placed on the left of the array and a coverslip placed gently over the array, enabling the probe to cover the array. The slides were placed in a humid airtight hybridisation chamber in a 42 °C water bath overnight. The slides were then washed in 1X SSC containing 0.03 % SDS for 10 min, allowing the coverslip to gently slide off, transferred to 0.2X SSC for 5 min and then 0.05X SSC for 5 min. The slides were dried by centrifugation.

2.2.20.9 Analysis of fluorescence and data processing

Data analysis was carried out by Dr Tim Gant. Fluorescence was measured using the GenePix 3.0 (version 3.0.0.85) software (Axon Instruments, Union City, USA). Feature sizes were determined using the inbuilt automated parameters in the first instance and then adjusted manually where appropriate. The fluorescence of each pixel within the feature was determined and the median fluorescence of these pixel measurements taken as the measure of fluorescence for the whole feature. The local background fluorescence was measured using the default parameters of GenePix 3.0. The raw feature data for each channel were globally centered by

reference to the median fluorescence of the whole feature set for that channel. To analyse the gene changes from the replicates of each of the three experiments, the absorbance data for both red and green channels were normalised. The data was normalized and processed to a final measure of differential gene expression, quantitated as a ratio of ET-743-treated over control, as previously described, using ConvertData version 3.4.0c (<http://www.le.ac.uk/cmht/twg1/array-fp.html>). Clustering analysis was performed by determination of the principal components of the score data using SIMCA-P (Umetrics, Bracknell, UK). The expression of genes which were significantly altered with reference to all the other genes on the same array, were used for a principal components analysis. Each microarray was kept as a separate entity for this analysis, as were the replicated clones on the microarrays. For the hepatic genes the expression of which was consistently up- or down-regulated by ET-743 (*cdc2a*, *ccnd1*, *abcbd1a*, *abcb1b* and *car 3*, see Results), homology between the mouse and the rat was established to be 98 % or above.

2.2.21 Preparation of membrane liver fractions for Western blotting

Approximately 2.5 g of liver was homogenised in 20 ml 0.1 M Tris containing 10 µg/mg pepstatin, 10 µg/mg leupeptin and 0.1 mM PMSF in isopropanol. The homogenate was spun at 1500 g for 10 min at 4 °C. The supernatant was removed, the pellet was resuspended and spun again. The supernatants were combined and spun at 100 000 g for 45 min at 4 °C. The pellet was resuspended in 10 ml Tris buffer, aliquoted and stored at -80 °C.

2.2.22 Polyacrylamide gel electrophoresis and Western blotting analysis, an overview

Proteins are denatured by sodium dodecyl sulphate (SDS) and separated due to size by electrophoresis. Proteins are transferred to a solid membrane for Western blotting analysis. For this procedure, an electric current is applied to the gel so that the separated proteins transfer through the gel and onto the membrane in the same pattern as they separate on the gel. All

sites on the membrane which do not contain blotted protein from the gel can then be non-specifically "blocked" so that antibody will not non-specifically bind to them. To detect the antigen blotted on the membrane, a primary antibody is added at an appropriate dilution and incubated with the membrane. In order to detect the antibodies which have bound, a second antibody is added. Finally after excess second antibody is washed free of the blot, a substrate is added which will precipitate upon reaction with the conjugate resulting in a visible band where the primary antibody has previously bound to the protein.

2.2.22.1 Preparation of the gel

The resolving gel solution was mixed and poured into a Hoeffer mini gel casting system. The gel was overlaid with water and left to set. Once set, the water was removed. The stacking gel solution was mixed and poured onto the resolving gel, a comb inserted and left to set.

7.5% Resolving gel solution

5 ml Acrylamide solution

5 ml Resolving gel buffer (1.5 M Tris-HCl, pH 8.8, 200 ml)

0.2 ml 10 % SDS

9.7ml ddH₂O

200 µl 10% Ammonium persulphate

15 µl TEMED

Stacking gel solution:

0.44 ml Acrylamide solution

0.83 ml Stacking gel buffer (0.5 M Tris-HCl, pH 6.8)

33 µl 10 % SDS

2.03 ml ddH₂O

25 µl 10 % Ammonium persulphate

3 µl TEMED

2.2.22.2 Loading and running the gels

The protein concentrations of the samples were determined by the Bradford assay (see 2.2.19). Equal volumes of protein sample and treatment buffer were mixed and boiled for 90 sec. The combs were removed from the gel and the wells washed with tank buffer. 25 μ l of samples (containing 10 μ g of protein) were loaded to each well alongside a prestained broad range protein molecular weight standard. The gel caster was filled with tank buffer. The samples were run through the gel at 150 V until the dye front ran off the bottom of the plate. Gels were removed and floated in transfer buffer. Proteins were transferred to a nitrocellulose membrane using a wet blotting system running at 100 V for 90 min. The membrane was blocked at 4°C in 5% non-fat milk in TBS-T.

Treatment buffer:

0.125 M stacking gel buffer

4 % SDS

20 % glycerol

0.02 % bromophenol blue

0.2 M DTT

ddH₂O

Tank buffer:

0.025 M Tris

0.192 M glycine

0.1 % SDS

ddH₂O

Transfer buffer:

48 mM Tris

39 mM glycine

20% methanol

0.037% SDS

2.2.22.3 Detection of P-glycoprotein expression

An antibody specific for p-glycoprotein (C129) was used at a dilution of 1:100 in 5 % milk in Tris buffered saline tween (TBS-T; 5 mM Tris pH 7.5, 15 mM NaCl, 0.1 % polyoxyethylene sorbitan monolaurate (Tween 20)) for 4 hours at 4°C on a mixing platform (Schrenk et al., 1993). Membranes were washed with TBS-T (3 washes x 10 min) and incubated with an anti-mouse HRP-linked secondary antibody (1:1000 dilution) in TBS-T for 1 hour. The signal was detected using an ECL detection system. Membranes were exposed to ECL hyperfilm for 30 sec and developed.

2.2.23 Cell cycle analysis

The object of the preparative method is to obtain intact nuclei. Nuclei are then stained with a fluorescent dye which intercalates with the DNA. Using a flow cytometer, a single nuclei suspension is forced to flow as single cells through a laser beam. The instrument measures fluorescent excitement and both forward and sideways light scatter. Sideways scatter reflect the density of a cell and forwards scatter reflects the size of a cell. The fluorescence is directly proportional to the total amount of DNA in each cell. Cells in G₂ and M phases of the cell cycle have double the DNA content of those in G₀ and G₁. Cells in S phase have DNA content lying between these extremes. The FACS machine plots a histogram of number of cells against DNA which reflects the state of the cell cycle (Ormerod, 1990).

Approximately 200 mg of liver was added to 10 ml of culture media and gently homogenised. The homogenate was filtered through a tea strainer. The cell suspension was centrifuged at 800 g for 5 min. The supernatant was removed and aspirated off. The pellet containing the cell nuclei was resuspended in 10 ml of stain detergent solution (100 ml of distilled water containing, 100 mg trisodium citrate, 56.4 mg NaCl, 30 µl Nonidet p-40, 10 ml propidium iodide (50 µg/ml), 100 µl Rnase) and mixed for 4 hours at 4 °C (Ormerod, 1990). The solution

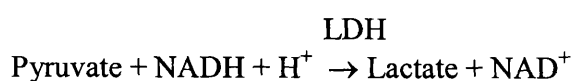
was filtered through a 100 µm pore nylon mesh. Flow cytometry analysis was performed using a FACS flow cytometer (Becton Dickinson) and Cell Quest software.

2.2.24 Isolation of primary rat hepatocytes

Hepatocytes were isolated from the liver of female Wistar rats by a 2 step *in situ* perfusion method (Seglen, 1976). The first step involved perfusion of the livers with buffer devoid of Ca^{2+} in order to irreversibly cleave desmosomal cell to cell interactions. In the second step, collagenase was added to the perfusion buffer to digest the extracellular matrix. The rat was anaesthetised with an i.p. injection of pentobarbitone (60 mg/kg) and prepared for perfusion. The abdominal cavity was opened and the heart injected with 0.5 ml heparin solution (2000 units/ml of saline). The hepatic portal vein was located and cannulated with a 20 GA cannular. The liver was perfused with the Hanks buffer saline solution (HBSS, without calcium, magnesium, sodium bicarbonate and phenol red but containing 1 mM ethylene glycol-bis (2-aminoethylether)-N, N, N', N'-tetraacetic acid (EGTA), and pre-saturated with carbogen, at a rate of 50 mls/min until the heart was clear of blood. The liver was then perfused with HBSS containing collagenase (100 mg/l.) and calcium chloride (332 mg/l). Perfusion continued until the liver showed signs of digestion. The softened liver was dissected out of the rat and transferred to a sterile beaker containing 50 ml William's E media (supplemented with 10 % FCS calf serum and penicillin/streptomycin 100 U/100 µg per ml) and gently stirred to dislodge the cells. The liver was gently pushed through a 100 µm mesh. The filtrate was centrifuged for 2 min at 50 g. The supernatant was removed and the pellet resuspended in 25 ml media. This was repeated twice and the cells were finally resuspended in 25 ml of media. Cells were counted using a haemocytometer. Hepatocyte viability determined by the trypan blue exclusion assay was routinely 85 % or higher.

2.2.25 Incubations with hepatocytes

Cell suspensions were diluted to 1×10^6 cells /ml of culture media (Williams E media containing 2 mM glutamine, 2 mM gentamicin, 10 nM insulin, 5 μ M transferrin solution, 5 mM nicotinamide, 0.75 μ g/ml zinc sulphate, 0.2 μ g/ml copper sulphate, 5 ng/ml sodium selenite, 30 nM dexamethasone sodium phosphate, 10 % FCS, penicillin/streptomycin 100 U/100 μ g per ml) and plated onto fibronectin coated 6 well plates and incubated at 37 °C in an atmosphere of 5 % CO₂ and 95 % air for 4 hours to attach. The supernatant medium was removed and fresh medium was added. Human hepatocytes were obtained from the Human Tissue Bank, De Monfort University, Leicester. Isolated human hepatocytes were cultured as described for rat hepatocytes. Hepatocytes were precultured for 24 hours, then exposed to fresh medium to which ET-743 dissolved in DMSO was added to yield final concentrations of 1 nM – 1 μ M. The final DMSO concentration was 1 %, which on its own did not affect hepatocyte viability. Hepatotoxicity was assessed by leakage of lactate dehydrogenase (LDH) into the medium. Samples of media were taken after 48, 72 and 96 hours for viability assessment by the LDH assay kit (Sigma-Aldrich). The method is a ultraviolet, kinetic method. LDH catalyses the following reaction and the decrease in absorbance at 340 nm due to the formation of the NAD is directly proportional to LDH activity.



Degree of leakage of LDH into the medium was expressed as a percentage (X) of total cellular LDH enzyme content. Total LDH content was established by adding Triton-X-100 to untreated hepatocyte cultures, which caused complete lysis. Viability was calculated as 100 minus X, and expressed as %.

For investigation of the effects of N-acetylcysteine on the hepatotoxicity of ET-743, hepatocytes were exposed to N-acetylcysteine (1 mM), and ET-743 was added one hour later.

2.2.26 Study of ET-743 levels in liver and plasma.

Female Wistar rats received ET-743 (40 µg/kg, i.v.) with or without pre-treatment with dexamethasone 24 hours prior to ET-743 (10 mg/kg p.o.). Blood and liver tissue was collected before and 30 min, 1, 3, 6, 12, 24 and 72 hours *post* treatment with ET-743. Blood samples were taken by cardiac puncture and placed in heparinised tubes. Plasma was obtained by centrifugation (2000 rpm, for 25 min). Liver was excised and homogenized (25% in phosphate buffer 0.2 M, pH 7.4). Liver homogenate was centrifuged (1000 g, 4°C). The supernatant was collected and frozen at -80°C until assayed. Quantification of ET-743 levels was performed by collaborators at Istituto di Ricerca Farmacologiche Mario Negri, Milan, Italy. An aliquot (0.3 ml) of supernatant was mixed with 0.7 ml ammonium acetate buffer (0.2M, pH 5.0), the mixture was kept on ice (30 min), centrifuged (1000 g for 10 min), and subjected to solid phase extraction (Bond Elut non-end-capped CN cartridges). Elution was carried out with methanolic hydrochloric acid (0.1 M, 2.5 ml). The elute was evaporated, the residue dissolved in mobile phase (200 µl), and an aliquot (20 µl) was injected onto the column. ET-743 was measured by HPLC coupled with electrospray ionization tandem mass spectrometry, as described by Rosing et al. (Rosing et al., 1998) using an API 3000 triple quadrupole mass-spectrometer (Applied Biosystem - Sciex, Toronto, Canada) operating in positive ion mode (standard TurboIonSpray source). A methanol-water (75:25, v/v) mixture containing 5 mM ammonium acetate and 4% (v/v) formic acid was used as the mobile phase. At a flow-rate of 200 µl/min, the mobile phase was pumped through a Zorbax Rx-C18 column (15 x 2.1 mm i.d., particle size 5 µm). The column outlet was connected directly to the TurboIon-Spray sample inlet without splitting. Ions were created at atmospheric pressure and were transferred to a triple quadrupole mass-spectrometer.

2.2.27 MCF-7 cells

MCF-7 cells were grown in RPMI-1640 medium supplemented with 10 % FCS and 2 nM glutamax. Cells at 70-80 % confluency were washed in PBS, trypsinised with T/E and pelleted

at 200 g for 3 min. Cells were re-seeded at required densities in flasks and maintained in an incubator at 37 °C in 5 % CO₂.

2.2.28 Effect of ET-743 on MCF-7 cell growth

MCF-7 cells were seeded at 2×10^6 cells /ml of medium into 6-well plates. The cells were incubated for 24 hours to plate down. The media was removed and replaced with fresh media containing ET-743 dissolved in DMSO to yield final concentrations of 0.1-1 nM or DMSO alone. Final concentration of DMSO was 1 %. After 48 hours, cells were trypsinised and counted using a Coulter counter (Beckman). The concentration of ET-743 found to inhibit cell growth by 50 % (IC₅₀) was 0.2 nM.

2.2.29 *In vitro* bioassay to assess the cytotoxicity of ET-743 after incubation with rat liver microsomes.

Aliquots of 400 µl ET-743 (20 nM) were pipetted into glass vials with 200 µl of 0.5 M phosphate buffer (pH 7.4) and 400 µl of NADPH generating system (3.25 mM NADP, 8.25 mM MgCl₂, 8.25 mM glucose-6-phosphate and 0.6 units/ml glucose-6-phosphate dehydrogenase). Next, 50 µl of microsomes previously prepared from dexamethasone treated (10 mg/kg, 24 hours prior to microsome preparation) or untreated rats and incubated at 37°C for 40 min in a shaking water bath. Control experiments were performed without microsomes. The reaction was terminated by adding 1 ml of ice-cold methanol. The samples were centrifuged at 200 g for 3 min to separate proteins. The supernatant was removed and 100 µl was added to MCF-7 cells in 2 mls of medium, seeded at 2×10^5 cells /ml of medium into 6-well plates, the previous day. The concentration of ET-743 in the wells was 0.2 nM. After 48 hours, cells were trypsinised and counted using a Coulter counter.

2.2.30 Statistical analysis

Data was analysed using Excel (Office 2000) and Origin 6.0. Results were subject to statistical analysis using Minitab (version 13) software package. Values were subjected to one-way analysis of variance (ANOVA) and statistical significance was established by *post hoc* Tukey's pairwise comparison.

CHAPTER 3

ET-743 hepatotoxicity

3.1 Introduction

Preclinical toxicity studies performed in mice, rats, dogs and monkeys demonstrated that liver was one of the main targets for ET-743 toxicity. Information regarding these toxicity studies has not been published. Hepatic effects were observed as an increase in liver enzymes as well as evidence of cholangitis (section 1.10.4). In some species the hepatotoxic effects were reversible, however in the female rat, the most sensitive species, the effects were irreversible. Patients who receive ET-743 frequently develop acute, but reversible transaminitis and subclinical cholangitis characterised by increases in ALP and/or bilirubin, which is not unlike the hepatotoxicity observed in preclinical toxicity studies. The female rat was chosen as the model in which to study the hepatotoxicity of ET-743 as it is the most susceptible with respect to the adverse hepatic side effects and therefore responses towards strategies designed to reduce the hepatotoxicity might be easy to detect.

The aim of the work described in this chapter was to fully characterise ET-743 liver toxicity in the female Wistar rat. This aim was achieved by detailed analysis of changes in liver biochemistry and liver pathology. In addition, cDNA microarray analysis was performed to identify hepatic gene changes during the development of cholestasis and the associated adaptive response after ET-743 treatment. The purpose of this study was to link the clinical chemistry and pathology of inflammation, cholestasis, necrosis and fibrosis to differential gene expression with the overall aim of increasing our understanding of the mechanisms of hepatotoxicity. Also, it may be possible to identify gene changes which may predict hepatic damage. Additionally, the liver pathology and clinical chemistry induced by ET-743 was compared in male and female rats not only to confirm the increase in sensitivity of the female rat, but also in an attempt to explain this gender related increase in toxicity.

The liver damage induced by another cholestatic agent, α -naphylisothiocyanate (ANIT), was also investigated in female Wistar rats in terms of biochemistry, pathology and hepatic gene expression and compared with that of ET-743. The specific question that was addressed was

Chapter 3

whether the gene changes observed after ET-743 treatment are generic to cholestasis and associated repair, or whether any gene expression changes are unique to ET-743.

Results

3.2 Effects of ET-743 on liver biochemistry

In a preliminary dose-finding experiment, ET-743 administered at 75 $\mu\text{g}/\text{kg}$, the maximum tolerated dose in the female rat, elicited severe toxicity, resulting in mortality. Therefore the dose was reduced to 40 $\mu\text{g}/\text{kg}$, which caused moderate toxicity but avoided mortality. Animals were killed at 6, 12, 24 hours; 2, 3, 6, 12, 24 or 48 days; or 3 months after administration. There were no acute effects at the time of injection of ET-743. Within 4-6 days after dosing, animals lost 15 % of their body weight, compared with controls and 2 deaths occurred at 6 days. Surviving animals started to gain weight at the same rate as untreated animals after 8 days. Rats had intense yellow stained urine for the first week after treatment. At autopsy, rats had yellow subcutaneous and other body fat, and enlarged livers.

Plasma levels of ALP, AST and total bilirubin were measured at each time point up to 3 months after a single dose of ET-743 at 40 $\mu\text{g}/\text{kg}$. Plasma levels of bilirubin started to increase 48 hours after treatment (figure 3.1) and on day 3, levels were elevated 7-fold compared to untreated rats. The bilirubin levels remained elevated until 12 days and reverted to basal levels by 24 days. Plasma levels of ALP and AST were elevated by approximately two-fold at 48 hours after treatment compared to controls (figure 3.1). Levels remained significantly elevated until 72 days and 96 days with respect to ALP and AST.

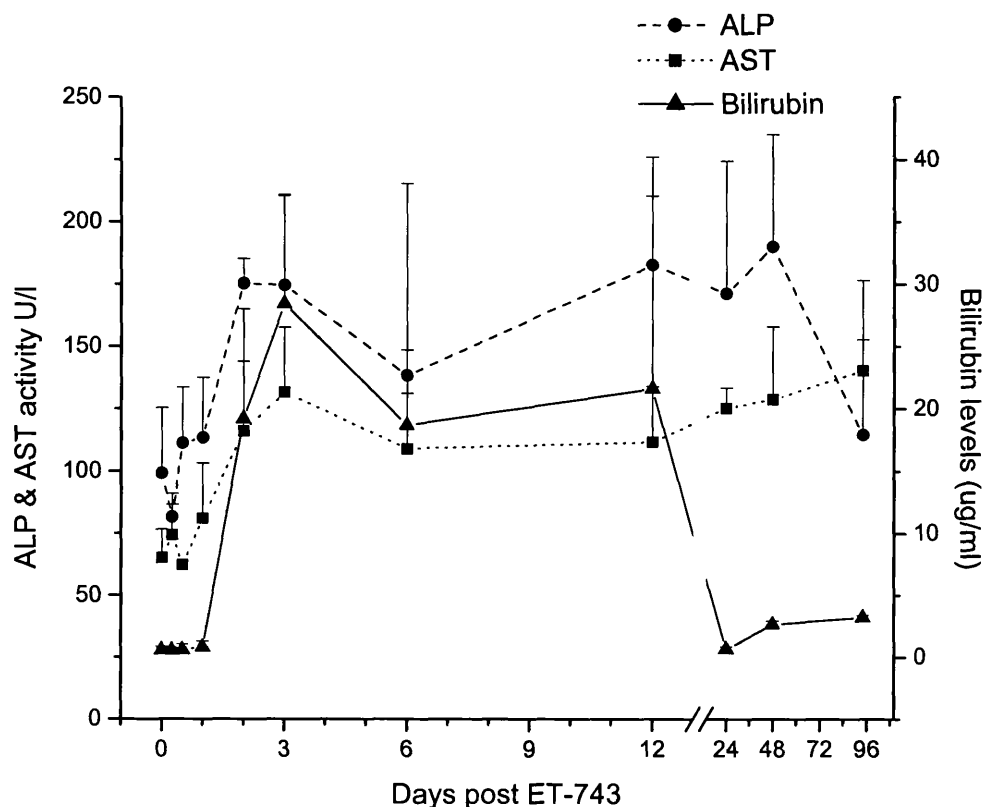


Figure 3.1 Time course of changes in concentration of total bilirubin and activities of liver enzymes alkaline phosphatase and aspartate aminotransferase in the plasma from female rats that received ET-743 (40 µg/kg, i.v.). Levels of bilirubin (▲) are presented in µg/ml (right axis) and activities of ALP (●) and AST (■) are given as units /litre (left axis). Values are the mean ± SD of four animals /time point. The values observed at the following time points are significantly different ($p < 0.05$ by ANOVA) from those measure in control rats: bilirubin, days 3,6,12; ALP, days 2, 3, 12, 24 and 48; AST, days 2, 3, 12, 24, 48 and 96.

Activities of CYP3A2, CYP1A1/2 and CYP2E1 were measured at 3, 6, 12, 24 and 48 days after a single i.v. dose of ET-743 (40 $\mu\text{g}/\text{kg}$). Levels of CYP1A1/2 and CYP 2E1 were significantly reduced at 3 days after treatment to almost unmeasurable levels compared to untreated rats (figure 3.2). Between 12 and 24 days the activities had returned to basal levels. The activity of CYP3A2 was diminished by 36 % at day 3 after administration, and this decrease persisted for up to 24 days. Levels of total microsomal cytochrome P450 protein were also measured and were decreased by 33 % after 3 days, which persisted up to 48 days (figure 3.2).

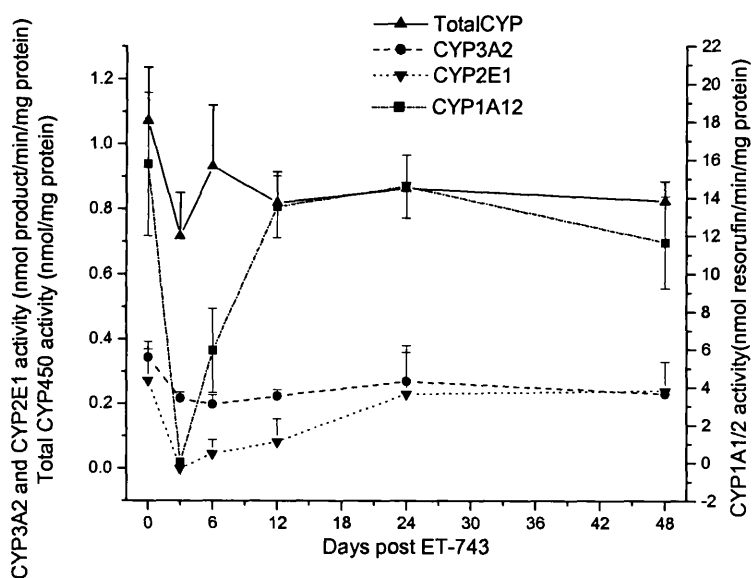


Figure 3.2 Time course of changes of cytochrome P450 protein levels and activities of CYP1A1/2, CYP2E and CYP3A2 in liver microsomes obtained from female rats that received ET-743 (40 $\mu\text{g}/\text{kg}$, i.v.). Concentrations are expressed as nmol cytochrome P450 protein/mg microsomal protein (\blacktriangle left axis) or as nmol product generated /min/mg microsomal protein for CYP3A2 (\bullet left axis), CYP2E1, (\blacktriangledown left axis) and CYP1A1/2 (\blacksquare right axis). Values are the mean \pm SD of four animals /time point. The values observed at the following points are significantly different ($p < 0.05$ by ANOVA) from those measured in control rats: total cytochrome P450, day 3; CYP3A and CYP2E1, days 3, 6 and 12; and CYP1A1/2, days 3 and 6.

3.3 Effect of ET-743 on liver cell pathology

Female Wistar rats received a single i.v. dose of ET-743 (40 µg/kg). Heart, kidney, pancreas and spleen were within normal limits. There was mild loss in cellularity of bone marrow at 12, 24 and 72 hours. In the small intestine, there was a degenerative change in the cells deep within the intestinal crypts as early as 6 hours after treatment. This degeneration was visible up to 24 hours but had disappeared by day 3. Livers obtained 6 and 12 hours after ET-743 administration did not show any signs of pathological change, whereas in livers obtained at 24 hours, there was focal degenerative alteration in the epithelial cells lining the larger bile ducts. By day 2, these changes were characterised by degenerative and patchy focal necrosis of bile duct epithelial cells in many bile ducts accompanied by a modest acute inflammatory infiltrate in all treated animals (figure 3.3 A and B). A day later, the damage was more pronounced with increased inflammation and early signs of regeneration of the epithelial cells characterised by enlarged cell cytoplasm and large irregular nuclei with occasional mitoses (figure 3.3 C). Six and 12 days after treatment with ET-743, bile ducts were surrounded by dense, poorly cellular, concentric fibrosis (sclerosis) and by mesenchymal cells that stained for α -smooth muscle actin (figure 3.3 E and F). After 24 days, the inflammation in the portal tract had diminished substantially, although periductal fibrosis remained prominent. Most hepatocytes showed relatively little alteration. In some treated rats, rounded focal zones of hepatic necrosis and haemorrhage were observed from day 2 which persisted up to 3 months (figure 3.3 D). Some focal pigmentation was observed around zones of necrosis at time points after 24 hours.

Electron microscopy showed that within 2 days after ET-743 administration there was focal injury in the epithelium of bile ducts including apoptosis, which resulted in the liberation of cell debris into the lumen (figure 3.4). Despite these slight changes in the biliary epithelium, most of the liver remained normal. The foci of hepatic necrosis and haemorrhage did not correlate with particular regions of the lobule. There was little or no inflammation within the foci. Hepatocytes immediately surrounding the focal lesions

tended to have rather more smooth endoplasmic reticulum than controls but were essentially within normal limits (figure 3.4). Abnormal mitochondria were evident in many necrotic cells.

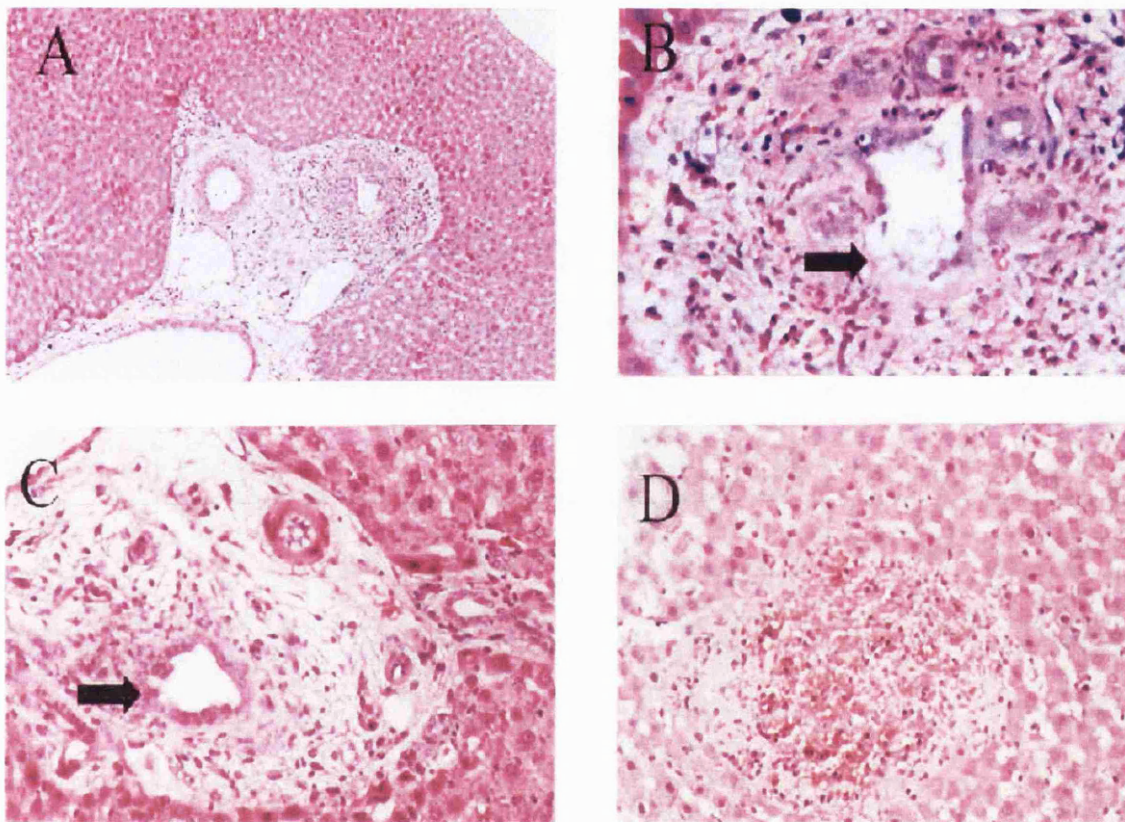


Figure 3.3 Photomicrographs of liver sections from female rats that received ET-743 (40 µg/kg, i.v.) 2 (A, B, D) or 3(C) days before tissue excision. Staining was by H & E. Magnification was X 50 in A; X 130 in C and D; and X 200 in B. The following features characterise manifestations of ET-743 hepatotoxicity: swelling of the portal tract with little alteration in the hepatic parenchyma (A); ulceration of the bile duct epithelium (arrow) and sparse inflammatory infiltrate (B); damage to the bile duct epithelium (arrow) and mild hyperplasia (C); and round focus of haemorrhagic necrosis (D). The sections are representative of four to eight separate animals. Histopathological analysis was carried out by Dr Peter Greaves.

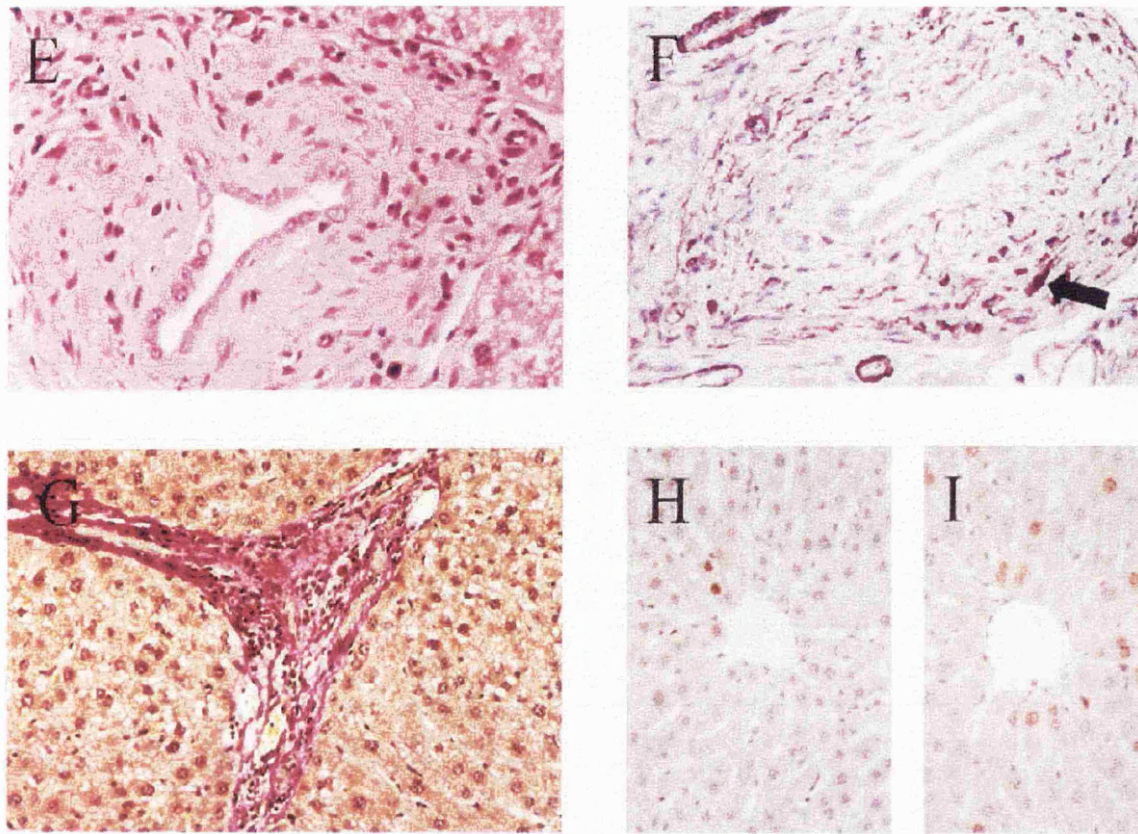


Figure 3.3 Photomicrographs of liver sections from female rats that received ET-743 (40 $\mu\text{g}/\text{kg}$, i.v.) 3 (I), 12 (E and F), or 48 days (G) before tissue excision and liver sections from an untreated rat (H). Staining was by H & E (E), immunoperoxidation for α -smooth muscle actin (F), van Gieson's stain (G), or Ki-67 antiserum (H and I). Magnification was X 130 in G, H and I; and X 200 in E and F. The following features characterise manifestations of ET-743 hepatotoxicity: peribiliary fibrosis and enlarged biliary epithelium cells (E); spindle cells staining for α -smooth muscle actin (for example see arrow in F); presence of dense residual collagen in the portal tract marked by red staining (G); and increased staining of nuclei for Ki-67 antigen (H and I). The sections are representative of four to eight separate animals.

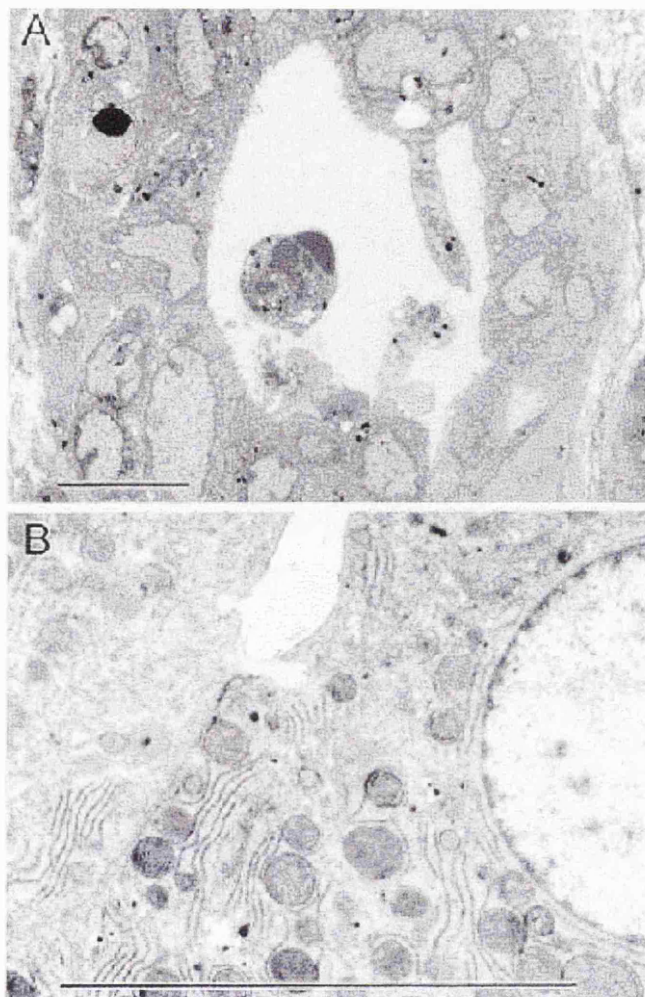


Figure 3.4 Electron micrographs of a bile duct (A) and a typical hepatocyte (B) observed in female rats 2 days after treatment with ET-743 (40 $\mu\text{g}/\text{kg}$, i.v.). In A, note focal injury, including some apoptosis, to bile duct epithelium with liberation of some cell debris into the lumen. The hepatocyte in B, which was located near a zone of necrosis, displays slightly more smooth endoplasmic reticulum than hepatocytes in control animals but is essentially within normal limits. Bars equals 10 μM . The micrographs are representative of four separate animals. Analysis by electron microscopy was performed by Dr David Dinsdale.

3.4 Effects of ET-743 on hepatic gene expression

The hepatic gene expression changes after ET-743 administration are displayed in tables 3.1 and 3.2. Among the cluster of up-regulated genes are the cell cycle genes *cdc2a* and *ccnd1*; the rodent homologues of human CDC2 and Cyclin D1, respectively and the three ABC transport genes *abcb1a* and *abcb1b*, which are equivalent to human ABCB1 and impart drug resistance, and *abcb4* which is implicated in phospholipid excretion (figure 3.5). The time course of expression of *abcb1a* and *abcb1b* mirrors the changes in serum bilirubin concentration (figure 3.6). In order to validate at the functional level the induction of *abcb1* gene expression by ET-743, Western blot analysis was performed to detect hepatic P-glycoprotein (P-gp) expression, encoded by *abcb1a* and *abcb1b*. Livers from three ET-743 treated rats and three untreated rats were removed for analysis of P-gp. As shown in figure 3.7, Western blot analysis revealed two bands at 140 and 170 kDa, probably corresponding to P-gp1 encoded by *abcb1* and P-gp2 encoded by *abcb4*. ET-743 treatment dramatically increased hepatic P-gp expression by 40-fold which is consistent with the increase in *abcb1* gene expression.

Genes consistently down regulated at 3 days after ET-743 administration were *cyp1a2*, *cyp3a11* and *cyp2e1*. The expression levels mirrored the down-regulation in the activity of CYP1A1/2, CYP3A4 and CYP2E1. Another cluster of genes consistently down regulated consisted of the haemoglobin genes, *hba-x*, *hba-a1*, *hbb-b1*, *hbb-bh1* and *hbb-y* (figure 3.8). One of the most prominent down-regulated genes was *car3*, carbonic anhydrase which reached a nadir on day 6 after administration of ET-743 (figure 3.9).

Gene symbol	Gene name
<i>Abcb4</i>	ATP-binding cassette, sub-family B (MDR/TAP), member 4
<i>Ltb</i>	lymphotoxin B
<i>Cdc2a</i>	cell division cycle 2 homolog A
<i>Mt1</i>	metallothionein 1
<i>Abcb1a</i>	ATP-binding cassette, sub-family B (MDR/TAP), member 1A
<i>Abcb1b</i>	ATP-binding cassette, sub-family B (MDR/TAP), member 1B
<i>Cdkn1a</i>	cyclin-dependent kinase inhibitor 1A
<i>Igfbp2</i>	insulin-like growth factor binding protein 2
<i>Mdu1</i>	solute carrier family 3, member 2
<i>Ifi10</i>	chemokine (C-X-C motif) ligand 10
<i>Arnt1</i>	aryl hydrocarbon receptor nuclear translocator-like
<i>Scd1</i>	stearoyl-Coenzyme A desaturase 1
<i>Apobec2</i>	apolipoprotein B editing complex 2
<i>Ccnd1</i>	cyclin D1
<i>Mt2</i>	metallothionein 2
<i>Fabp2</i>	fatty acid binding protein 2, intestinal
<i>Krt2-8</i>	keratin complex 2, basic, gene 8
<i>Ptmb10</i>	thymosin, beta 10
<i>Cd63</i>	Cd63 antigen
<i>Col5a2</i>	procollagen, type V, alpha 2
<i>Apoa1</i>	apolipoprotein A-I
<i>Tubb5</i>	tubulin, beta 5
<i>Krt2-4</i>	keratin complex 2, basic, gene 4
<i>Krt1-19</i>	keratin complex 1, acidic, gene 19
<i>Sat</i>	spermidine/spermine N1-acetyl transferase
<i>Pcna</i>	proliferating cell nuclear antigen
<i>App</i>	amyloid beta (A4) precursor protein
<i>Egr1</i>	early growth response 1
<i>Gstm1</i>	glutathione S-transferase, mu 1
<i>Emp3</i>	epithelial membrane protein 3
<i>Gstm2</i>	glutathione S-transferase, mu 2
<i>Cd151</i>	CD151 antigen
<i>Gfap</i>	glial fibrillary acidic protein
<i>Odc</i>	ornithine decarboxylase, structural
<i>Actg</i>	actin, gamma, cytoplasmic
<i>Lpl</i>	lipoprotein lipase
<i>Hpxn</i>	hemopexin
<i>Clu</i>	clusterin
<i>H2-T23</i>	histocompatibility 2, T region locus 23
<i>H2-T10</i>	histocompatibility 2, T region locus 10
<i>Col3a1</i>	procollagen, type III, alpha 1

<i>Anxa2</i>	annexin A2
<i>Synd1</i>	syndecan 1
<i>Hmgcr</i>	3-hydroxy-3-methylglutaryl-Coenzyme A reductase
<i>Pbx1</i>	pre B-cell leukemia transcription factor 1
<i>H2-K</i>	histocompatibility 2, K region
<i>Glns-ps1</i>	glutamine synthetase pseudogene 1
<i>Hes6</i>	hairy and enhancer of split 6, (<i>Drosophila</i>)
<i>Mif</i>	macrophage migration inhibitory factor
<i>Tuba4</i>	tubulin, alpha 4
<i>Cola2</i>	procollagen, type I, alpha 1
<i>Ctsb</i>	cathepsin B
<i>Dag1</i>	dystroglycan 1

Table 3.1 Genes up-regulated at one or more time points after ET-743 administration (40 µg/kg, i.v.) in female rats. Groups of three ET-743-treated rats were paired with three untreated rats and were killed at 6 hours and 1, 2, 3, 6, and 24 days after dosing. Gene expression changes were determined by cDNA microarrays. For the genes listed, expression was up-regulated in all three arrays for a particular time point and the mean change in gene expression was greater than two-fold. Genes have been named in order of greatest up-regulation.

Gene symbol	Gene name
<i>Ltc4</i>	leukotriene C4 synthase
<i>Mh3</i>	myosin, heavy polypeptide 3, skeletal muscle, embryonic
<i>Gypa</i>	glycophorin A
<i>H3f3a</i>	H3 histone, family 3A
<i>Tbxa2r</i>	thromboxane A2 receptor
<i>Hba-a1</i>	hemoglobin alpha, adult chain 1
<i>Tgfb3</i>	transforming growth factor, beta 3
<i>Ier2</i>	immediate early response 2
<i>Zfp144</i>	Zinc finger protein 144
<i>3110023K12</i>	RIKEN cDNA 3110023K12 gene
<i>Gp49</i>	glycoprotein 49 B
<i>Nkx2</i>	NK2 transcription factor related, locus 6
<i>Zic4</i>	zinc finger protein of the cerebellum 4
<i>Spnb3</i>	spectrin beta 3
<i>Car3</i>	carbonic anhydrase 3
<i>Sez6</i>	seizure related gene 6
<i>Cryba</i>	crystallin, beta A2
<i>Rad50</i>	RAD50 homolog
<i>Prkm3</i>	mitogen activated protein kinase 3
<i>Zfp67</i>	zinc finger protein 67
<i>Orct11</i>	solute carrier family 22 (organic anion transporter), member 6
<i>Hba-x</i>	hemoglobin X, alpha-like embryonic chain in Hba complex
<i>Smarca</i>	SWI/SNF related, matrix associated, actin dependent regulator of chromatin, subfamily a, member 3
<i>Tgfb1i1</i>	transforming growth factor beta 1 induced transcript 1
<i>Itm2</i>	integral membrane protein 2A
<i>Akr1b1</i>	aldo-keto reductase family 1, member B
<i>Apba2</i>	amyloid beta (A4) precursor protein-binding, family A, member 2
<i>Hbb-bh</i>	hemoglobin Z, beta-like embryonic chain
<i>Myd116</i>	myeloid differentiation primary response gene 116
<i>Hexb</i>	hexosaminidase B
<i>Hbb-b1</i>	hemoglobin, beta adult major chain
<i>Pdi2</i>	peptidyl arginine deiminase, type II
<i>Lox</i>	lysyl oxidase
<i>Nr2cl</i>	nuclear receptor subfamily 2, group C, member 1
<i>Atf4</i>	activating transcription factor 4
<i>Rab4a</i>	RAB4A, member RAS oncogene family
<i>Cea2</i>	pregnancy specific glycoprotein 17
<i>Sipal</i>	signal-induced proliferation associated gene 1
<i>Mcccl</i>	methylcrotonoyl-Coenzyme A carboxylase 1 (alpha)
<i>Mup</i>	major urinary protein 2
<i>Madh</i>	MAD homolog 5

<i>Hbb-y</i>	hemoglobin Y, beta-like embryonic chain
<i>Apoa4</i>	apolipoprotein A-IV
<i>Hmr</i>	nuclear receptor subfamily 4, group A, member 1
<i>Ptgs1</i>	prostaglandin-endoperoxide synthase 1
<i>Cyp3a11</i>	Cytochrome P450 3a11
<i>Egf</i>	epidermal growth factor
<i>Tcf2</i>	transcription factor 2
<i>Per</i>	period homolog 1
<i>Rnf19</i>	ring finger protein (C3HC4 type) 19
<i>Dlgh3</i>	discs, large homolog 3
<i>Nbl1</i>	neuroblastoma, suppression of tumorigenicity 1
<i>Cdx2</i>	caudal type homeo box 2
<i>Ykt6</i>	prenylated SNARE protein
<i>Sdf1</i>	chemokine (C-X-C motif) ligand 12
<i>Itk</i>	IL2-inducible T-cell kinase
<i>Rad9</i>	RAD9 homolog
<i>G6pc</i>	glucose-6-phosphatase, catalytic
<i>Cyp1a2</i>	Cytochrom p450 1a2
<i>Terf1</i>	telomeric repeat binding factor 1
<i>Ptpn16</i>	dual specificity phosphatase 1
<i>Top2b</i>	topoisomerase (DNA) II beta
<i>Itp1</i>	inositol 1,4,5-triphosphate receptor 1
<i>Mrpp1f3</i>	mitogen regulated protein, proliferin 3
<i>Tfam</i>	transcription factor A, mitochondrial
<i>Rpl18</i>	ribosomal protein L18
<i>Flt4</i>	FMS-like tyrosine kinase 4
<i>Myc</i>	myelocytomatosis oncogene
<i>Spilc1</i>	serine palmitoyltransferase, long chain base subunit 1
<i>Cyp2e1</i>	Cytochrom P450 2e1
<i>Prkar1b</i>	protein kinase, cAMP dependent regulatory, type I beta
<i>44921525H23</i>	RIKEN cDNA 4921525H23 gene
<i>Anp32</i>	acidic (leucine-rich) nuclear phosphoprotein 32 family, member A

Table 3.2 Genes down-regulated at one or more time point after ET-743 (40 µg/kg, i.v.) administration in female rats. Groups of three ET-743-treated rats were paired with three untreated rats and were killed at 6 hours and 1, 2, 3, 6, and 24 days after dosing. Gene expression changes were determined by cDNA microarrays. For the genes listed, expression was down-regulated in all three arrays for a particular time point and the mean change in gene expression was greater than two-fold. Genes have been named in order of greatest down-regulation.

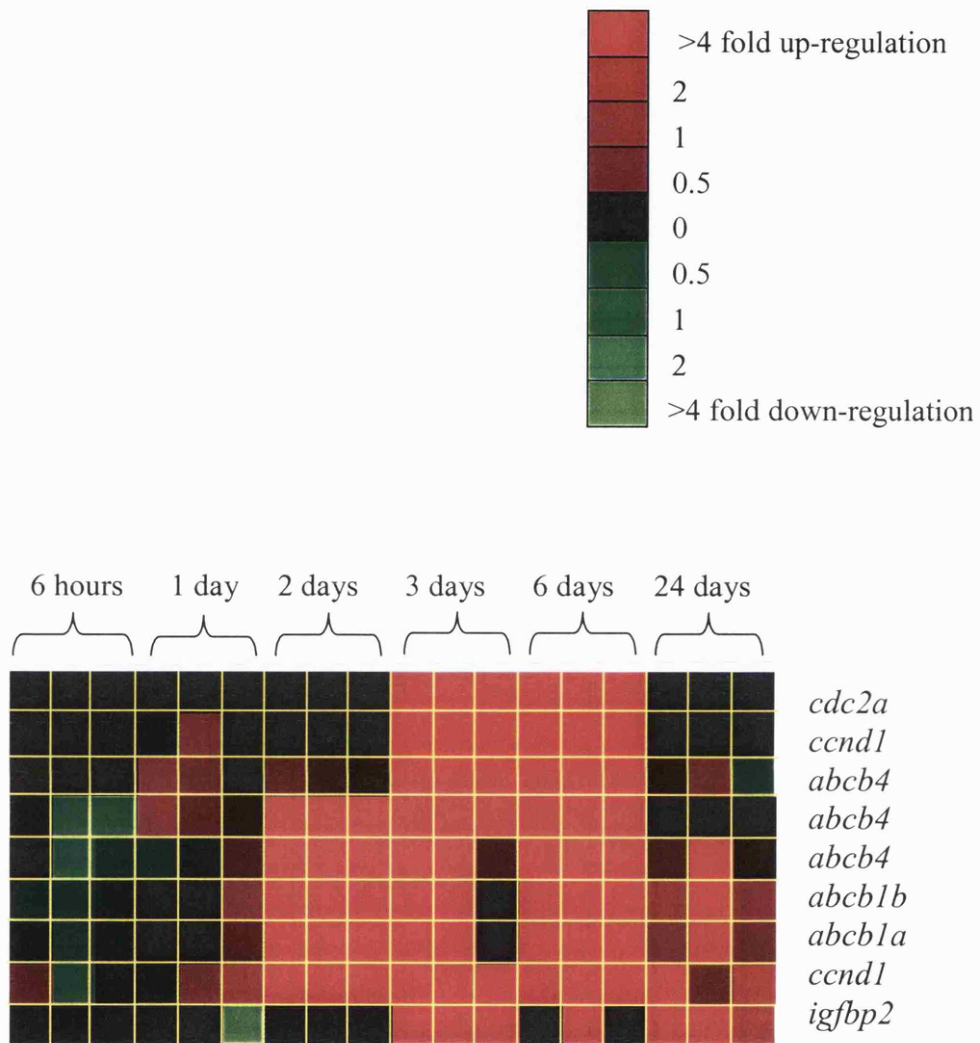


Figure 3.5 A cluster of genes up-regulated after ET-743 (40 $\mu\text{g}/\text{kg}$, i.v.) administration. The gene expression patterns were determined by cDNA microarray. At each time point, three arrays were used for each pair of rats; treated and control. Genes were clustered depending on gene expression pattern.

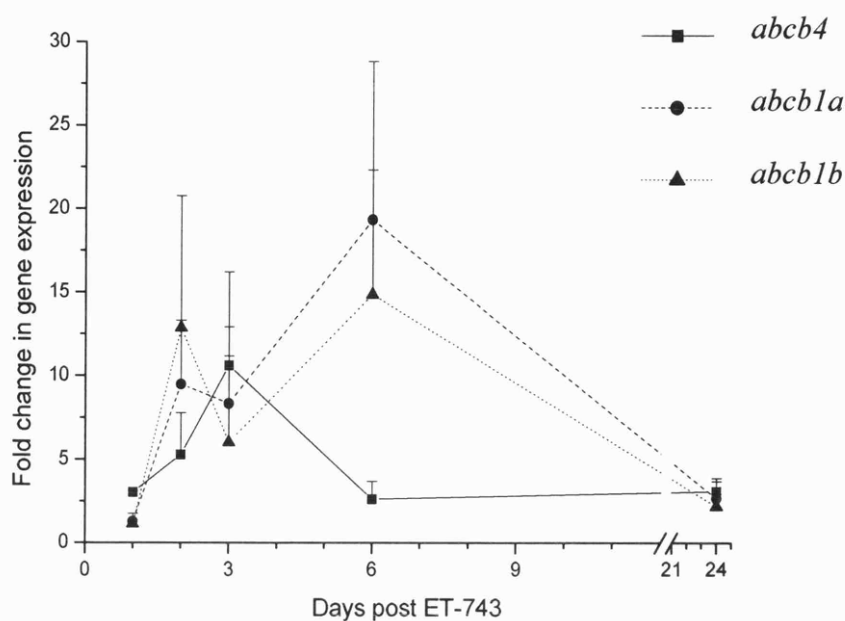


Figure 3.6 Time course of changes in hepatic expression of ABC genes *abcb4* (■), *abcb1a* (●) and *abcb1b* (▲) in livers of female rats that received ET-743 (40 µg/kg, i.v.). The gene expression patterns were determined by cDNA microarray. The normalized intensity values from the hybridisation of the RNA from treated rats at 2, 3 and 6 day time points for *abcb1a* and *abcb1b* were significantly different ($p < 0.05$ by ANOVA) from the values of control rat RNA hybridised on the same microarray. The SDs indicate the variability in the measure of the ratio of treated: control rats.

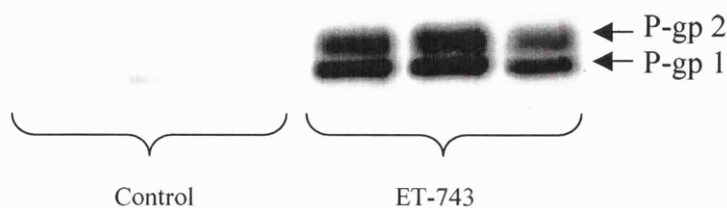


Figure 3.7 Western blot showing the expression of P-glycoprotein in the liver after ET-743 treatment (40 µg/kg, i.v.), compared to control liver. Proteins were extracted from three ET-743-treated and three control animals, killed 3 days after treatment.

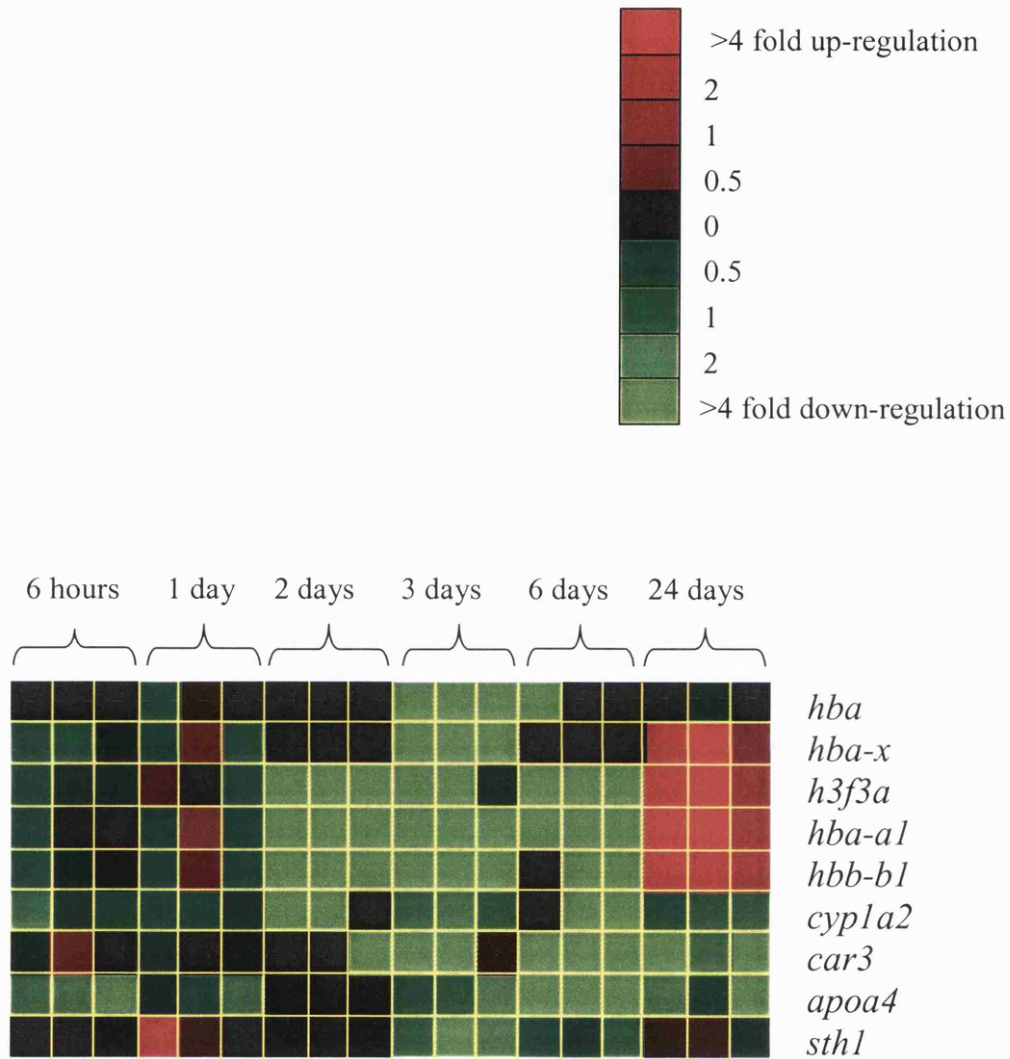


Figure 3.8 A cluster of genes down-regulated after ET-743 (40 µg/kg, i.v.) administration. The gene expression patterns were determined by cDNA microarray. At each time point, three arrays were used for each pair of rats; treated and control. Genes were clustered depending on gene expression pattern.

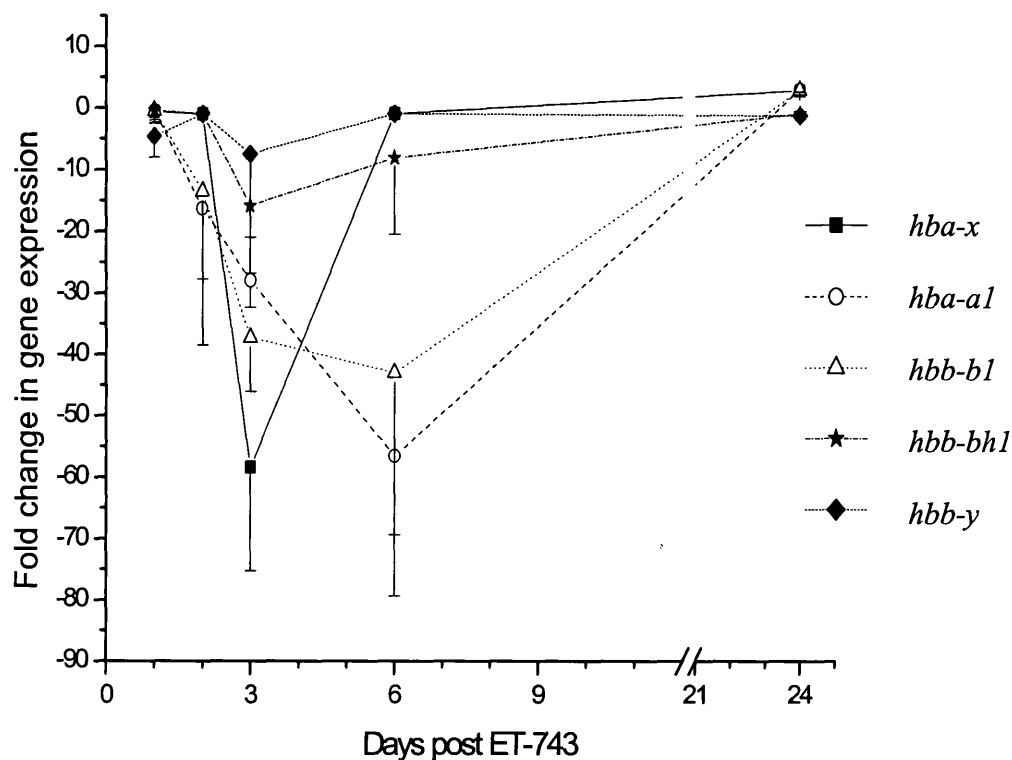


Figure 3.9 Time course of changes in expression in *hba-x* (■), *hba-a1* (○), *hbb-b1* (△), *hbb-bh1* (★) and *hbb-y* (◆) genes in livers of female rats that received ET-743 (40 $\mu\text{g}/\text{kg}$, i.v.). Gene expression was determined by cDNA microarray. The normalized intensity values from the hybridisation of the RNA from treated rats at 3 and 6 day time points for *hba-x*, *hba-a1*, *hbb-b1* and *hbb-bh1* genes and the 6 day point for *hba-a1* and *hbb-b1* were significantly different ($p < 0.05$ by ANOVA) from the values for control rat RNA hybridised on the same microarray. The SDs indicate the variability in the measure of the ratio of treated: control rats.

3.5 Effects of ET-743 on indices of hepatic cell proliferation

The dramatic increase in hepatic expression of *cdc2a* determined by DNA microarray peaked on day 3 after administration of ET-743 (figure 3.10). It remained elevated until day 6 and by day 24 had returned to basal levels. A similar pattern in expression was observed for *ccnd1*, although the elevation was smaller and persisted until day 24. Staining for Ki-67, a marker of DNA synthesis, in liver nuclei from rats that had received ET-743 was significantly elevated in comparison with that in control rats [figure 3.3 (H and I) and figure 3.11]. The ET-743-induced increase in Ki-67 proliferation index was comparable with increases in *cdc2a* expression. The peak in Ki-67 index occurred at 6 days and returned to basal levels by day 12. In addition, staining for proliferating cell nuclear antigen was markedly elevated in ET-743-treated rats 3 days after dosing compared to control animals. Consistent with these increases in markers of hepatic cellular proliferation, the liver weights were significantly elevated after ET-743 treatment compared to controls. Liver weights peaked at 12 days after ET-743 treatment, 6 days after the peak in *cdc2a* gene expression and Ki-67 index (figure 3.11). Due to this evidence of hepatic cell proliferation it was decided to investigate the distribution of liver cells at different stages of the cell cycle. There were subtle but significant changes in the cell cycle after ET-743 treatment. The proportion of S-phase hepatocytes increased from 0 % in control to 7.3 ± 1.5 % after ET-743 treatment, whereas the number of cells in G1 and G2-M respectively amounted to 62.6 ± 7.2 % and 37 ± 7.2 % in control rats and 61.0 ± 5.2 % and 31.4 ± 5.3 % in treated rats (figure 3.12).

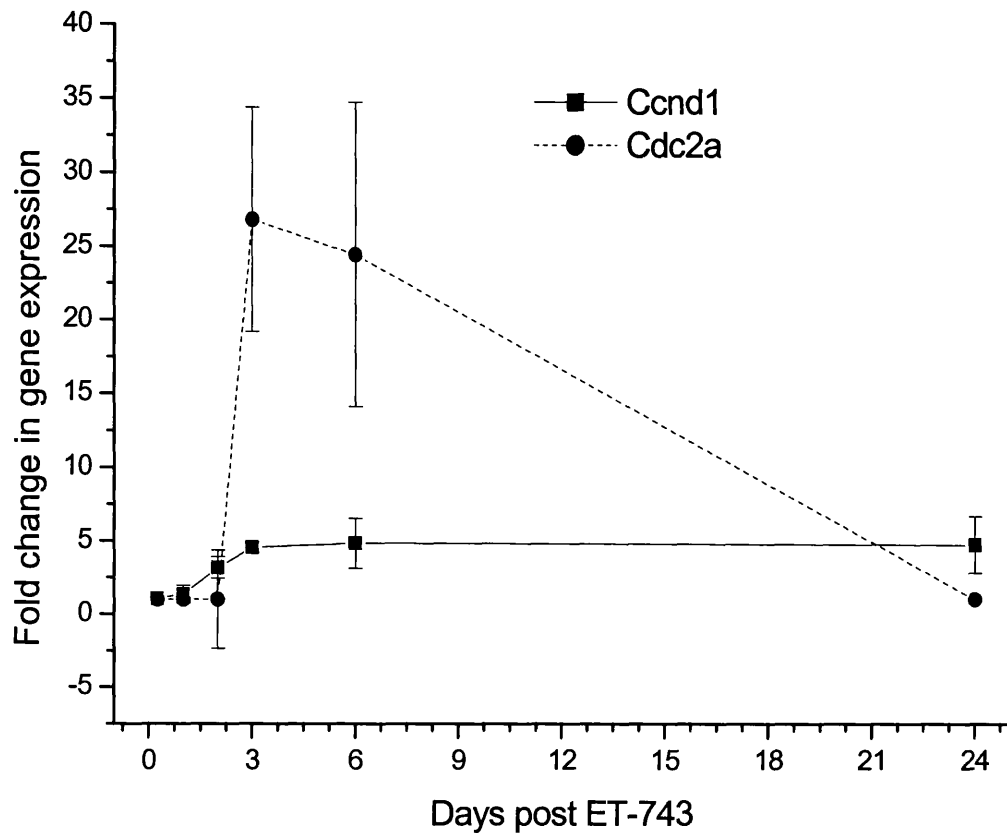


Figure 3.10 Time course of changes in expression of *cdc2a* (●) and *ccnd1* (■) genes in livers of female rats that received ET-743 (40 $\mu\text{g}/\text{kg}$, i.v.). The gene expression patterns were determined by cDNA microarray. The normalized intensity values from the hybridisation of the RNA from treated rats at 3 and 6 day time points for both genes and the 24 day point for *ccnd1* were significantly different ($p < 0.05$ by ANOVA) from the values for control rat RNA hybridised on the same microarray. The SDs indicate the variability in the measure of the ratio of treated: control rats.

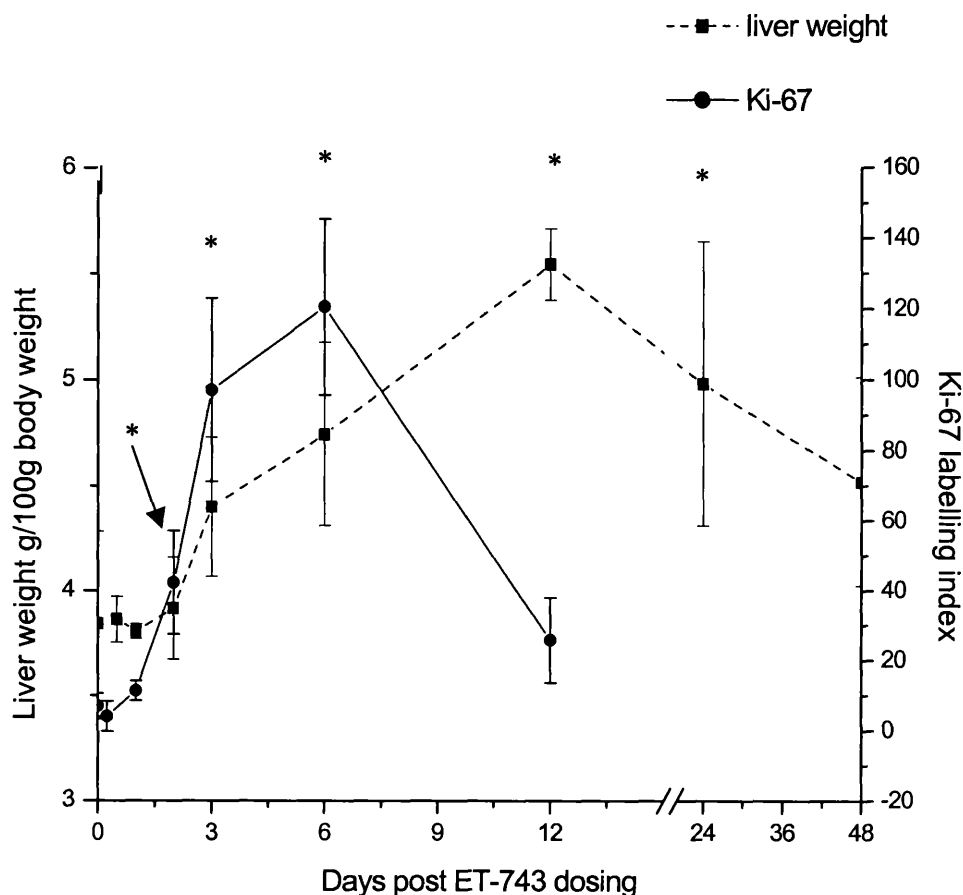


Figure 3.11 Time course of changes in liver weight (■) and Ki-67 (●) labelled nuclei in female rats that received ET-743 (40 $\mu\text{g}/\text{kg}$, i.v.). Liver weight values are expressed as the ratio of liver weight (in grams) at each time point: 100g of the pre-treated body weight of the respective animal. Nuclei were stained with Ki-67 antiserum, and Ki-67 labelling index denotes the number of stained nuclei/1000 hepatocyte nuclei. Values are the mean \pm SD of 4 rats/time points. Stars indicate that values are significantly different from those of the corresponding controls ($p < 0.05$ by ANOVA).

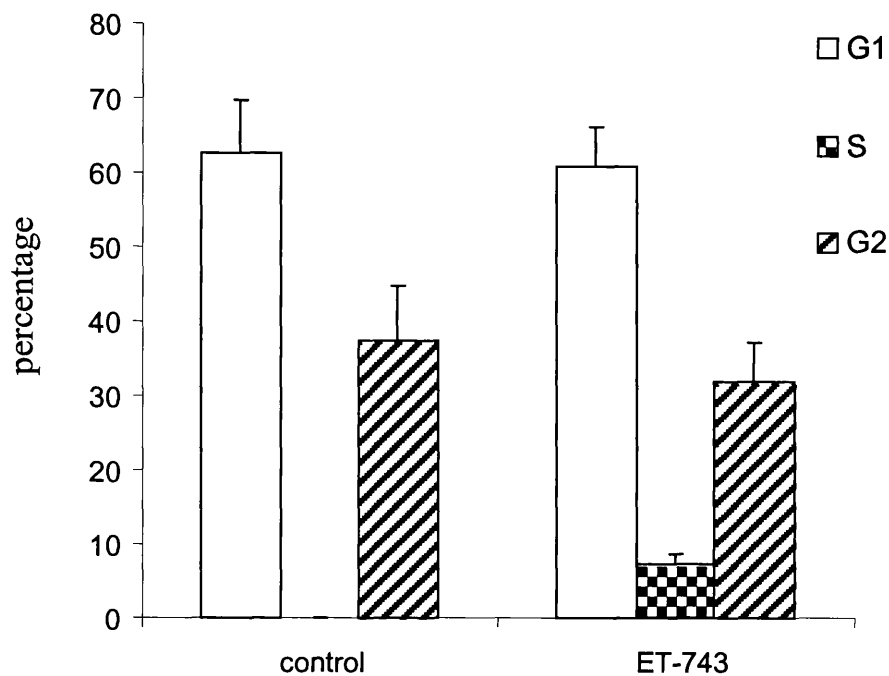


Figure 3.12 Change in liver cell cycle distribution in rats given ET-743 (40 $\mu\text{g}/\text{kg}$, i.v.), compared to untreated rats. Livers were removed 3 days after i.v. ET-743 (40 $\mu\text{g}/\text{kg}$) administration and FACS analysis was performed. The proportion of cells in the different phases of the cycle is expressed as percentage of total cells. Values obtained are the mean \pm SD from four rat livers.

3.6 Effects of ET-743 on liver biochemistry and pathology in male rats

In an orientation experiment male rats were dosed i.v with. ET-743 at either 40 or 80 $\mu\text{g}/\text{kg}$ body weight. Eight rats were dosed at 40 $\mu\text{g}/\text{kg}$ ET-743 and killed at either 3 or 12 days. Four rats were treated with 80 $\mu\text{g}/\text{kg}$ ET-743, two were culled at 3 days and due to severe weight loss, two were culled at 5 days. In male rats, 40 $\mu\text{g}/\text{kg}$ ET-743 had no effect on plasma bilirubin, AST or ALP levels, whereas the same dose produced marked increases in female rats. Pathological examination of rats given 40 $\mu\text{g}/\text{kg}$ revealed slightly irregular bile duct epithelia and sparse degenerative biliary cells 3 days after dosing with mild peribiliary fibrosis at day 12. When the dose of ET-743 was increased to 80 $\mu\text{g}/\text{kg}$ there was a two-fold elevation in the levels of ALP and AST and a 6-fold elevation in plasma bilirubin levels (figure 3.13). Similarly, the pathology of the liver sections mimicked the pathology observed in female rats after administration of 40 $\mu\text{g}/\text{kg}$ in both character and extent.

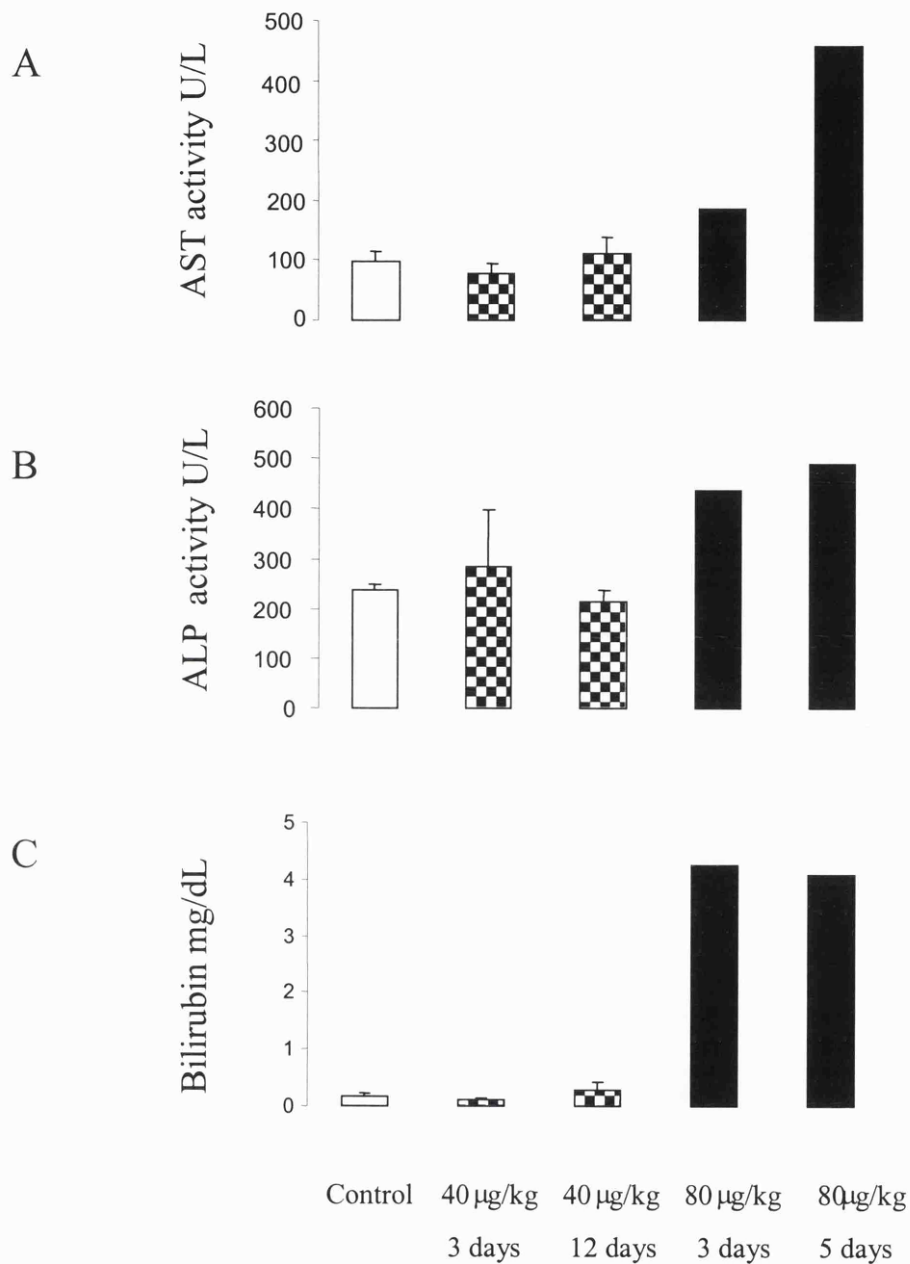


Figure 3.13 Plasma aspartate aminotransferase (A), alkaline phosphatase (B), and bilirubin (C) levels in male rats after ET-743 at two dose levels. Rats dosed i.v. at 40 µg/kg (chequered bars) were killed 3 and 12 days after dosing, while rats dosed i.v. at 80 µg/kg (filled bars) were killed 3 and 5 days after dosing. Values shown for control (open bars) and 40 µg/kg rats are the mean \pm SD for four animals. Values for 80 µg/kg are the mean for two animals.

3.7 The effect of ANIT on liver pathology, biochemistry and gene expression changes

The effects of a single oral dose of ANIT (100 mg/kg, p.o.) on markers of liver injury were investigated. ANIT caused a two-fold elevation in ALP and AST and a six-fold elevation in plasma bilirubin compared to untreated rats at two days after administration (figure 3.14). By day 6 the levels of ALP, AST and bilirubin had returned to basal levels. At 2 days after administration, ANIT produced degenerative alterations in bile duct epithelium that were associated with localised portal tract inflammation and oedema. Bile ducts had undergone repair by 6 days but the repair was associated with fibrosis around the larger bile ducts and some proliferation of bile duct or oval cells. In some animals there were rounded foci of hepatocellular necrosis in the regions of bile duct damage.

Hepatic gene expression changes were measured at 2 and 6 days after treatment. Among the genes that were consistently up-regulated were the ATP-binding cassette genes, *abcb1a*, *abcb1b* and *abcb4* (figure 3.15). There was a significant increase at 2 days after treatment that returned to basal levels at 6 days. The cell cycle genes up-regulated after ET-743 treatment were not altered by ANIT. Some wound repair genes such as *krt2-8*, *krt2-6a*, *krt1-19*, *krt2-4*, *cola1* and *col3a1* were up-regulated by both ET-743 and ANIT (figure 3.15 and 3.16). Genes significantly down regulated by both ET-743 and ANIT included *ptpn16*, *sth2*, *g6pc*, *car3*, *igh-6* and *pklr*.

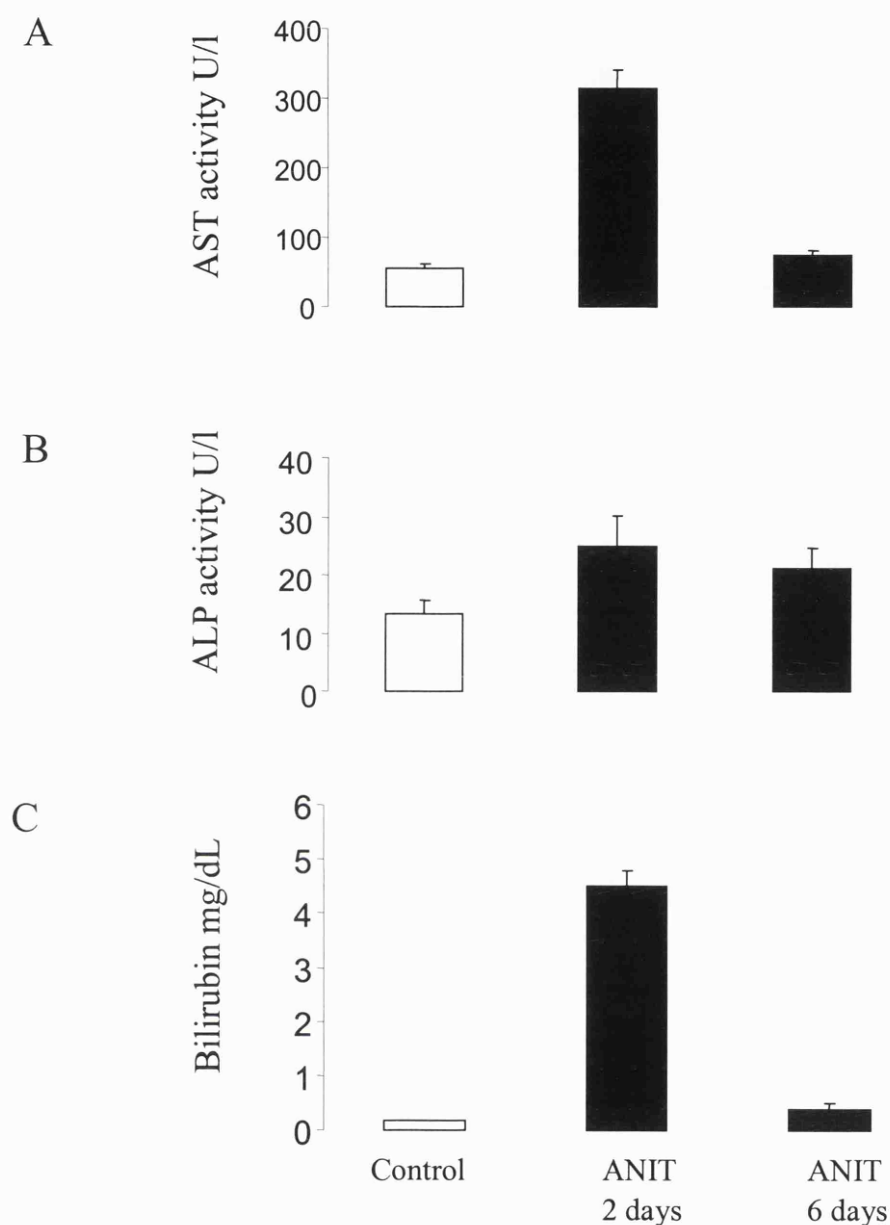


Figure 3.14 Plasma aspartate aminotransferase (A), alkaline phosphatase (B) and bilirubin (C) measured in female Wistar rats after ANIT treatment (100 mg/kg, p.o.) (filled bars) or vehicle only (open bars). Values are the Mean \pm SD of four animals. Values obtained for ALP, AST and bilirubin at 2 days after ANIT administration were significantly different to controls ($p < 0.05$ by ANOVA).

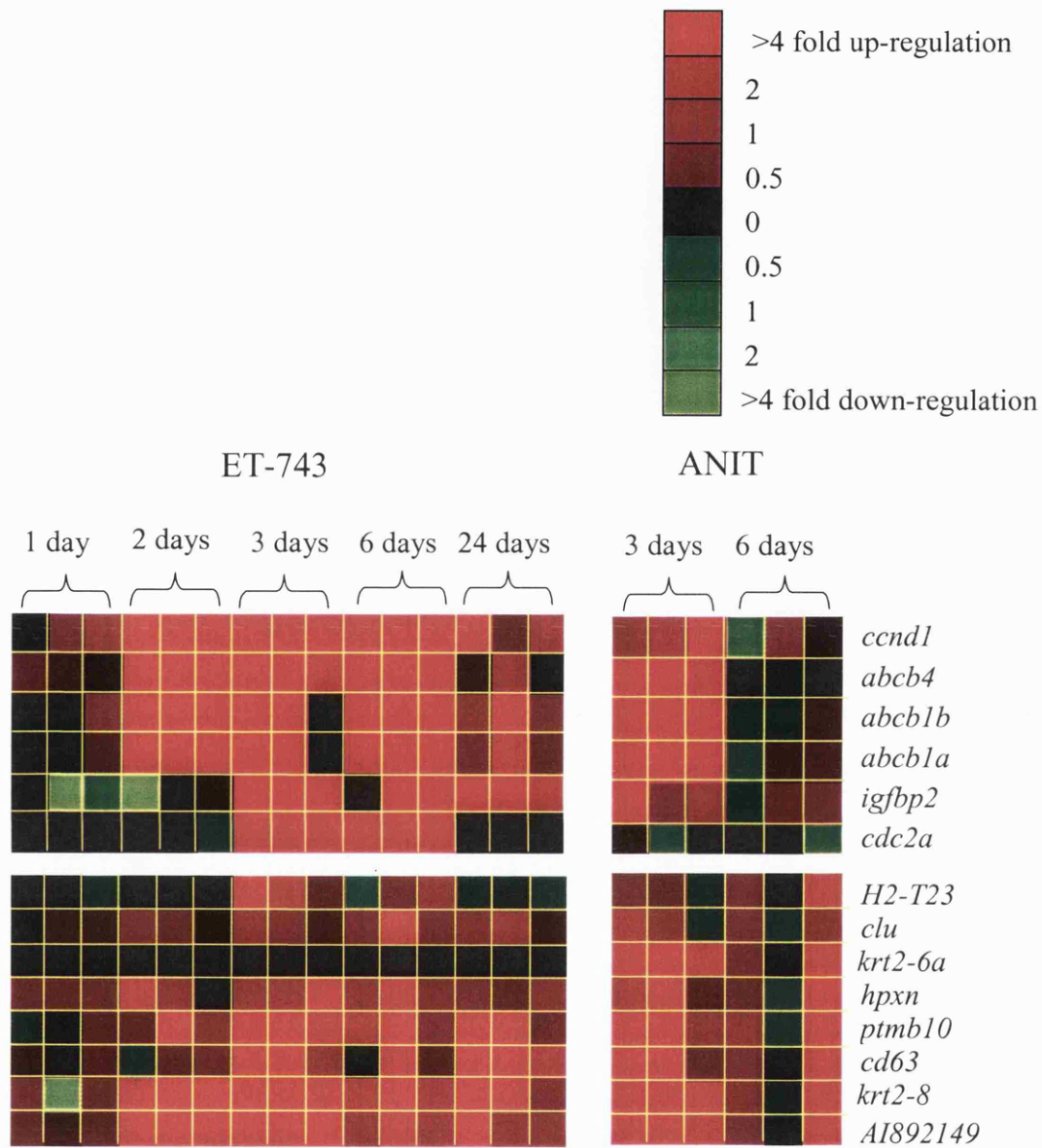


Figure 3.15 Genes changes after ANIT (100 mg/kg, p.o.) and ET-743 (40 µg/kg, i.v.) administration. The gene expression patterns were determined by cDNA microarray. At each time point, three arrays were used for each pair of rats; treated and control. Genes were clustered depending on gene expression pattern.

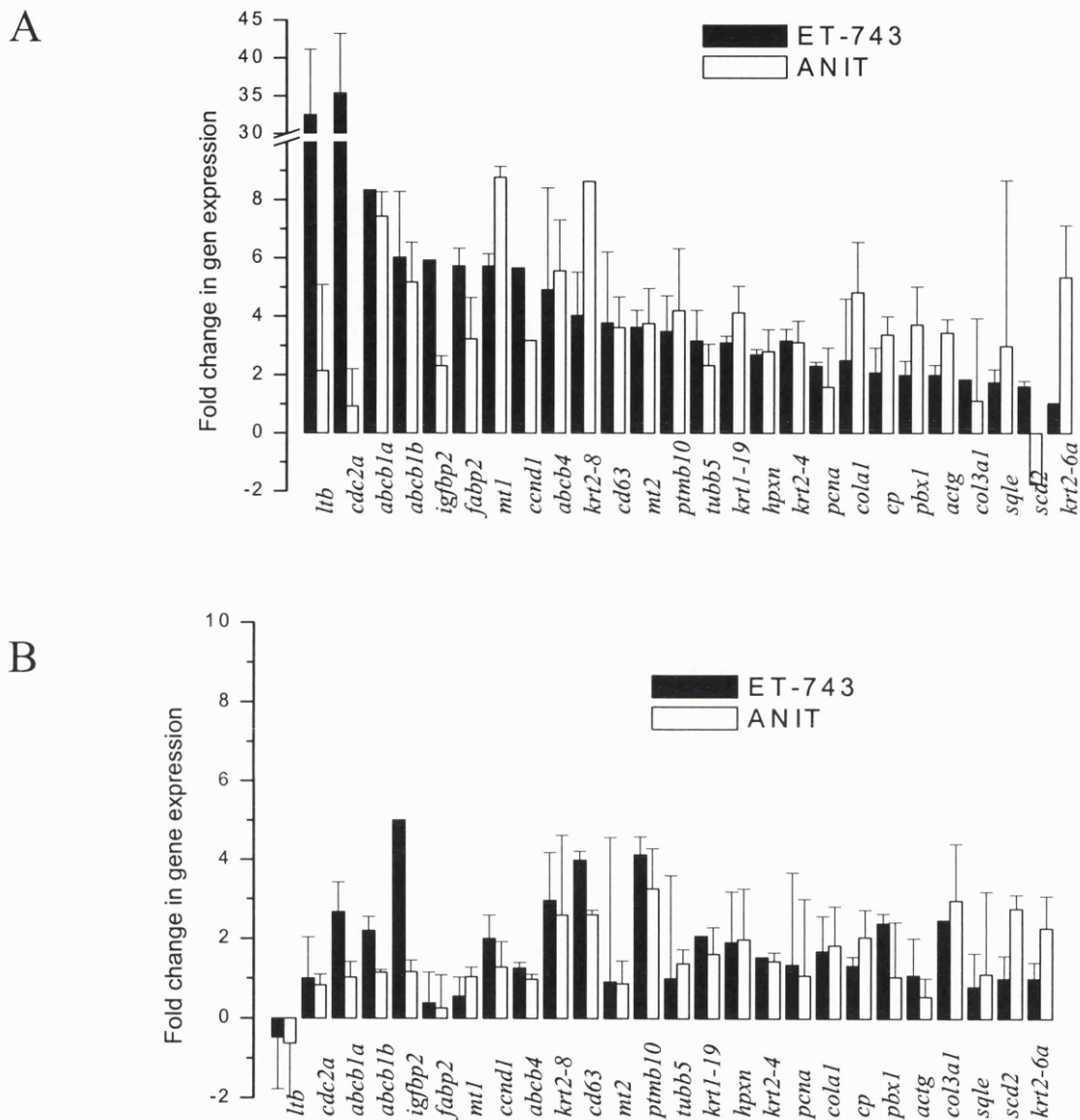


Figure 3.16 The gene expression changes at 2 days post ANIT (100 mg/kg, p.o.) and 3 days post ET-743 (40 μ g/kg, i.v.) (A) and 6 days post ANIT and 12 days post ET-743 (B) after ET-743 (filled bars) or ANIT treatment (open bars). The values are the mean \pm SD from 3 arrays for each treatment. The genes shown are in order of decreasing expression as determined in the analysis of ET-743 treatment. There is a good correlation between genes up-regulate by ET-743 and genes up-regulated by ANIT, except *cdc2a*.

3.8 Discussion

The results suggest that the novel anti-cancer drug ET-743 induces an unusual form of hepatotoxicity in rats, which differs from the adverse effects described for traditional cytotoxic drugs such as methotrexate and cyclophosphamide. In the female rat, a single i.v. dose of 40 $\mu\text{g}/\text{kg}$ of ET-743 caused damage to the bile duct epithelia followed by peribiliary fibrosis. Bile duct damage accompanied by inflammation was first evident 24 hours after dosing and reached maximal levels at 3 days. Fibrosis around damaged bile ducts was observed 3 days after dosing and increased dramatically over the following week. These hepatic lesions were accompanied by a dramatic elevation in plasma bilirubin levels and moderate increase in plasma ALP and AST.

There was a decrease in the activity of hepatic cytochrome P450 enzymes CYP3A2, CYP1A1/2 and CYP2E1 after ET-743 treatment. Most cytochrome P450 activity is associated with hepatocytes, which show minimal damage at 3 days after ET-743 dosing, whereas CYP1A1/2 and CYP2E show 90 % inhibition and CYP3A2 shows 40 % inhibition. Therefore, it is possible that ET-743 has a direct effect on CYP, associated with its metabolism. CYP3A2 appears to be the major CYP catalysing ET-743 metabolism in the rat (Reid et al., 2002) and therefore ET-743 must be a substrate for CYP3A. ET-743 may inhibit CYP3A activity by reversible, competitive binding. CYP1A1/2 may also play a minor role in ET-743 metabolism, yet ET-743 inhibits CYP1A1/2 activation by 90 %. Therefore, ET-743 or its metabolites may irreversibly bind to CYP1A1/2 causing destruction of the isozymes. Another explanation for the diminished CYP activity is provided by investigators examining liver damage induced by bile duct-ligation (Chen et al., 1998; Tateishi et al., 1998). They report that in bile-duct ligated rats, there was a reduction of hepatic microsomal CYP levels. Moreover, the changes in activity of individual microsomal enzymes were non-uniform. The authors suggest that bile acids inhibit the activity of microsomal enzymes in the livers of bile-duct ligated rats. The pathophysiology of bile-duct ligation resembles cholestasis, and therefore it is possible that the cholestasis induced by ET-743 is inhibiting hepatic microsomal CYP activity.

ANIT is often used as a model to investigate intrahepatic cholestasis (see chapter 1.7). The results show that the liver damage produced by ANIT and ET-743 are very similar, but not identical. Broadly, ANIT-treated rats showed more acute inflammation of portal tracts at 2 days and less fibrosis at 6 days than rats treated with ET-743. The hepatic gene expression changes after treatment with both compounds were remarkably similar. The increased expression of the *abcb1a* and *abcb1b* genes with both compounds coincided with dramatic elevations of bilirubin. Therefore, the gene changes may be generic to the cholestasis and an adaptive response to the damage. This interpretation is based on the previous observation that expression of these genes was raised in cholestatic livers of rats and monkeys (Schrenk et al., 1993). Increased expression of the *abcb1a* and *abcb1b* genes coincided with an increase in the P-gp levels. P-gp (MDR1), located on the apical hepatocyte membrane, is thought to participate in biliary excretion, acting as an efflux transporter that extrudes drugs from the cells (Lin et al., 1999). A possible explanation for the increased expression is that P-gp is induced in response to the damage and is responsible for the elimination of the toxic compound from the liver. In analogy, the down regulation of expression of *car3* gene with both ET-743 and ANIT is probably the consequence of hepatobiliary damage rather than a direct response to ET-743 proper because it has been shown to occur in mouse liver after exposure to griseofulvin (Gant et al, unpublished observation).

One of the most striking results of the DNA microarray analysis of hepatic gene expression after ET-743 treatment is the increased expression of the cell cycle genes *cdc2a* and *ccnd1*. The time course of change in expression of the *cdc2a* gene resembles the time course of the ET-743-induced alterations in liver weight and Ki-67 labelling. These observations suggest that ET-743 elicits a mitogenic wave in the liver by induction of DNA synthesis. This was supported by cell cycle analysis, which showed there were an increased number of liver cells in S phase of the cell cycle after ET-743 treatment. In addition, staining of proliferating cell nuclear antigen was increased and there was a prominent presence of mitotic figures in ET-743-treated livers. In contrast, ANIT treatment had no effect on the expression of the cell cycle genes and Ki-67 staining showed that there was not the striking increase in hepatocyte proliferation observed with ET-743. Stimulation of mitogenesis has not been observed thus far

as a generic mechanistic feature of hepatotoxic drugs. Therefore, it seems to be specific to ET-743, and is probably the result of a direct effect of ET-743 on *cdc2a* transcription, which drives the cell cycle in the liver.

An unusual feature of the ET-743 induced damage is its persistence. Bile duct fibrosis and increased plasma levels of AST were observed as late as 3 months after a single dose, and levels of plasma ALP were elevated for up to 2 months. In contrast, bilirubin levels were elevated for a relatively short time and returned to control levels between 12 and 24 days. In a preliminary pharmacokinetic study, hepatic drug levels in rats 6 hours after i.v. administration of ET-743 were approximately 37 pmoles/g liver and diminished to 4 pmoles/g liver after 72 hours. Therefore, very low levels of ET-743 are present in the liver after 3 days, yet there is still significant liver damage. It is not known whether the long-term persistence of the liver damage is related to the continuous presence of harmful levels of a toxic metabolite, or to late consequences of the initial bile duct damage and subsequent fibrosis. In contrast to the long persistence of the damage in the female rat, transaminitis in patients in phase I trials of ET-743 was not dose limiting (Delalogue et al., 2001; Ryan et al., 2001; Taamma et al., 2001; van Kesteren et al., 2000), as it had returned to normal levels before the next drug cycle, 3 weeks later. This difference indicates that in relation to humans, the female rat model exaggerates some aspects of ET-743- induced damage.

The results confirm the preclinical toxicity reports that the female rat is more sensitive than the male. ET-743 at 40 µg/kg, which caused severe liver damage in females, produced only slight pathological change in males. Twice the dose given to females was required to produce similar toxicity in males. Nevertheless, qualitatively similar changes in pathology and biochemistry were observed by ET-743 in both genders.

In conclusion, ET-743 produces an unusual form of liver damage characterised by a primary insult to the bile duct epithelium with inflammation and bilirubinaemia followed by peribiliary fibrosis. The pathological damage appears to be irreversible up to 3 months after a single dose in the female rat. There were changes in gene expressions related to the toxicity and associated

repair. However, the most dramatic gene changes were up-regulation of two cell cycle genes which was accompanied by a wave of mitogenesis, not observed with other hepatotoxic compounds. The female Wistar rat was more sensitive than the male as twice the dose of ET-743 was required in males to produce a similar toxicity in females. Although the female rat is very sensitive to the toxicity induced by ET-743, some features of the liver toxicity described here have been observed in patients. Liver toxicity starts as cholangitis followed by hepatitis in both the rat and the human and the main difference is the intensity of the damage. Therefore, the female rat is a suitable model to investigate treatment regimes designed to reduce the hepatotoxicity of ET-743 in man.

CHAPTER 4

Evaluation of the protective efficacy
of dexamethasone against ET-743
induced hepatotoxicity *in vivo*

4.1 Introduction

Altering the metabolism of a xenobiotic is often the key to modifying its toxicity. Data concerning ET-743 metabolism are very limited (section 1.10.5). However, studies suggest that CYP3A is the major CYP involved in ET-743 metabolism. *In vitro* metabolism was characterised using male and female rat microsomes (Kuffel et al., 1997). NADPH-dependent ET-743 metabolism was greater with male rat microsomes than with female rat microsomes as measured by disappearance of ET-743. In addition, metabolism was induced by pre-treatment with dexamethasone and phenobarbitone, but not 3-methylcholanthrene, which induce CYP3A, CYP2B and CYP1A respectively (Reid et al., 2002). Microsomal metabolism of ET-743 was reduced by inhibitors of CYP3A, CYP2C and CYP1A and by anti-rat CYP3A2 serum. CYP3A2 appears to be the major CYP catalysing ET-743 metabolism in the rat. In addition, metabolites of ET-743 were discovered in a study using human lymphoblasts expressing the CYP3A4 isoform (Rinehart et al., 1999).

As dexamethasone is a well-known inducer of CYP3A (see chapter 1.5.1), it was considered that the effect of dexamethasone on ET-743 hepatotoxicity was worthy of investigation. The choice of dexamethasone has more than one implication. Patients receive dexamethasone during treatment for chemotherapy-induced emesis. Furthermore, initial results suggest that dexamethasone pre-treatment enhances the efficacy of ET-743. In an early *in vivo* experiment using a B16 tumour model in male rats, dexamethasone treatment 24 hours prior to ET-743 increased the tumour growth inhibition compared to ET-743 alone (unpublished work commissioned by PharmaMar). The tumour growth inhibition of the dexamethasone and ET-743 combination was 65 % compared with 19 % and 9 % for ET-743 or dexamethasone alone, respectively.

The use of dexamethasone as an anti-emetic was precluded during phase I trials due to concerns about inducing hepatic metabolism of ET-743 (Puchalski et al., 2002). However, in consideration of the unexpectedly severe nausea and vomiting experienced by the initial patients entered into phase II trials, dexamethasone was soon incorporated as a regular

component of the anti-emetic regime. The first preliminary assessment of the effects of dexamethasone on the pharmacokinetics of ET-743 in patients in a phase II trial was recently published (Puchalski et al., 2002). Dexamethasone (10 mg) was administered i.v. shortly before ET-743 infusions. The mean \pm SD of the area under the plasma versus time profile (AUC) of ET-743 was 38.1 ± 15.4 ng/ml x h for the group of patients who received dexamethasone and 48.5 ± 20.3 ng/ml x h for those who did not. Although the difference between these mean AUC values was 27 %, it did not achieve statistical significance ($p=0.08$). The incidence of nausea and vomiting was 48 % in patients receiving dexamethasone and 69 % in those who did not. Furthermore, the incidence of severe transaminitis was 25 % lower in patients who received dexamethasone. Dexamethasone co-treatment appeared to decrease the incidence of severe toxicity as well as the AUC of ET-743.

In this chapter the effect of dexamethasone on ET-743-induced hepatotoxicity is explored in the female Wistar rat model. Different doses and schedules of dexamethasone were investigated to find the optimal dose that protects the liver against ET-743-mediated toxicity. The prevention of the detrimental effects to the liver by dexamethasone was adjudged by changes in the activity of plasma ALP and AST and plasma bilirubin levels, pathological examination and cDNA microarray analysis. In addition, microarray analysis was performed after dexamethasone treatment, in the absence of ET-743, to identify possible gene changes which may give rise to its protective effect. To gain further insight into the mechanisms by which dexamethasone may affect ET-743-mediated toxicity, levels of ET-743 in the liver and plasma of rats were measured after dexamethasone pre-treatment in a separate project conducted by colleagues at the Mario Negri Institute in Milan. In order to justify exploration of the dexamethasone hepatoprotection strategy in the clinic, it is of paramount importance to demonstrate that dexamethasone does not adversely affect the anti-tumour activity of ET-743. Therefore, the effect of the combination of ET-743 and dexamethasone on antineoplastic activity was explored in five rodent models by colleagues in Italy.

Results

4.2 Effect of dexamethasone pre-treatment on ET-743-induced liver damage

Female Wistar rats were pre-treated with a single dose of dexamethasone (1-20 mg/kg p.o., dissolved in glycerol formal,) 24 hours prior to a hepatotoxic dose of ET-743 (40 µg/kg i.v.). Blood samples and liver tissue were collected from rats 3 days after administration of ET-743 (40 µg/kg) with or without dexamethasone (1-20 mg/kg) pre-treatment. Plasma levels of ALP, AST and bilirubin were measured at 3 days after ET-743 treatment, the time point at which liver damage was maximal in rats which received ET-743 alone (Figure 4.1). ET-743 administered on it own elicited hepatic damage as reflected by dramatically raised bilirubin and elevated ALP and AST in the plasma (chapter 3.1). A single dose of dexamethasone administered alone at all dose levels caused loss of up to 10 % body weight within a day of administration, and this weight loss was not dose related. Rats treated with 1 or 5 mg/kg of dexamethasone prior to ET-743 had decreased levels of ALP and AST activity compared to levels measured in rats after ET-743 treatment alone (Figure 4.1). Dexamethasone pre-treatment at 5 mg/kg also reduced the ET-743-induced elevation of plasma bilirubin level, but at 1 mg/kg dexamethasone had no effect on the elevated bilirubin levels elicited by ET-743. Dexamethasone at 10 mg/kg and 20 mg/kg abolished the ET-743 induced liver changes in that the elevation of all three indicators of hepatic damage was abrogated. Dexamethasone alone had no effect on ALP, AST or bilirubin.

In a separate study the protective effect of dexamethasone (10 mg/kg, p.o.) against ET-743 mediated hepatotoxicity was investigated at two additional time points, 6 days and 12 days. Dexamethasone abolished the ET-743 induced liver changes, as the elevation of all three indicators of hepatic damage was abrogated, at both time points, resembling the results observed after 3 days (data not shown).

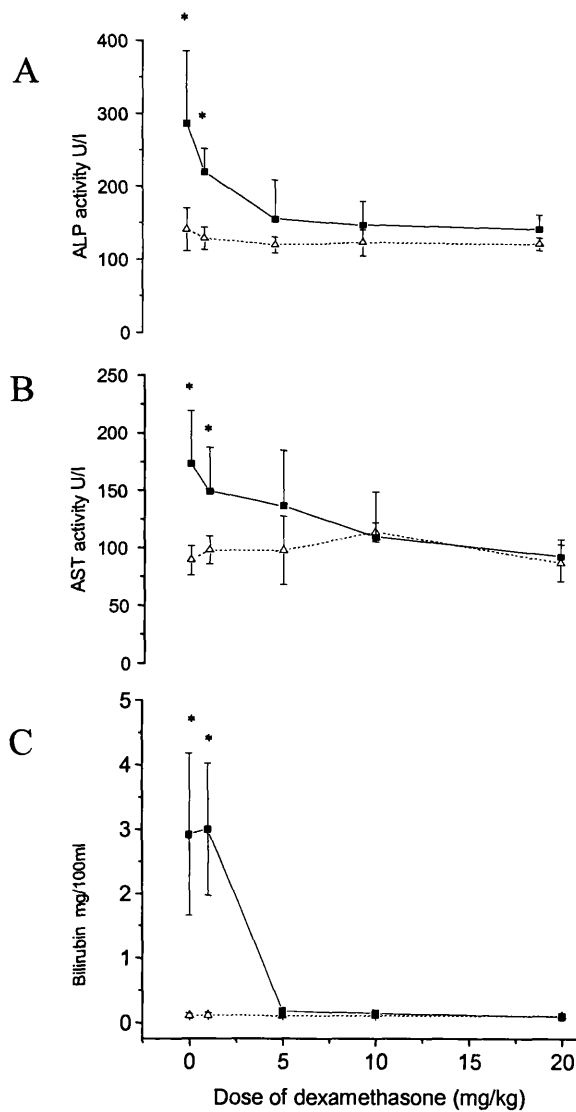


Figure 4.1 Dose dependency of the effect of dexamethasone administered p.o. 24 hours prior to ET-743 (40 $\mu\text{g}/\text{kg}$, i.v.) on ET-743 induced elevations of plasma activity of alkaline phosphatase (A), aspartate aminotransferase (B) and of plasma bilirubin levels (C) in female rats when measured 3 days after ET-743. Triangles reflect values observed in rats which received dexamethasone alone, or glycerol formal, the vehicle for dexamethasone (0 mg/kg dexamethasone), squares denote values in rats which received the combination or ET-743 alone (0 mg/kg dexamethasone). Values are the mean \pm SD of 5 animals. Stars indicate that values are significantly different ($p < 0.05$ by ANOVA) from levels in animals which did not receive ET-743.

The histopathological examination underpins the biochemical results described above. Livers of animals which received ET-743 alone revealed degenerative and inflammatory changes in the biliary epithelium (see chapter 3.3). Round zones of haemorrhagic hepatocellular necrosis were also present. Rats which received dexamethasone alone did not exhibit significant liver changes, except for slight hepatic vacuolation, conceivably due to lipid, and clear cell change, probably caused by glycogen. Dexamethasone pre-treatment, at 20 mg/kg, completely abrogated the histopathological changes in the liver induced by ET-743 and at 10 mg/kg histopathological changes were minimal (figure 4.2). At 5 mg/kg dexamethasone reduced the severity of the bile duct damage generated by ET-743 in all rats and one animal was completely damage-free. There was little evidence that dexamethasone at 1 mg/kg significantly reduced the biliary damage produced by ET-743. However, the absence of overt hepatocellular necrosis following ET-743 treatment suggested that dexamethasone at 1 mg/kg did mitigate the hepatocellular damage induced by ET-743 to some extent.

The protective efficacy of dexamethasone at 10 mg/kg was also evaluated in livers obtained at 6 and 12 days after administration of ET-743. Dexamethasone strongly attenuated the histopathological manifestations in the liver elicited by ET-743, as observed at 3 days after administration.

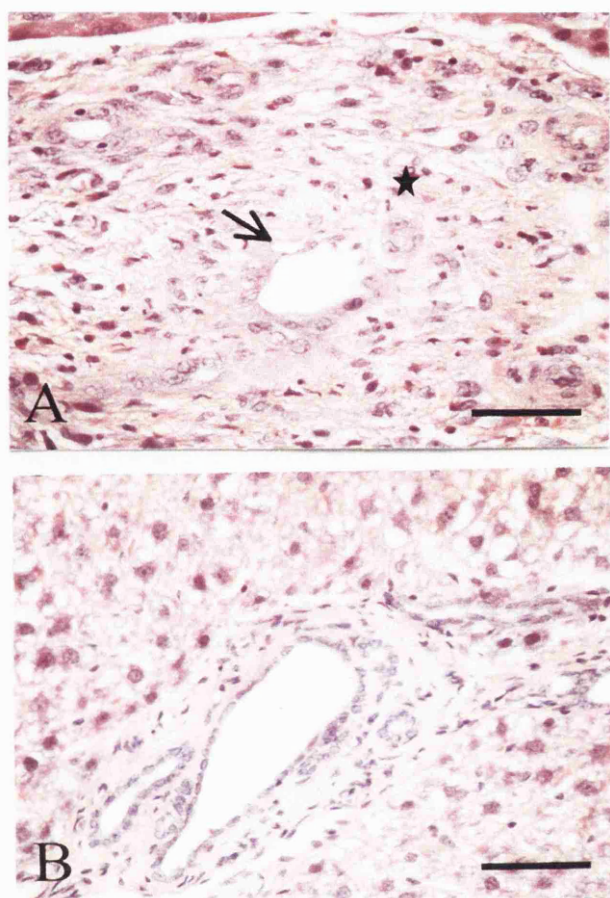


Figure 4.2 Liver section from female Wistar rats which received ET-743 (40 $\mu\text{g}/\text{kg}$, i.v.) alone (A), or 24 hours after dexamethasone (10 mg/kg , p.o.)(B). Liver sections were taken 3 days after ET-743 dosing. Note in A the swollen, thickened portal tract with a sparse infiltrate of inflammatory cells (star) and the damaged bile duct (arrow), which is lined by degenerative epithelium, characteristics of ET-743 induced changes in livers of female rats. In contrast, after dexamethasone pre-treatment (B) a comparable portal tract is indistinguishable from controls. Sections are representative of five separate animals. Bar equals 100 μm . Histopathological analysis was carried out by Dr Peter Greaves.

4.3 The effect of dexamethasone on ET-743 hepatotoxicity when both are administered concurrently

Dexamethasone is often administered in the clinic at the same time as cytotoxic drugs in order to prevent drug-induced emesis. Therefore co-administration of ET-743 with high-dose dexamethasone as a potential hepatoprotectant and anti-emetic would clearly be clinically beneficial. In order to investigate whether co-administration of dexamethasone shows protection against ET-743-induced liver damage, a study was performed in which rats were treated with dexamethasone (10 mg/kg, p.o.) immediately before a single i.v. dose of ET-743 (40 µg/kg). Blood samples and liver tissue were collected from rats 3 days after treatment. Plasma ALP activity and bilirubin levels in animals which received dexamethasone just before ET-743 were as elevated as levels measured in animals which received ET-743 alone (Figure 4.3). Moreover, plasma AST activity in animals which received the combination was 4-fold higher than when measured in animals which received dexamethasone alone. Likewise, histopathological examination of the liver sections revealed that concurrent treatment of dexamethasone and ET-743 failed to abrogate ET-743-induced liver damage. There was similar portal tract inflammation and bile duct damage. In fact, swelling of the portal tract was marginally greater in two rats which received the combination, and the livers of these rats showed more foci of haemorrhagic hepatocellular necrosis than livers in rats treated with ET-743 alone.

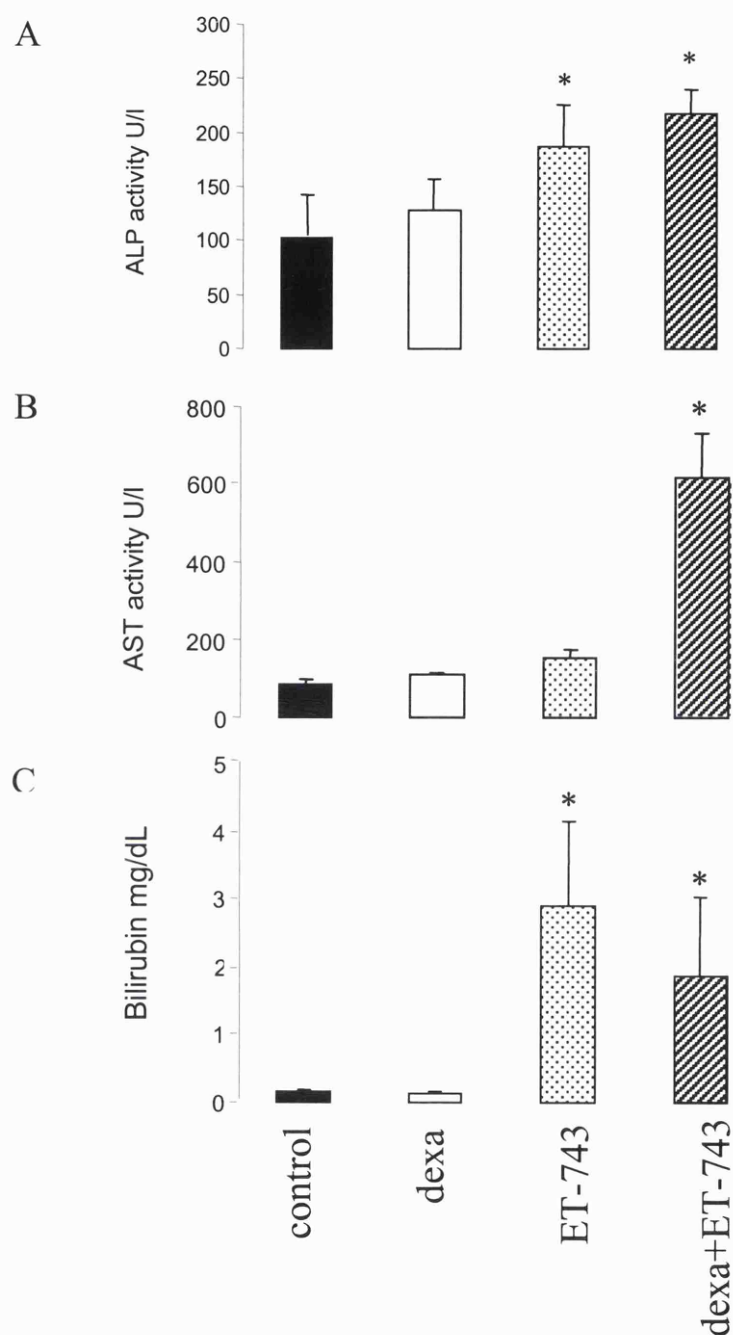


Figure 4.3 The effect of dexamethasone administered p.o. immediately prior to ET-743 (40 $\mu\text{g}/\text{kg}$, i.v.) on ET-743-induced elevation of plasma activity of alkaline phosphatase (A), aspartate aminotransferase (B) and of plasma bilirubin levels (C) in female rats measured 3 days after ET-743. Values are the mean \pm SD of 4 animals. Stars indicate that values are significantly different ($p < 0.05$ by ANOVA) from levels in animals which did not receive ET-743.

4.4 Effect of pre-treatment with dexamethasone on changes in hepatic gene expression caused by ET-743

The hepatotoxicity of ET-743 is accompanied by changes in the expression of a variety of hepatic genes (chapter 3.4). In order to assess whether dexamethasone pre-treatment at a hepatoprotective dose abrogates these changes, hepatic gene expression changes were analysed in livers obtained 3 days after administration of ET-743 using a cDNA microarray containing 4700 hybridisable ESTs. For the analysis of differential gene expression, each rat treated with ET-743, dexamethasone, or the combination was paired with a rat which received the vehicle only. Figure 4.4 shows the 24 most abundantly expressed hepatic genes induced by ET-743 alone versus their expression pattern in animals which received ET-743 after pre-treatment with dexamethasone. Among the hepatic genes up-regulated by ET-743 alone were, the cell cycle genes *cdc2a*, *ccnd1*, and the two drug resistance coding ABC transport genes *abcb1a* and *abcb1b* (see chapter 3.4). The expression of the genes which were up-regulated by ET-743 were reduced to control levels by pre-treatment with dexamethasone, with the exception of the genes coding for metallothionein 1 and 2, which remained elevated (figure 4.4 and 4.5).

Treatment with ET-743 alone resulted in the down-regulation of several genes, including *cyp1a*, *cyp2e1* and *cyp3a25*. Pre-treatment with dexamethasone abolished the decrease in expression of these genes caused by ET-743 alone (figure 4.5). In addition, the ET-743-induced down-regulation of expression of the haemoglobin genes, *hbb-b1*, *hbb-y*, *hba-a1* and *hba-x* was partially ameliorated by dexamethasone pre-treatment.

Dexamethasone is reported to have many pharmacological effects. However, the microarray expression profile of hepatic RNA from rats treated with dexamethasone only, compared to control rats, showed that dexamethasone alone induced very few gene changes. As the liver samples were taken at 4 days after dexamethasone treatment, any effect on gene expression changes was probably transitory and therefore no longer detectable at that time

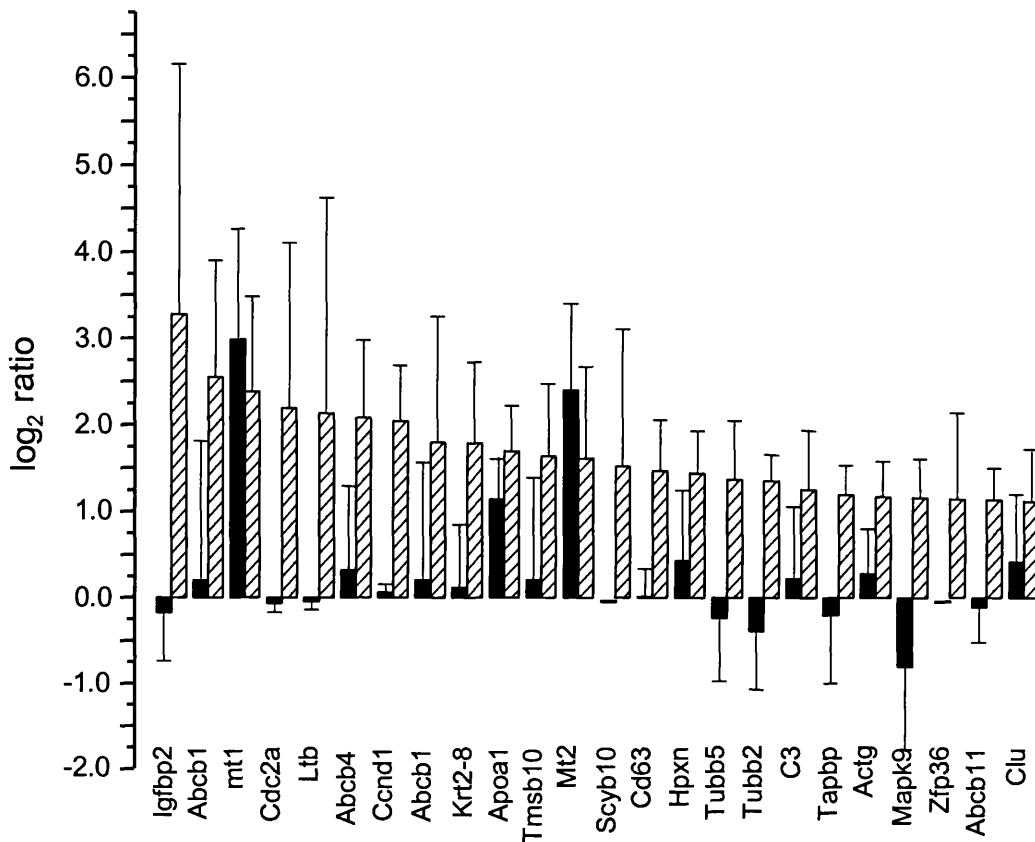


Figure 4.4 Gene expression changes elicited by ET-743 (40 $\mu\text{g}/\text{kg}$, i.v.) without pre-treatment (hatched bars) and after pre-treatment with dexamethasone (10 mg/kg , p.o.) (closed bars) in livers of female rats. Values are expressed as log ratio of fold expression \pm SD. Rats received dexamethasone (10 mg/kg , p.o.) 24 hours prior to ET-743 (40 $\mu\text{g}/\text{kg}$, i.v.) and livers were taken 3 days after ET-743. Rats treated with ET-743 or the combination of ET-743 with dexamethasone were each paired with control (untreated rats). Three pairs of rats were used for each comparison. Plotted for each gene are the Log_2 ratios, \pm SD, of the change of expression of treated versus untreated rats. The genes shown are ordered by decreasing expression ratio as determined in the analysis of ET-743 treatment versus control. The elaboration of the gene expression data was conducted by Dr Tim Gant.

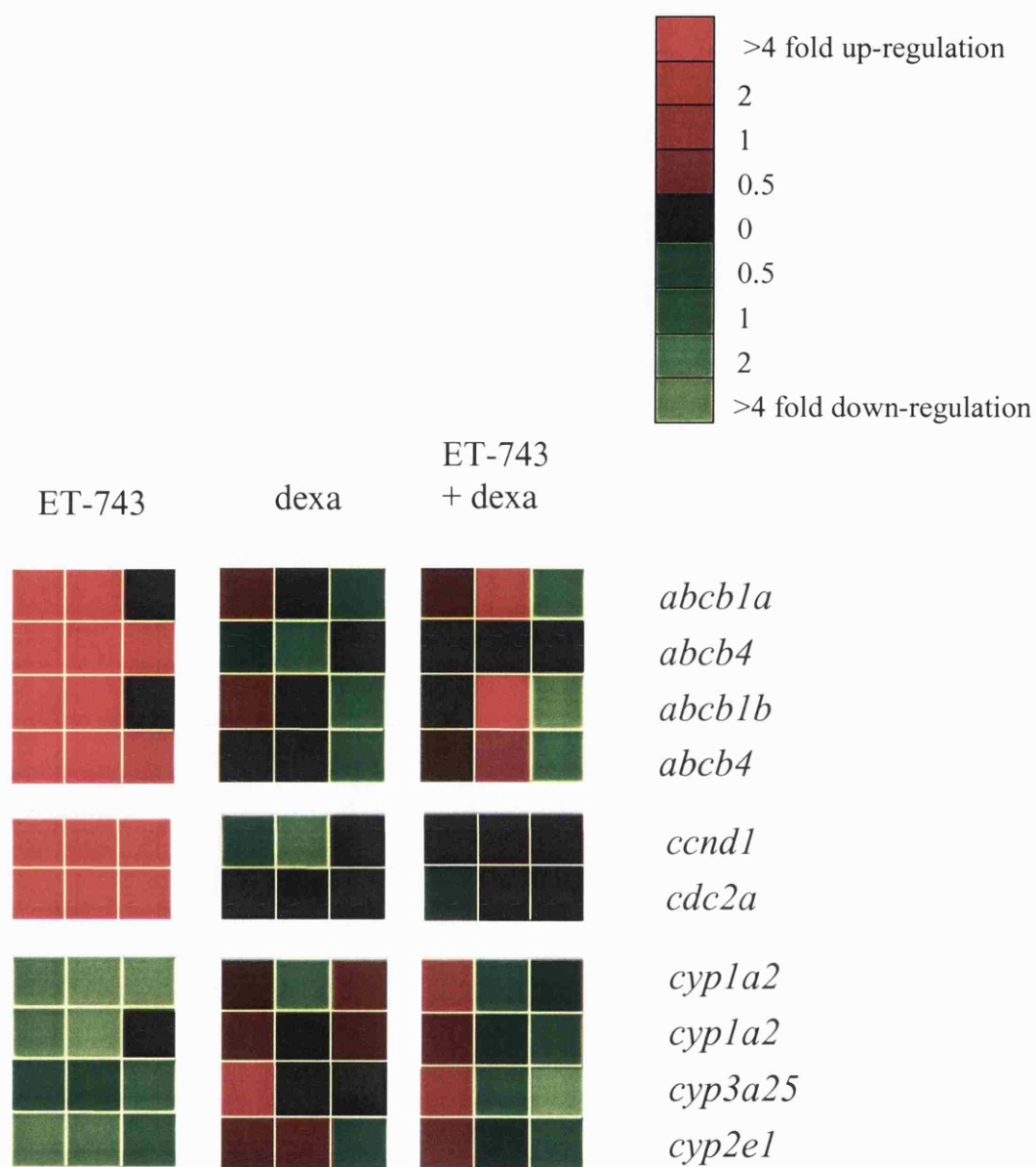


Figure 4.5 Gene expression changes in livers of female rats elicited by ET-743 (40 $\mu\text{g}/\text{kg}$, i.v.), dexamethasone (10 mg/kg , p.o.) and the combination. Gene expression patterns were determined by cDNA microarray using livers obtained 3 days after ET-743, which is the time point of maximal hepatotoxicity. Rats treated with ET-743, dexamethasone or the combination were paired with control (untreated rats). Rats received dexamethasone (10 mg/kg , p.o.) 24 hours prior to ET-743 (40 $\mu\text{g}/\text{kg}$, i.v.). Three pairs of rats were used for each comparison.

4.5 Effect of dexamethasone on hepatic CYP3A

Further microarray analysis was carried out to find clues to possible mechanisms by which dexamethasone protects the rat liver against ET-743-induced liver damage. Livers were obtained from pairs of untreated rats and rats which received dexamethasone (10 mg/kg) one day prior to RNA isolation. This enabled the analysis to be carried out exactly at the time point at which ET-743 would have been injected in the experiments in which the combination was studied. Dexamethasone up-regulated the expression of a number of genes by 2.5-fold or more (Figure 4.6 and Table 4.1) A number of the genes found to be up-regulated are involved in cellular metabolism, these include glyceraldehyde-3-phosphate dehydrogenase and aldolase 1, which are involved in glycolysis, malate dehydrogenase, which catalyses the conversion of oxaloacetate and malate in the Krebs cycle, and arginase 1, which catalyses the conversion of arginine into ornithine in the Urea cycle. Other genes found to be up-regulated are involved in biosynthesis. Phosphoenolpyruvate carboxykinase catalyses the first step of hepatic and renal gluconeogenesis, sialyltransferase is involved in the biosynthesis of sialylated glycoproteins and glycolipids, and fatty acid synthase catalyses the last step in the fatty acid biosynthetic pathway. The phase II metabolising enzyme, UDP-glucuronosyltransferases, which catalyses the glucuronidation of endogenous and exogenous substrates was up-regulated by 4.5-fold. The most dramatic induction was observed for the cytochrome P450 genes *cyp3a11* (23.2-fold induction), *cyp3a16* (18.1-fold induction), *cyp3a25* (13.2-fold) and *cyp3a13* (10.2-fold).

CYP3A activity was measured in microsomes obtained from rats 24 hours after dexamethasone treatment. The specific activity of the enzymes was measured using a fluorometric assay that measures the oxidative de-benzoylation of 7-benzyloxyquinolone to 7-hydroxyquinolone. Dexamethasone treatment resulted in a dose-dependent increase in the activity of the enzyme. The optimal hepato-protective dose of dexamethasone, 10 mg/kg, produced a 7-fold increase in CYP3A activity compared to untreated rats, whereas the moderately protective dose of 5 mg/kg produced a 3-fold increase in CYP3A activity (Figure 4.7). This result suggests that the increase in *cyp3a* gene expression elicited by dexamethasone in the rat liver predicts elevated CYP3A enzyme activity. It is therefore conceivable that

dexamethasone-mediated induction of CYP3A contributes to the protection by dexamethasone against the hepatotoxicity of ET-743.

At the same time CYP3A activity was measured and compared in untreated male and female rats. The basal level of CYP3A activity was significantly higher in male rats compared to females, as reported in the literature (Jager et al., 1999) (Figure 4.7). The basal level of activity in the males was similar to the level of activity in the females after induction with 10 mg/kg dexamethasone. This finding supports the hypothesis that the gender difference in sensitivity towards the hepatotoxicity of ET-743 is related to the gender differences in CYP3A expression.

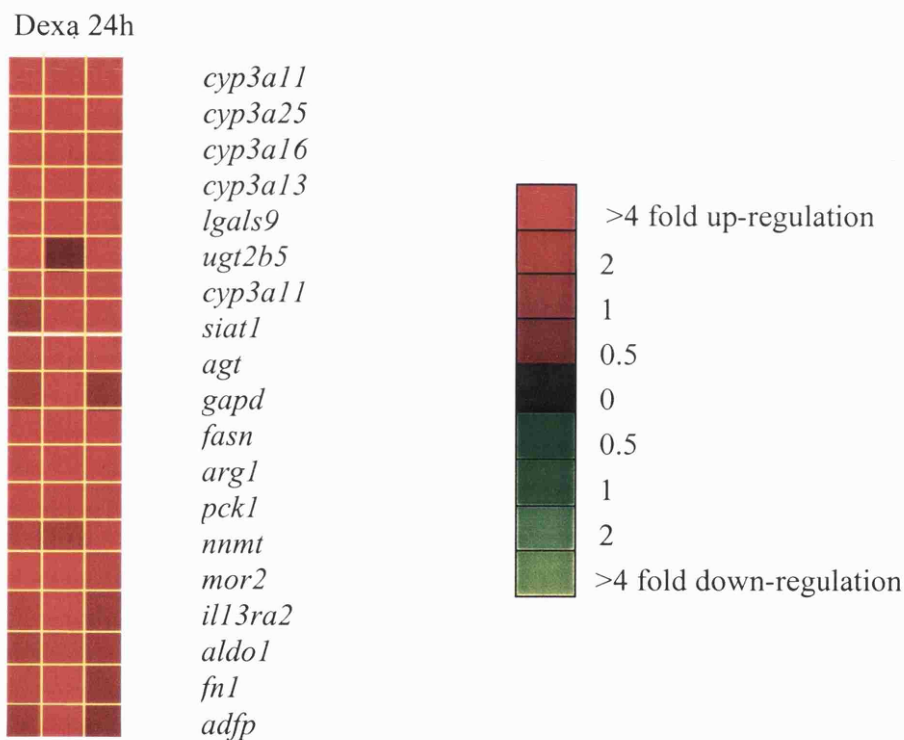


Figure 4.6 Gene expression changes in livers of female Wistar rats 24 hours after oral administration of dexamethasone (10 mg/kg, p.o.). Gene expression patterns were determined by cDNA. Rats treated with dexamethasone were paired with control (untreated rats). Three pairs of rats were used for each comparison.

Gene symbol	Gene name	Fold change	
		Mean	SD
<i>Cyp3a11</i>	Cyp3a11	23.2	14.5
<i>Cyp3a16</i>	Cyp3a16	18.1	9.0
<i>Cyp3a25</i>	Cyp3a25	13.2	2.9
<i>Cyp3a13</i>	Cyp3a13	10.2	3.7
<i>Fasn</i>	Fatty acid synthase	7.5	2.9
<i>Lgals9</i>	Galectin	5.2	1.2
<i>UGT2b5</i>	UDP-glucuronosyltransferase 2B	4.5	2.3
<i>Mor2</i>	Malate dehydrogenase	3.6	0.8
<i>Pck1</i>	Phosphoenolpyruvate carboxykinase	3.5	1.4
<i>Siat1</i>	Sialyltransferase	3.5	1.1
<i>Agt</i>	Angiotensinogen	3.3	0.9
<i>Arg1</i>	Arginase 1	3.2	0.1
<i>Fnl</i>	Fibronectin 1	3.1	0.8
<i>Gapd</i>	Glyceraldehyde 3 phosphate dehydrogenase	3.0	1.1
<i>Nnmt</i>	Nicotinamide N-methyltransferase	2.8	0.3
<i>Il13ra2</i>	Interleukin 13 receptor a2	2.7	0.5
<i>Adpf</i>	Adipophilin	2.6	0.6
<i>Aldo1a</i>	Aldolase1, A isoform	2.6	0.3

Table 4.1. Gene expression changes elicited by dexamethasone (10 mg/kg, p.o.) in livers of female rats 24 hours after dosing. Rats treated with dexamethasone were paired with rats which received glycerol formal, the vehicle for ET-743. Values are the mean ratio of fold expression of three pairs of rats.

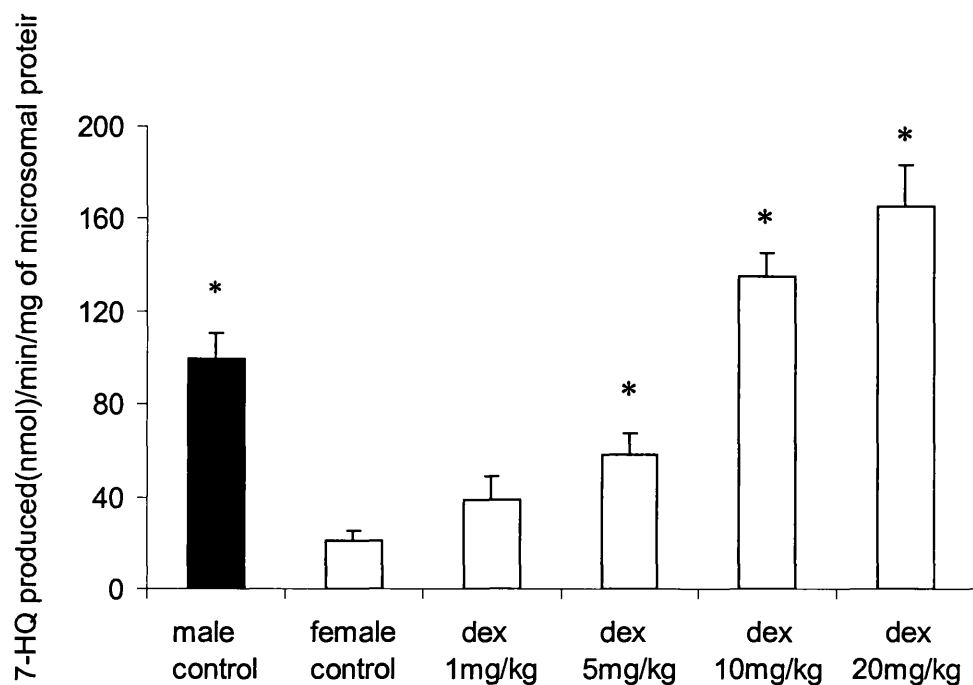


Figure 4.7 CYP3A activity in female rats treated with oral dexamethasone (1-20 mg/kg, p.o.) compared to untreated female rats (open bars) and untreated male (filled bar). CYP3A activity was measured by the conversion of 7-BQ to 7-HQ by microsomes prepared from rat livers 24 hours after dexamethasone administration. Values, expressed as the amount of 7-HQ produced (nm) /min/gram of microsomal protein, are the mean \pm SD of four animals. Stars indicate values are significantly different to female controls ($p < 0.05$ by ANOVA).

4.6 Effect of pre-treatment with dexamethasone on levels of ET-743 in the liver and blood

On the basis of the results presented in chapter 4.5, it is conceivable that dexamethasone-induced CYP3A enzymes in rat liver oxidise ET-743 to a non-hepatotoxic species at a faster rate than livers of rats which have not been pre-treated with dexamethasone. If this hypothesis is correct, it follows that increased metabolism of ET-743 by dexamethasone-induced CYP3A isozymes leads to decreased levels of parent ET-743 in the liver compared to treatment with ET-743 without CYP3A pre-induction. Levels of ET-743 were measured in liver and plasma of rats which had been pre-treated with an optimal hepatoprotective dose of dexamethasone (10 mg/kg, p.o.), and these were compared with animals which had received ET-743 only. ET-743 was measured by HPLC coupled to electrospray ionisation tandem mass spectrometry by collaborators at the Mario Negri Institute, Milan, Italy. Figure 4.8 shows that the levels of ET-743 measured in the livers from rats pre-treated with dexamethasone were dramatically lower than those levels measured in livers from animals which did not receive dexamethasone. At one hour after administration of ET-743 liver levels were 37 pmols/g liver tissue, whereas the levels in animals pre-treated with dexamethasone were 5 pmols/g liver tissue. In contrast, dexamethasone pre-treatment neither changed the shape of the plasma concentration versus time curve, nor decreased systemic exposure to ET-743, as measured by the area under the plasma concentration versus time curve (AUC between and 0 and 6 hours after dosing). AUC values, shown in table 4.2, were not significantly different from animals which received ET-743 alone or after dexamethasone pre-treatment.

<u>Treatment</u>	<u>AUC</u>	
	Mean (ng/ml.h)	SD
ET-743 alone	1.65	0.87
Dexamethasone and ET-743	1.75	0.29

Table 4.2 The AUC values for plasma between 0 and 6 hours obtained from rats which received ET-743 alone or ET-743 after dexamethasone pre-treatment (n=4).

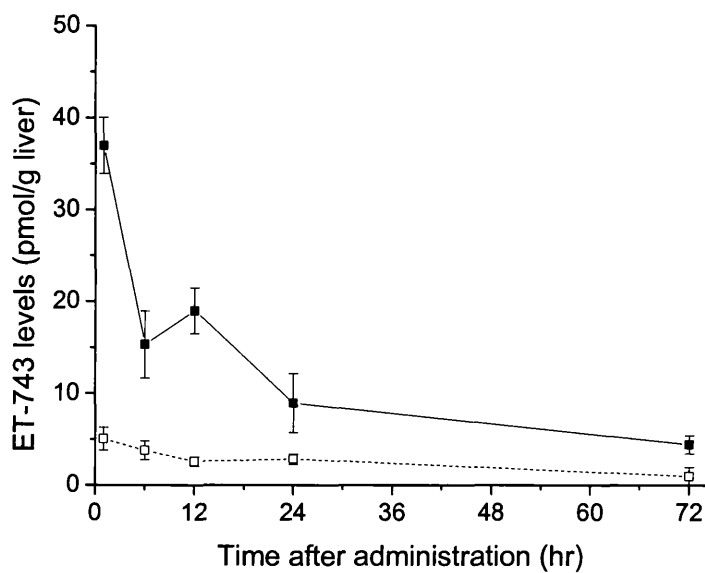


Figure 4.8 Effect of pre-treatment with dexamethasone on the disposition of ET-743 in liver tissue of female rats. Values reflect ET-743 levels in the liver of rats which received ET-743 (40 $\mu\text{g}/\text{kg}$, i.v.) 24 hours after either dexamethasone (10 mg/kg, p.o.) (open squares) or glycerol formal, the vehicle for dexamethasone (closed squares). Values are the mean \pm SD of four rats.

4.7 Effect of pre-treatment with dexamethasone on anti-tumour activity of ET-743

In order to justify exploration of dexamethasone pre-treatment in the clinic it is of paramount importance to demonstrate that dexamethasone does not adversely affect the anti-tumour activity of ET-743. This work was carried out by collaborators at the Mario Negri Institute, Milan using a number of rodent models. The anti-tumour activity was initially studied in female Fischer rats bearing the 13762 mammary carcinoma. The animals received dexamethasone 9 days *post* tumour implantation and 24 hours later ET-743 was administered. Tumour weight was determined on days 14 and 17 *post* tumour implantation. Both dexamethasone (10 mg/kg, i.p.) and ET-743 (40 µg/kg, i.v.) individually exhibited anti-tumour activity, and the combination was not inferior to either of that of the single agents (figure 4.9). On day 14 *post* tumour implantation, the tumour weight inhibition (TWI) was 34 % after ET-743 treatment and 42% after dexamethasone treatment. The TWI of the combination was 57 %, which is 68 or 36 % greater than the values observed with either ET-743 or dexamethasone, respectively, alone.

The activity of ET-743 with dexamethasone pre-treatment was also investigated in murine tumour models of melanoma (B-16), reticulum cell sarcoma (M5076), ovarian carcinoma (IGROV-1) and rhabdomyosarcoma (TE-671) (Table 4.3). A variety of dosing regimes and dose levels of ET-743 were used in order to account for differential sensitivities of the individual models and to allow discrimination between efficacies of the individual constituents. Dexamethasone given as repeated i.p. doses (see table 4.3) exhibited significant anti-neoplastic activity on its own in the murine B16 melanoma and IGROV-1 ovarian tumour model. In none of the rodent models investigated was the combination less efficacious than ET-743 administered alone. Moreover, in three of the models investigated, the 13762, B16 and TE-671 models the combination was clearly more efficacious than ET-743 alone.

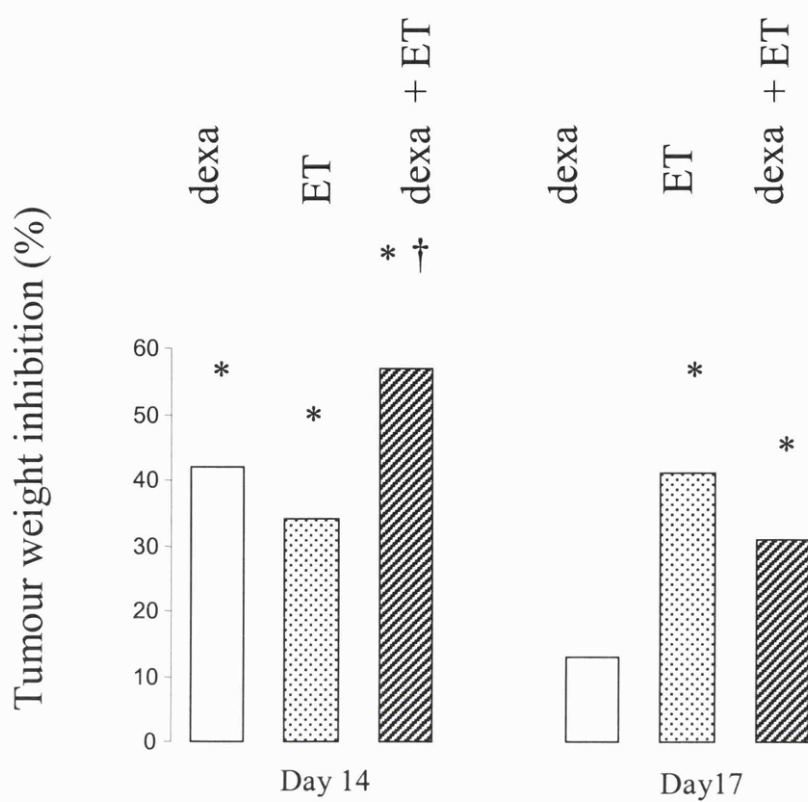


Figure 4.9 Anti-tumour activity of dexamethasone (10 mg/kg, i.p.), ET-743 (40 µg/kg, i.v.) or ET-743 in combination with dexamethasone given 24 hours prior to ET-743, in female Fischer rats bearing the 13762 mammary carcinoma. Tumour weight in control rats was 1.60 ± 0.27 g (mean \pm SE), stars indicate that tumour weight values were significantly reduced ($p < 0.01$ by Fisher's test) compared to controls, dagger indicates that tumour weight in animals which received the combination was significantly different from that in rats on ET-743 only ($p < 0.05$ by Fisher's test). For method of TWI calculation see chapter 2.2.9.

<u>Tumor model</u>	<u>Dose schedule</u>		<u>TWI (%)¹</u>		
	Dexa ²	ET-743 ³	Dexa	ET-743	Combination
B-16 ⁴	40 mg/kg on days 7, 8, 9, 14, 15, 16 ⁸	0.15 mg/kg on days 10 and 17	52 ^{**}	45 ^{**}	69 ^{**} ,↓
M5076 ⁵	40 mg/kg on days 11, 12, 13, 18, 19, 20	0.15 mg/kg on days 14 and 21	10	64 ^{**}	65 ^{**}
IGROV-1 ⁶	40 mg/kg on days 8, 9, 10, 15, 16, 17, 22, 23, 24	0.2 mg/kg on days 11, 18, 25	41 [*]	56 ^{**}	60 ^{**}
TE-671 ⁷	20 mg/kg on days 12, 13, 14, 15	0.2 mg/kg on day 15	15	33 [*]	68 ^{**} ,↓

Table 4.3 Activity of dexamethasone, ET-743 and the combination against mouse B-16 melanoma, M5076 reticulum sarcoma, IGROV-1 ovarian carcinoma and TE-671 rhabdomyosarcoma.

¹ TWI = tumour weight inhibition = $100 - (T/C \times 100)$, with T = tumour weight of treated animals, C = tumour weight of control animals.

² dexamethasone via the i.p. route

³ ET-743 via the i.v. route

⁴ tumour weight evaluated on day 23, control tumours weighed 6.13 ± 0.59 g (mean \pm S.E.)

⁵ tumour weight evaluated on day 32, control tumours weighed 2.89 ± 0.25 g (mean \pm S.E.)

⁶ tumour weight evaluated on day 32, control tumours weighed 3.84 ± 1.11 g (mean \pm S.E.)

⁷ tumour weight evaluated on day 34, control tumours weighed 4.90 ± 0.22 g (mean \pm S.E.)

⁸ days *post* tumor implantation

* tumour weight significantly different from untreated mice ($p < 0.05$, Fisher's test)

** tumour weight significantly different from untreated mice ($p < 0.01$, Fisher's test)

↓ tumour weight significantly different from ET-743-treated mice ($p < 0.05$, Fisher's test)

4.8 *In vitro* bioassay to predict toxicity of ET-743 metabolites

The results described so far hint at the possibility that dexamethasone induces CYP3A isozymes which increase the metabolism of ET-743 in the liver to a less hepatotoxic species. In an attempt to support this hypothesis and to measure the cytotoxicity of possible ET-743 metabolites, an *in vitro* experiment was performed using a breast tumour cell line. Potential metabolites were generated by incubating ET-743 with microsomes from untreated and dexamethasone treated rats. MCF-7 cells were treated with the supernatant from the incubates and cell number was determined 48 hours after treatment. ET-743 (0.2 nM) applied directly to the cells resulted in $41 \% \pm 4.9$ inhibition of cell growth (Figure 4.10). MCF-7 cells treated with supernatant from microsomes incubated with ET-743 inhibited cell growth by $25 \pm 3.7 \%$ whilst MCF-7 cells treated with supernatant from microsomes obtained from dexamethasone treated rats then incubated with ET-743 inhibited cell growth $11 \pm 2.9 \%$. These results suggest that enzymes in the liver convert ET-743 to a less cytotoxic species and that the conversion to a less cytotoxic species is further increased after pre-treatment with dexamethasone. This finding is consistent with the hypothesis that dexamethasone induces the metabolism of ET-743 to a less toxic species in the liver.

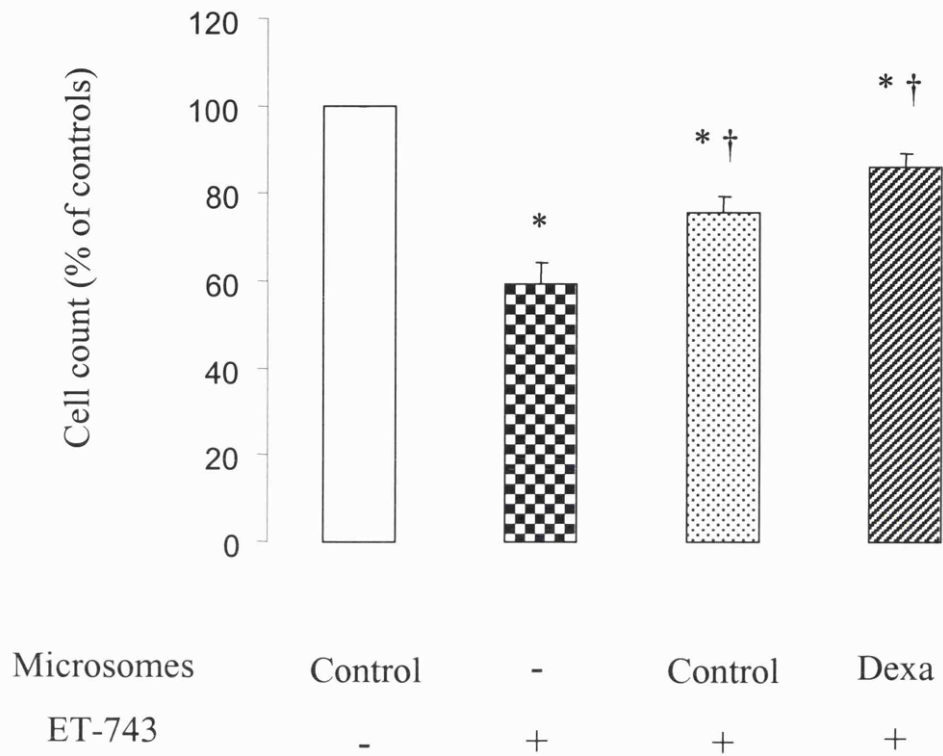


Figure 4.10 The effect of ET-743, and ET-743 after microsomal metabolism on cytotoxicity towards MCF-7 cells. ET-743 was incubated with microsomes from control rats, dexamethasone treated rats or without microsomes, as described in section 2.2.29. The incubation mixture containing ET-743 and/or metabolites, was added to MCF-7 cells and the cytotoxicity was determined by comparing the cell count with that of untreated cells (cells treated with incubates of microsomes without ET-743). The number of untreated cells was 4×10^5 , and this was taken as 100 %. Values are the mean \pm SD from 3 incubations. Star indicates that cell counts were significantly different to controls ($p < 0.05$ by ANOVA), and daggers indicate that cell counts were significantly different to those after ET-743 treatment.

4.9 Discussion

A single dose of dexamethasone administered alone at all dose levels caused loss of up to 10 % body weight within a day of administration, and this weight loss was not dose related. This body weight loss made dexamethasone treated animals more vulnerable to subsequent treatment with ET-743. There is little information in the literature about the adverse effects of dexamethasone, which is frequently used in rodents to induce CYP3A activity. Possible reasons for the weight loss after dexamethasone treatment include decreased food intake, decreased food absorption or increased metabolic rate.

Pre-treatment with high-dose dexamethasone afforded dramatic protection against the detrimental effects of ET-743 as reflected by plasma levels of bilirubin and activity of liver enzymes AST and ALP, and by pathological change. Dexamethasone also abolished almost all the alterations in hepatic gene expression which accompanied ET-743-mediated liver damage. The timing of administration of dexamethasone in relation to that of ET-743 was shown to be crucial, as co-administration failed to protect the rat liver against ET-743, and may even have exacerbated the liver changes.

Dexamethasone possesses numerous pharmacological activities including activation of many transcription factors and anti-inflammatory stimuli, many of which could conceivably contribute to its ability to protect rat liver from the adverse effects of ET-743. Results of the microarray analysis suggest that the expression of a number of genes was altered 24 hours after a hepatoprotective dose of ET-743. Many of the genes were involved in fatty acid synthesis, carbohydrate metabolism and gluconeogenesis, which are known effects of glucocorticoids. The most highly up-regulated genes were four genes coding for members of the CYP3A family. Consistent with this up-regulation of gene expression, CYP3A activity was significantly elevated after dexamethasone treatment, suggesting that protection by dexamethasone is due to induction of CYP3A and thus increased metabolic removal of ET-743. This notion is supported by the fact that pre-treatment with dexamethasone resulted in a dramatic suppression of hepatic ET-743 levels. *In vitro* metabolism studies have shown that

ET-743 is metabolised to three species, N-desmethyl ET-743 (ET-729) and two molecules generated by oxidative degradation of the drug (section 1.10.5). However, no metabolites of ET-743 could be identified in the plasma or liver from rats treated with dexamethasone and ET-743. Therefore, alternative explanations cannot be discarded. Dexamethasone may exert its effects by elevated bile flow and consequent increase in the rate of ET-743 elimination from the liver.

The observation that co-administration failed to protect the rat liver against ET-743, and may even have exacerbated the liver changes was unexpected. Possible reasons why concurrent dexamethasone treatment failed to decrease hepatotoxicity may be that it takes 24 hours for dexamethasone to induce CYP activity, assuming that CYP activity is the mechanism by which dexamethasone pre-treatment protects against ET-743 hepatotoxicity. The histopathology findings and the results of the AST assay suggest that co-administration of dexamethasone with ET-743 increases ET-743 toxicity. One possible explanation for this effect may be that dexamethasone causes an initial fall in CYP activity which results in a reduced metabolism of ET-743. This explanation requires further investigation.

The genes coding for metallothionein 1 and 2, were up-regulated by ET-743 and expression was still elevated after pre-treatment with dexamethasone. These two genes were the only genes in which expression did not return to control levels after dexamethasone pre-treatment. Metallothioneins are cysteine-rich metal binding proteins with a high affinity for heavy metal ions. Although the biological functions of metallothioneins have not been fully elucidated, they are thought to play an important role in detoxification of toxic elements such as cadmium and mercury. They are also highly expressed during liver regeneration, as a result of a series of growth stimulators (Friedman et al., 1984). The possibility that metallothionein could participate in a DNA synthesis-related process through donation or abstraction of zinc to and from transcription factors has been inferred from *in vitro* studies (Moffatt and Denizau, 1997). Overexpression of metallothionein is often accompanied by increased resistance towards a variety of alkylating agents and chemotherapeutic drugs. The latter two physiological processes might explain the over expression of metallothioneins in response to

ET-743 treatment. Metallothionines are inducible by glucocorticoids as well as metals and two glucocorticoid response elements have been found to regulate expression of the metallothionine genes (Kelly et al., 1997), which might explain why the genes encoding for metallothionine 1 and 2 were up-regulated by a combination of dexamethasone and ET-743.

The results from the *in vitro* bioassay intimate that in dexamethasone-treated rat liver ET-743 is metabolised to a less cytotoxic species. This suggestion stems from the finding that incubations of ET-743 with microsomes from dexamethasone treated rats were less toxic to MCF-7 cells than incubations of ET-743 and microsomes from untreated rats.

Most importantly, dexamethasone did not interfere with the anti-tumour activity of ET-743, as in none of the five models tested was the anti-tumour activity of the combination less effective than that of ET-743 alone. Interestingly, in three tumour models the combination was more efficacious than ET-743 alone. Dexamethasone pre-treatment failed to decrease ET-743 plasma levels despite the dramatic decrease in liver levels. This finding suggests that the systemic availability of ET-743 is not diminished by high-dose dexamethasone. These findings taken together suggest that while dexamethasone pre-treatment decreases hepatic levels of ET-743, it does not interfere markedly with the steps that determine the rate of elimination from the systemic circulation and does not interfere with its anti-tumour activity.

The finding that dexamethasone pre-treatment had no effect on the plasma AUC whilst dramatically lowering ET-743 in the liver, is difficult to explain. Discussions with pharmacokinetic specialists did not provide clarifying explanations. There are two issues which may hint at possible explanations. Firstly, Dr. Zuchetti, who did the ET-743 analysis, clearly indicated that, whilst the choice of time points allowed the calculation of plasma AUC values, the time points were not optimally chosen, more early intervals would have been desirable to describe possible effects of dexamethasone on ET-743 disposition. This lack of early time point data leaves the possibility that dexamethasone caused a considerable change in the early part of the plasma concentration versus time curve, which our design would not have allowed to discover. Secondly, it seems important to consider that plasma AUC is

dependent on clearance, and clearance is governed by a series of uptake and elimination equilibria, especially from the blood into the liver and from the liver into the bile. It is just conceivable that the uptake of ET-743 into the liver is very slow and is thus the rate-determining step in the overall plasma clearance of the drug. If this was the case, even drastic changes in clearance of the drug from the liver by increased metabolism and/or increased bile flow and thus increased elimination of the parent drug from the liver would not affect drastically plasma clearance, as it is governed by the liver uptake equilibrium. As no examples were found in the literature to support the validity of this explanation attempt, this explanation needs to be interpreted with appropriate caution.

In a phase II study, patients who received dexamethasone (10 mg/kg) just prior to ET-743 infusion had a diminished incidence of severe toxicity (Puchalski et al., 2002). This finding is in contrast to the situation in rats in which simultaneous administration of dexamethasone and ET-743 enhanced toxicity. Whilst the true effect of dexamethasone on the toxicity of ET-743 in humans is difficult to delineate from the study by Puchalski *et al*, as the effect was not significant, the study may allow some careful interpretations as to differences and similarities between the situation in humans and in rats. Dexamethasone pre-treatment 24 hours prior to ET-743 abolished ET-743-induced hepatotoxicity in rats. ET-743-induced hepatotoxicity in humans is less severe than that reported in the female rat, and hepatic changes are generally reversible in patients. It is conceivable that the mechanisms by which ET-743 induces hepatic damage differ between rats and humans, and that such differences lead to different susceptibilities towards amelioration by dexamethasone. Similarly, the mechanism by which dexamethasone protects against ET-743-induced damage may differ between humans and rats. The biological response to ET-743 using a long term pre-treatment interval for dexamethasone in rats may be related to dexamethasone's effect on CYP3A-induced metabolism, whereas the effect of the shorter pre-treatment interval in humans may be due to the anti-inflammatory effects of dexamethasone. Another explanation as to why dexamethasone pre-treatment was effective when given immediately prior to ET-743 in human but not effective when given immediately before ET-743 in rats may be due to the different dosing schedules of ET-743. In patients ET-743 is administered over 24 h by infusion, whereas in the rat model, ET-743 is

administered as a single bolus. Therefore, the peak ET-743 plasma concentration occurs immediately after administration in rats, whereas in patients plasma ET-743 levels will rise during the first few hours of infusion and then plateau as the drug is metabolised and eliminated. In humans low levels of ET-743 are in the blood for at least 24 hours after dexamethasone administration. The finding that administration of dexamethasone 24 hours prior to ET-743 in the rat significantly ameliorated ET-743-mediated hepatotoxicity, suggests that it may be possible to increase the beneficial effects of dexamethasone in patients by increasing the time period between administration of dexamethasone and that of ET-743. A dosing regime based on this premise should be evaluated in patients.

The doses of dexamethasone given to patients are considerably lower than those given in this study to rats. High-dose dexamethasone therapy is used clinically in conditions in which immunosuppression and anti-inflammation are desired, such as systemic lupus, erythematosus, renal transplantation, steroid resistant nephritic syndrome and crescentic glomerulonephritis. The adverse effects of high-dose dexamethasone treatment include hypertension, arrhythmias, hypokalemia, psychosis and susceptibility to infection (Hari and Srivastava, 1998; Sprung et al., 1984). Therefore it may be difficult to use such high doses of dexamethasone in patients as have been used in rats in the experiment described here. However, there is a powerful rationale to fully evaluate the potential clinical usefulness of pre-treatment with dexamethasone in cancer patients who receive ET-743.

CHAPTER 5

Evaluation of the protective efficacy of β -naphthoflavone, phenobarbitone and N-acetylcysteine against ET-743–induced toxicity *in vivo*

5.1 Introduction

Dexamethasone pre-treatment has been shown to abrogate ET-743-mediated hepatotoxicity in the female rat model without impeding its anti-tumour activity (chapter 4). Protection by dexamethasone pre-treatment was accompanied by a dramatic reduction in hepatic levels of ET-743, implicating induction of hepatic clearance of ET-743, perhaps *via* metabolic enzymes, as the mechanism by which dexamethasone exerts its beneficial effect. Dexamethasone induces CYP3A which is thought to play a major role in ET-743 metabolism (Reid et al., 2002; Reid et al., 1996). However, other CYPs may also play a role in oxidative metabolism of ET-743. *In vitro* metabolism of ET-743 in rat liver microsomes was induced by pre-treatment with phenobarbitone, an inducer of CYP2B, CYP2C and CYP3A (Reid et al., 1996). Whilst inhibition of ET-743 metabolism was observed with inhibitors of CYP2C, CYP1A and CYP3A. When ET-743 was incubated with lymphocytes expressing specific CYPs, CYP2A and CYP3A2 had the greatest ability to metabolise ET-743, and substantial ET-743 metabolism was also observed for CYP2C6, CYP2D1 and CYP2E1 (Reid et al., 2002).

Conjugation with glutathione is a major mechanism for the elimination of toxic compounds. Depletion of glutathione renders cells more susceptible to the toxic effects of drugs, reactive metabolites and other xenobiotics in which toxicity is due to nucleophilic attack. In the case of paracetamol overdose, the sulfate and glucuronic acid conjugation pathway become saturated and the cytochrome P450 pathway becomes critical, since it generates a toxic metabolite which can deplete intracellular glutathione and lead to cell injury and death (chapter 1.6). The alkylating anti-cancer drugs, mechlorethamine, chlorambucil and cyclophosphamide deplete hepatocyte GSH resulting in lipid peroxidation and cytotoxicity in isolated hepatocytes (Khan et al., 1992). In such cases where GSH is depleted, N-acetylcysteine can replenish intrahepatocellular stores of thiol moieties and increase levels of glutathione, thus buttressing the cell's capacity to detoxify potentially harmful chemically reactive drug-derived species (Burgunder et al., 1989; Rumack et al., 1981). Not all glutathione conjugation reactions lead to detoxification. An instructive example is ANIT, which produces cholestasis,

hyperbilirubinemia, and bile duct epithelial cell necrosis in rats, changes which are not dissimilar to those induced by ET-743 (see chapter 3.7). This agent undergoes metabolic reaction with glutathione to generate a dithiocarbamate intermediate (Carpenter-Deyo et al., 1991). The conjugate is thought to be transported into the bile, where it can revert back to glutathione and α -naphylisothiocyanate resulting in the accumulation in the biliary tract of the latter at cytotoxic concentrations. To date, there is no information on the effect of ET-743 on glutathione levels and whether ET-743 is detoxified by a GSH-dependent pathway.

In the work described in this chapter the effects of three modulators of drug metabolism on ET-743-induced liver damage are investigated and observations important to the hepatotoxicity of ET-743 in rats extended. The hepatoprotective capacity of β -naphthoflavone, phenobarbitone and N-acetylcysteine are compared with that of dexamethasone *in vivo*. β -Naphthoflavone and phenobarbitone induce primarily cytochrome P450 (CYP) enzyme families 1A1/2 and 2B, respectively (chapter 1.5.1), and can thus increase the rate of oxidative metabolic disposition of suitable drug substrates. In addition the levels of non-protein thiols levels are investigated after ET-743 administration and the protective effect of N-acetylcysteine on ET-743-mediated hepatotoxicity assessed.

Results

5.2 Effect of β -naphthoflavone, phenobarbitone and N-acetylcysteine on ET-743-induced elevations of plasma indicators of hepatotoxicity

Rats were pre-treated with β -naphthoflavone, phenobarbitone or N-acetylcysteine before they received ET-743. The effect of pre-treatment with these agents on ET-743 mediated hepatic alterations, as indicated by levels of bilirubin, ALP and AST in the plasma, are shown in figure 5.1. ET-743 administered on its own elicited dramatically raised biochemical indicators in the plasma, as seen previously (section 3.1). Pre-treatment with β -naphthoflavone, administered on 3 consecutive days 24 hours prior to ET-743, ameliorated the ET-743-induced liver changes in that all three indicators of hepatic damage observed on day 3 were indistinguishable from those measured in untreated rats. The protective effect lasted partially for 12 days as the levels of AST and bilirubin in rats pre-treated with β -naphthoflavone remained at levels measured in untreated rats, but ALP levels were as elevated as those seen in rats treated with ET-743 only. Pre-treatment with phenobarbitone for one week prior to administration of ET-743 had no significant effect on the elevated levels of AST and ALP activity induced by ET-743. However it prevented the ET-743-induced elevations of plasma bilirubin levels at both 3 days and 12 days. Pre-treatment with N-acetylcysteine had no protective effect, as levels of bilirubin, AST and ALP were as elevated as those in animals which received ET-743 only. As described in the previous chapter, also observed here, dexamethasone given 24 hours prior to ET-743 completely abolished the ET-743-induced rise in plasma bilirubin, ALP and AST for at least 12 days.

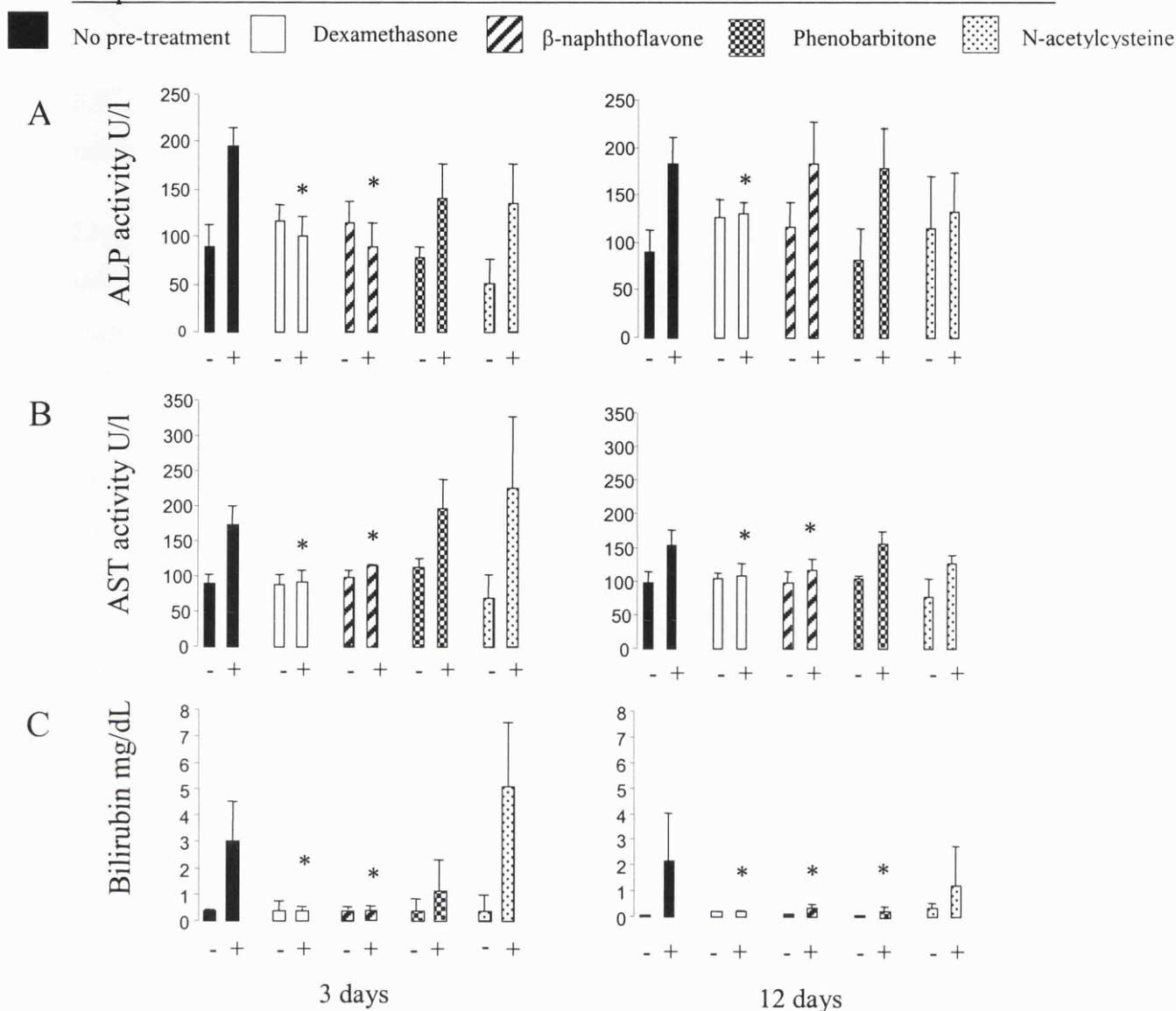


Figure 5.1 The effect of dexamethasone, β -naphthoflavone, phenobarbitone and N-acetylcysteine when administered prior to ET-743 (40 μ g/kg, i.v.) on ET-743 induced increases in the plasma activities of ALP, (A), AST (B) and of plasma levels of bilirubin (C) in female Wistar rats. Dexamethasone was dosed at 20 mg/kg, p.o. 24 hours prior to ET-743. Doses for β -naphthoflavone, phenobarbitone and N-acetylcysteine are given in section 2.2.6. Indicators of hepatic damage were measured 3 and 12 days after ET-743 administration. Plus and minus signs represent rats treated with ET-743 or the vehicle (water), respectively. Values are the mean \pm SD of 4 animals. Star indicates that values are significantly different ($p < 0.05$ by ANOVA) from activities and levels in animals which received ET-743 only.

5.3 Effects of β -naphthoflavone, phenobarbitone and N-acetylcysteine on ET-743 induced histopathological changes in liver

Livers of animals which received only ET-743 (40 μ g/kg, i.v.) revealed degenerative and inflammatory changes in the biliary epithelium (figure 5.2B) compared to livers of control rats (figure 5.2A). Pre-treatment with β -naphthoflavone abolished the degenerative and inflammatory effects on the biliary epithelium on day 3 (figure 5.2D). At 12 days the peri-biliary fibrosis was less marked in the β -naphthoflavone pre-treated rats, compared to rats that had received ET-743 alone. However, β -naphthoflavone treatment appeared to have little effect on the degree of hepatocellular necrosis induced by ET-743 at 12 days. In rats pre-treated with phenobarbitone, inflammatory changes in the bile ducts were less severe than in rats on ET-743 only, but differences were slight. Rats which had received N-acetylcysteine followed by ET-743 displayed increased biliary damage compared with rats treated with ET-743 alone (figure 5.2C). In one animal on the combination, focal areas of bile duct epithelium showed complete necrosis. Nevertheless, there was no evidence of any increase in the extent of hepatocellular necrosis in these animals

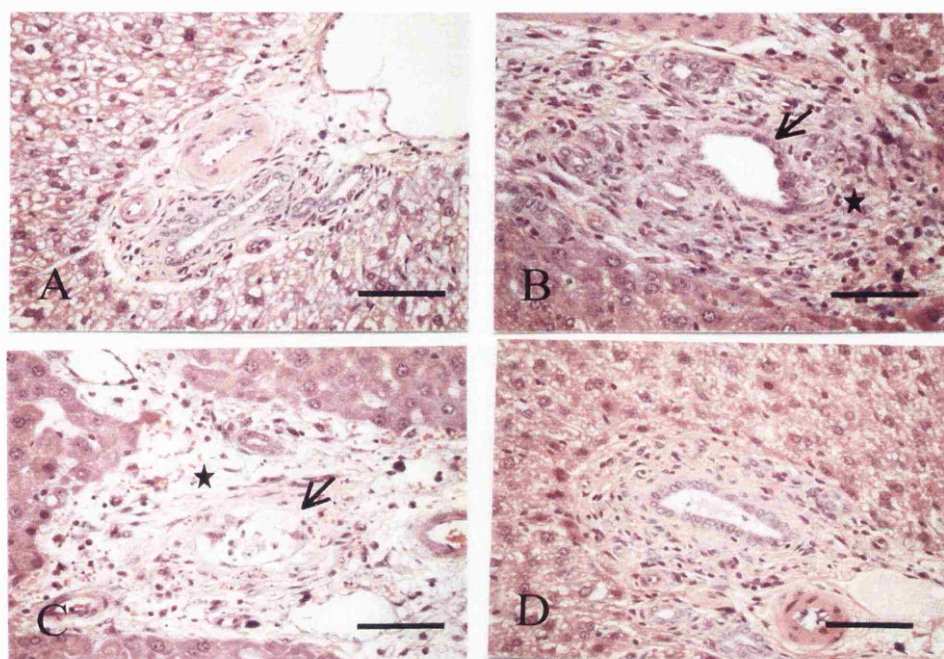


Figure 5.2 The effect of N-acetylcysteine and β -naphthoflavone on ET-743-induced changes in liver pathology. Photomicrographs of liver sections from control (vehicle treated) female Wistar rats (A) and from rats that received ET-743 alone (B) or ET-743 one hour after N-acetylcysteine (C) or 24 hours after β -naphthoflavone (D). Doses for β -naphthoflavone and N-acetylcysteine are given in section 2.2.6. Liver tissues were excised 3 days after administration of ET-743. Staining was by haematoxylin and eosin. Note in B the enlarged, thickened portal tract with a sparse infiltrate of inflammatory cells (star) and the damaged bile duct (arrow), which is lined by degenerative and reactive epithelium, characteristics of ET-743 induced changes in liver of female rats. The features are somewhat intensified by N-acetylcysteine (C) as shown by the almost total necrosis of the bile duct epithelium (arrow) and the surrounding swelling and cell debris (star) in the portal tract. In contrast, in livers of rats pre-treated with β -naphthoflavone (D), comparable portal tracts are almost indistinguishable from controls. Sections are representative of four animals. Bar equals 100 μ m. Histopathological analysis was carried out by Dr Peter Greaves.

5.4 Effects of ET-743 on hepatic glutathione levels

In order to investigate the effect of ET-743 on hepatic glutathione levels, levels of glutathione were measured in rat liver three days after administration of ET-743. The concentration of glutathione in liver after ET-743 treatment was elevated by 16 % (figure 5.3).

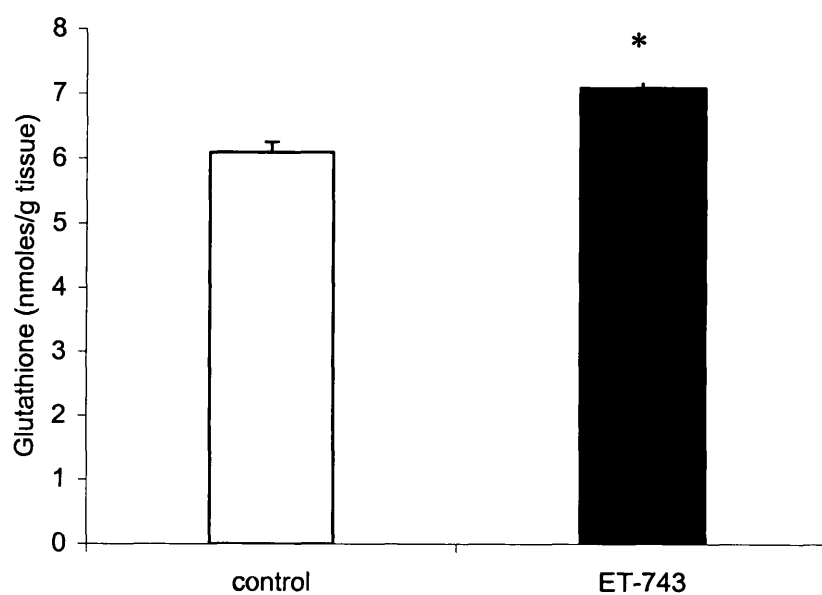


Figure 5.3 The effect of ET-743 on hepatic glutathione levels. Glutathione was measured in livers from animals three days after administration of ET-743 (40 $\mu\text{g}/\text{kg}$, i.v.) or vehicle (water). Values are the mean \pm SD of three animals. Star indicates that values are statistically significant ($p < 0.05$ by ANOVA).

5.5 Discussion

Pre-treatment with β -naphthoflavone and phenobarbitone ameliorated the detrimental effect of ET-743 on rat liver. The protection provided by β -naphthoflavone and phenobarbitone *in vivo* was not as efficacious as that afforded by dexamethasone. Reduction of ET-743-mediated hepatotoxicity by β -naphthoflavone persisted only for a short time, and that by phenobarbitone was weak, as reflected by significant suppression of elevation of only one biochemical indicator, bilirubin, but not of the others. Another agent, N-acetylcysteine, failed to protect rat livers against ET-743 altogether.

The protection afforded by dexamethasone was accompanied by dramatically decreased hepatic levels of ET-743 and by up-regulated CYP3A enzyme levels, suggesting that protection by dexamethasone is the consequence of the increased clearance of the drug from the liver, possibly mediated by metabolism involving CYP3A (see chapter 4). CYP families other than CYP3A, such as CYPs1A, 2A and 2C, have been potentially implicated as minor contributors to the overall hepatic metabolism of ET-743 (Reid et al., 2002; Reid et al., 1996). On the basis of these findings, tentative inferences can be made as to the mechanisms by which β -naphthoflavone and phenobarbitone ameliorated the effects of ET-743 on the rat liver. Like dexamethasone, β -naphthoflavone and phenobarbitone are inducers of oxidative drug metabolism, the former of CYP1A, the latter of a variety of CYPs, mainly CYP2B but also CYP3A (Nebert and Gonzalez, 1987). Raised CYP enzyme levels consequent to pre-treatment with β -naphthoflavone and phenobarbitone may have been, at least in part, responsible for their protective efficacy. It is important to note though that these agents possess a variety of physiological effects which may contribute to protection. In the case of phenobarbitone it is well known that it induces liver bile flow (Berman et al., 1983) and this property may well have been involved with the protection afforded by phenobarbitone. In experiments with Gunn rats, an animal model displaying hyperbilirubinemia, administration of inducers of CYP1A such β -naphthoflavone were shown to decrease plasma bilirubin levels (Kapitulnik and Ostrow, 1978). This study led to the hypothesis that the CYP1A family might

be involved in an alternate pathway of bilirubin elimination in Gunn rats that lack the normal detoxification pathway via glucuronidation. Supporting this concept CYP1A1 was shown to catalyse bilirubin degradation *in vitro* (De Matteis et al., 1991). In addition to CYP1A1/2 induction, β -naphthoflavone is known to induce phase II enzymes such as DT- diaphorase and UDP-glucuronosyl transferase, which may play a role in the protection against the adverse effect of ET-743 towards the liver (Saarikoski et al., 1998; Favreau and Pickett, 1995).

β -naphthoflavone has been shown to induce CYP1A1 in the lungs by 20-fold (Ioannides and Parke, 1990). When a single i.v. injection of a drug is given, high concentrations are seen first in the right heart and lung. Therefore, assuming that CYP1A2 is involved in ET-743 metabolism, it is possible that β -naphthoflavone induction of CYP1A2 in the lung results in increased metabolism of ET-743 in this tissue and as a result a lower concentration of parent compound reaches the liver. Dexamethasone has also been shown to induce CYP3A activity in mouse lung (Haag et al., 2003), therefore, it is possible that dexamethasone may also increase metabolism of ET-743 in the rat lung resulting in lower levels of parent compound reaching the liver. Phenobarbitone has no significant effect on CYP activity in rat lung (Lee et al., 1998).

The untoward hepatic effects of many hepatotoxicants, which comprise alkylating or arylating moieties, or which generate such functionalites *via* metabolism, can efficiently be counteracted by strategies leading to the elevation of intracellular thiols (DeLeve and Kaplowitz, 1991). In contrast, other agents can undergo metabolic toxification by reaction with glutathione. As N-acetylcysteine pre-treatment failed to reduce ET-743-induced hepatotoxicity, it is unlikely that the hepatic damage produced by ET-743 treatment were caused by reactive electrophiles, which escape efficient detoxification by reacting with glutathione. In addition, it was demonstrated that ET-743 at the hepatotoxic dose used in this study did not deplete glutathione levels in rat liver. Levels of ET-743 were found to be approximately 40 pmols/g tissue after a hepatotoxic dose ET-743 (40 μ g/kg, i.v.) and it is unlikely that such low levels would deplete the liver glutathione levels. Therefore, if ET-743 does react covalently with non-protein thiols, the levels of hepatic thiol stores are probably

more than adequate for efficient metabolic transformation. All these findings suggest that hepatic glutathione does not detoxify ET-743. There was even an indication of increased ET-743 toxicity after pre-treatment with N-acetylcysteine especially on histopathological observation. These findings hint at the possibility that ET-743 reacts with GSH to generate a hepatotoxic species, in analogy to the mechanism by which ANIT is thought to cause hepatotoxicity. In addition, as found with ANIT treatment, hepatic glutathione levels were elevated after ET-743 exposure, but only to a small extent. Nevertheless, as the increase of ET-743-induced hepatic changes by N-acetylcysteine and the increase in non-protein thiols were not profound, the suggestion that ET-743 reacts with GSH to form a hepatotoxic species has to be drawn with caution and requires further experimental verification.

Of all the potential protectants tested thus far dexamethasone and β -naphthoflavone were most promising, the former displaying high, the latter moderate, efficacy, as potential antidotes against ET-743-induced hepatotoxicity. In light of the fact that dexamethasone and β -naphthoflavone were effective at reducing ET-743-induced hepatotoxicity, it is conceivable that increased oxidative metabolism of ET-743 is a mechanism which limits its hepatotoxic potential.

6.1 Introduction

Most of the current understanding of liver damage caused by xenobiotics has been obtained in animal models. Preclinical data cannot be easily extrapolated to humans due to species differences in the metabolism and elimination of foreign compounds. In the light of the current trend to reduce animal experimentation, liver cells in incubation or culture are often used to screen drugs for hepatotoxic potential and to reveal insights into mechanisms by which they may exert such toxicity (chapter 1.9). *In vitro* methods have been used to predict the *in vivo* liver toxicity of well known hepatotoxicants, such as paracetamol (Paillard et al., 1999) and carbon tetrachloride (Frazier, 1993). A major advantage of *in vitro* systems is the ability to use the systems to make direct comparisons between humans and rodents, thereby helping in the extrapolation of observations from laboratory animals to humans. However, it is important to explore for each new drug to what extent experiments using hepatocytes *in vitro* can reliably predict potential hepatotoxicity which may occur *in vivo*.

In this chapter, the toxicity of ET-743 to cultured hepatocytes isolated from female rats is investigated and the usefulness of this *in vitro* model to predict aspects of ET-743-mediated hepatotoxicity is assessed. The protective activity of dexamethasone, β -naphthoflavone, phenobarbitone and N-acetylcysteine against ET-743 hepatic changes displayed *in vivo* was also tested *in vitro* in cultured hepatocytes isolated from rats which have undergone appropriate pre-treatment. In addition, the similarity of response to ET-743 of liver cells from both rats and humans is assessed in a preliminary fashion.

Results

6.2 Effect of ET-743 on hepatocytes isolated from female rats

Initially the toxicity of ET-743 to hepatocytes was assessed using hepatocytes in suspension. Hepatocytes in suspension only remain viable for up to 6 hours, during which time ET-743 at concentrations of 1 nM to 1 μ M had no or only slight detrimental effects. As a result, isolated hepatocytes were cultured, which extended their viability to about a week. Incubation of cultured rat hepatocytes with ET-743 resulted in a time and dose-dependent decrease in cell viability (Figure 6.1). Viability of hepatocytes after 48 hours exposure to ET-743 at 1 nM, 10 nM, 100 nM and 1 μ M was 78 ± 3 , 65 ± 7 , 54 ± 2 and 46 ± 7 % of control viability, respectively. After 96 hours viability at these dose levels was 67 ± 2 , 28 ± 3 , 21 ± 4 and 8 ± 1 %, respectively when compared to controls. DMSO alone had no significant effect on hepatocyte viability.

The concentrations of ET-743 required to kill cultured hepatocytes were surprisingly high compared to the concentrations which were reported to have anti-proliferative effects in tumour cell lines. For example the IC_{50} for ET-743 in Calu-3 (NSCLC), HT-29 (colon) and MCF-7 (breast) cells were reported to be 0.3 nM, 0.6 nM and 0.2 nM, respectively, after 3 days of continuous exposure (Jimeno et al., 1996). An orientation experiment was performed using MCF-7 cells to confirm that the ET-743 used in these studies had not degraded. MCF-7 cells were exposed to ET-743 at 0.1 nM, 0.2 nM 0.5 nM and 1 nM for 48 hours, continuously. Cell numbers were counted and the results are shown in figure 6.2. In MCF-7 cells there was a dose-dependent decrease in cell number after incubation with ET-743. The IC_{50} of ET-743 was found to be approximately 0.2 nM which corresponds to the IC_{50} value reported by Jimeno et al. and suggests that the ET-743 used in these experiments is intact. The IC_{50} of ET-743 in MCF-7 cells is approximately 500-fold lower than the concentration required to kill 50 % of cultured hepatocytes which suggests that *in vitro* hepatocytes are far less sensitive to the cytotoxic effects of ET-743 than MCF-7 cells

Exposure of human hepatocytes to 100 nM ET-743 resulted in a time- and dose-dependent decrease in cell viability which was comparable to, but slightly less severe than, that seen in cultures of rat hepatocytes (figure 6.3). These results hint at the possibility that under the experimental conditions used here, human hepatocytes are less susceptible than rat liver cells towards the direct cytotoxic effect of ET-743.

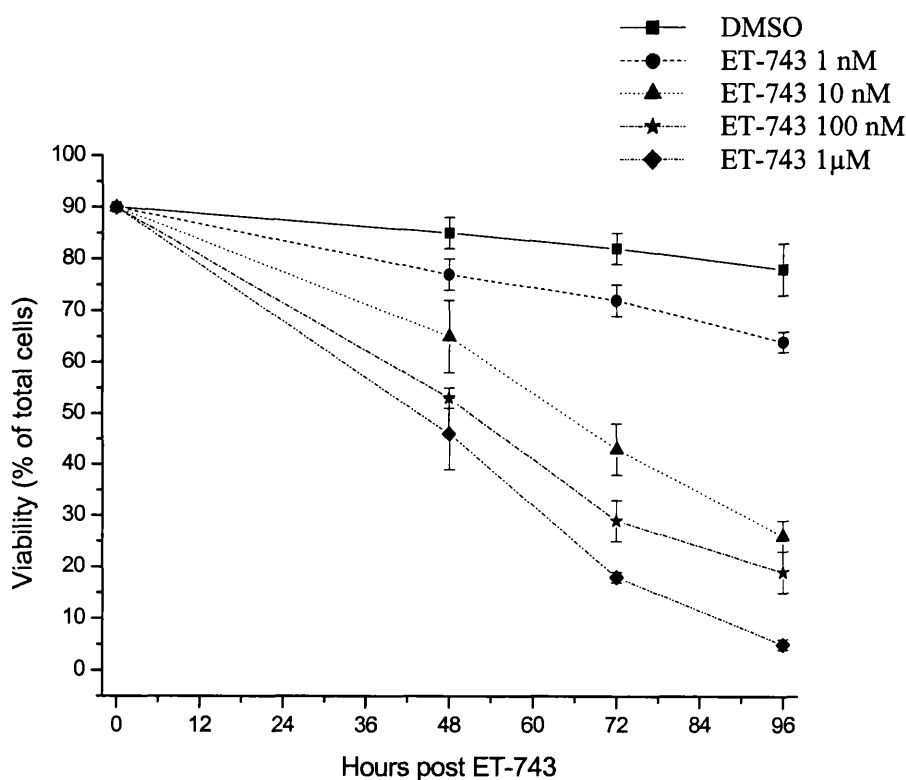


Figure 6.1 Effect of ET-743 on viability of hepatocytes isolated from female Wistar rats. Hepatocyte cultures were exposed to ET-743 (1nM, 10nM, 100nM or 1 μ M) or the vehicle (DMSO). Hepatocyte viability was assessed by measurement of LDH in the cellular supernatant. Viability was calculated by expressing the LDH in the culture as percentage (X) of the value obtained in untreated cultures in which all cells were destroyed to cause maximal LDH release, and by subtracting X from 100 (as described in chapter 2.2.25). Values are the mean \pm SD of three experiments

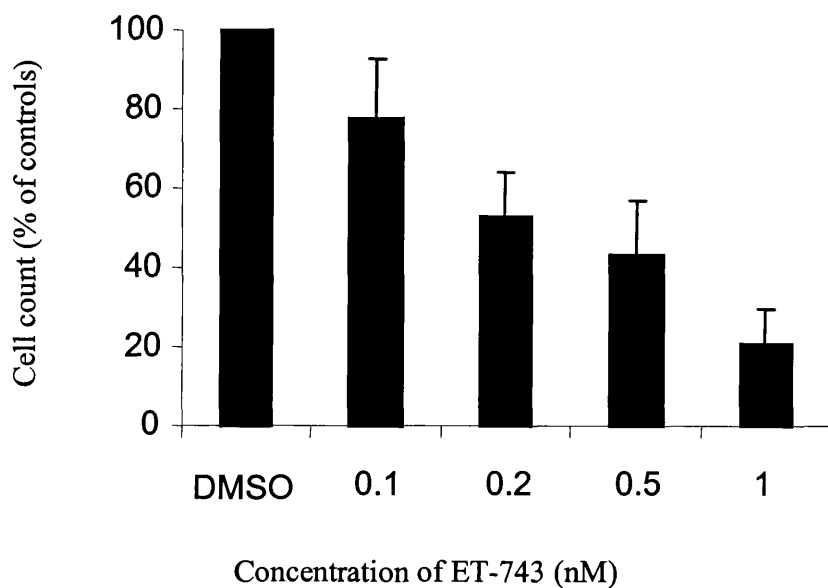


Figure 6.2 Effect of ET-743 on MCF-7 cell proliferation. MCF-7 cells were exposed to ET-743 or DMSO, the vehicle, for 48 hours. Cells were counted and the cell count was expressed as a percentage of the control cells (DMSO). Values are the mean \pm SD of three incubations

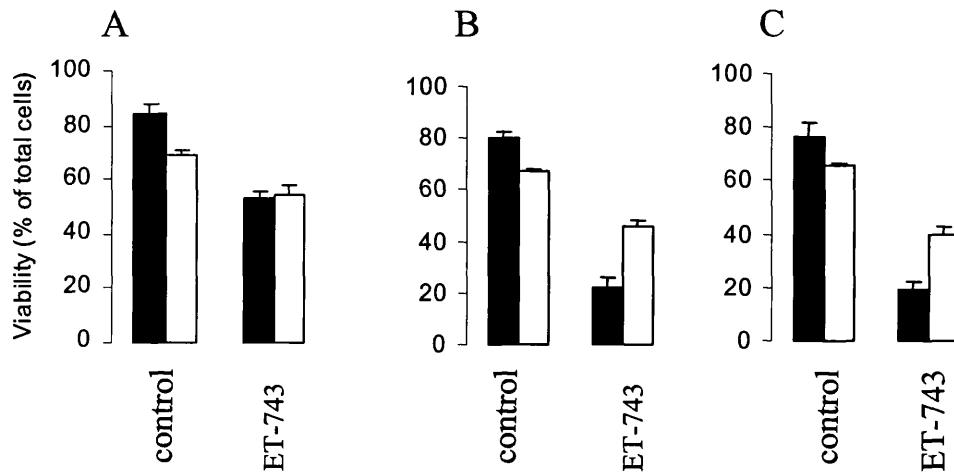


Figure 6.3 Effect of ET-743 on viability of hepatocytes from rats (closed bars) and humans (open bars) after 48 (A), 72 (B) and 96 hours (C) exposure to the drug. Hepatocyte cultures were exposed to ET-743 (100 nM) or the vehicle (DMSO, see 'control' bars). Hepatocyte viability was assessed by measurement of LDH in the cellular supernatant. Viability was calculated by expressing the LDH in the culture as percentage (X) of the value obtained in untreated cultures in which all cells were destroyed to cause maximal LDH release, and by subtracting X from 100. Values are the mean \pm SD of three experiments.

6.3 Effects of dexamethasone, β -naphthoflavone, phenobarbitone and N-acetylcysteine on ET-743 induced toxicity in hepatocytes

The effect of pre-treatment of rats with dexamethasone, β -naphthoflavone or phenobarbitone and of the co-incubation of hepatocytes with N-acetylcysteine, on the cytotoxicity of ET-743 (1 nM- 1 μ M) was explored *in vitro*. Figure 6.4 shows that the viability of liver cells from control (no pre-treatment) rats and rats which had been pre-treated with dexamethasone, β -naphthoflavone or phenobarbitone were equally susceptible to the toxic potential of ET-743, as reflected by LDH release. Likewise inclusion of N-acetylcysteine (1 mM) in cultures of hepatocytes from untreated rats did not alter cell viability after ET-743 treatment.

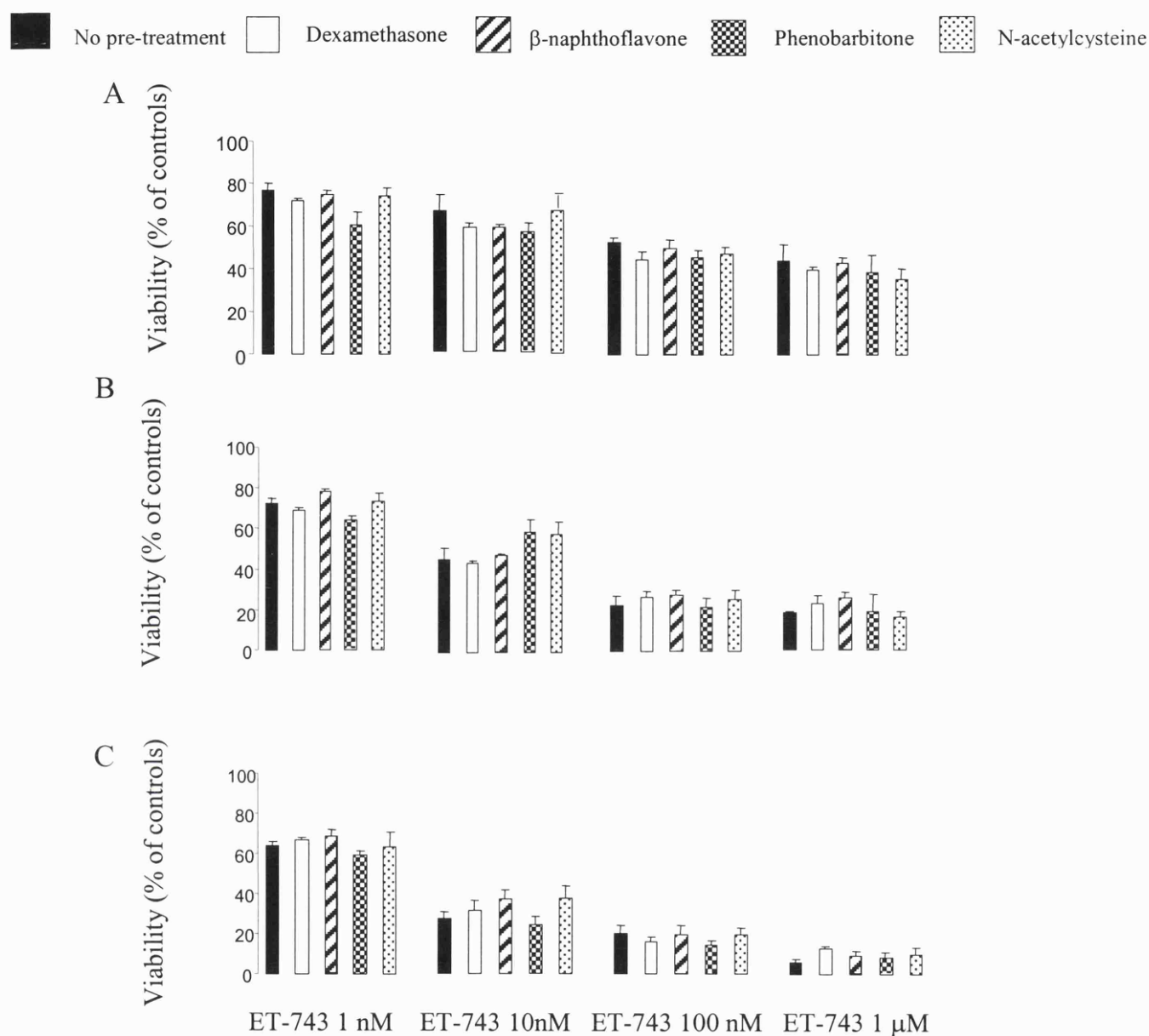


Figure 6.4 Effect of ET-743 on viability of hepatocytes isolated from rats which have been pre-treated with dexamethasone, β -naphthoflavone, or phenobarbitone or of cells which have been incubated with N-acetylcysteine. For doses of dexamethasone, β -naphthoflavone, phenobarbitone and N-acetylcysteine see section 2.2.7. Hepatocyte viability was measured at 48 (A), 72 (B) and 96 hours (C) after commencement of ET-743 treatment. Hepatocyte viability was assessed by measurement of LDH in the cellular supernatant. Values are expressed as percentage with respect to the viability of hepatocytes which were untreated at the respective time point ('controls'). Values are the mean \pm SD of 3 separate experiments.

6.4 Discussion

Hepatic ET-743 levels, determined in rats after i.v. administration of the drug, were found to be approximately 40 pmol/g tissue after one hour and falling to 10 pmol/g tissue after 24 hours (chapter 4.6). These concentrations of ET-743 measured in liver after a hepatotoxic dose of the drug are equivalent to 40 and 10 nM which are close to the concentration of ET-743 which was shown to be toxic in cultured rat hepatocytes *in vitro*. ET-743 measured in liver, removed from rats at 72 hours after they had received an intravenous dose of ET-743 (40 µg/kg), were approximately 5 nM (figure 4.8). Histopathological examination of livers from rats 72 hours after an i.v. dose of ET-743 (40 µg/kg) revealed degeneration and necrosis of the bile duct epithelium associated with inflammation, whilst the majority of hepatocytes appeared normal. In comparison, the viability of cultured hepatocytes exposed continuously to 10 nM ET-743 for 72 hours was only 45 %. It is probable that manifestations of ET-743-induced hepatic damage in the rat requires the structural integrity of the whole liver, and ET-743 accumulates in the bile duct, thus giving rise to the primary lesion whilst the hepatocytes are exposed to lower concentrations and are initially less affected by the drug. Therefore, the greater degree of toxicity displayed by cultured hepatocytes exposed to ET-743 compared to hepatocytes *in vivo*, may be because *in vitro*, hepatocytes are continually exposed to a relatively high concentration of ET-743, whereas *in vivo*, hepatocytes are transiently exposed to lower concentrations whilst bile duct cells are exposed to probably very high concentrations of ET-743, as the biliary system excretes the drug.

Pre-treatment with dexamethasone, β-naphthoflavone or phenobarbitone at doses which protected rat livers against the hepatotoxicity of ET-743 *in vivo* failed to influence cytotoxicity exerted by ET-743 in hepatocytes *in vitro*. This approach of induction of CYPs by phenobarbitone and β-naphthoflavone *in vivo* followed by hepatocyte isolation and culture has been used to investigate metabolic activation of several hepatotoxins (Hammond and Fry, 1991). At the same doses as those used in the experiments described here, phenobarbitone and β-naphthoflavone enhanced the toxicity of procenes I and II, 6-thiopurine, 4-ipomeanol, 2-methylfuran, compared to control cultures, whilst phenobarbitone also enhanced the toxicity

of valproic acid and butylated hydroxytoluene. The cytotoxicity of these compounds is mediated by CYP-dependent activation, and it is possible to use induction by phenobarbitone and β -naphthoflavone followed by exposure *in vitro* to detect metabolism-mediated cytotoxicity. The finding that induction by dexamethasone, β -naphthoflavone or phenobarbitone failed to influence cytotoxicity exerted by ET-743 in hepatocytes *in vitro* might suggest that the cytotoxicity exerted by ET-743 is insensitive to increased hepatic CYP activity. The alteration in toxicity *in vivo* following pre-treatment with dexamethasone, β -naphthoflavone or phenobarbitone may engage mechanisms alternative to those involving CYP induction, such as increased bile flow or induction of phase II enzymes, as discussed in chapter 5. Another explanation is that dexamethasone, β -naphthoflavone and phenobarbitone protect against ET-743 mediated toxicity *in vivo* by inducing CYP activity in biliary epithelium cells. Although CYP enzymes are most abundant in hepatocytes, a number of isoforms have been identified in biliary epithelium cells (Lakehal et al., 1999). In addition, Shen et al have demonstrated that CYP1A1/2 in intrahepatic biliary epithelial cells can be significantly increased by pre-treatment of rats with β -naphthoflavone (Shen et al., 1998). The finding that CYP inducer pre-treatment protected against ET-743-induced toxicity in the rat but inducer pre-treatment had no effect on ET-743 toxicity in cultured hepatocytes suggests that hepatocytes in culture are unlikely to be a suitable model to aid with the discovery of agents which prevent the detrimental hepatic effects of ET-743.

In conclusion, cultured hepatocytes do not provide a suitable model for studying the hepatotoxicity of ET-743. Therefore strategies designed to investigate and eliminate ET-743 mediated hepatotoxicity need to be tested *in vivo*. Alternatively, it is conceivable that sophisticated experimental designs involving hepatocytes and bile cells in co-culture may be required to model *in vitro* hepatic changes mediated by ET-743 *in vivo*. Co-cultures of rat hepatocytes and biliary epithelial cells have been used to study the effects of triiodothyronine and thyroxine on GST activities and proteins in the liver (Vanhaecke et al., 2001).

CHAPTER 7

Evaluation of the protective efficacy
of indole-3-carbinol against ET-743
induced hepatotoxicity

7.1. Introduction

Indole-3-carbinol (I3C) is a hydrolysis product of glucobrassin, a compound that occurs naturally in large amounts in a number of vegetables of the brassica genus e.g. cabbage, cauliflower, brussels sprouts (McDanell et al., 1988). I3C has received considerable attention as a dietary modulator of carcinogenesis (see chapter 1.5.1). I3C has been documented to be chemopreventative against cancer in a number of animal models and is being investigated in clinical trials as a potential chemopreventive agent against breast cancer and ovarian cancer in humans (Bradfield and Bjeldanes, 1987; Manson et al., 1997; Stoner et al., 2002).

One possible mechanism for the effects of I3C is through its ability to induce phase I and II drug metabolising enzymes and increase clearance of chemical carcinogens (Wattenberg et al., 1985). Indole-3-carbinol has been shown to inhibit aflatoxin B₁-induced hepatocarcinogenesis (Manson et al., 1997). Rats pre-treated with I3C (0.5 % in the diet) for two weeks prior to administration of aflatoxin B₁ manifested induction of CYP1A1, CYP1A2, CYP2B1/2 and CYP 3A1 in liver as well as induction of glutathione-S-transferase. Induction of phase I and II enzymes corresponded with increased formation of the less toxic metabolic metabolites such as aflatoxin M₁ (AFM₁) and aflatoxin Q₁ (AFQ₁). In a different study, after 7 days of feeding 0.2 % I3C, the levels of hepatic CYP1A1 were increased 24-fold with a more modest 2 to 4-fold increase in CYP1A2, CYP 3A1/2 and CYP2B1/2 (Stresser et al., 1994). Other studies have shown that dietary I3C induces phase II enzymes UDP-glucuronosyl transferase and NADPH: quinone reductase (Shertzer and Sainsbury, 1991).

I3C pre-treatment one hour prior to carbon tetrachloride produced a decrease in carbon tetrachloride-mediated necrosis in the liver. Carbon tetrachloride-induced liver toxicity is due to free radical metabolites which produce a large myriad of specific cellular events, including alterations in protein turnover, calcium homeostasis and lipid peroxidation (Shertzer et al., 1987). The authors suggest that I3C or its metabolites may act as natural antioxidants and protect against free radical mediated toxicity. In addition, I3C feeding for 3 weeks at 0.1 % in the diet weakened the toxic effects of trichothecene T-2 mycotoxin (Kravchenko et al., 2001).

The protective effect of I3C was probably due to its ability to activate enzymes participating in the biotransformation and detoxification of trichothecene T-2 mycotoxin.

I3C is rapidly converted in the gastro-intestinal tract through a series of acid catalysed condensation reactions to oligomers including dimers, trimers and tetramers. A number of studies suggest found that acid condensation products have profound effects on xenobiotic and oestrogen metabolism. Evidence to support this hypothesis includes the observation that oral, but not i.p. administration of I3C led to an induction of hepatic CYP1A activity, and acid treatment of I3C generated a reaction mixture that induced CYP activity after i.p. and oral administration (Bradfield and Bjeldanes, 1987). Two condensation products of I3C, diindolylmethane (DIM) and indolylcarbazole (ICZ) have received the most attention as active species responsible for enzyme induction, although there are a number of other metabolites that have yet to be fully investigated. A number of acid condensation products of I3C have been shown to be potent Ah receptor agonists which may be responsible for the ability of I3C when given in the diet to induce CYP1A1 and CYP1A2 (Bjeldanes et al., 1991; Chen et al., 1996).

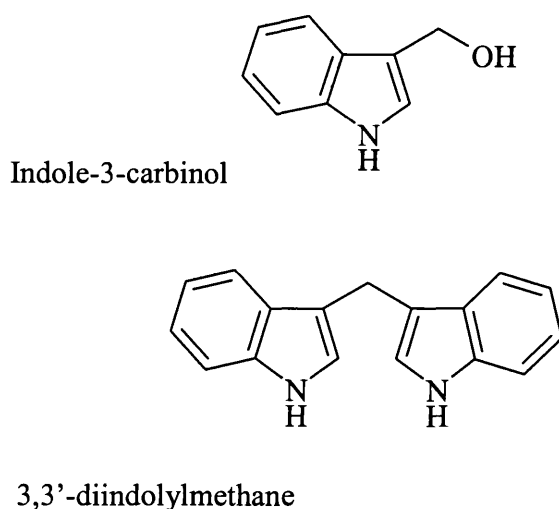


Figure 7.1 Structure of I3C and one of its condensation products, DIM.

The aim of the experiments in this chapter was to investigate the effects of I3C on ET-743 induced hepatotoxicity. Initially a high dose of I3C was administered, 0.5 % in the diet, to assess its protective effects, and in a second study the dose was reduced to 0.1 % in the diet. Due to the condensation reaction in the stomach, I3C is only present in the liver transiently, whereas the condensation products, of which DIM is the most abundant, remain in the liver for longer periods but at lower concentrations (Anderton et al, unpublished data). For example, in mice given a single oral dose of I3C (250 mg/kg), maximal levels of I3C, 166 μM , were detected in the liver at 15 min after administration, but I3C could not be detected at 1 hour after dosing, whereas the highest concentration of DIM was 14.6 μM , detected at 2 hours, and 2.4 μM detected at 24 hours after I3C dosing (Mark Anderton, personal communication). In comparison with I3C, DIM is stable and has a relatively long half-life. In the light of this knowledge, another experiment was performed to investigate whether the protective effect of I3C against ET-743-mediated hepatotoxicity was due to its acid condensation product, DIM. As I3C is thought to protect against aflatoxin hepatocarcinogenesis by inducing metabolising enzymes, especially CYP1A, the activity of CYP1A and CYP3A were measured after I3C and DIM administration to identify a possible mechanism for protection against ET-743-induced liver damage.

Results

7.2 The effect of I3C pre-treatment on ET-743-induced liver changes

In an experiment to assess the effect of feeding I3C in the diet (0.5 % in the diet for 7 days prior to ET-743 and throughout the study) on ET-743 hepatotoxicity, ALP and AST activity and bilirubin levels were measured at 3 and 9 days after ET-743 dosing. As expected, levels of ALP and AST were increased by ET-743 at 3 and 9 days after dosing when compared to levels measured in untreated animals and animals treated with I3C alone. Similarly, bilirubin levels were elevated 20-fold in rats which received ET-743 when compared to untreated control animals or animals which received I3C alone. However, administration of I3C in the diet for one week prior to ET-743 caused a reduction in ALP activity and bilirubin levels, compared to levels seen in unprotected animals (figure 7.2) although the modest increase in AST levels caused by ET-743 alone was not reduced in rats which received the combination of I3C and ET-743.

Histopathological examination showed that in the livers of rats treated with ET-743 alone there was damage to the bile ducts at 3 days, followed by sclerosis at 9 days, as seen in previous experiments (chapter 3.3). After administration of I3C (0.5 % in the diet), a single dose of ET-743 produced significantly less biliary damage, compared with rats given ET-743 alone (figure 7.3). In rats given both I3C and ET-743, only slightly irregular bile duct epithelium and very sparse degenerate biliary cells were observed on day 3 with some mild peribiliary fibrosis on day 9. Control animals and those which received I3C alone appeared normal.

In a second experiment, the dietary concentration of I3C was reduced to 0.1 %. As before, ET-743 alone elicited hepatic damage as reflected by dramatically raised bilirubin and elevated ALP and AST in the plasma (figure 7.4). Administration of 0.1 % I3C in the diet one week before ET-743 did not decrease AST and ALP activity, when compared with levels induced by ET-743 treatment alone. However, bilirubin levels were reduced in animals that received the combination, compared to rats which received ET-743 alone, even though the reduction was

not statistically significant. Pathological examination of liver sections supported these results. In rats fed 0.1 % I3C, followed by a single dose of ET-743 there was no evidence of a decrease in severity of bile duct damage at 3 days when compared to animals which received ET-743 alone. Moreover, at 9 days, biliary fibrosis in rats which received both ET-743 and I3C was as intense as that in rats which were treated with ET-743 alone.

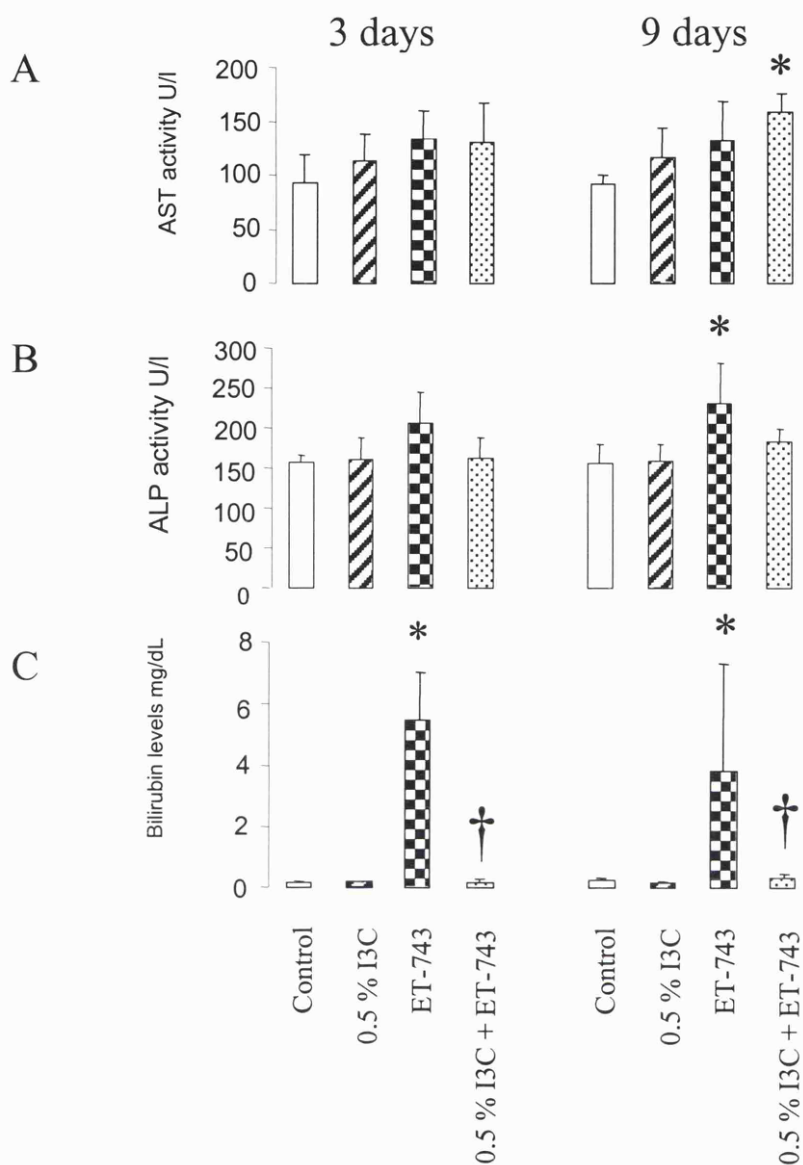


Figure 7.2 Effect of 0.5 % I3C in the diet on ET-743 induced elevations of plasma activity of aspartate aminotransferase (A), alkaline phosphatase (B) and of plasma bilirubin levels (C) in female rats. I3C, at 0.5 % in the diet, was administered for one week prior to ET-743 (40 $\mu\text{g}/\text{kg}$, i.v.) and throughout the study. Rats were culled and plasma indicators of toxicity were measured at 3 and 9 days *post* ET-743. Values are the mean \pm SD for 5 animals. Stars indicate that values are significantly greater ($p < 0.05$ by ANOVA) than activities and levels in animals which did not receive ET-743. Daggers indicate that values for the combined treatment are significantly less ($p < 0.05$ % by ANOVA) than activities and levels in animals which received ET-743 only.

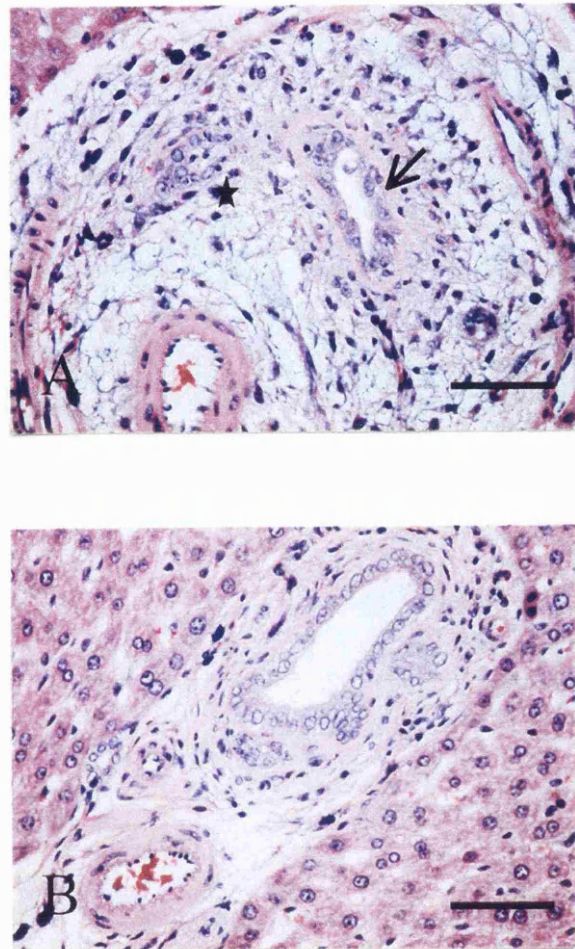


Figure 7.3 Photomicrographs of liver section from female Wistar rats which received ET-743 (40 $\mu\text{g}/\text{kg}$ i.v.) alone (A) or after 0.5 % I3C in the diet for one week prior to ET-743 and throughout the study period (B). Note in A the swollen, thickened portal tract with an infiltrate of inflammatory cells (star) and the damaged bile duct (arrow), which is lined by degenerative epithelium, characteristics of ET-743 induced changes in livers of female rats. In contrast, after I3C pre-treatment (B) a comparable portal tract is indistinguishable from controls. Sections are representative of five separate animals. Bar equals 100 μm . Histopathological analysis was carried out by Dr Peter Greaves.

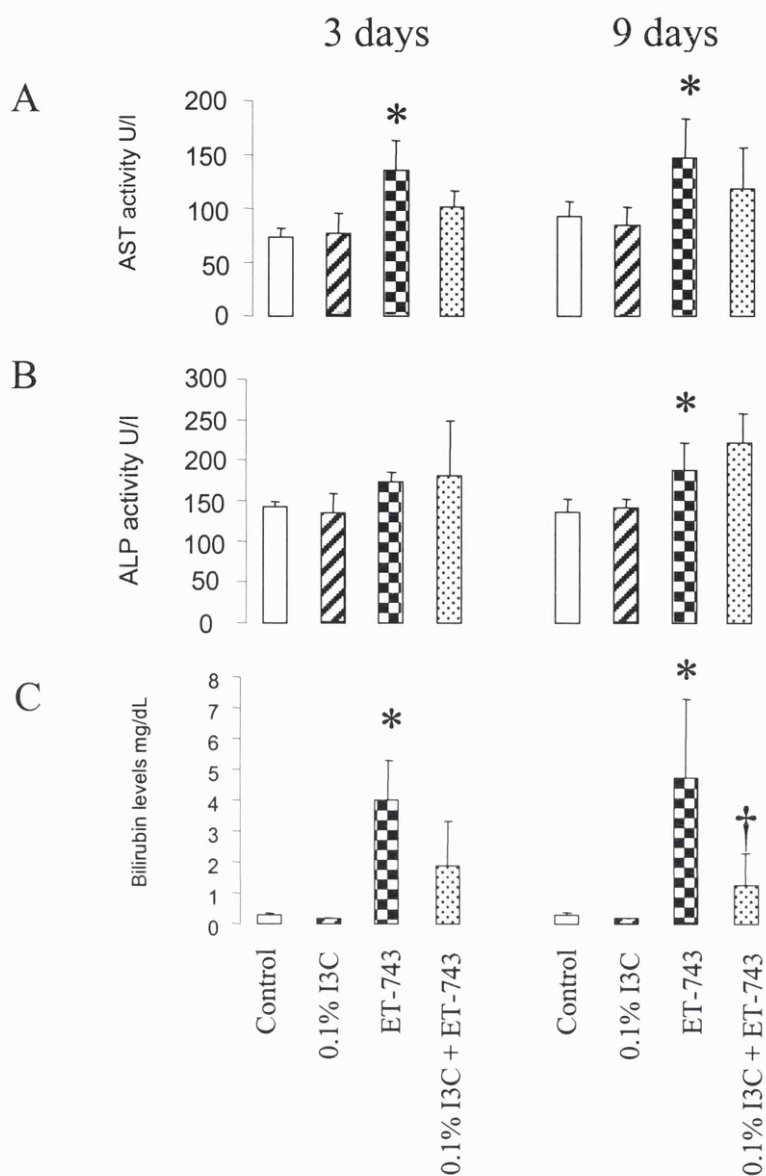


Figure 7.4 Effect of 0.1 % I3C in the diet on ET-743 induced elevations of plasma activity of aspartate aminotransferase (A), alkaline phosphatase (B) and of plasma bilirubin levels (C) in female rats. I3C, at 0.1 % in the diet, was administered for one week prior to ET-743 (40 $\mu\text{g}/\text{kg}$, i.v.) and throughout the study. Rats were culled and plasma indicators of toxicity were measured at 3 and 9 days *post* ET-743. Values are the mean \pm SD of 5 animals. Stars indicate that values are significantly greater ($p < 0.05$ by ANOVA) than activities and levels in animals which did not receive ET-743. Daggers indicate that values for the combined treatment are significantly less ($p < 0.05$ % by ANOVA) from activities and levels in animals which received ET-743 only.

7.3 The effect of DIM pre-treatment on ET-743-induced liver changes

I3C undergoes extensive condensation reactions under the acidic conditions of the stomach. One of the main acid condensation product is DIM (figure 7.1), which is a result of the condensation of two molecules of I3C. I3C at 0.5 % in the diet is equal to approximately 400 mg/kg or 2.72 mmol/kg, therefore, assuming all of the I3C molecules dimerise to form DIM, the maximum amount of DIM which could theoretically be produced is 50 % of the concentration of I3C. Much lower levels of DIM are formed after I3C dosing compared to levels measured after DIM dosing. In a recent study by Anderton et al (unpublished) the levels of DIM were measured in the livers of mice after a single oral dose of I3C (250 mg/kg or 1.7 mmol/kg) or DIM (250mg/kg or 1 mmol/kg). The maximum levels of DIM measured in the liver were 14 nmol/g after a single dose of I3C, compared to 170 nmol/g measured after DIM administration. Therefore, the levels of DIM after similar doses of I3C or DIM are approximately 12-fold higher after DIM administration compared to I3C administration. To investigate the possibility that the protective effect of 0.5 % I3C in the diet against ET-743-induced hepatotoxicity is due to its conversion to DIM, an experiment was designed to investigate the effect of 0.2 % DIM on ET-743-mediated hepatotoxicity. This dose far exceeds the concentration of DIM likely to be formed from I3C in the stomach after 0.5 % I3C.

ET-743 alone elicited hepatic damage as reflected by dramatically raised bilirubin and elevated ALP and AST in the plasma as seen in previous experiments. Administration of 0.2 % DIM in the diet one week before ET-743 and throughout the experiment did not decrease AST and ALP activity when compared with levels induced by ET-743 treatment alone (figure 7.5). However, bilirubin levels were reduced in animals that received the combination, compared to rats, which received ET-743 alone, but the reduction was not significant. Pathological examination of liver sections endorse these findings. In rats fed 0.2 % DIM, there was no evidence of a decrease in the severity of bile duct damage induced by ET-743 at 3 days after dosing when compared to animals which received ET-743 alone. Moreover, at 9 days biliary fibrosis in rats, which received the combination of ET-743 and I3C, was as severe as that in rats, which were treated with ET-743 alone.

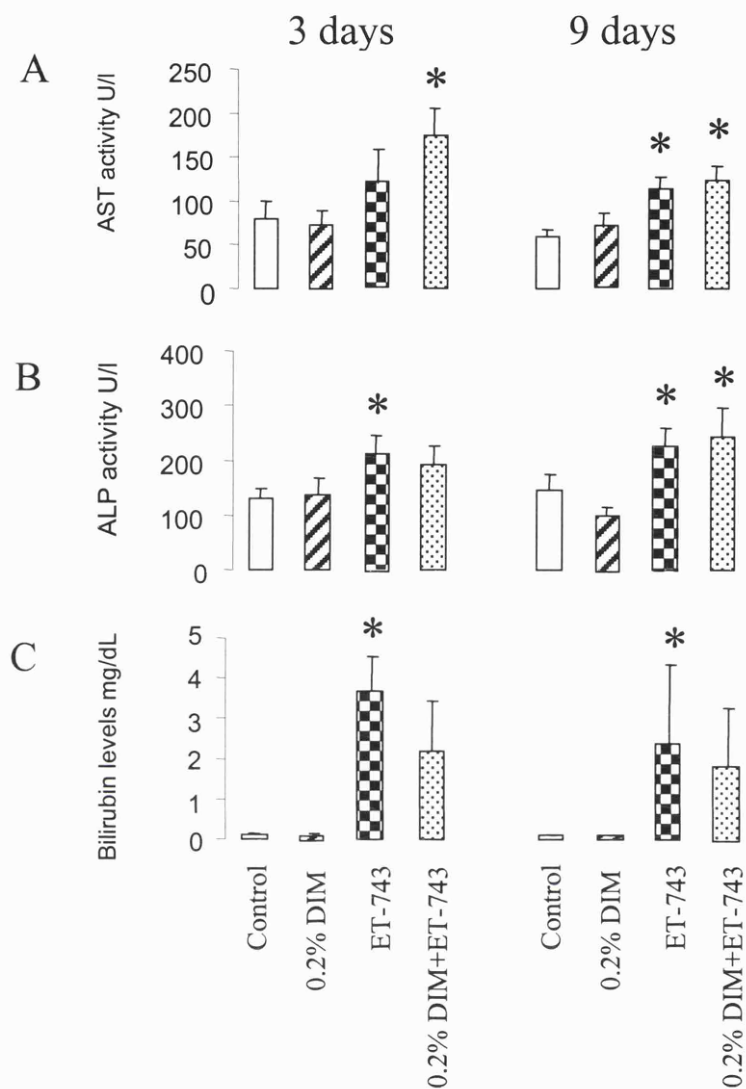


Figure 7.5 Effect of 0.2 % DIM in the diet on ET-743-induced elevations of plasma activity of aspartate aminotransferase (A), alkaline phosphatase (B) and of plasma bilirubin levels (C) in female rats. DIM, at 0.2 % in the diet, was administered for one week prior to ET-743 (40 $\mu\text{g}/\text{kg}$, i.v.) and throughout the study. Rats were culled and plasma indicators of hepatotoxicity were measured at 3 and 9 days *post* ET-743. Values are the mean \pm SD of 5 animals. Stars indicate that values are significantly different ($p < 0.05$ by ANOVA) from activities and levels in animals which did not receive ET-743.

7.4 The effect of I3C on hepatic cytochrome P450 enzymes

The experiments described in chapter 4 hint at the possibility that dexamethasone-induced CYP3A enzymes in rat liver oxidise ET-743 to a non-hepatotoxic species. As β -naphthoflavone also suppressed the toxicity, induction of CYP1A enzymes may also be a mechanism of protection against ET-743-induced hepatotoxicity. I3C is an inducer of oxidative drug metabolism, and raised CYP enzyme levels may play a role in the mechanism by which I3C ameliorated the adverse effects of ET-743 in the rat liver. In order to investigate this hypothesis, the levels of induction of CYP3A and CYP1A1/2 were measured in microsomes taken from rats one week after administration of 0.5 % I3C, the time point at which ET-743 would have been injected in the combination studies. In addition, the induction of CYPs by a hepatoprotective dose of I3C was compared with that of DIM at a dose that was found to have little effect on ET-743-mediated hepatotoxicity. As shown in figure 7.6, at 0.5 % in the diet, I3C increased the rate of oxidative de-benzoylation of 7-BQ, the model substrate for CYP3A activity, by 2.6-fold, whereas DIM increased the rate only by 1.7-fold. In addition, I3C increased CYP1A1/2 activity by 15.3-fold compared to 0.2 % DIM, which increased the rate only 3.1-fold (figure 7.7).

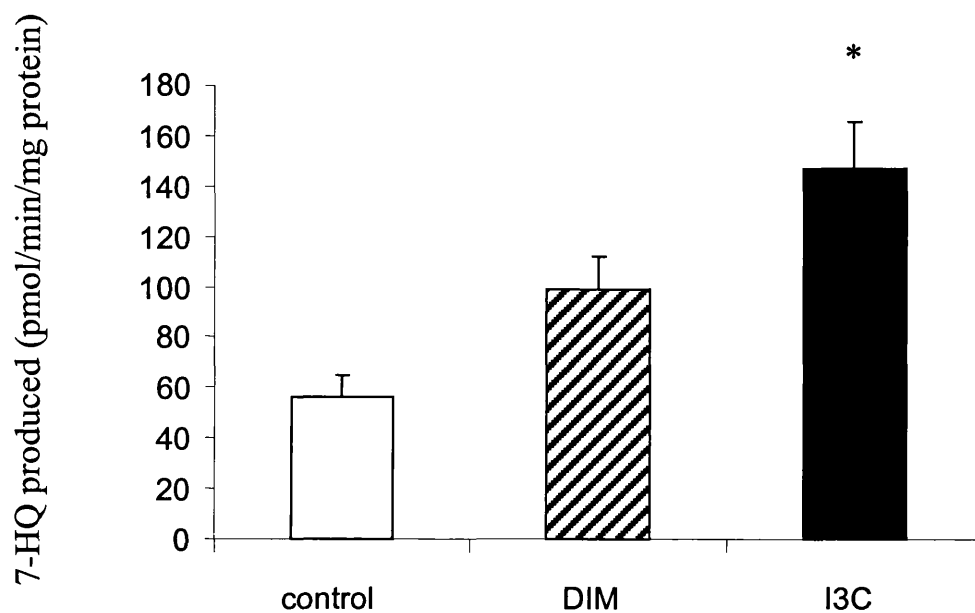


Figure 7.6 CYP3A activity in female rats after 0.5 % I3C (closed bars) or 0.2 % DIM (striped bars) feeding for one week compared to untreated rats (open bars). CYP3A activity was measured by the conversion of 7-BQ to 7-HQ by microsomes prepared from rat livers after 7 days of I3C and DIM feeding. Values, expressed as the rate of formation of 7-HQ in pmol /min/gram of microsomal protein are the mean \pm SD of four animals. Stars indicate values are significantly different to controls ($p < 0.05$ by ANOVA).

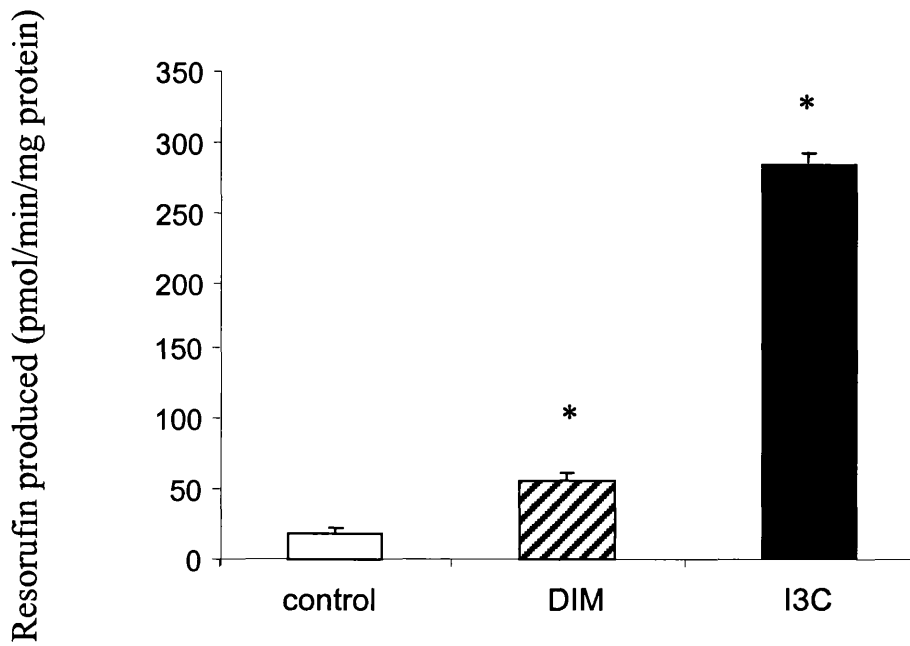


Figure 7.7 CYP1A1/2 activity in female rats after 0.5 % I3C (closed bars) or 0.2 % DIM (striped bars) feeding for one week compared to untreated female rats (open bars). CYP3A activity was measured by the conversion of ethoxyresorufin to resorufin by microsomes prepared from rat livers after 7 days of I3C and DIM feeding. Values, expressed as the rate of formation resorufin in pmol /min/gram of microsomal protein are the mean \pm SD of four animals. Stars indicate values are significantly different to controls ($p < 0.05$ by ANOVA).

7.5 Discussion

Treatment with I3C at 0.5 % in the diet for one week prior to ET-743 and throughout the experiment ameliorated ET-743-induced hepatotoxicity. The protective effect was reflected by significant suppression of the elevation of bilirubin and ALP normally induced by ET-743, and prevention of ET-743 induced pathological damage. Furthermore, this protection persisted for up to 12 days after ET-743 administration. In contrast, the lower dose of I3C, 0.1 % in the diet, failed to significantly protect against the detrimental effects of ET-743 on rat liver. DIM pre-treatment at 0.2 % in the diet did not significantly reduce the biochemical indicators of hepatotoxicity. This result would suggest that the protection afforded by 0.5 % I3C is not due to the condensation product, DIM, as the concentration of DIM in the stomach after feeding 0.2 % DIM far exceeds the concentration of DIM in the stomach achieved after feeding of 0.5 % I3C. However, condensation products other than DIM formed under acid conditions may be responsible for the protection afforded by I3C. Two such products, indolylcarbazole (ICZ) and 2-(indol-3-ylmethyl)-3,3-diindolylmethane (LTr-1) have been reported to contribute to the action of I3C and there are a number of other metabolites yet to be investigated (Brignall, 2001).

Dexamethasone and β -naphthoflavone were effective at reducing ET-743-induced hepatotoxicity, possibly by increasing oxidative metabolism of ET-743 to a less hepatotoxic species, through induction CYP3A and CYP1A, respectively. Increased oxidative metabolism of ET-743 may also be the mechanism by which I3C prevents ET-743-induced liver damage. I3C at 0.5 % induced hepatic CYP3A by 2.6-fold compared with 0.2 % DIM which induced CYP3A by 1.7-fold. This induction was not as impressive as that achieved by a hepatoprotective dose of dexamethasone, 10 mg/kg, which induced CYP3A 7-fold, and a moderately hepatoprotective dose of 5 mg/kg which induced CYP3A 3-fold. In addition, I3C significantly induced CYP1A activity 15.3-fold, whereas DIM induced the enzyme by a more modest 3.1-fold. The finding, that I3C induced CYP to a similar degree as a moderately hepatoprotective dose of dexamethasone, 5 mg/kg, would suggest that induction of CYP3A is likely to be the mechanism of protection by I3C. In addition, because CYP1A activity was

elevated so strongly by I3C, and β -naphthoflavone was also effective at protecting against the liver (see chapter 5), induction of CYP1A may perhaps contribute to the mechanism by which I3C protects against ET-743-induced hepatotoxicity. Furthermore, other mechanism such as elevation of phase II enzymes and increased bile flow may also play a role in the reduction of ET-743-mediated toxicity by I3C.

DIM is more stable than I3C and remains in the liver for longer, but it was less effective than I3C at inducing CYP1A. Bjeldanes et al compared the Ah receptor-binding affinities of the condensation products of I3C. I3C had the lowest binding affinity for the Ah-receptor, which is in contrast with the biological potency of I3C as an inducer of CYP1A activity in the whole animal (Bjeldanes et al., 1991). The condensation product ICZ had the highest binding affinity for the Ah receptor followed by LTr-1, and DIM. These results would suggest that the ability of I3C, when given in the diet, to induce CYP1A1 is due to its condensation products binding to the Ah receptor rather than I3C itself. Therefore, both DIM and I3C have relatively low binding affinity for the Ah receptor, but I3C is converted into condensation products under acid condition which are potent Ah receptor agonists and lead to induction of CYP1A activity.

High dose I3C, 0.5 % in the diet, which is equivalent to approximately 400 mg/kg rat body weight/day, showed protection against ET-743 hepatotoxicity without any I3C treatment related side effects. In studies in which mice received large doses of I3C, up to 700 mg/kg/day, there were no toxic effects (Grubbs et al., 1995). I3C is a dietary agent and possibly innocuous in comparison to dexamethasone, which has a number of adverse effects in humans. However, high doses of I3C equivalent to the doses given to rats in these studies have not been given to humans before and may cause some adverse reactions. Nevertheless, I3C may still be less harmful than dexamethasone and therefore could prove to be safer than dexamethasone in the clinic for protection against ET-743-induced hepatotoxicity. In order to justify exploration of the I3C hepatoprotection strategy in the clinic, it is vital to demonstrate that I3C does not adversely affect the anti-tumour activity of ET-743. The anti-tumour effect of I3C in combination with ET-743 is currently being investigated by collaborators in Milan.

CHAPTER 8

Final discussion

8.1 Final discussion

The work described in this thesis has provided the following seven novel insights into the hepatotoxicity of ET-743:

1) The hepatotoxicity exerted by ET-743 is characterised by a primary insult to the bile ducts illustrated by degeneration and focal patchy necrosis associated with inflammation. Hepatocytes were essentially normal after ET-743 administration, apart from focal zones of hepatic necrosis in some treated animals (chapter 3). In preclinical toxicity studies, hepatic damage caused by ET-743 were characterised as cholangitis, however this is the first time extensive histopathological examinations have been performed in conjunction with electron microscopy to characterise the hepatotoxicity.

2) The pathological damage and elevated liver enzymes generated by ET-743 in the female Wistar rat persist for at least 3 months (chapter 3). This finding differs from the results of the preclinical toxicity studies in mice, dogs and monkeys in which hepatic toxicities were resolved after 3-4 weeks. Furthermore, it has been reported that the haematological and pathological effects were generally reversible in rats (Jimeno et al., 1996).

3) For the first time microarray analysis was performed to explore gene expression changes which may identify the biological events underlying the unwanted hepatic effects of ET-743 (chapter 3). Microarray technology was also used to assess whether dexamethasone abrogates the hepatic gene expression changes produced by ET-743. Microarray technology is often used to monitor changes in expression of thousands of genes in response to drug treatment. In this project, microarray technology has been used as an innovative tool to characterise specific gene changes associated with toxicity, and to monitor these specific gene changes to predict abrogation of toxicity.

4) ET-743-induced liver toxicity is coupled with enhanced liver cell proliferation involving up-regulation of the *cdc2a* and *ccnd1* genes (chapter 3). This is an unusual and possible unique property for a cytotoxic anti-cancer agents.

5) Single high-dose dexamethasone pre-treatment prevents the deleterious effects of ET-743, on liver function, structure and gene changes in the rat, without compromising its experimental anti-tumour activity (chapter 4). Whereas, simultaneous dexamethasone and ET-743 treatment enhanced the ET-743-induced hepatotoxicity. Suppression of the toxicity was associated with an induction of CYP3A and dramatic reduction in hepatic ET-743 levels, which intimate that ET-743 increases the metabolic removal of ET-743.

6) Pre-treatment with β -naphthoflavone and phenobarbitone also displayed some efficacy as potential antidotes against ET-743-induced hepatotoxicity (chapter 5). Furthermore, another CYP inducer, I3C, abrogated the detrimental effects on the liver induced by ET-743 (chapter 7). The results suggest that CYP induction may play a role in the mechanism of protection against ET-743 hepatotoxicity.

7) For the first time cultured hepatocytes have been used to investigate the mechanism by which ET-743 causes hepatotoxicity. Cultured hepatocytes exposed to ET-743 displayed a greater degree of toxicity compared to hepatocytes *in vivo* (chapter 6). Pre-treatment with dexamethasone, β -naphthoflavone or phenobarbitone, at doses which decreased the toxicity of ET-743 in the female rat *in vivo*, failed to influence cytotoxicity exerted by ET-743 in hepatocytes *in vitro*. Therefore, this work suggests that hepatocytes in culture are not a suitable model for the discovery of agents which protect against the detrimental effects of ET-743.

The rat is an important preclinical model in anti-cancer drug development and is often used to predict drug toxicity and disposition in humans. However, the differences in CYP3A enzymes between rats and humans and the interspecies difference in metabolism of ET-743 has led to the suggestion that the female rat is not a suitable model to evaluate ET-743 liver toxicity in humans. In addition, the female rat is the species most sensitive to ET-743 hepatotoxicity in which the toxicity is irreversible, whereas manifestations of damage induced by ET-743 in humans, acute transaminitis and subclinical cholangitis, are generally reversible after 3 weeks. The liver changes in the female rat and human are not dissimilar but the damage is more

intense in the female rat. Therefore, the female rat is a suitable experimental model to study the effects of possible antidotes on ET-743-induced hepatotoxicity. However any conclusions drawn from the results obtained in rats need to be extrapolated to the clinic with utmost caution.

A possible reason for the high susceptibility of the female rat to the hepatotoxic potential of ET-743 is the low basal activity of CYP3A compared to other species. Female rats were more sensitive than male rats and this increased sensitivity corresponded with significantly lower CYP3A activity (chapter 3). Similar CYP3A activities were observed in the male rat and humans (Tomlinson et al., 1997). In addition, the mouse is reported to be very similar to the male rat regarding CYP3A activity (Bogaards et al., 2000). The similarity in CYP3A activity between the male rat, mouse and human might explain the lower sensitivity to ET-743 hepatotoxicity in these species compared to female rats. In humans, CYP3A does not exhibit gender difference, and therefore there should not be gender dimorphism in metabolism and toxicity of ET-743.

In this thesis several antidotes have been investigated for their efficacy in limiting ET-743 induced hepatotoxicity in the female rat. It seems worthwhile to discuss the potential use of these agents in the clinic and to consider which further investigations in cancer patients may lead to strategies to reduce ET-743-mediated hepatotoxicity.

Dexamethasone was the most effective agent at preventing against ET-743-mediated hepatotoxicity. Furthermore, dexamethasone pre-treatment did not interfere with the anti-tumour activity, and the combination may even be more efficacious than ET-743 alone. Dexamethasone therapy is given at low doses in clinical trials with ET-743 to reduce the chemotherapy related emesis, but the effect of dexamethasone on the hepatotoxicity has not been fully evaluated. Higher doses of dexamethasone are given to patients in circumstances in which immunosuppression and antiinflammation are desired, however, it is associated with adverse effects. High doses of dexamethasone equivalent to the dose of 10 mg/kg, which was found to be hepatoprotective in rats, are probably too high to use in humans. Nevertheless,

tolerable high doses of dexamethasone, such as 10 mg per person, deserve investigation in patients for protection against ET-743-induced hepatotoxicity. The timing of pre-treatment seems to be crucial in the rat, as dexamethasone given 24 hours prior to ET-743 was hepatoprotective, but when given concurrently with ET-743, the toxicity was enhanced. A clinical trial should be designed to investigate the effects of high-dose dexamethasone 24 hours prior to ET-743 infusion. A randomised clinical trial would be required consisting of two arms, in one arm, patients should receive low-dose dexamethasone concurrently with ET-743, as in previous ET-743 phase II trials, and in the second arm, patients should receive high-dose dexamethasone 24 hours prior to ET-743. The effect of dexamethasone on the hepatotoxicity and anti-tumour activity should be evaluated.

If the hypothesis is correct that dexamethasone protects against ET-743 by inducing CYP3A and increasing the metabolic removal of ET-743, then other CYP3A inducers may be equally effective as dexamethasone. The antibiotic rifampicin is perhaps the most potent inducer of CYP3A4 in clinical use (Pichard et al., 1990). In patients treated with rifampicin (600 mg per day for 4 days) there was a 5-fold increase in CYP3A activity compared to untreated patients, measured by excretion of urinary 6 β -hydroxycortisol (Ged et al., 1989). As discussed in chapter 4, an increase in CYP3A activity between 3 and 7-fold, in rats following dexamethasone pre-treatment corresponded with abrogation of the hepatotoxicity induced by ET-743. Assuming that induction of CYP3A is the mechanism by which dexamethasone protects against ET-743, then rifampicin pre-treatment may be a possible antidote to ET-743-induced hepatotoxicity in humans. Rifampicin is used for the treatment of tuberculosis at doses of up to 600 mg per day. During therapy, rifampicin is usually well tolerated, however, adverse side-effects are common in intermittent rifampicin intake. These side-effects include febrile reaction, eosinophilia, leucopenia, thrombocytopenia, purpura, haemolysis and shock, hepatotoxicity and nephrotoxicity (BNF). Rifampicin at high doses can cause cholestasis and liver dysfunction (Scheuer et al., 1974) and might therefore intensify ET-743 hepatotoxicity. Therefore, rifampicin should be tested, initially in the rat model used in this project to evaluate its effect on ET-743-induced hepatotoxicity.

Induction of CYP3A by I3C is a rare example of induction of this isoform by a naturally occurring component of human diet (Stresser et al., 1994). The finding that high-dose I3C was effective at protecting rat liver against ET-743-induced hepatotoxicity provides a powerful rationale for an investigation into the protective effect of I3C in the clinic. The results of the work presented here allow the conclusion that 0.5 % I3C pre-treatment, which equals approximately 400 mg/kg rat/day, eliminated almost completely the biliary damage induced by ET-743, whereas 0.1 % I3C, which equals approximately 80 mg/kg rat/day, had very little effect. Based on the Freireich equation (Freireich et al., 1966) which has been used to compare the maximum tolerated doses of anti-cancer drugs in man and different animal species, 400 mg/kg in rats equates to 2.8 g/m², and for a 70 kg human with a body surface area of 1.8 m², the dose of I3C which was hepatoprotective in rats is equal to 5 g in human. The chemopreventive potential of I3C has been well documented in animal models, yet few clinical trials have been performed. In a clinical trial to investigate the effect of I3C on oestrogen metabolism, women received 400 mg/day I3C for 3 months and no adverse effects were noted (Bradlow et al., 1994). This dose is considerably lower than the equivalent dose of 400mg/kg / day given to the rat, which was found to be hepatoprotective. As a detailed dose ranging study for I3C has not been performed in this investigation, a concentration somewhere between 0.1 and 0.5 % may also be effective against ET-743-induced liver toxicity. It is not known whether the degree of CYP induction by I3C is comparable in humans and rats, or whether the level of CYP induction to increase oxidative metabolism of ET-743 is equal in rats and humans. Therefore, it may be possible to achieve induction of CYP and increased oxidative metabolism of ET-743 in humans with daily doses of I3C lower than 5 g.

The data regarding the effect of I3C on hepatocarcinogenesis in animals initiated by aflatoxin B₁ are contradictory. Several studies have been performed in rainbow trout in which I3C administered prior to aflatoxin B₁ showed a protective effect against hepatocarcinogenesis (Bailey et al., 1987a; Goeger et al., 1986). However, when the aflatoxin administration preceded I3C treatment, promotion of liver tumours was noted (Bailey et al., 1987b; Dashwood, 1998). I3C tumour promoting activity has also been observed in a colon cancer model. Administration of I3C combined with wheat bran and cholesterol before, during and

after treatment with the colon carcinogen dimethylhydrazine enhanced tumour incidence in the colon (Pence et al., 1986). In another rat model, I3C enhanced liver and thyroid neoplasia when given one week after a 3 week initiation period with N-diethylnitrosamine (DEN), N-methylnitrosourea (NMU) and dihydroxy-di-N-propyl-nitrosamine (DHPN) (Kim et al., 1997). The possibility of tumour promotion by I3C in humans is unknown and therefore I3C should be given to patient with utmost prudence. Whether I3C pre-treatment affects the anti-tumour activity of ET-743 in rodent tumour models is currently being evaluated by collaborators in Milan.

β -Naphthoflavone was effective at reducing ET-743 induced hepatotoxicity leading to the hypothesis that CYP1A may be involved in the oxidative metabolism of ET-743. The finding that I3C at 0.5 % in the diet prevented ET-743-induced hepatotoxicity, and the same dose also induced CYP1A1/2 activity by 15-fold is consistent with this hypothesis. β -Naphthoflavone is frequently used in animal models to induce CYP1A, but there is no record of its use in the clinic. There is also a suggestion that β -naphthoflavone may be carcinogenic (McKillop and Case, 1991). Therefore, β -naphthoflavone could perhaps not be given to cancer patients as a protective strategy.

Both dexamethasone and I3C at high concentrations prevented ET-743-induced hepatotoxicity. An alternative strategy would be to combine dexamethasone and I3C at lower doses. The two agents in combination may sufficiently induce CYP3A to increase oxidative metabolism by the required amount. The protective effect of a combination of dexamethasone and I3C against ET-743-induced hepatotoxicity should firstly be evaluated in the female Wistar rat. If the combination was successful, then a clinical trial may be warranted. The combination of dexamethasone and I3C, at lower doses than those used to evaluate the agents individually, might well reduce the adverse effects associated with high doses of the two agents.

Throughout the history of development of novel chemotherapeutic agents there are many examples of drugs with interesting anti-tumour activity but with toxicity which prevented

progress and development in the clinic. In some cases toxicities were detected early, whereas for some agents, unwanted side-effects have become apparent much later in clinical trials. The work in this thesis provides novel insights into the hepatotoxicity of ET-743 and strategies for elimination of its unwanted hepatic effects. If ET-743 was still in the early stages of development this information would perhaps have facilitated a better approach to ET-743 development. ET-743 is currently in phase II/III clinical trials but the interesting findings concerning strategies to eliminate its hepatotoxicity may still have an impact on the future clinical use of ET-743.

BIBLIOGRAPHY

Bibliography

- Amromin G, Delman R, Shanbran E. Liver damage after chemotherapy for leukemia and lymphoma. *Gastroenterology* 1962; 42: 401-10.
- Arias IM. Multidrug resistance genes, p-glycoprotein and the liver. *Hepatology* 1990; 12: 159-65.
- Armstrong RN. Glutathione S-transferases: structure and mechanism of an archetypical detoxication enzyme. *Adv Enzymol Relat Areas Mol Biol* 1994; 69: 1-44.
- Aubrey D. Massive hepatic necrosis after cyclophosphamide. *British Medical Journal* 1970; 3: 588.
- Aviles A, Herrera J, Ramos E, Ambriz R, Aguirre J, Pizzuto J. Hepatic injury during doxorubicin therapy. *Arch Pathol Lab Med* 1984; 108: 912-3.
- Awasthi YC, Sharma R, Singhal SS. Human glutathione S-transferases. *Int J Biochem* 1994; 26: 295-308.
- Bacon AM, Rosenberg SA. Cyclophosphamide hepatotoxicity in a patient with systemic lupus erythematosus. *Ann Intern Med* 1982; 97: 62-3.
- Bailey G, Selivonchick D, Hendricks J. Initiation, promotion, and inhibition of carcinogenesis in rainbow trout. *Environ Health Perspect* 1987a; 71: 147-53.
- Bailey GS, Hendricks JD, Shelton DW, Nixon JE, Pawlowski NE. Enhancement of carcinogenesis by the natural anticarcinogen indole-3-carbinol. *J Natl Cancer Inst* 1987b; 78: 931-4.
- Beijnen JH. Pharmacokinetic parameters: predictive factors for ET-743 tolerability/safety profile. *European Cancer Conference Satellite Symposium* 2001; 37.
- Beijnen JH, Rosing H, Cvitkovic E. Pharmacokinetics (PK) and pharmacodynamics (PD) of ET-743 (ecteinascidin-743) in phase I trials. *Proc Am Soc Clin Oncol* 1999; 18: 163.
- Belay ED, Bresee JS, Holman RC, Khan AS, Shahriari A, Schonberger LB. Reye's syndrome in the United States from 1981 through 1997. *N Engl J Med* 1999; 340: 1377-82.
- Berkowitz RS, Goldstein DP, Bernstein MR. Ten year's experience with methotrexate and folinic acid as primary therapy for gestational trophoblastic disease. *Gynecol Oncol* 1986; 23: 111-8.

Bibliography

- Berman JS, Hiley CR, Wilson AC. Comparison of the effects of the hypolipidaemic agents ICI53072 and clofibrate with those of phenobarbitone on liver size, blood flow and DNA content in the rat. *Br J Pharmacol* 1983; 78: 533-41.
- Bernuau J, Rueff B, Benhamou JP. Fulminant and subfulminant liver failure: definitions and causes. *Semin Liver Dis* 1986; 6: 97-106.
- Berry MN, Friend DS. High-yield preparation of isolated rat liver parenchymal cells: a biochemical and fine structural study. *J Cell Biol* 1969; 43: 506-20.
- Bjeldanes LF, Kim JY, Grose KR, Bartholomew JC, Bradfield CA. Aromatic hydrocarbon responsiveness-receptor agonists generated from indole-3-carbinol in vitro and in vivo: comparisons with 2,3,7,8-tetrachlorodibenzo-p-dioxin. *Proc Natl Acad Sci U S A* 1991; 88: 9543-7.
- Bjork O, Eklof O, Willi U, Ahstrom L. Veno-occlusive disease and peliosis of the liver complicating the course of Wilms' tumour. *Acta Radiol Diagn (Stockh)* 1985; 26: 589-97.
- Black SD, Coon MJ. P-450 cytochromes: structure and function. *Adv Enzymol Relat Areas Mol Biol* 1987; 60: 35-87.
- Blum RH, Carter SK, Agre K. A clinical review of bleomycin--a new antineoplastic agent. *Cancer* 1973; 31: 903-14.
- Bogaards JJ, Bertrand M, Jackson P, Oudshoorn MJ, Weaver RJ, van Bladeren PJ, et al. Determining the best animal model for human cytochrome P450 activities: a comparison of mouse, rat, rabbit, dog, micropig, monkey and man. *Xenobiotica* 2000; 30: 1131-52.
- Bonfanti M, La Valle E, Fernandez Sousa Faro JM, Faircloth G, Caretti G, Mantovani R, et al. Effect of ecteinascidin-743 on the interaction between DNA binding proteins and DNA. *Anticancer Drug Des* 1999; 14: 179-86.
- Boobis AR, Sesardic D, Murray BP, Edwards RJ, Singleton AM, Rich KJ, et al. Species variation in the response of the cytochrome P-450-dependent monooxygenase system to inducers and inhibitors. *Xenobiotica* 1990; 20: 1139-61.
- Boyer JL. New concepts of mechanisms of hepatocyte bile formation. *Physiol Rev* 1980; 60: 303-26.

Bibliography

- Bradfield CA, Bjeldanes LF. Structure-activity relationships of dietary indoles: a proposed mechanism of action as modifiers of xenobiotic metabolism. *J Toxicol Environ Health* 1987; 21: 311-23.
- Bradford MM. A rapid and sensitive method for the quantitation of microgram quantities of protein utilizing the principle of protein-dye binding. *Anal Biochem* 1976; 72: 248-54.
- Bradlow HL, Michnovicz JJ, Halper M, Miller DG, Wong GY, Osborne MP. Long-term responses of women to indole-3-carbinol or a high fiber diet. *Cancer Epidemiol Biomarkers Prev* 1994; 3: 591-5.
- Braunschweiger PG, Schiffer LM. Growth kinetics of mammary tumor 13762 in rats previously cured by chemotherapy. *J Natl Cancer Inst* 1980; 64: 671-4.
- Brignall MS. Prevention and treatment of cancer with indole-3-carbinol. *Altern Med Rev* 2001; 6: 580-9.
- Broggini M, D'Incalci M. Modulation of transcription factor--DNA interactions by anticancer drugs. *Anticancer Drug Des* 1994; 9: 373-87.
- Burgunder JM, Varriale A, Lauterburg BH. Effect of N-acetylcysteine on plasma cysteine and glutathione following paracetamol administration. *Eur J Clin Pharmacol* 1989; 36: 127-31.
- Burke MD, Mayer RT. Ethoxyresorufin: direct fluorimetric assay of a microsomal O-dealkylation which is preferentially inducible by 3-methylcholanthrene. *Drug Metab Dispos* 1974; 2: 583-8.
- Carlson GP. Influence of ethanol on microsomal p-nitrophenol hydroxylation and ethoxyresorufin deethylation in rat liver and lung. *J Toxicol Environ Health* 1991; 32: 153-9.
- Carpenter-Deyo L, Marchand DH, Jean PA, Roth RA, Reed DJ. Involvement of glutathione in 1-naphthylisothiocyanate (ANIT) metabolism and toxicity to isolated hepatocytes. *Biochem Pharmacol* 1991; 42: 2171-80.
- Chang AE, Schneider PD, Sugarbaker PH, Simpson C, Culnane M, Steinberg SM. A prospective randomized trial of regional versus systemic continuous 5-fluorodeoxyuridine chemotherapy in the treatment of colorectal liver metastases. *Ann Surg* 1987; 206: 685-93.

Bibliography

- Chen I, Safe S, Bjeldanes L. Indole-3-carbinol and diindolylmethane as aryl hydrocarbon (Ah) receptor agonists and antagonists in T47D human breast cancer cells. *Biochem Pharmacol* 1996; 51: 1069-76.
- Chen J, Robertson G, Field J, Liddle C, Farrell GC. Effects of bile duct ligation on hepatic expression of female-specific CYP2C12 in male and female rats. *Hepatology* 1998; 28: 624-30.
- Chen TR, Dorotinsky C, Macy M, Hay R. Cell identity resolved. *Nature* 1989; 340: 106.
- Clark P, Hsia Y, Huntsman R. Toxic complications of treatment with 6-mercaptopurine. Two cases with hepatic necrosis and intestinal ulceration. *British Medical Journal* 1960; 1: 393-95.
- Crooke ST, Bradner WT. Mitomycin C: a review. *Cancer Treat Rev* 1976; 3: 121-39.
- Curigliano G, Bauer J, Capri G. Ecteinascidin 743 (ET-743) in ovarian cancer: activity in xenografts and preliminary results of an ongoing study in patients failing platinum-taxanes. *Proceedings of the AACR-NCI-EORTC International conference on Molecular Targets and Cancer Therapeutics: Discovery, Biology and Clinical Applications* 2001: 78a.
- da Rocha AB, Lopes RM, Schwartzmann G. Natural products in anticancer therapy. *Curr Opin Pharmacol* 2001; 1: 364-9.
- Dahm LJ, Bailie MB, Roth RA. Relationship between alpha-naphthylisothiocyanate-induced liver injury and elevations in hepatic non-protein sulfhydryl content. *Biochem Pharmacol* 1991; 42: 1189-94.
- Dahm LJ, Roth RA. Protection against alpha-naphthylisothiocyanate-induced liver injury by decreased hepatic non-protein sulfhydryl content. *Biochem Pharmacol* 1991; 42: 1181-8.
- Damia G, Silvestri S, Carrassa L, Filiberti L, Faircloth GT, Liberi G, et al. Unique pattern of ET-743 activity in different cellular systems with defined deficiencies in DNA-repair pathways. *Int J Cancer* 2001; 92: 583-8.
- Danielson UH, Mannervik B. Kinetic independence of the subunits of cytosolic glutathione transferase from the rat. *Biochem J* 1985; 231: 263-7.

Bibliography

- Dashwood RH. Indole-3-carbinol: anticarcinogen or tumor promoter in brassica vegetables? *Chem Biol Interact* 1998; 110: 1-5.
- De Matteis F, Dawson SJ, Boobis AR, Comoglio A. Inducible bilirubin-degrading system of rat liver microsomes: role of cytochrome P450IA1. *Mol Pharmacol* 1991; 40: 686-91.
- DeLeve LD, Kaplowitz N. Glutathione metabolism and its role in hepatotoxicity. *Pharmacol Ther* 1991; 52: 287-305.
- Delalogue S, Yovine A, Taamma A, Riofrio M, Brain E, Raymond E, et al. Ecteinascidin-743: a marine-derived compound in advanced, pretreated sarcoma patients--preliminary evidence of activity. *J Clin Oncol* 2001; 19: 1248-55.
- DeLeve LD, Kaplowitz N. Glutathione metabolism and its role in hepatotoxicity. *Pharmacol Ther* 1991; 52: 287-305.
- DeLeve LD, Kaplowitz N. Mechanisms of drug-induced liver disease. *Gastroenterol Clin North Am* 1995; 24: 787-810.
- Demetri G, Manola J, Harmon D. Ecteinascidin-743 (ET-743) induces durable responses and promising 1-year survival rates in soft tissue sarcomas (STS): final results of phase II and pharmacokinetic studies in the U.S.A. *Proc Am Soc Clin Oncol* 2001; 20: 363a.
- DeRisi JL, Iyer VR, Brown PO. Exploring the metabolic and genetic control of gene expression on a genomic scale. *Science* 1997; 278: 680-6.
- Desmet VJ, Krstulovic B, Van Damme B. Histochemical study of rat liver in alpha-naphthyl isothiocyanate (ANIT) induced cholestasis. *Am J Pathol* 1968; 52: 401-21.
- DeVita VT, Trujillo NP, Blackman AH, Ticktin HE. Pulmonary manifestations of primary hepatic carcinoma. *Am J Med Sci* 1965; 250: 428-36.
- Donehower R, Abeloff M, Perry M. *Chemotherapy*. New York: Churchill Livingstone, 1995.
- Donehower RC, Karp JE, Burke PJ. Pharmacology and toxicity of high-dose cytarabine by 72-hour continuous infusion. *Cancer Treat Rep* 1986; 70: 1059-65.
- Doria MI, Jr., Shepard KV, Levin B, Riddell RH. Liver pathology following hepatic arterial infusion chemotherapy. Hepatic toxicity with FUDR. *Cancer* 1986; 58: 855-61.
- Einhorn M, Davidson I. Hepatotoxicity of mercaptopurine. *JAMA* 1964; 188: 802-806.
- Eisen MB, Brown PO. DNA arrays for analysis of gene expression. *Methods Enzymol* 1999; 303: 179-205.

Bibliography

- Ellison RR, Holland JF, Weil M, Jacquillat C, Boiron M, Bernard J, et al. Arabinosyl cytosine: a useful agent in the treatment of acute leukemia in adults. *Blood* 1968; 32: 507-23.
- Erba E, Bergamaschi D, Bassano L, Damia G, Ronzoni S, Faircloth GT, et al. Ecteinascidin-743 (ET-743), a natural marine compound, with a unique mechanism of action. *Eur J Cancer* 2001; 37: 97-105.
- Erlinger S. Hepatocyte bile secretion: current views and controversies. *Hepatology* 1981; 1: 352-9.
- Erlinger S. What is cholestasis in 1985? *J Hepatol* 1985; 1: 687-93.
- Erlinger S. Review article: new insights into the mechanisms of hepatic transport and bile secretion. *J Gastroenterol Hepatol* 1996; 11: 575-9.
- Favreau LV, Pickett CB. The rat quinone reductase antioxidant response element. Identification of the nucleotide sequence required for basal and inducible activity and detection of antioxidant response element-binding proteins in hepatoma and non-hepatoma cell lines. *J Biol Chem* 1995; 270: 24468-74.
- Fentem JH, Fry JR. Comparison of the effects of inducers of cytochrome P450 on Mongolian gerbil and rat hepatic microsomal monooxygenase activities. *Xenobiotica* 1991; 21: 895-904.
- Formelli F, Cleris L. Synthetic retinoid fenretinide is effective against a human ovarian carcinoma xenograft and potentiates cisplatin activity. *Cancer Res* 1993; 53: 5374-6.
- Frazier JM. In vitro models for toxicological research and testing. *Toxicol Lett* 1993; 68: 73-90.
- Friedman JM, Chung EY, Darnell JE, Jr. Gene expression during liver regeneration. *J Mol Biol* 1984; 179: 37-53.
- Freireich EJ, Gehan EA, Rall DP, Schmidt LH, Skipper HE. Quantitative comparison of toxicity of anticancer agents in mouse, rat, hamster, dog, monkey, and man. *Cancer Chemother Rep* 1966; 50: 219-44.
- Fromenty B, Pessayre D. Impaired mitochondrial function in microvesicular steatosis. Effects of drugs, ethanol, hormones and cytokines. *J Hepatol* 1997; 26 Suppl 2: 43-53.
- Ganey PE, Bailie MB, VanCise S, Colligan ME, Madhukar BV, Robinson JP, et al. Activated neutrophils from rat injured isolated hepatocytes. *Lab Invest* 1994; 70: 53-60.

Bibliography

- Garcia-Rocha M, Garcia-Gravalos MD, Avila J. Characterisation of antimetabolic products from marine organisms that disorganise the microtubule network: ecteinascidin 743, isohomohalichondrin-B and LL-15. *Br J Cancer* 1996; 73: 875-83.
- Ged C, Rouillon JM, Pichard L, Combalbert J, Bressot N, Bories P, et al. The increase in urinary excretion of 6 beta-hydroxycortisol as a marker of human hepatic cytochrome P450III_A induction. *Br J Clin Pharmacol* 1989; 28: 373-87.
- George CB, Mansour RP, Redmond J, 3rd, Gandara DR. Hepatic dysfunction and jaundice following high-dose cytosine arabinoside. *Cancer* 1984; 54: 2360-2.
- Gilman A, Philips F. The biological action and therapeutic applications of beta-chloroethyl amine and sulphides. *Science* 1946; 103: 409-411.
- Glatt H. Sulfotransferases in the bioactivation of xenobiotics. *Chem Biol Interact* 2000; 129: 141-70.
- Goeger DE, Shelton DW, Hendricks JD, Bailey GS. Mechanisms of anti-carcinogenesis by indole-3-carbinol: effect on the distribution and metabolism of aflatoxin B1 in rainbow trout. *Carcinogenesis* 1986; 7: 2025-31.
- Goldberg JW, Lidsky MD. Cyclophosphamide-associated hepatotoxicity. *South Med J* 1985; 78: 222-3.
- Goldfarb S, Singer E, Popper H. Experimental cholangitis due to alpha-naphthylisothiocyanate. *American Journal of Pathology* 1962; 40: 685-695.
- Gomez MR, Benzick AE, Rogers LK, Heird WC, Smith CV. Attenuation of acetaminophen hepatotoxicity in mice as evidence for the bioavailability of the cysteine in D-glucose-L-cysteine in vivo. *Toxicol Lett* 1994; 70: 101-8.
- Gonzalez FJ. The molecular biology of cytochrome P450s. *Pharmacol Rev* 1988; 40: 243-88.
- Gonzalez FJ, Nebert DW. Evolution of the P450 gene superfamily: animal-plant 'warfare', molecular drive and human genetic differences in drug oxidation. *Trends Genet* 1990; 6: 182-6.
- Govindan VM, Faulstich H, Wieland T, Agostini B, Hasselbach W. In-vitro effect of phalloidin on plasma membrane preparation from rat liver. *Naturwissenschaften* 1972; 59: 521-2.
- Greaves P. *Histopathology of preclinical toxicity studies*: Elsevier, 2000.

Bibliography

- Green DM, Finklestein JZ, Norkool P, D'Angio GJ. Severe hepatic toxicity after treatment with single-dose dactinomycin and vincristine. A report of the National Wilms' Tumor Study. *Cancer* 1988; 62: 270-3.
- Green L, Donehower RC. Hepatic toxicity of low doses of mithramycin in hypercalcemia. *Cancer Treat Rep* 1984; 68: 1379-81.
- Grubbs CJ, Steele VE, Casebolt T, Juliana MM, Eto I, Whitaker LM, et al. Chemoprevention of chemically-induced mammary carcinogenesis by indole-3-carbinol. *Anticancer Res* 1995; 15: 709-16.
- Hari P, Srivastava RN. Pulse corticosteroid therapy with methylprednisolone or dexamethasone. *Indian J Pediatr* 1998; 65: 557-60.
- Hayes JD, Judah DJ, McLellan LI, Kerr LA, Peacock SD, Neal GE. Ethoxyquin-induced resistance to aflatoxin B1 in the rat is associated with the expression of a novel alpha-class glutathione S-transferase subunit, Yc2, which possesses high catalytic activity for aflatoxin B1-8,9-epoxide. *Biochem J* 1991; 279 (Pt 2): 385-98.
- Hendriks HR, Fiebig HH, Giavazzi R, Langdon SP, Jimeno JM, Faircloth GT. High antitumour activity of ET743 against human tumour xenografts from melanoma, non-small-cell lung and ovarian cancer. *Ann Oncol* 1999; 10: 1233-40.
- Honkakoski P, Negishi M. Regulatory DNA elements of phenobarbital-responsive cytochrome P450 CYP2B genes. *J Biochem Mol Toxicol* 1998; 12: 3-9.
- Honkakoski P, Zelko I, Sueyoshi T, Negishi M. The nuclear orphan receptor CAR-retinoid X receptor heterodimer activates the phenobarbital-responsive enhancer module of the CYP2B gene. *Mol Cell Biol* 1998; 18: 5652-8.
- Hoogstraten B, Gottlieb JA, Caoili E, Tucker WG, Talley RW, Haut A. CCNU (1-(2-chloroethyl)-3-cyclohexyl-1-nitrosourea, NSC-79037) in the treatment of cancer. Phase II study. *Cancer* 1973; 32: 38-43.
- Hutter R, Shipkey F, Tan C. Hepatic fibrosis in children with acute leukaemia: A complication of therapy. *Cancer* 1960; 13: 288-307.
- Infield G. *Disasters at Bari*. New York: MacMillan, 1971.
- Ioannides C, Parke DV. The cytochrome P450 I gene family of microsomal hemoproteins and their role in the metabolic activation of chemicals. *Drug Metab Rev* 1990; 22: 1-85.

Bibliography

- Izbicka E, Lawrence R, Raymond E, Eckhardt G, Faircloth G, Jimeno J, et al. *In vitro* antitumor activity of the novel marine agent, ecteinascidin-743 (ET-743, NSC-648766) against human tumors explanted from patients. *Ann Oncol* 1998; 9: 981-7.
- Jager W, Correia MA, Bornheim LM, Mahnke A, Hanstein WG, Xue L, et al. Ethynylestradiol-mediated induction of hepatic CYP3A9 in female rats: implication for cyclosporine metabolism. *Drug Metab Dispos* 1999; 27: 1505-11.
- Jean PA, Bailie MB, Roth RA. 1-naphthylisothiocyanate-induced elevation of biliary glutathione. *Biochem Pharmacol* 1995; 49: 197-202.
- Jean PA, Roth RA. Naphthylisothiocyanate disposition in bile and its relationship to liver glutathione and toxicity. *Biochem Pharmacol* 1995; 50: 1469-74.
- Jimeno J, Faircloth G, Cameron L, Meely K, Vega E, Gomez A, et al. Progress in the acquisition of new marine-derived anticancer compounds : development of ecteinascidin-743 (ET-743). *Drugs of the Future* 1996; 21: 1155-65.
- Jin S, Gorfajn B, Faircloth G, Scotto KW. Ecteinascidin 743, a transcription-targeted chemotherapeutic that inhibits MDR1 activation. *Proc Natl Acad Sci U S A* 2000; 97: 6775-9.
- Johnson DH, Greco FA, Wolff SN. Etoposide-induced hepatic injury: a potential complication of high-dose therapy. *Cancer Treat Rep* 1983; 67: 1023-4.
- Kapitulnik J, Ostrow JD. Stimulation of bilirubin catabolism in jaundiced Gunn rats by an induced of microsomal mixed-function monooxygenases. *Proc Natl Acad Sci U S A* 1978; 75: 682-5.
- Kedderis GL. Biochemical basis of hepatocellular injury. *Toxicol Pathol* 1996; 24: 77-83.
- Kelly EJ, Sandgren EP, Brinster RL, Palmiter RD. A pair of adjacent glucocorticoid response elements regulate expression of two mouse metallothionein genes. *Proc Natl Acad Sci U S A* 1997; 94: 10045-50.
- Kemeny N, Daly J, Reichman B, Geller N, Botet J, Oderman P. Intrahepatic or systemic infusion of fluorodeoxyuridine in patients with liver metastases from colorectal carcinoma. A randomized trial. *Ann Intern Med* 1987; 107: 459-65.
- Kemper B. Regulation of cytochrome P450 gene transcription by phenobarbital. *Prog Nucleic Acid Res Mol Biol* 1998; 61: 23-64.

Bibliography

- Kennedy BJ. Metabolic and toxic effects of mithramycin during tumor therapy. *Am J Med* 1970; 49: 494-503.
- Kennedy BJ, Brown JH, Yarbrow JW. Mithramycin (NSC-24559) therapy for primary glioblastomas. *Cancer Chemother Rep* 1965; 48: 59-63.
- Khan S, Ramwani JJ, O'Brien PJ. Hepatocyte toxicity of mechlorethamine and other alkylating anticancer drugs. Role of lipid peroxidation. *Biochem Pharmacol* 1992; 43: 1963-7.
- Kim DJ, Han BS, Ahn B, Hasegawa R, Shirai T, Ito N, et al. Enhancement by indole-3-carbinol of liver and thyroid gland neoplastic development in a rat medium-term multiorgan carcinogenesis model. *Carcinogenesis* 1997; 18: 377-81.
- King CD, Rios GR, Green MD, Tephly TR. UDP-glucuronosyltransferases. *Curr Drug Metab* 2000; 1: 143-61.
- King PD, Perry MC. Hepatotoxicity of chemotherapeutic and oncologic agents. *Gastroenterol Clin North Am* 1995; 24: 969-90.
- King R. *Cancer Biology*: Prentice Hall, 2000.
- Kountouras J, Billing BH, Scheuer PJ. Prolonged bile duct obstruction: a new experimental model for cirrhosis in the rat. *Br J Exp Pathol* 1984; 65: 305-11.
- Kravchenko LV, Avren'eva LI, Guseva GV, Posdnyakov AL, Tutel'yan VA. Effect of nutritional indoles on activity of xenobiotic metabolism enzymes and T-2 toxicity in rats. *Bull Exp Biol Med* 2001; 131: 544-7.
- Krell H, Hoke H, Pfaff E. Development of intrahepatic cholestasis by alpha-naphthylisothiocyanate in rats. *Gastroenterology* 1982; 82: 507-14.
- Kretzschmar M. Regulation of hepatic glutathione metabolism and its role in hepatotoxicity. *Exp Toxicol Pathol* 1996; 48: 439-46.
- Kuffel MJ, Reid JM, Ames MM. Cytochrome P450 catalysed metabolism of Ecteinascidin 743 by rat and human liver microsomes. *Proc Am Ass Cancer Res* 1997; 38: abstract 596.
- Le Cesne A, Blay J, Judson I. ET-743 is an active drug in adult soft-tissue sarcoma. *Proc Am Soc Clin Oncol* 2001; 20: 353a.

Bibliography

- Leonard TB, Neptun DA, Popp JA. Serum gamma glutamyl transferase as a specific indicator of bile duct lesions in the rat liver. *Am J Pathol* 1984; 116: 262-9.
- Lin JH, Chiba M, Chen IW, Nishime JA, deLuna FA, Yamazaki M, et al. Effect of dexamethasone on the intestinal first-pass metabolism of indinavir in rats: evidence of cytochrome P-450 3A [correction of P-450 A] and p-glycoprotein induction. *Drug Metab Dispos* 1999; 27: 1187-93.
- Lopez Lazaro L, van Kesteren C, Hoekman K. Ecteinascidin (ET-743) pharmacokinetics (PK): overview of phase I and advanced phase II results. *Eur J Cancer* 2001; 37: S66.
- Lyons L, Studdiford JS, Sommaripa AM. Treatment of acetaminophen overdose with N-acetylcysteine. *N Engl J Med* 1977; 296: 174-5.
- Mackenzie AH. Hepatotoxicity of prolonged methotrexate therapy for rheumatoid arthritis. *Cleve Clin Q* 1985; 52: 129-35.
- Manson MM, Ball HW, Barrett MC, Clark HL, Judah DJ, Williamson G, et al. Mechanism of action of dietary chemoprotective agents in rat liver: induction of phase I and II drug metabolizing enzymes and aflatoxin B1 metabolism. *Carcinogenesis* 1997; 18: 1729-38.
- Manson MM, Gescher A, Hudson EA, Plummer SM, Squires MS, Prigent SA. Blocking and suppressing mechanisms of chemoprevention by dietary constituents. *Toxicol Lett* 2000; 112-113: 499-505.
- Manson MM, Hudson EA, Ball HW, Barrett MC, Clark HL, Judah DJ, et al. Chemoprevention of aflatoxin B1-induced carcinogenesis by indole-3-carbinol in rat liver--predicting the outcome using early biomarkers. *Carcinogenesis* 1998; 19: 1829-36.
- Martinez EJ, Corey EJ, Owa T. Antitumor activity- and gene expression-based profiling of ecteinascidin Et 743 and phthalascidin Pt 650. *Chem Biol* 2001; 8: 1151-60.
- McDanell R, McLean AE, Hanley AB, Heaney RK, Fenwick GR. Chemical and biological properties of indole glucosinolates (glucobrassicins): a review. *Food Chem Toxicol* 1988; 26: 59-70.
- McIlvanie S, MacCarthy J. Hepatitis in association with prolonged 6-mercaptopurine therapy. *Blood* 1959; 14: 80-90.

Bibliography

- McIntosh S, Davidson DL, O'Brien RT, Pearson HA. Methotrexate hepatotoxicity in children with leukemia. *J Pediatr* 1977; 90: 1019-21.
- McKillop D, Case DE. Mutagenicity, carcinogenicity and toxicity of beta-naphthoflavone, a potent inducer of P448. *Biochem Pharmacol* 1991; 41: 1-7.
- Meyers LL, Beierschmitt WP, Khairallah EA, Cohen SD. Acetaminophen-induced inhibition of hepatic mitochondrial respiration in mice. *Toxicol Appl Pharmacol* 1988; 93: 378-87.
- Minuzzo M, Marchini S, Brogginini M, Faircloth G, D'Incalci M, Mantovani R. Interference of transcriptional activation by the antineoplastic drug ecteinascidin-743. *Proc Natl Acad Sci U S A* 2000; 97: 6780-4.
- Mirsalis J, Schinder-Horvat J, Tomaszewski J. Preclinical toxicity studies. *Proc Am Soc Clin Oncol* 1996; 37: 2556.
- Moffatt P, DenizEAU F. Metallothionein in physiological and physiopathological processes. *Drug Metab Rev* 1997; 29: 261-307.
- Moore B, Seaman F, Hurley LH . NMR-based model of an ecteinascidin 743-DNA adduct. *J Am Chem Soc* 1997; 119: 5475-6.
- Morris LE, Guthrie TH, Jr. Busulfan-induced hepatitis. *Am J Gastroenterol* 1988; 83: 682-3.
- Muller M, Jansen PL. Molecular aspects of hepatobiliary transport. *Am J Physiol* 1997; 272: G1285-303.
- Nebert DW, Jones JE. Regulation of the mammalian cytochrome P1-450 (CYP1A1) gene. *Int J Biochem* 1989; 21: 243-52.
- Nebert DW, Gonzalez FJ. P450 genes: structure, evolution, and regulation. *Annu Rev Biochem* 1987; 56: 945-93.
- Nicotera P, Bellomo G, Orrenius S. The role of Ca²⁺ in cell killing. *Chem Res Toxicol* 1990; 3: 484-94.
- Nicotera P, Hartzell P, Davis G, Orrenius S. The formation of plasma membrane blebs in hepatocytes exposed to agents that increase cytosolic Ca²⁺ is mediated by the activation of a non-lysosomal proteolytic system. *FEBS Lett* 1986; 209: 139-44.
- Ormerod M. Flow cytometry: A practical approach. Oxford, United Kingdom: IRL Press, 1990

Bibliography

- Paciucci PA, Sklarin NT. Mitoxantrone and hepatic toxicity. *Ann Intern Med* 1986; 105: 805-6.
- Paillard F, Finot F, Mouche I, Prenez A, Vericat J. Use of primary cultures of rat hepatocytes to predict toxicity in the early development of new chemical entities. *Toxicology in vitro* 1999; 13: 693-700.
- Pascussi JM, Drocourt L, Gerbal-Chaloin S, Fabre JM, Maurel P, Vilarem MJ. Dual effect of dexamethasone on CYP3A4 gene expression in human hepatocytes. Sequential role of glucocorticoid receptor and pregnane X receptor. *Eur J Biochem* 2001; 268: 6346-58.
- Pendergrast WJ, Jr., Drake WP, Mardiney MR, Jr. A proper sequence for the treatment of B16 melanoma: chemotherapy, surgery, and immunotherapy. *J Natl Cancer Inst* 1976; 57: 539-44.
- Pence BC, Buddingh F, Yang SP. Multiple dietary factors in the enhancement of dimethylhydrazine carcinogenesis: main effect of indole-3-carbinol. *J Natl Cancer Inst* 1986; 77: 269-76.
- Pereira TM, Carlstedt-Duke J, Lechner MC, Gustafsson JA. Identification of a functional glucocorticoid response element in the CYP3A1/IGC2 gene. *DNA Cell Biol* 1998; 17: 39-49.
- Perry MC. Chemotherapeutic agents and hepatotoxicity. *Semin Oncol* 1992; 19: 551-65.
- Pettavel J, Gardiol D, Bergier N, Schnyder P. Fatal liver cirrhosis associated with long-term arterial infusion of floxuridine. *Lancet* 1986; 2: 1162-3.
- Phillips F, Sternberg S, Hamilton L. The toxic effects of 6-mercaptopurine and related compounds. *Ann N Y Acad Sci* 1957; 60: 283-96.
- Pichard L, Fabre I, Fabre G, Domergue J, Saint Aubert B, Mourad G, et al. Cyclosporin A drug interactions. Screening for inducers and inhibitors of cytochrome P-450 (cyclosporin A oxidase) in primary cultures of human hepatocytes and in liver microsomes. *Drug Metab Dispos* 1990; 18: 595-606.
- Pitot H, Loeb D. *Fundamentals of Oncology*. New York: Marcel Dekker, 2002.
- Pizzuto J, Aviles A, Ramos E, Cervera J, Aguirre J. Cytosine arabinoside induced liver damage: histopathologic demonstration. *Med Pediatr Oncol* 1983; 11: 287-90.

Bibliography

- Plaa GL, Priestly BG. Intrahepatic cholestasis induced by drugs and chemicals. *Pharmacol Rev* 1976; 28: 207-73.
- Podurgiel BJ, McGill DB, Ludwig J, Taylor WF, Muller SA. Liver injury associated with methotrexate therapy for psoriasis. *Mayo Clin Proc* 1973; 48: 787-92.
- Pollera CF, Ameglio F, Nardi M, Vitelli G, Marolla P. Cisplatin-induced hepatic toxicity. *J Clin Oncol* 1987; 5: 318-9.
- Pommier Y, Kohlhagen G, Bailly C, Waring M, Mazumder A, Kohn KW. DNA sequence- and structure-selective alkylation of guanine N2 in the DNA minor groove by ecteinascidin 743, a potent antitumor compound from the Caribbean tunicate *Ecteinascidia turbinata*. *Biochemistry* 1996; 35: 13303-9.
- Pratt W, Ruddon R, Ensminger W. The Anticancer drugs. In: 2 E, editor. New York: Oxford University Press, 1994.
- Priestman T. *Cancer Chemotherapy: an introduction*: Springer-Verlag, 1989.
- Pritchard J, Raine J, Wallendszus K. Hepatotoxicity of actinomycin-D. *Lancet* 1989; 1: 168.
- Puchalski TA, Ryan DP, Garcia-Carbonero R, Demetri GD, Butkiewicz L, Harmon D, et al. Pharmacokinetics of ecteinascidin 743 administered as a 24-h continuous intravenous infusion to adult patients with soft tissue sarcomas: associations with clinical characteristics, pathophysiological variables and toxicity. *Cancer Chemother Pharmacol* 2002; 50: 309-19.
- Quattrochi LC, Yockey CB, Barwick JL, Guzelian PS. Characterization of DNA-binding proteins required for glucocorticoid induction of CYP3A23. *Arch Biochem Biophys* 1998; 349: 251-60.
- Reichen J, Simon FR. Mechanisms of cholestasis. *Int Rev Exp Pathol* 1984; 26: 231-74.
- Reid JM, Kuffel MJ, Ruben SL, Morales JJ, Rinehart KL, Squillace DP, et al. Rat and human liver cytochrome P-450 isoform metabolism of ecteinascidin 743 does not predict gender-dependent toxicity in humans. *Clin Cancer Res* 2002; 8: 2952-62.
- Reid JM, Walker DL, Ames MM. Preclinical pharmacology of ecteinascidin 729, a marine natural product with potent antitumor activity. *Cancer Chemother Pharmacol* 1996; 38: 329-34.

Bibliography

- Renwick AB, Lewis DF, Fulford S, Surry D, Williams B, Worboys PD, et al. Metabolism of 2,5-bis(trifluoromethyl)-7-benzyloxy-4-trifluoromethylcoumarin by human hepatic CYP isoforms: evidence for selectivity towards CYP3A4. *Xenobiotica* 2001; 31: 187-204.
- Rinehart KL. Antitumor compounds from tunicates. *Med Res Rev* 2000; 20: 1-27.
- Rinehart KL, Morales JJ, Reid JM, Reymundo I, Floriano P, Garcia-Gravalos L. Metabolites of Ecteinascidin 743. Patent WO 1999; 99/58125.
- Rosing H, Hillebrand MJ, Jimeno JM, Gomez A, Floriano P, Faircloth G, et al. Quantitative determination of Ecteinascidin 743 in human plasma by miniaturized high-performance liquid chromatography coupled with electrospray ionization tandem mass spectrometry. *J Mass Spectrom* 1998; 33: 1134-40.
- Roth RA, Dahm LJ. Neutrophil- and glutathione-mediated hepatotoxicity of alpha-naphthylisothiocyanate. *Drug Metab Rev* 1997; 29: 153-65.
- Roth RA, Hewett JA. The cholestatic agent, alpha-naphthylisothiocyanate, stimulates superoxide release by rat neutrophils in vitro. *Lab Invest* 1990; 62: 736-41.
- Ruddon R. *Cancer Biology*. New York: Oxford University Press, 1995.
- Rumack BH, Peterson RC, Koch GG, Amara IA. Acetaminophen overdose. 662 cases with evaluation of oral acetylcysteine treatment. *Arch Intern Med* 1981; 141: 380-5.
- Ryan DP, Supko JG, Eder JP, Seiden MV, Demetri G, Lynch TJ, et al. Phase I and pharmacokinetic study of ecteinascidin 743 administered as a 72-hour continuous intravenous infusion in patients with solid malignancies. *Clin Cancer Res* 2001; 7: 231-42.
- Saarikoski ST, Ikonen TS, Oinonen T, Lindros KO, Ulmanen I, Husgafvel-Pursiainen K. Induction of UDP-glycosyltransferase family 1 genes in rat liver: different patterns of mRNA expression with two inducers, 3-methylcholanthrene and beta-naphthoflavone. *Biochem Pharmacol* 1998; 56: 569-75.
- Schneider J, Kinne D, Fracchia A, Pierce V, Anderson KE, Bradlow HL, et al. Abnormal oxidative metabolism of estradiol in women with breast cancer. *Proc Natl Acad Sci USA* 1982; 79: 3047-51.

Bibliography

- Schrenk D, Gant TW, Preisegger KH, Silverman JA, Marino PA, Thorgeirsson SS. Induction of multidrug resistance gene expression during cholestasis in rats and nonhuman primates. *Hepatology* 1993; 17: 854-60.
- Scheuer PJ, Summerfield JA, Lal S, Sherlock S. Rifampicin hepatitis. A clinical and histological study. *Lancet* 1974; 1: 421-5.
- Schuetz EG, Schmid W, Schutz G, Brimer C, Yasuda K, Kamataki T, et al. The glucocorticoid receptor is essential for induction of cytochrome P-450B by steroids but not for drug or steroid induction of CYP3A or P-450 reductase in mouse liver. *Drug Metab Dispos* 2000; 28: 268-78.
- Schuetz JD, Schuetz EG, Thottassery JV, Guzelian PS, Strom S, Sun D. Identification of a novel dexamethasone responsive enhancer in the human CYP3A5 gene and its activation in human and rat liver cells. *Mol Pharmacol* 1996; 49: 63-72.
- Seeman P. The membrane actions of anesthetics and tranquilizers. *Pharmacol Rev* 1972; 24: 583-655.
- Seglen PO. Preparation of isolated rat liver cells. *Methods Cell Biol* 1976; 13: 29-83.
- Shepard KV, Levin B, Faintuch J, Doria MI, DuBrow RA, Riddell RH. Hepatitis in patients receiving intraarterial chemotherapy for metastatic colorectal carcinoma. *Am J Clin Oncol* 1987; 10: 36-40.
- Shertzer HG, Niemi MP, Reitman FA, Berger ML, Myers BL, Tabor MW. Protection against carbon tetrachloride hepatotoxicity by pretreatment with indole-3-carbinol. *Exp Mol Pathol* 1987; 46: 180-9.
- Shertzer HG, Sainsbury M. Intrinsic acute toxicity and hepatic enzyme inducing properties of the chemoprotectants indole-3-carbinol and 5,10-dihydroindeno[1,2-b]indole in mice. *Food Chem Toxicol* 1991; 29: 237-42.
- Shorey J, Schenker S, Suki WN, Combes B. Hepatotoxicity of mercaptopurine. *Arch Intern Med* 1968; 122: 54-8.
- Skett P. Problems in using isolated and cultured hepatocytes for xenobiotic metabolism/metabolism based toxicity testing-solutions? *Toxicology in vitro* 1994; 8: 491-504.

Bibliography

- Sparidans RW, Rosing H, Hillebrand MJ, Lopez-Lazaro L, Jimeno JM, Manzanares I, et al. Search for metabolites of ecteinascidin 743, a novel, marine-derived, anti-cancer agent, in man. *Anticancer Drugs* 2001; 12: 653-66.
- Sprung CL, Caralis PV, Marcial EH, Pierce M, Gelbard MA, Long WM, et al. The effects of high-dose corticosteroids in patients with septic shock. A prospective, controlled study. *N Engl J Med* 1984; 311: 1137-43.
- Stoner G, Casto B, Ralston S, Roebuck B, Pereira C, Bailey G. Development of a multi-organ rat model for evaluating chemopreventive agents: efficacy of indole-3-carbinol. *Carcinogenesis* 2002; 23: 265-72.
- Stresser DM, Bailey GS, Williams DE. Indole-3-carbinol and beta-naphthoflavone induction of aflatoxin B1 metabolism and cytochromes P-450 associated with bioactivation and detoxication of aflatoxin B1 in the rat. *Drug Metab Dispos* 1994; 22: 383-91.
- Stresser DM, Blanchard AP, Turner SD, Erve JC, Dandeneau AA, Miller VP, et al. Substrate-dependent modulation of CYP3A4 catalytic activity: analysis of 27 test compounds with four fluorometric substrates. *Drug Metab Dispos* 2000; 28: 1440-8.
- Sueyoshi T, Kawamoto T, Zelko I, Honkakoski P, Negishi M. The repressed nuclear receptor CAR responds to phenobarbital in activating the human CYP2B6 gene. *J Biol Chem* 1999; 274: 6043-6.
- Sznol M, Ohnuma T, Holland JF. Hepatic toxicity of drugs used for hematologic neoplasia. *Semin Liver Dis* 1987; 7: 237-56.
- Taamma A, Misset JL, Riofrio M, Guzman C, Brain E, Lopez Lazaro L, et al. Phase I and pharmacokinetic study of ecteinascidin-743, a new marine compound, administered as a 24-hour continuous infusion in patients with solid tumors. *J Clin Oncol* 2001; 19: 1256-65.
- Takahashi N, Li WW, Banerjee D, Scotto KW, Bertino JR. Sequence-dependent enhancement of cytotoxicity produced by ecteinascidin 743 (ET-743) with doxorubicin or paclitaxel in soft tissue sarcoma cells. *Clin Cancer Res* 2001; 7: 3251-7.
- Takebayashi Y, Goldwasser F, Urasaki Y, Kohlhagen G, Pommier Y. Ecteinascidin 743 induces protein-linked DNA breaks in human colon carcinoma HCT116 cells and is

Bibliography

- cytotoxic independently of topoisomerase I expression. *Clin Cancer Res* 2001; 7: 185-91.
- Takebayashi Y, Pourquier P, Yoshida A, Kohlhagen G, Pommier Y. Poisoning of human DNA topoisomerase I by ecteinascidin 743, an anticancer drug that selectively alkylates DNA in the minor groove. *Proc Natl Acad Sci U S A* 1999; 96: 7196-201.
- Talmadge JE, Key ME, Hart IR. Characterization of a murine ovarian reticulum cell sarcoma of histiocytic origin. *Cancer Res* 1981; 41: 1271-80.
- Tateishi T, Watanabe M, Nakura H, Tanaka M, Kumai T, Kobayashi S. Liver damage induced by bile duct ligation affects CYP isoenzymes differently in rats. *Pharmacol Toxicol* 1998; 82: 89-92.
- Testa B, Jenner P. Inhibitors of Cytochrome P-450s and their mechanism of action. *Drug Metab Rev* 1981; 12: 1-117.
- Tolman KG, Clegg DO, Lee RG, Ward JR. Methotrexate and the liver. *J Rheumatol* 1985; 12 Suppl 12: 29-34.
- Tomlinson ES, Maggs JL, Park BK, Back DJ. Dexamethasone metabolism in vitro: species differences. *J Steroid Biochem Mol Biol* 1997; 62: 345-52.
- Tran A, Housset C, Boboc B, Tourani JM, Carnot F, Berthelot P. Etoposide (VP 16-213) induced hepatitis. Report of three cases following standard-dose treatments. *J Hepatol* 1991; 12: 36-9.
- Tribble DL, Aw TY, Jones DP. The pathophysiological significance of lipid peroxidation in oxidative cell injury. *Hepatology* 1987; 7: 377-86.
- Tuchweber B, Weber A, Roy CC, Yousef IM. Mechanisms of experimentally induced intrahepatic cholestasis. *Prog Liver Dis* 1986; 8: 161-78.
- Turton NJ, Judah DJ, Riley J, Davies R, Lipson D, Styles JA, et al. Gene expression and amplification in breast carcinoma cells with intrinsic and acquired doxorubicin resistance. *Oncogene* 2001; 20: 1300-6.
- Underwood JC, Shahani RT, Blackburn EK. Jaundice after treatment of leukemia with busulphan. *Br Med J* 1971; 1: 556-7.

Bibliography

- Valoti G, Nicoletti MI, Pellegrino A, Jimeno J, Hendriks H, D'Incalci M, et al. Ecteinascidin-743, a new marine natural product with potent antitumor activity on human ovarian carcinoma xenografts. *Clin Cancer Res* 1998; 4: 1977-83.
- Vanhaecke T, Derde MP, Vercruyse A, Rogiers V. Hydroxypropyl-beta-cyclodextrin as delivery system for thyroid hormones, regulating glutathione S-transferase expression in rat hepatocyte co-cultures. *Biochem Pharmacol* 2001; 61: 1073-8.
- van Kesteren C, Cvitkovic E, Taamma A, Lopez-Lazaro L, Jimeno JM, Guzman C, et al. Pharmacokinetics and pharmacodynamics of the novel marine-derived anticancer agent ecteinascidin 743 in a phase I dose-finding study. *Clin Cancer Res* 2000; 6: 4725-32.
- Vang O, Frandsen H, Hansen KT, Nielsen JB, Andersen O. Modulation of drug-metabolising enzyme expression by condensation products of indole-3-ylcarbinol, an inducer in cruciferous vegetables. *Pharmacol Toxicol* 1999; 84: 59-65.
- Walters D, Robinson RG, Dick-Smith JB, Corrigan AB, Webb J. Poor response in two cases of juvenile rheumatoid arthritis to treatment with cyclophosphamide. *Med J Aust* 1972; 2: 1070.
- Wani M, Taylor H, Wall M, Coggon P, McPhail A. Plant antitumour agents. VI. The isolation and structure of taxol, a novel antileukemia and antitumour agent from *Taxus brevifolia*. *J Am Chem Soc* 1971; 93: 2325-7.
- Watkins PB. Role of cytochromes P450 in drug metabolism and hepatotoxicity. *Semin Liver Dis* 1990; 10: 235-50.
- Wattenberg LW, Hanley AB, Barany G, Sparnins VL, Lam LK, Fenwick GR. Inhibition of carcinogenesis by some minor dietary constituents. *Princess Takamatsu Symp* 1985; 16: 193-203.
- Weber BL, Tanyer G, Poplack DG, Reaman GH, Feusner JH, Miser JS, et al. Transient acute hepatotoxicity of high-dose methotrexate therapy during childhood. *NCI Monogr* 1987: 207-12.
- Weinstein GD. Methotrexate. *Ann Intern Med* 1977; 86: 199-204.
- White IN. The role of liver glutathione in the acute toxicity of retrorsine to rats. *Chem Biol Interact* 1976; 13: 333-42.

Bibliography

- Williams DE, Reed RL, Kedzierski B, Dannan GA, Guengerich FP, Buhler DR. Bioactivation and detoxication of the pyrrolizidine alkaloid senecionine by cytochrome P-450 enzymes in rat liver. *Drug Metab Dispos* 1989; 17: 387-92.
- Wong GY, Bradlow L, Sepkovic D, Mehl S, Mailman J, Osborne MP. Dose-ranging study of indole-3-carbinol for breast cancer prevention. *J Cell Biochem Suppl* 1997; 28-29: 111-6.
- Wright AE, Forleo DA, Gunawardana GP, Gunasekera SP, Koehn FE, McConnell OJ. Antitumour tetrahydroisoquinoline alkaloids from the colonial ascidian *Ecteinascidia turbinata*. *J Org Chem* 1990; 55: 4508-12.
- Yarbro JW, Kennedy BJ. A comparison of the rate of recovery from inhibition of RNA synthesis in mouse liver and transplantable glioma. *Cancer Res* 1967; 27: 1779-82.
- Yasumori T, Chen L, Nagata K, Yamazoe Y, Kato R. Species differences in stereoselective metabolism of mephenytoin by cytochrome P450 (CYP2C and CYP3A). *J Pharmacol Exp Ther* 1993; 264: 89-94.
- Yi JR, Lu S, Fernandez-Checa J, Kaplowitz N. Expression cloning of the cDNA for a polypeptide associated with rat hepatic sinusoidal reduced glutathione transport: characteristics and comparison with the canalicular transporter. *Proc Natl Acad Sci USA* 1995; 92: 1495-9.
- Yovine A, Riofrio M, Brain E. Ecteinascidin-743 given as 24 hour intravenous continuous infusion (IVCI) every 3 weeks: results of a Phase II trial in patients (PTS) with pretreated soft tissue sarcoma (PSTS). *Proc Am Soc Clin Oncol* 2001; 20: 363a.
- Zepek L, Yovine A, Brain E, Turpin F, Taamma A, Riofrio M, et al. Preliminary results of phase II study of ecteinascidin-743(ET-743) with the 24 hour (H) continuous infusion (CI)q3 weeks schedule in pretreated advanced/metastatic breast cancer (A/MBC) patients (Pts). *Proceedings of the 11th NCI-EORTC-AACR Symposium on New Drugs in Cancer Therapy*. Amsterdam, The Netherlands 2000: 85a.
- Zewail-Foote M, Hurley LH. Ecteinascidin 743: a minor groove alkylator that bends DNA toward the major groove. *J Med Chem* 1999; 42: 2493-7.
- Zewail-Foote M, Li VS, Kohn H, Bearss D, Guzman M, Hurley LH. The inefficiency of incisions of ecteinascidin 743-DNA adducts by the UvrABC nuclease and the unique

Bibliography

structural feature of the DNA adducts can be used to explain the repair-dependent toxicities of this antitumor agent. *Chem Biol* 2001; 8: 1033-49.

Zimmerman HJ. Drug-induced liver disease. *Drugs* 1978; 16: 25-45.

Zimmerman HJ. Hepatotoxicity. *Dis Mon* 1993; 39: 675-787.

Zimmerman HJ, Ishak KG. General aspects of drug-induced liver disease. *Gastroenterol Clin North Am* 1995; 24: 739-57.

Zimmerman HJ, Lewis JH. Drug-induced cholestasis. *Med Toxicol* 1987; 2: 112-60.

APPENDIX

Publications

Papers

Donald S, Verschoyle RD, Edwards R, Judah DJ, Davies R, Riley J, Dinsdale D, Lopez-Lazaro L, Smith AG, Gant TW, Greaves P, Gescher AJ. Hepatobiliary damage and changes in hepatic gene expression caused by the antitumor drug ecteinascidin-743 (ET-743) in the female rat. *Cancer Res* 2002 62 (15): 4256-4262

Donald S, Verschoyle RD, Greaves P, Gant TW, Colombo T, Zaffaroni M, Frapolli R, Zucchetti M, D'Incalci M, Meco D, Riccardi R, Lopez-Lazaro L, Jimeno J, Gescher AJ. Complete protection by high-dose dexamethasone against the hepatotoxicity of the novel antitumor drug Yondelis (ET-743) in the rat. *Cancer Res*, submitted

Donald S, Verschoyle RD, Greaves P, Orr S, Lopez-Lazaro L, Jimeno J, Gescher AJ. Comparison of four modulators drug metabolisms protectants against the hepatotoxicity of the novel antitumor drug Yondelis (ET-743) in the female rat and in hepatocytes *in vitro*. *Biochem Pharmacol*, submitted.

Abstracts

Donald S, Verschoyle R, Greaves P, Colombo T, Frapolli R, D'Incalci M, Lopez-Lazaro L, Gescher AJ. Modulation of the hepatotoxicity of Ecteinascidin 743 (ET-743) in the rat. *Clin Cancer Research* 2001 7 (11): 271 Suppl.

Donald S, Verschoyle R, Gant T, Greaves P, Colombo T, Frapolli R, D'Incalci M, Lopez-Lazaro L, Gescher AJ. High-dose dexamethasone (dex) protects against the hepatotoxicity of yondelis (ET-743) in the rat. *European journal of cancer* 38: Suppl 7. 2002.

Hepatobiliary Damage and Changes in Hepatic Gene Expression Caused by the Antitumor Drug Ecteinascidin-743 (ET-743) in the Female Rat¹

Sarah Donald, Richard D. Verschoyle, Richard Edwards, David J. Judah, Reginald Davies, Joan Riley, David Dinsdale, Luis Lopez Lazaro, Andrew G. Smith, Timothy W. Gant, Peter Greaves, and Andreas J. Gescher²

Department of Oncology [S. D., R. D. V., A. J. G.] and Medical Research Council Toxicology Unit [R. E., D. J. J., R. D., J. R., D. D., A. G. S., T. W. G., P. G.], University of Leicester, Leicester LE1 9HN, United Kingdom, and PharmaMar SA, 28760 Tres Cantos, Madrid, Spain [L. L.]

ABSTRACT

Ecteinascidin-743 (ET-743) is a novel marine-derived anticancer drug with clinical activity in soft tissue sarcoma and ovarian cancer. Reversible transaminitis and subclinical cholangitis have frequently been described in patients who receive ET-743. To facilitate understanding of this adverse effect and help design suitable therapeutic rescue strategies, we characterized the hepatic effects of ET-743 in rats. Female rats received ET-743 (single dose, 40 $\mu\text{g}/\text{kg}$) i.v., and liver changes were assessed from 6 h up to 3 months after dosing by histopathology, immunohistochemistry, electron microscopy, hepatic and plasma biochemistry, and DNA microarray analysis. At 24 h posttreatment and beyond, livers displayed degeneration and patchy focal necrosis of bile duct epithelial cells associated with mild inflammation followed by fibrosis. Sporadic and focal zones of hepatic necrosis and hemorrhage were observed from day 2 onward, although the majority of hepatocytes appeared normal as judged by electron microscopy. Pathological alterations persisted up to 3 months after dosing. Plasma levels of total bilirubin were elevated up to 7-fold over those in untreated rats from day 2 onward and returned to control values by day 24. Activities of alkaline phosphatase and aspartate aminotransferase in plasma were elevated for 2 and 3 months, respectively. Activities of the hepatic microsomal drug-metabolizing enzymes cytochrome P-450 A1/2, CYP2E1, and CYP3A2 were decreased. DNA microarray analysis of livers from ET-743-treated animals showed a dramatic increase in the expression of ATP binding cassette transport genes *Abcb1a* and *Abcb1b*, which impart resistance to anticancer drugs, and of *Cdc2a* and *Ccnd1*, the rodent homologues of human cell cycle genes *CDC2* and *cyclin D1*, respectively. The cell cycle gene expression changes mirrored ET-743-induced increases in liver weight and Ki-67 labeling of liver nuclei. The results suggest that the toxicity exerted by ET-743 in the rat liver is a consequence of biliary rather than hepatocellular damage and that it is accompanied by a wave of mitogenic activity, which may be driven by the transcriptional increase in *Cdc2a* expression.

INTRODUCTION

Ecteinascidin 743 (ET-743) is a tetrahydroisoquinoline alkaloid isolated from the marine tunicate *Ecteinascidia turbinata* that possesses potent antineoplastic activity against a variety of human tumor xenografts grown in athymic mice *in vivo*, including melanoma and ovarian and breast carcinoma (1–3). In clinical Phase I studies of ET-743, promising responses were observed in patients with sarcoma and breast and ovarian carcinoma (4–7). The drug is currently under investigation in Phase II trials in cancer patients with a variety of neoplastic diseases. Patients who received ET-743 by prolonged infusions over 24–72 h experienced myelosuppression and frequently acute (but reversible) transaminitis and subclinical cholangitis char-

acterized by increases in ALP³ and/or bilirubin. Preclinical acute toxicity studies conducted in mice, rats, dogs, and monkeys demonstrated liver toxicity as an important side effect of ET-743, as evidenced by an increase in plasma levels of liver-specific enzymes and pathological manifestations of cholangitis (8). In these studies, the female rat was identified as the species with the highest susceptibility to the hepatotoxic potential of ET-743 and showed treatment-related blood chemistry alterations not unlike those accompanying hepatotoxicity seen in the clinical trials of ET-743 (4–7).

The mechanism of antineoplastic action of ET-743 is not yet fully understood, and the mechanisms responsible for its hepatotoxic potential are unknown. The drug has been shown to bind to the minor groove of DNA and alkylate the N2 position of guanine at specific sequences (9). At pharmacologically active concentrations, ET-743 caused perturbations of the cell cycle with a decrease in the rate of progression of S-phase cells toward G₂ and a prolonged blockade in G₂-M (10). The drug inhibited the binding of several transcription factors to DNA (11–13), prominent among them nuclear factor Y (12, 13), which activates transcription of some cell cycle genes. Therefore, the perturbations of the cell cycle machinery exerted by ET-43 may be caused, at least in part, by its ability to inhibit nuclear factor Y transactivation. Cells deficient in nucleotide excision repair ability were resistant to the cytotoxic potential of ET-743 (14), a finding that suggests that the mode of cytotoxicity of ET-743 is distinctly different from that of other DNA-interactive cytotoxicants.

Taken together, these results characterize ET-743 as a new drug with anticancer activity and a novel, albeit still somewhat obscure, mechanism of antineoplastic activity. In light of the paucity of information available on details of its hepatotoxic potential, we investigated its hepatotoxicity *in vivo* in the female rat, the rodent species that seems to be most sensitive to this adverse effect of ET-743, by detailed analysis of ET-743-induced changes in liver pathology, biochemistry, and accompanying gene expression profiles. The overall aim of the study was to increase our understanding of the hepatotoxicity of ET-743 and identify biological events underlying the observed hepatic alterations that may ultimately be exploited by novel therapeutic regimens or drug combinations designed to alleviate this adverse effect.

MATERIALS AND METHODS

Animals and Treatments. ET-743 was obtained from PharmaMar SA (Madrid, Spain), the drug manufacturer. Experiments were conducted as stipulated by Project License 80/1250 granted to the MRC Toxicology Unit by the United Kingdom Home Office. Groups of four female Wistar rats (230–260 g) received either a single dose of ET-743 (40 $\mu\text{g}/\text{kg}$) i.v. or the vehicle (water) via the lateral tail vein. In a preliminary dose-finding orientation experiment, ET-743 administered at 75 $\mu\text{g}/\text{kg}$, the maximum tolerated dose in the female rat, elicited severe toxicity, resulting in mortality. Therefore the dose was reduced to 40 $\mu\text{g}/\text{kg}$, which caused toxicity but avoided mortality. This dose is close to 1500 $\mu\text{g}/\text{m}^2$ (approximately 38 $\mu\text{g}/\text{kg}$), the dose recommended to be

Received 1/24/02; accepted 5/24/02.

The costs of publication of this article were defrayed in part by the payment of page charges. This article must therefore be hereby marked *advertisement* in accordance with 18 U.S.C. Section 1734 solely to indicate this fact.

¹ Supported in part by Medical Research Council Toxicology Unit core grant funding and a grant from PharmaMar SA (Madrid, Spain).

² To whom requests for reprints should be addressed, at Medical Research Council Toxicology Unit, University of Leicester, Leicester LE1 9HN, United Kingdom. Phone: 44-116-252-5618; Fax: 44-116-252-5616; E-mail: ag15@le.ac.uk.

³ The abbreviations used are: ALP, alkaline phosphatase; AST, aspartate aminotransferase; MRC, Medical Research Council; CYP, cytochrome P-450; ABC, ATP binding cassette.

infused in Phase II studies in patients (5). Animals were killed 6, 12, or 24 h; 2, 3, 6, 12, 24, or 48 days; or 3 months after administration. Blood was obtained by cardiac puncture, and blood cells were separated from plasma by centrifugation. Slices of liver were excised and fixed in buffered formalin (10%). The remaining liver tissue was homogenized in ice-cold 50 mM Tris-KCl buffer containing 0.25 M sucrose (pH 7.4). For isolation of liver microsomes, the homogenate was centrifuged (10,000 × g, 20 min, 4°C), and the supernatant was then removed and spun at 100,000 × g for 60 min at 4°C (15). The microsomal pellet was resuspended in fresh buffer and recentrifuged (100,000 × g) for an additional 60 min. The resulting pellet was suspended in 0.25 M phosphate buffer containing 30% glycerol, stored at -80°C, and thawed before analysis. The Bradford assay was used to determine protein concentration.

Selected tissues other than liver (including stomach, small intestine, thymus, spleen, heart, lungs, kidneys, and bone marrow) from rats killed at periods of up to 3 days after treatment were taken for histological examination.

Histopathology and Immunocytochemistry. Tissues were fixed in neutral buffered formalin and embedded in paraffin wax. Sternum samples were decalcified for examination of bone marrow cellularity. Sections (5-μm thick) were cut and stained with H&E. Selected hepatic sections were stained with van Gieson's stain for collagen.

Ki-67 was demonstrated in sections of formalin-fixed, paraffin wax-embedded liver tissue at all time points between 6 h and 12 days after dosing. Sections were dewaxed in xylene, immersed in water, and microwaved in citrate buffer (pH 6.0) for 30 min at 700 W. A primary polyclonal rabbit antibody to a 1086-bp Ki-67 motif-containing cDNA fragment (NCL-Ki67p; Novocastra) was applied at a dilution of 1:500 for 3 h at room temperature. Normal rabbit immunoglobulin (X0903; DAKO) was used as a negative control. The primary antibody was detected with the DAKO Duet System (K0492; DAKO). Positive nuclei were visualized using 3,3'-diaminobenzidine tetrahydrochloride, and sections were lightly counterstained with hematoxylin. The total number of nuclei/unit area was calculated by counting the number of nuclei in a rectangular frame (0.32 × 0.225 mm) using the ×40 Diaplan microscope objective on the H&E-stained sections, and counting was repeated in 10 randomly chosen frames. The proliferation index was calculated as the number of Ki-67-stained nuclei/1000 hepatocyte nuclei.

The presence of α-smooth muscle actin was demonstrated using a mouse monoclonal antibody (clone 1A4, IgG2a, DAKO M 0851) against the NH₂-terminal decapeptide of human α-smooth muscle actin. Sections were pretreated as described above, and the primary antibody was applied at a dilution of 1:100 for 3 h at room temperature. Mouse IgG2a-negative control antibody (X0943; DAKO) was used as control. The primary antibody was detected as described above. The peroxidase label was visualized using the VIP substrate kit (SK-4600; Vector Laboratories) followed by a light hematoxylin counterstain.

Electron Microscopy. Livers were fixed by vascular perfusion with 2% glutaraldehyde in 0.1 M sodium cacodylate buffer (pH 7.4) and stored overnight (4°C) in the fixative. Slices (<1-mm thick) were postfixed with 1% osmium tetroxide/1% potassium ferrocyanide, stained *en bloc* with 5% uranyl acetate, and embedded in Taab epoxy resin (Taab Ltd.). Ultrathin sections were examined unstained or after staining with lead citrate and/or uranyl acetate.

Measurement of Liver Enzymes, Bilirubin, and Cytochrome P450 Isoenzymes, and Cell Cycle Distribution. Plasma levels of ALP, AST, and total plasma bilirubin were measured using commercially available kits and established protocols (Sigma, St. Louis, MO). Total microsomal cytochrome P450 protein content was determined by the method of Adams *et al.* (15), and activities of liver microsomal enzymes associated with cytochrome P450 isoforms CYP1A1/2, CYP2E1, and CYP3A2 were measured according to Burke *et al.* (16), Carlson (17), and Chang and Yeung (18) using ethoxyresorufin, 4-nitrophenol, and 7-benzyloxy-4-trifluoromethylcoumarin, respectively, as substrates.

Cell cycle analysis on liver nuclei from control and ET-743-treated rats was performed as described previously using fluorescence-assisted cell-sorting scan (19).

Microarray Studies. In a separate study, female Wistar rats were treated as described above with ET-743, and the liver of each treated rat was paired with liver from an age-matched vehicle-treated control rat. Groups of three ET-743-treated rats paired with three untreated rats were killed 6 h and 1, 2, 3, 6, and 24 days after dosing. Analysis of hepatic gene expression was carried out using

cDNA microarrays containing approximately 4700 hybridizable mouse expressed sequence tags derived from IMAGE clones obtained from Research Genetics (Huntsville, AL) or from the MRC Human Gene Mapping Project.⁴ At each time point, one array was used for each pair of rats, and the individual RNAs were labeled with Cy3 or Cy5. The labels were reversed for subsequent hybridizations. Microarray preparation, RNA labeling, and hybridization were performed as described previously by Turton *et al.* (20). The clones of interest were sequenced to confirm identity. Where differential expression was determined, sequence homology with the appropriate rat gene was assessed to confirm that cross-hybridization between the species could occur. Pixel intensity for both the features and the background was assessed using GenePix software (Axon Instruments, Union City, CA) version 3.0.6 and an Axon 4000A scanner. The data were normalized and processed to a final measure of differential gene expression, quantitated as a ratio of ET-743-treated:control, as described previously (20), using ConvertData version 3.4.0c.⁵ Clustering analysis was performed by determination of the principal components of the score data (20) using SIMCA-P (Umetrics, Bracknell, United Kingdom). The expression of genes that were significantly altered with reference to all of the other genes on the same array were used for a principal components analysis. Each microarray was kept as a separate entity for this analysis, as were the replicated clones on the microarrays. For the hepatic genes, the expression of which was consistently up- or down-regulated by ET-743 (*Cdc2a*, *Ccnd1*, *Abcb1a*, *Abcb1b*, and *Car 3*, see "Results"), homology between the mouse and the rat was established to be 98% or greater. Data supplementing the microarray results shown in Figs. 4 and 5 are contained on the World Wide Web.⁵

Statistical Analysis. Significance of differences was assessed using one-way ANOVA followed by Tukey's *post hoc* test.

RESULTS

Effect of ET-743 on Liver Pathology. To study liver changes induced by ET-743, female rats received a single dose of ET-743 (40 μg/kg) i.v. Within 4–6 days after dosing, animals lost 15% of their body weight, compared with controls. Whereas livers obtained 6 and 12 h after ET-743 administration did not show signs of pathological change, the epithelial cells lining the larger bile ducts in some animals displayed focal degenerative alterations at 24 h after treatment. By days 2 and 3, these changes involved many bile ducts in all treated animals. Livers were characterized by degeneration and patchy focal necrosis of bile duct epithelial cells associated with a modest acute inflammatory infiltrate on day 2 and thereafter (Fig. 1, A and B). A day later, these alterations were more pronounced and accompanied by increased inflammation (Fig. 1C) and early signs of regeneration of the epithelial cells characterized by enlarged cell cytoplasm and large irregular nuclei with occasional mitoses. Six and 12 days after treatment with ET-743, bile ducts were surrounded by dense, poorly cellular, concentric fibrosis (sclerosis) (Fig. 1E) and by mesenchymal cells that stained for α smooth muscle actin (Fig. 1F). After 24, 48, and 92 days, the inflammation in the portal tract had diminished substantially, although periductal fibrosis remained prominent (Fig. 1G). Blood vessels appeared histologically within normal limits. In some treated rats, rounded focal zones of hepatic necrosis and hemorrhage were observed from day 2 onward, with little or no inflammation (Fig. 1D). These alterations persisted up to 3 months. Some focal pigmentation was seen around zones of necrosis at time points >24 h after administration of ET-743. Apart from these foci of necrosis, most hepatocytes showed relatively little alteration on light microscopic examination, except that mitotic activity was evident 3 days after treatment.

Electron microscopy showed that within 2 days after administration of ET-743, there was focal injury including some apoptosis in the epithelium of bile ducts, often resulting in the liberation of

⁴ <http://www.htgmp.mrc.ac.uk>.

⁵ http://www.le.ac.uk/cmht/microarray_lab/Home.

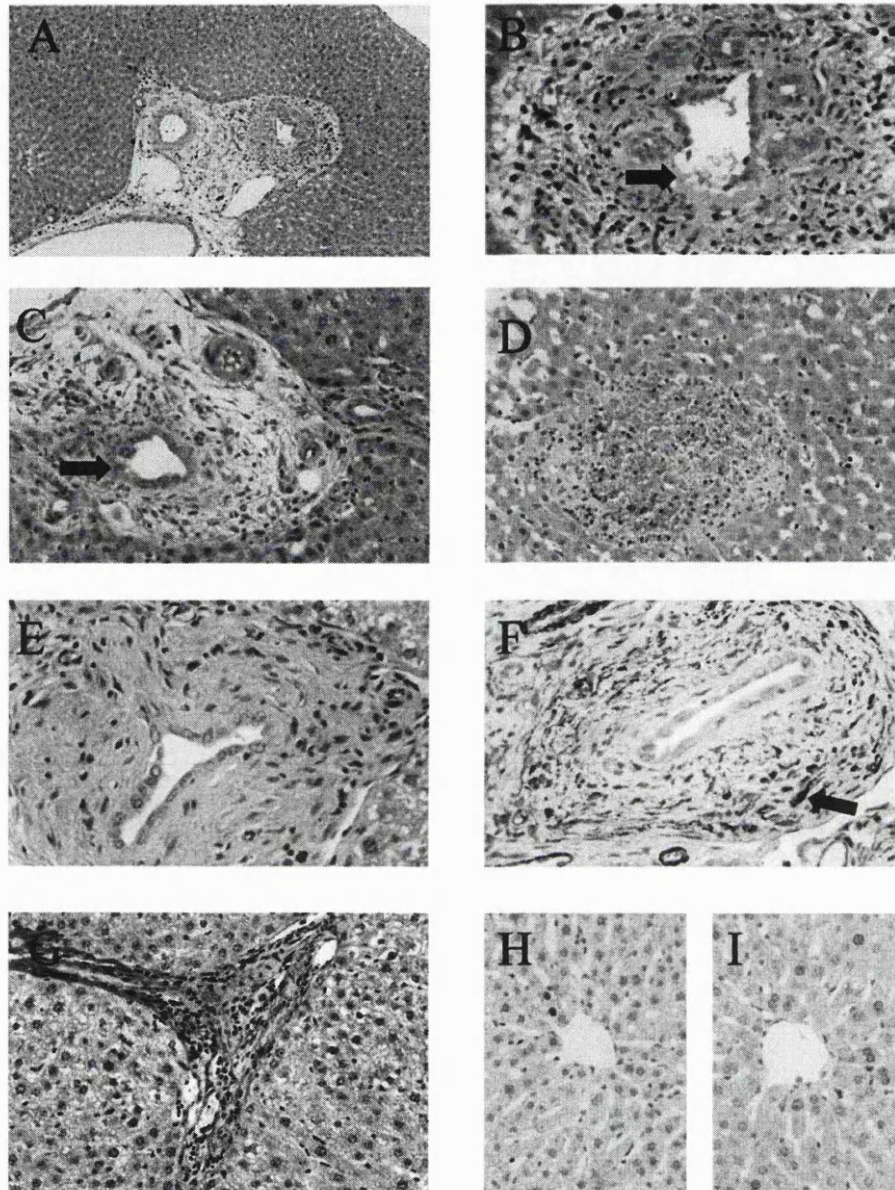


Fig. 1. Liver sections from female rats that received ET-743 (40 $\mu\text{g}/\text{kg}$, i.v.) 2 (A, B, and D), 3 (C and E), 12 (E and F), or 48 days (G) before tissue excision and liver sections from an untreated rat (H). Staining was by H&E (A–E), immunoperoxidase for α -smooth muscle actin (F), van Gieson's stain (G), or Ki-67 antiserum (H and I). Magnification was $\times 50$ in A; $\times 130$ in C, D, G, H, and I; and $\times 200$ in B, E, and F. The following features characterize manifestations of ET-743 hepatotoxicity: swelling of the portal tract with little alteration in the hepatic parenchyma (A); ulceration of the bile duct epithelium (arrow) and sparse inflammatory infiltrate (B); damage to the bile duct epithelium (arrow) and mild hyperplasia (C); round focus of hemorrhagic necrosis (D); peribiliary fibrosis and enlarged biliary epithelial cells (E); spindle cells staining for α -smooth muscle actin (for example, see arrow in F); presence of dense residual collagen in the portal tract marked by red staining (G); and increased staining of nuclei for Ki-67 antigen (H and I). The sections are representative of four to eight separate animals. For details of histopathology and immunohistochemistry, see "Materials and Methods."

cell debris into the lumen (Fig. 2A). Most of the liver remained largely normal. The foci of hepatic necrosis (oncosis) and hemorrhage did not correlate with particular regions of the lobule. The tight junctions isolating bile canaliculi, even between severely damaged cells, were usually intact. Despite the presence of numerous erythrocytes within these foci, there was little or no inflammation. Abnormal mitochondria were evident in many necrotic cells and probably represented a phenomenon secondary to the necrosis. Hepatocytes immediately surrounding the focal lesions tended to have rather more smooth endoplasmic reticulum than controls, and it was dispersed throughout the cytoplasm rather than aggregated in large clumps (Fig. 2B). Apparently normal hepatocytes were immediately adjacent to affected cells. Venous endothelial cells were often distended in affected zones, which did not seem to be a primary injury because intact endothelial cells were present overlying oncotic hepatocytes. The endothelial lining of sinusoids was largely undamaged, but some sinusoids were blocked by erythrocytes, neutrophils, platelets, and luminal fibrin.

As far as ET-743-induced extrahepatic damage is concerned, there was a degenerative change in the small intestine to cells deep within the intestinal crypts as early as 6 h after treatment. This degeneration was visible up to 24 h but had disappeared by day 3. Pancreatic ducts in the head of pancreas were not systematically sectioned, but in sections in which they were visible, their appearance was entirely normal. There was also mild loss in cellularity of bone marrow at 12, 24, and 72 h. The thymus tissue examined showed little or no definite evidence of loss in cellularity, and the appearance of the other organs investigated was within normal limits.

In an orientation experiment, male rats were investigated instead of females. In male rats, 40 $\mu\text{g}/\text{kg}$ ET-743, the dose that had elicited the changes described above in female animals, caused only slightly irregular bile duct epithelia and sparse degenerate biliary cells 3 days after dosing and additional mild peribiliary fibrosis at day 12. Nevertheless, 80 $\mu\text{g}/\text{kg}$ ET-743 was profoundly toxic in male rats and caused changes to bile ducts and necrosis in liver cells that mimicked

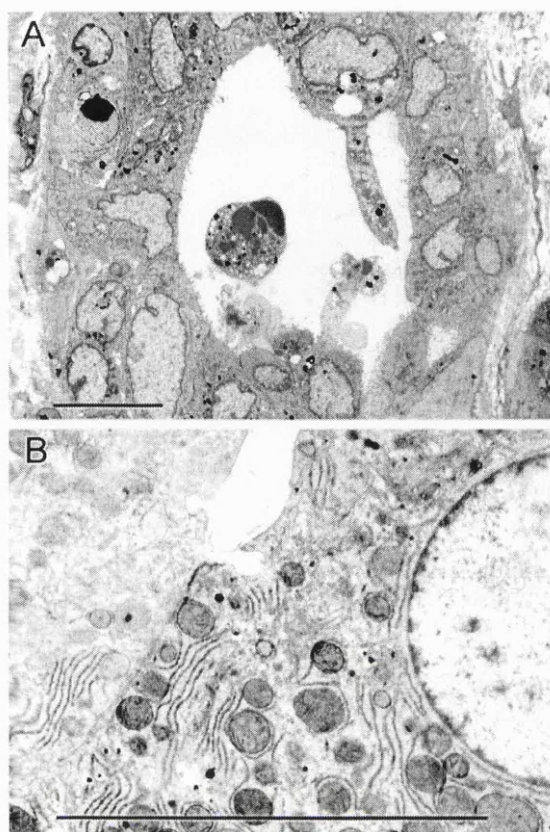


Fig. 2. Electron micrographs of (A) a bile duct and (B) a typical hepatocyte observed in female rats 2 days after treatment with ET-743 (40 $\mu\text{g}/\text{kg}$, i.v.). In A, note focal injury, including some apoptosis, to bile duct epithelium with liberation of some cell debris into the lumen. The hepatocyte in B, which was found near a zone of necrosis, displays slightly more smooth endoplasmic reticulum than hepatocytes in control animals but is otherwise essentially within normal limits. Bars, 10 μm . The micrographs are representative of four separate animals. For details of electron microscopy, see "Materials and Methods."

in character and extent the liver pathology observed in female rats after administration of 40 $\mu\text{g}/\text{kg}$ ET-743.

Effect of ET-743 on Liver Biochemistry. Plasma levels of total bilirubin started to increase >24 h after female rats had received ET-743, and at 3 days, levels were elevated 7-fold over controls (Fig. 3A). This elevation persisted until at least 12 days and returned to basal levels by day 24. Levels of liver enzymes ALP and AST were significantly raised from 48 h after administration of ET-743 onward (Fig. 3A). Maximal elevation of ALP and AST levels was approximately 2-fold over control levels by day 3, and the rise in AST activity persisted up to 3 months after administration, the furthest time point examined. In male rats, plasma levels of bilirubin, ALP, and AST were not affected by the dose of ET-743 (40 $\mu\text{g}/\text{kg}$) that elicited marked elevation in females. However 80 $\mu\text{g}/\text{kg}$ ET-743 increased the biochemical markers of hepatotoxicity in male rats as dramatically as seen with the lower dose in females.

ET-743 also affected the activities of hepatic microsomal drug-metabolizing cytochrome P450 enzymes (Fig. 3). Activities of CYP3A2, CYP1A1/2, and CYP2E1 were investigated in female rats because these enzymes have been implicated in ET-743 metabolism (21). Levels of the latter two were dramatically decreased to almost unmeasurable levels 3 days after administration and returned to control values within 12–24 days. The activity of CYP3A2 was decreased by up to 37% at day 3 after administration, and this decrease persisted for up to 12 days. Levels of total microsomal cytochrome P450 protein were diminished by 33% after 3 days.

Effect of ET-743 on Hepatic Gene Expression. Gene expression profiles were analyzed using one microarray for each of the three pairs of female rats per time point. A cluster of genes was consistently down-regulated, and this cluster included the cytochrome P450 genes *Cyp1a2*, *Cyp3a11*, and *Cyp3a13*, mirroring the down-regulation in activity of CYP1A1/2, CYP3A2, and CYP2E1 (see Fig. 3), and *Car3*, which codes for carbonic anhydrase 3. *Car3* expression levels reached a nadir on day 6 after administration of ET-743 (data not shown), past the time point of maximal biochemical manifestation of hepatic damage, which was day 3. Among the cluster of overexpressed genes were the cell cycle genes *Cdc2a* and *Ccnd1* (Fig. 4A); the rodent homologues of human *CDC2* and *cyclin D1*, respectively; and the two ABC transport genes *Abcb1a* and *Abcb1b*, which are equivalent to human *ABCB1* and impart drug resistance. The time course of expression of *Abcb1a* and *Abcb1b* (Fig. 5) mirrors the changes in serum bilirubin

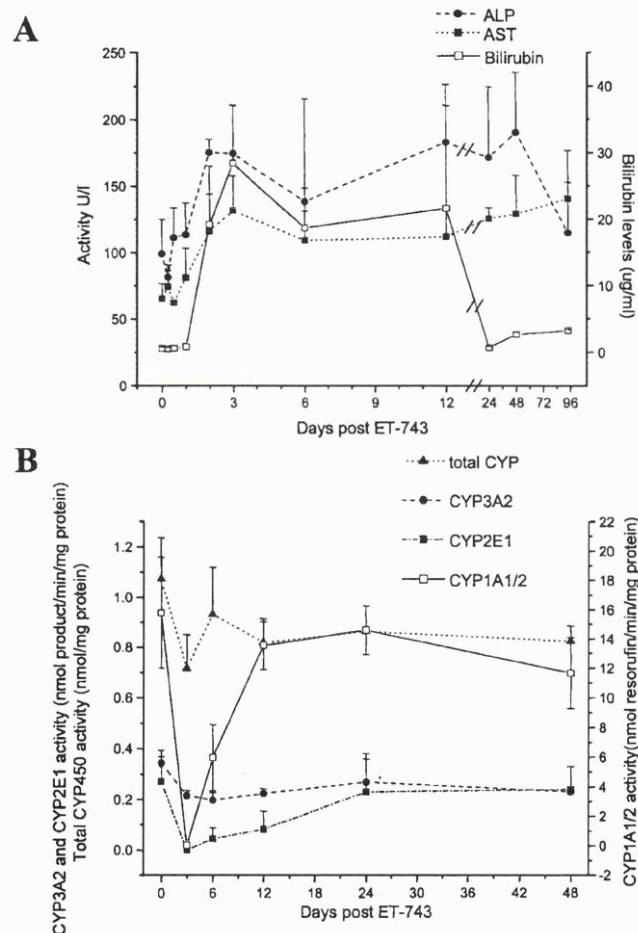


Fig. 3. Time course of changes in concentration of total bilirubin and activities of liver enzymes ALP and AST in the plasma (A) and of cytochrome P450 protein levels and activities of CYP1A1/2, CYP2E1, and CYP3A2 in liver microsomes (B) obtained from female rats that received ET-743 (40 $\mu\text{g}/\text{kg}$, i.v.). In A, levels of bilirubin (\square) are presented in $\mu\text{g}/\text{ml}$ (right axis), and activities of ALP (\bullet) and AST (\blacksquare) are given as units/liter (left axis). Concentrations in B are expressed as nmol cytochrome P450 protein/mg microsomal protein (\blacktriangle , left axis) or as nmol product of one of the following substrates generated/min/mg microsomal protein: 7-benzoyloxy-4-trifluoromethyl coumarin (CYP3A2, \bullet , left axis); 4-nitrophenol (CYP2E1, \blacksquare , left axis); or ethoxresorufin (CYP1A1/2, \square , right axis). Note that the abscissa in A is not linear with time beyond the 12 h time point. Values are the mean \pm SD of 4 animals/time point. The values observed at the following time points are significantly different ($P < 0.05$) from those measured in control rats: bilirubin, days 3, 6, and 12; ALP, days 2, 3, 12, 24, and 48; AST, days 2, 3, 12, 24, 48, and 96; total cytochrome P450, day 3 only; CYP3A2 and CYP2E1, days 3, 6, and 12; and CYP1A1/2, days 3 and 6. For details of measurement of bilirubin levels and enzyme activities, see "Materials and Methods."

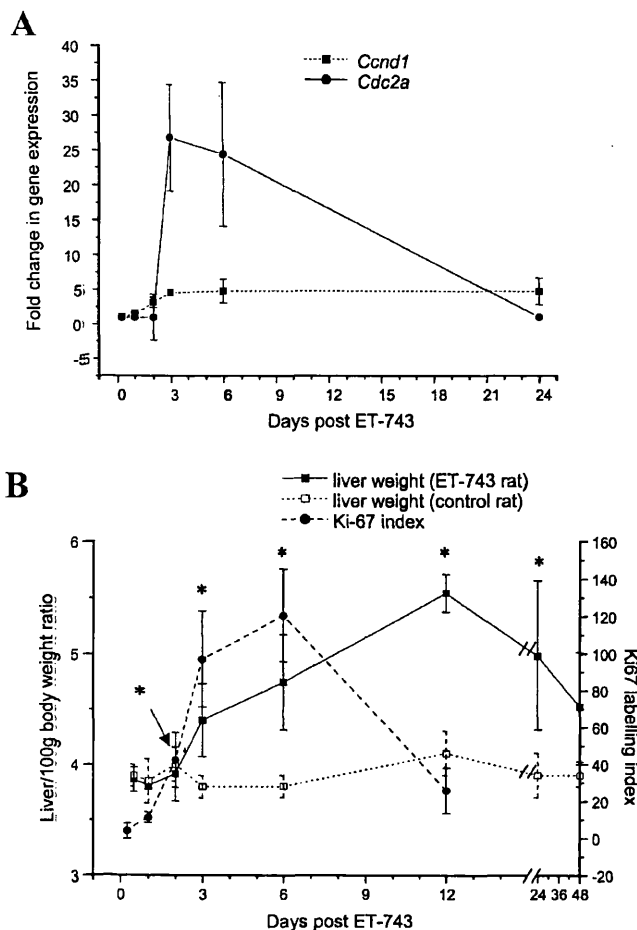


Fig. 4. Time course of changes (A) in hepatic expression of *Cdc2a* (●) and *Cnd1* genes (■), and (B) in liver weight (■, left axis) and Ki-67 labeling of hepatic nuclei (●, right axis) in female rats that had received ET-743 (40 $\mu\text{g}/\text{kg}$, i.v.). Changes in liver weight of control rats are also shown (□, left axis). Gene expression patterns (A) were determined by cDNA microarray. The normalized intensity values from the hybridization of the RNA from treated rats at the 3 and 6 day time points for both genes and the 24 day point for *Cnd1* were significantly different ($P < 0.05$) from the values of control rat RNA hybridized on the same microarray. The SDs reflect the variability in the measure of the ratio of treated:control rats. Liver weight values (B) are expressed as the ratio of liver weight (in grams) at the time point: 100 g of the pretreatment body weight of the respective animal. Nuclei were stained with Ki-67 antiserum, and Ki-67 labeling index (B) denotes the number of stained nuclei/1000 hepatocyte nuclei. Note that the abscissa in B is not linear with time beyond the 12 h time point. Values are the mean \pm SD of 4 rats/time point, asterisks indicate that values are significantly different from those of the corresponding controls ($P < 0.05$). For details of DNA microarray analysis and Ki-67 labeling, see "Materials and Methods."

concentration (Fig. 3). The expression of none of the other 45 ABC genes among the expressed sequence tags on the microarray was altered by ET-743. ABC genes unaffected by ET-743 include *Abcb4* (Fig. 5), which is implicated in phospholipid excretion.

Effect of ET-743 on Indices of Hepatic Cell Proliferation. The increase in hepatic expression of *Cdc2a* determined by DNA microarray peaked on day 3 after administration of ET-743. It remained elevated through at least day 6 and returned to basal levels on day 24 (Fig. 4A). *Cnd1* expression followed a similar pattern, except that the elevation was smaller and maintained through day 24 (Fig. 4A). The *Cdc2a* gene expression changes were similar to ET-743-induced changes in hepatic Ki-67 proliferation index. The peak in Ki-67 proliferation and *Cdc2a* expression occurred at 6 days and 9 days, respectively, before the peak in liver weight (Fig. 4B). Staining for Ki-67, a marker of DNA synthesis, in liver nuclei of animals that had

received ET-743 was significantly elevated in comparison with that in control rats (Fig. 1, H and I, and Fig. 4B). Similar to the results shown here for Ki-67 (Fig. 1, H and I), staining for proliferating cell nuclear antigen was substantially elevated in ET-743-treated rats 3 days after dosing compared with control animals (data not shown). The weight of livers of ET-743-treated animals increased from day 2 after dosing onward and reached a zenith on day 12 (Fig. 4B). Furthermore, consistent with an ET-743-mediated increase in hepatocyte cycle activity, liver cell cycle distribution underwent significant, albeit subtle, alteration by ET-743. The proportion of S-phase hepatocytes increased from 0% in control rats to $7.3 \pm 1.5\%$ (mean \pm SD; $n = 4$) in rats 3 days after administration of ET-743, whereas the number of hepatocytes in G_1 and G_2 -M, respectively, amounted to $62.6 \pm 7.2\%$ and $37.4 \pm 7.2\%$ in control animals and $61.0 \pm 5.2\%$ and $31.4 \pm 5.3\%$ in treated rats.

DISCUSSION

Various cancer chemotherapeutic agents are known to possess the potential to damage the liver (22). Methotrexate is a prominent example, which has been reported to cause steatosis and cirrhosis in patients (23). The results described above suggest that the novel anticancer drug ET-743 induces an unusual form of hepatotoxicity in rats, which differs from the adverse hepatic effects described for traditional cytotoxic drugs. In the female rat, a clinically relevant single i.v. dose of 40 $\mu\text{g}/\text{kg}$ ET-743 caused damage to bile duct epithelia followed by peribiliary fibrosis. Bile duct damage accompanied by inflammation and repair was first evident 24 h after dosing. In contrast, cytotoxic damage by ET-743 to the rapidly proliferating cells of the small intestine was observed by 6 h. Fibrosis around damaged bile ducts increased dramatically over the following week. The pathological alterations were accompanied by defects of liver function, as reflected by a dramatic elevation of plasma bilirubin levels, moderate increases in plasma levels of ALP and AST, a marker of cholestasis, and a decrease in activities of hepatic cytochrome P450 enzymes CYP3A2, CYP1A1/2, and CYP2E1. These observations are consistent with the notion that ET-743 induces biliary cholestasis, which in turn might elicit elevation in expression of the *Abcb1a* and *Abcb1b* genes as an adaptive response. This interpretation is based on the previous observation that expression of these genes was raised in cholestatic livers of rats and monkeys (24). In analogy, the down-

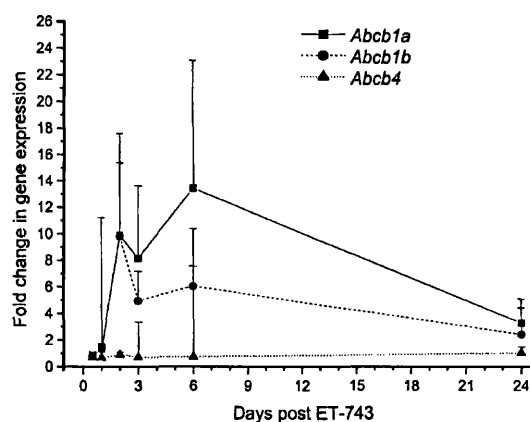


Fig. 5. Time course of changes in expression of ABC genes *Abcb1a* (■), *Abcb1b* (●), and *Abcb4* (▲) in livers of female rats that received ET-743 (40 $\mu\text{g}/\text{kg}$, i.v.). Gene expression was determined by cDNA microarray. For details, see "Materials and Methods." The normalized intensity values from the hybridization of the RNA from treated rats at the 2, 3, and 6 day time points for *Abcb1a* and *Abcb1b* were significantly different ($P < 0.05$) from the values of control rat RNA hybridized on the same microarray. The SDs indicate the variability in the measure of the ratio of treated:control rats.

regulation of expression of the *Car 3* gene described above may also be the consequence of hepatobiliary injury rather than a direct response to ET-743 proper because it has been shown to occur in the livers of rodents exposed to the hepatotoxicant griseofulvin.⁶

It is unknown whether the reduction in CYP3A2, CYP1A1/2, and CYP2E1 levels observed here in the rat also occurs in humans. If it did, it might be important in the planning of sequential combination chemotherapy involving ET-743 and drugs such as Taxol, which undergo cytochrome P450-mediated deactivation. The decrease in CYP activities, if it occurs in humans, probably does not impact the pharmacokinetics of the parent drug because ET-743 pharmacokinetics were unaltered when the drug was administered repeatedly via 24-h infusion (6).

Experiments in which ET-743 was incubated with isolated hepatocytes from rats or humans suggest that concentrations of the drug as high as 0.01–1 nmol/ml are required to damage hepatocytes directly (data not shown). In a preliminary study, hepatic drug levels in rats 6 h after i.v. administration of ET-743 (40 µg/kg) were just above 1 pmol/g tissue and declined thereafter.⁷ These results render it unlikely that concentrations of ET-743 required to elicit toxicity in isolated liver cells *in vitro* were achieved in liver tissue for time periods sufficient to explain the damage observed after administration of ET-743 *in vivo*. Instead, it is probable that manifestation of ET-743-mediated hepatic damage in the rat requires the structural integrity of the whole liver. This conclusion is consistent with the fact that the primary and most important lesion was found in the bile ducts. It is conceivable that drug accumulates in the bile duct, thus precipitating the primary lesion. This hypothesis needs experimental validation.

A prominent feature of the ET-743-induced hepatic toxicity described here is the persistence of the damage. Bile duct fibrosis and increased plasma levels of AST were observed as late as 3 months after administration, and levels of ALP were elevated for up to 2 months. In contrast, bilirubin remained elevated until some time between days 12 and 24. It remains to be investigated whether the long-term persistence of liver damage induced by ET-743 is related to continued harmful levels of a ET-743 metabolite in the liver. Nevertheless, it appears more likely that these delayed manifestations are late consequences of the initial bile duct damage and ensuing fibrosis. It is important to note that in contrast to the long persistence of elevation of AST and ALP in the female rat, transaminitis in patients in the Phase I trials of ET-743 was not dose limiting (4–7), and it had resolved before the subsequent course of drug was administered after a 3-week drug-free interval. This difference indicates that in relation to humans, the female rat model used in this study exaggerates some aspects of ET-743-induced hepatic lesions. Differences in susceptibility to ET-743-induced hepatotoxicity are also highlighted by the fact that the dose required to elicit damage in livers of male rats was twice as high as that which caused hepatic toxicity in female animals. This finding suggests that at comparable doses, male rats are less sensitive than female animals to the adverse effects of the drug. Nevertheless, qualitatively similar changes in pathology and biochemical marker levels were induced by the drug in animals of either gender. Concentrations of ET-743 that precipitate toxicity in the liver are as yet unknown. Therefore, it is conceivable that the observed gender difference in susceptibility reflects differences in liver exposure to ET-743, perhaps as a consequence of gender-related discrepancies in ability to metabolize the drug.

The most striking result of the DNA microarray analysis of hepatic gene expression precipitated by ET-743 is the increased expression of

the cell cycle genes *Cdc2a* and *Ccnd1*. The time course of change in expression of the *Cdc2a* gene resembles the time course of the ET-743-induced alterations in liver weight and Ki-67 labeling. These observations suggest that ET-743 elicits a mitogenic wave in the liver by induction of DNA synthesis, a proposition that is further supported by augmented staining of hepatic nuclei for proliferating cell nuclear antigen, the increased proportion of liver cells in S phase, and the prominent presence of mitotic figures in livers of animals that had received ET-743. To our knowledge, such stimulation of mitogenesis has hitherto not been observed as a generic mechanistic feature of hepatotoxic drugs. Therefore, it is unlikely to be a nonspecific compensatory reaction of the tissue to the ET-743-induced lesion. Instead the mitogenic wave seems to be a ET-743-specific phenomenon, and it is probably the corollary of a direct effect of ET-743 on hepatic *Cdc2a* transcription, which in turn drives the cell cycle. Whether or not patients exposed to ET-743 experience a similar mitogenic wave and increase in liver mass is not known and should be monitored in future studies.

In conclusion, the toxicity exerted by ET-743 in the rat liver is characterized by a primary insult to the bile duct epithelium, long duration of altered liver pathology, and enhanced liver cell proliferation involving up-regulation of the *Cdc2a* and *Ccnd1* genes. It has to be stressed that the animal model chosen here to study ET-743 hepatotoxicity, the female rat, seems among all species hitherto investigated to be most exquisitely sensitive to the hepatotoxic potential of ET-743. Other species including humans are less likely to experience the adverse effects described here. Nevertheless, manifestations of hepatotoxicity have been observed in the clinical evaluation of the drug, and therefore it is conceivable that some of the features of toxicity delineated here in the female rat are applicable to patients. These features may provide the basis for the design of treatment regimens designed to reduce the hepatotoxic potential of ET-743.

ACKNOWLEDGMENTS

We thank Jennifer Edwards and Lynda Wilkinson for the histological preparations and Judy McWilliam (all at the MRC Toxicology Unit) for electron microscopy.

REFERENCES

- Izbicka, E., Lawrence, R., Raymond, E., Eckhardt, G., Jimeno, J., Clark, G., and Von Hoff, D. D. *In vitro* antitumor activity of the novel marine agent ecteinascidin-743 (ET-743, NSC-648766) against human tumors explanted from patients. *Ann. Oncol.*, **9**: 981–987, 1998.
- Hendriks, H. R., Fiebig, H. H., Giavazzi, R., Langdon, S. P., Jimeno, J. M., and Faircloth, G. T. High antitumor activity of ET-743 against human tumour xenografts from melanoma, non-small cell lung cancer and ovarian cancer. *Ann. Oncol.*, **10**: 1233–1240, 1999.
- Valoti, G., Nicoletti, M. I., Pellegrino, A., Jimeno, J. M., Hendriks, H., D'Incalci, M., Faircloth, G., and Giavazzi, R. Ecteinascidin-743, a new marine product with potent antitumor activity on human ovarian carcinoma xenografts. *Clin. Cancer Res.*, **4**: 1977–1983, 1998.
- Tamma, A., Misset, J. L., Riosio, M., Guzman, C., Brain, E., Lopez-Lazaro, L., Rosing, H., Jimeno, J. M., and Cvitkovic, E. Phase I and pharmacokinetic study of ecteinascidin-743, a new marine compound, administered as a 24-hour continuous infusion in patients with solid tumors. *J. Clin. Oncol.*, **19**: 1256–1265, 2001.
- Delalage, S., Yovine, A., Tamma, A., Riosio, M., Brain, E., Raymond, E., Cottu, P., Goldwasser, F., Jimeno, J., Misset, J. L., Marty, M., and Cvitkovic, E. Ecteinascidin-743, a marine derived compound in advanced, pretreated sarcoma patients: preliminary evidence of activity. *J. Clin. Oncol.*, **19**: 1248–1255, 2001.
- Van Kesteren, C., Cvitkovic, E., Tamma, A., Lopez-Lazaro, L., Jimeno, J. M., Guzman, C., Mathot, R. A. A., Schellens, J. H. M., Misset, J. L., Brain, E., Hillebrand, M. J. X., Rosing, H., and Beijnen, J. H. Pharmacokinetics and pharmacodynamics of the novel marine-derived anticancer agent ecteinascidin 743 in a Phase I dose-finding study. *Clin. Cancer Res.*, **6**: 4725–4732, 2000.
- Ryan, D. P., Supko, J. G., Eder, J. P., Seiden, M. V., Demetri, G., Lynch, T. J., Fischman, A. J., Davis, J., Jimeno, J., and Clark, J. W. Phase I and pharmacokinetic study of ecteinascidin 743 administered as a 72-hour continuous intravenous infusion in patients with solid malignancies. *Clin. Cancer Res.*, **7**: 231–242, 2001.
- Mirsalis, J. C., Schindler-Horvat, J. E., Tomaszewski, J. E., Fairchild, D. G., Hill, J. R., Tyson, C. A., Schweikart, K. M., Turner, N. A., Sells, D., and Donohue, S. J.

⁶ T. W. Gant, P. R. Baus, B. Clothier, J. Riley, R. Davies, D. J. Judah, R. E. Edwards, J. A. Styles, E. George, P. Greaves, and A. G. Smith, unpublished observations.

⁷ H. Rosing and J. H. Beijnen, personal communication.

HEPATOTOXICITY OF ET-743

- Preclinical toxicology studies of ecteinascidin 743. *Proc. Am. Assoc. Cancer Res.*, *37*: 375, 1996.
9. Pommier, Y., Kohlhagen, G., Bailly, C., Waring, M., Mazumder, A., and Kohn, K. W. DNA sequence- and structure-selective alkylation of guanine N2 in the DNA minor groove: by ecteinascidin 743, a potent antitumor compound from the Caribbean tunicate *Ecteinascidia turbinata*. *Biochemistry*, *35*: 13303-13309, 1996.
 10. Takebayashi, Y., Goldwasser, F., Urasaki, Y., Kohlhagen, G., and Pommier, Y. Ecteinascidin-743 induces protein-linked DNA breaks in human colon carcinoma HCTT116 cells and is cytotoxic independently of topoisomerase I expression. *Clin. Cancer Res.*, *7*: 185-191, 2001.
 11. Jin, S., Gorfajn, B., Faircloth, G., and Scotto, K. W. Ecteinascidin 743, a transcription-targeted chemotherapeutic that inhibits MDR1 activation. *Proc. Natl. Acad. Sci. USA*, *97*: 6775-6779, 2000.
 12. Minuzzo, M., Marchini, S., Brogini, M., Faircloth, G., D'Incalci, M., and Mantovani, R. Interference of transcriptional activation by the antineoplastic drug ecteinascidin-743. *Proc. Natl. Acad. Sci. USA*, *97*: 6780-6784, 2000.
 13. Bonifanti, M., LaValle, E., Fernandez-Sousa-Faro, J. M., Faircloth, G., Caretti, G., Mantovani, R., and D'Incalci, M. Effect of ecteinascidin-743 on the interaction between DNA binding proteins and DNA. *Anticancer Drug Des.*, *14*: 179-186, 1999.
 14. Erba, E., Bergamaschi, D., Bassano, L., Darnia, G., Ronzoni, S., Faircloth, G. T., and D'Incalci, M. Ecteinascidin-743 (ET-743), a natural marine compound with a unique mechanism of action. *Eur. J. Cancer*, *37*: 97-105, 2001.
 15. Adams, D. J., Seilman, S., Ameliazad, Z., Oesch, F., and Wolf, C. R. Identification of human cytochrome P450 analogues to forms induced by phenobarbital and 3-methylcholanthrene in the rat. *Biochem. J.*, *232*: 869-876, 1985.
 16. Burke, M. D., Thompson, S., Elcombe, C. R., Halpert, J., Haaparanta, T., and Mayer, R. T. Ethoxy-, pentoxy- and benzyloxy-phenoxazones and homologues: a series of substrates to distinguish between different induced cytochromes P450. *Biochem. Pharmacol.*, *34*: 3337-3345, 1985.
 17. Carlson, G. P. Influence of ethanol on microsomal *p*-nitrophenol hydroxylation and ethoxyresorufin deethylation in rat liver and lung. *J. Toxicol. Environ. Health*, *32*: 153-159, 1991.
 18. Chang, T. K. H., and Yeung, R. K. Y. Effect of *trans*-resveratrol on 7-benzyloxy-4-trifluoromethylcoumarin *O*-dealkylation catalysed by human recombinant CYP3A4 and CYP3A5. *Can. J. Physiol. Pharmacol.*, *79*: 220-226, 2001.
 19. Ormerod, M. G. *Flow Cytometry: A Practical Approach*. Oxford, United Kingdom: IRL Press, 1990.
 20. Turton, N. J., Judah, D. J., Riley, J., Davies, R., Lipson, D., Styles, J. A., Smith, A. G., and Gant, T. W. Gene expression and amplification in breast carcinoma cells with intrinsic and acquired doxorubicin resistance. *Oncogene*, *20*: 1300-1306, 2001.
 21. Kuffel, M. J., Reid, J. M., and Ames, M. M. Cytochrome P450 catalyzed metabolism of ecteinascidin 743 by rat and human liver microsomes. *Proc. Am. Assoc. Cancer Res.*, *38*: 596, 1997.
 22. King, P. D., and Perry, M. C. Hepatotoxicity of chemotherapeutic and oncologic agents. *Gastroenterol. Clin. N. Am.*, *24*: 969-990, 1995.
 23. Reynolds, F. S., and Lee, W. M. Hepatotoxicity after long-term methotrexate therapy. *South. Med. J.*, *79*: 536-539, 1986.
 24. Schrenk, D., Gant, T. W., Preisegger, K. H., Silverman, J. A., Marino, P. A., and Thorgeirsson, S. S. Induction of multidrug resistance gene expression during cholestasis in rats and non-human primates. *Hepatology*, *17*: 854-860, 1993.